# Immunological and biochemical characterisation of the NSP4 protein of human rotavirus strains RV4 and RV5

By

Jacqueline Frances Bermingham

A thesis submitted in fulfillment of the
requirements for the degree of
Doctor of Philosophy
2011

Faculty of Life and Social Sciences
Swinburne University of Technology
Australia

# Abstract

Rotavirus has been identified as the major aetiological agent of severe dehydrating gastrointestinal disease in the young of humans and animal species. Of particular significance is the pleoitropic properties of the rotavirus non-structural protein 4 (NSP4), the first identified viral enterotoxin. NSP4 has been widely documented to play an integral role in disease pathogenesis and morphogenesis.

The induction of cell-mediated and humoral responses to NSP4 has been demonstrated in both humans and in animal models. The enterotoxigenic and cytopathic properties of rotavirus infection has been associated with the inherent ability of extracellular and intracellular NSP4 respectively, to perturb the calcium homeostasis of host cells. This study aimed to investigate the ability of the NSP4 protein of two prototype human rotavirus strains, RV4 and RV5 to mobilise intracellular calcium *in vitro* and to evoke a humoral response in naturally infected children and vaccine recipients.

The baculovirus expression system (BEVS) was used to produce hexa-his-tagged ($His_6$)-NSP4 fusion peptides in *Spodoptera frugiperda* (*Sf*-21 cells). The purified proteins were then used in (a) an α-NSP4 indirect ELISA and (b) intracellular calcium mobilisation studies.

The results obtained from the α-NSP4 specific immunoglobulin ELISA demonstrated that natural rotavirus infection and vaccination evoked an NSP4-specific humoral response, which was both heterotypic and/or homotypic. The dominant isotype-specific serum response was to α-NSP4 IgG. For children naturally infected with a G1 RV strain, the response was both homotypic and heterotypic, with 80% of samples reactive with NSP4 of genotype B (G1) and 60% to NSP4 genotype A (G2). The α-NSP4 IgA response was detected solely for children infected with a strain homotypic to the coating antigen and with a seroconversion rate of 29%. No NSP4-specific IgA was detected for vaccine recipients and the IgG response was less than for naturally infected children. Preliminary data indicated that the proximal location of the $His_6$-tag on NSP4 of the RV4 strain influenced the antigenic properties of the protein.

The studies on the effects of NSP4 derived from animal rotavirus strains (predominantly non-human primate strains) and to whole virus on perturbations to intracellular calcium homeostasis has been well established. This study aimed to investigate the ability of human rotaviruses and their corresponding NSP4 to alter the intracellular calcium concentration of cultured renal cells. Two methods for monitoring intracellular calcium concentrations were undertaken; (a) spectrofluorimetric detection of cell populations in suspension and (b) epifluorescence microscopy of cell monolayers. The results acquired from this study demonstrated that SA11 infection and the exogenous application of NSP4 induced changes to the intracellular calcium homeostasis of mammalian cell populations and single cells respectively. An apparent caloric stress effect, arising from the sequential exposure of uninfected mammalian cells to mild hypothermia and hyperthermia was observed to enhance the cytopathic effect of all three strains (SA11, RV4 and RV5) investigated.

# Acknowledgements

First and foremost, I would like to extend the deepest gratitude to my principal supervisor, Associate Professor Enzo Palombo. Many thanks for introducing me to the wonderful world of rotavirus, and for your unwavering optimism and belief in both my ability as a researcher and in the merits of this work. To my co-supervisor, Dr Tony Barton, thank you for broadening my practical skills, expanding my knowledge of protein biochemistry and for your boundless contributions to seemingly endless troubleshooting.

Much appreciation to Dr Carl Kirkwood of the Murdoch Children's Research Institute for his guidance and support with the development of the NSP4-specific ELISA. Your knowledge has been invaluable.

My sincerest gratitude to Professor Andrew Wood for your advice on all things calcium.

Great appreciation is extended to the technical staff, Ngan Nguyn, Soula Mougas and Chris Key.

To my beautiful girls, Carly Gamble, Sarah McLean, Jacqui McRae, Danielle Tilmanis and Kelly Walton for your support, advice, encouragement and much needed source of laughter and respite from the stresses of a PhD. To Kel and Carly in particular, a heart-felt thank you to two amazing women, I am truly blessed to have experienced this journey with you.

Daniel Eldridge, thank you for always being there. You were a constant source of optimism, humour and support, and your friendship will always be treasured.

To all my dearly loved friends, especially Michelle Dal Pozzo and Catherine Whiting and family, for always lending an ear (and shoulder) and allowing me to escape from my PhD.

To my family, in particular my parents and My Juzzii, thank you for your continued support throughout my seemingly endless academic pursuits. For all that I have achieved and for all that I am, it is a testament to your love, sacrifices and belief in me. In loving memory of my grandparents, Gladys and Frank Kennedy, who taught me to believe in myself.

Lastly, to my amazing husband Dr Gordon Bewsell, for your endless patience, support, love, encouragement, humour and understanding throughout this whole experience. I am now finally thesis-free Coasters and looking forward to the next chapters in our life together. Our time is finally our own.

# Declaration

I, Jacqueline Bermingham declare, to the best of my knowledge, that the material contained within this thesis has not been accepted for the award of Doctor of Philosophy or any other degree or diploma, nor has it been previously published or written by another, except where due reference is made. I also declare that where the work is based on joint research or publications, I have disclosed the relative contribution of the respective individuals.

Jacqueline Bermingham
May 2011

# Table Of Contents

## Chapter 2

### Production of recombinant histidine-tagged NSP4 proteins

## Chapter 3

### Immunogenicity of NSP4

## Chapter 5

### Summary and Future Directions

# List Of Figures

# List Of Tables

# List Of Abbreviations

| | |
|---|---|
| 1° Ab | primary antibody |
| 2° Ab | secondary antibody |
| aa | amino acid |
| Ab | antibody |
| *Ac*MNPV | *Autographa californica* multi nuclear polyhedrosis virus |
| Ag | antigen |
| AM | acetoxymethylester |
| $amp^R$ | ampicillin resistance gene |
| ASC | antibody secretory cells |
| bp | base pairs |
| BEVS | Baculovirus expression vector system |
| BSA | bovine serum albumin |
| $[Ca^{2+}]_i$ | intracellular calcium concentration |
| CaM | calmodulin |
| CFTR | cystic fibrosis transmembrane conductance regulator |
| CPE | cytopathic effect |
| Csp's | cold shock proteins |
| CT | checkerboard titration |
| CTB | cholera toxin subunit B |
| C-terminal | carboxyl terminal |
| DLP | double layered particle |
| DMEM | Dulbecco's modified eagle medium |
| DMSO | dimethyl sulfoxide |
| DNA | deoxyribonucleic acid |
| d.p.i. | days post inoculation |
| dsRNA | double stranded RNA |
| ECB | extracellular buffer |
| ECM | extracellular matrix |
| EDTA | ethylenediaminetetracetic acid |
| EGFP | enhanced green florescent protein |
| EGTA | ethylene glycol-bis (2-aminoethyl)-N,N,N',N'-tetraacetic acid |

| | |
|---|---|
| EIA | enzyme immunoassay |
| ELISA | enzyme-linked immunosorbent assay |
| EM | electron microscope |
| ENS | enteric nervous system |
| ER | endoplasmic reticulum |
| ERGIC | endoplasmic reticulum golgi intermediate compartment |
| FBS | foetal bovine serum |
| FFU | fluorescent-focus units |
| FITC | fluorescein isothiocyanate |
| GALT | gut associated lymphoid tissue |
| HEPES | N-2-Hydroxyethyl piperazine-N-2-ethane sulphonic acid |
| $His_6$ | hexa-histidine |
| h.p.i. | hours post inoculation |
| HRP | horse radish peroxidase |
| HRV | human rotavirus |
| Hsc | constitutively expressed Hsp's |
| Hsp's | heat shock proteins |
| IFN | interferon |
| Ig | immunoglobulin |
| IgA | immunoglobulin A |
| IgG | immunoglobulin G |
| IL | interleukin |
| IMAC | immobilised metal affinity chromatography |
| $IP_3$ | inositol 1,4,5-triphosphate |
| ISVD | interspecies-variable domain |
| kbp | kilo base pair |
| kDa | kilo Dalton |
| M13 | myosin light chain kinase |
| MCRI | Murdoch Children's Research Institute |
| MCS | multiple cloning site |
| MDA | membrane destabilising activity |
| MDCK-1 | Madin-Darby canine kidney cells |
| MOI | multiplicity of infection |

| | |
|---|---|
| mRNA | messenger RNA |
| NA | neuraminidase |
| NFDM | Carnation non-fat dry milk |
| NI-NTA | nickel-nitrilo triacetic |
| NSP4 | non-structural protein 4 |
| nt | nucleotide(s) |
| N-terminal | amino terminal |
| NTPs | nucleotide tri-phosphates |
| OD | optical density |
| ORF | open reading frame |
| PBS | phosphate buffered saline |
| PBS-T | phosphate buffered saline and Tween-20 |
| PCR | polymerase chain reaction |
| Pen/Strep | penicillin/streptomyocin |
| PFU | polyhedrin forming units |
| pI | isoelectric point |
| PLC | phospholipase C |
| PM | plasma membrane |
| RDRP | RNA-dependent-RNA polymerase |
| RE | restriction endonuclease |
| RER | rough endoplasmic reticulum |
| RIs | replication intermediates |
| RNA | ribonucleic acid |
| RT-PCR | reverse transcription - PCR |
| RV | rotavirus |
| RV4C | C-terminal $His_6$-tagged NSP4 protein of strain RV4 |
| RV4N | N-terminal $His_6$-tagged NSP4 protein of strain RV4 |
| RV5C | C-terminal $His_6$-tagged NSP4 protein of strain RV5 |
| RV5N | N-terminal $His_6$-tagged NSP4 protein of strain RV5 |
| rpm | revolutions per minute |
| SA | sialic acid |
| SAP | shrimp alkaline phosphatase |
| SCID | severe combined immune deficiency |

| | |
|---|---|
| SDS | sodium dodecyl sulphate |
| SDS-PAGE-SRB | sodium dodecyl sulphate- polyacrylamide gel electrophoresis-sample reducing buffer |
| SERCA | sarcoplasmic endoplasmic reticulum ATPase (SERCA) pumps |
| *Sf* | *Spodoptera frugiperda* |
| SGLTI | $Na^+$-D-glucose symporter |
| siRNAs | small interfering RNAs |
| STB | shiga toxin B subunit |
| SV40 | simian virus 40 |
| TE | Tris-EDTA |
| TLP | triple layered particle |
| TMB | 3,3',5,5'-Tetramethylbenzidine |
| UV | ultra violet |
| VLPs | virus like particles |
| VP | virus particle |

# 1

# Literature review

## 1.1 Introduction

Rotavirus (RV) is the major cause of severe dehydrating infantile gastroenteritis worldwide, implicated in 111 million diarrhoeal episodes and accounting for 25 million clinic visits and 2 million hospitalisations of children under the age of 5 years annually (reviewed in Angel *et al.*, 2007). The annual mortality rate attributed to RV infection is estimated to be in excess of 600,000, with children residing in developing countries (the Indian subcontinent, sub-Saharan Africa, Central and South America) accountable for approximately 95% of these deaths (Parashar *et al*., 2006). In Australia, RV illness is responsible for an estimated 22,000 emergency department visits, 10,000 hospitalisations and 1 death annually (Galati *et al*., 2006).

RV has been identified as the major aetiological agent of nosocomial infections contributing to 27 and 32% of all RV disease cases within developed and developing countries, respectively (Fischer *et al.*, 2004; Gleizes *et al.*, 2006; Moreira *et al.*, 2009). In addition to the human cost, the burden of RV-related medical and societal costs in the USA is estimated to be approximately $400 million and $1 billion respectively (Ward *et al*., 2004).

Comparable morbidity rates between developing and industrialised countries indicate that conventional prevention strategies (improved sanitation and hygiene) employed in the control of other diarrhoeal illnesses are ineffective in the control of RV. Taken in conjunction with the high mortality rate in developing countries, a consequence of

inadequate therapeutic care and the high incidence of nosocomial infection, the importance of developing efficient and cost-effective vaccine strategies is paramount.

RV is not restricted to human hosts, with pathogenesis observed in the young of an extensive number of mammalian and avian species inclusive of both domestic and wild animals. RV was first detected in suckling mice in the late 1940's (Cheever and Mueller, 1947) and subsequently identified in 1963 as RV strain EDIM; the first non-bacterial diarrhoeal agent (Adams and Crafts, 1963). Upon discovery of RV in epithelial cells from duodenal biopsies (Bishop *et al.*, 1973) and faecal specimens (Flewett *et al.*, 1973) of children afflicted with gastroenteritis, its significance as a causative agent of severe dehydrating diarrhoeal illness in young children was realised.

## 1.2 Transmission, clinical features, diagnosis and treatment of rotavirus

The resistance to physical inactivation and the shedding of large numbers of virus particles in faeces may contribute to the efficient transmission of human rotaviruses (HRVs). In addition, contaminated water has been identified as an important vehicle for transmission of RVs, in particular for Group B RVs (Hopkins *et al*., 1984; Tao *et al*., 1984).

RV is transmitted *via* the faecal to oral route, but there is speculation that the respiratory route may be an additional mode of transmission, due in part, to the detection of virus particles in nasopharyngeal secretions (Azevedo *et al.,* 2005; Crawford *et al.,* 2006; reviewed in Estes and Kapikian, 2007). It is estimated that as many as $10^{11}$ infectious particles per gram of faeces may be shed by children with diarrhoea (Flewett, 1983), whilst the human infectious dose may be as low as $10^{1}$ infectious particles (Ward *et al*., 1986).

RV particles are quite stable, surviving on environmental surfaces at low humidity and at ≤25°C for days (Sattar *et al.*, 1989), within stool at ambient temperatures (30 to 35°C) for approximately 2.5 months (Fischer *et al.*, 2002a) and have an approximate 50% survival rate on human fingers after 60 minutes (Ansari *et al*., 1988). Standard

hygiene practices, inclusive of hand washing and the disinfection of inanimate objects with 70% ethanol or chlorine based disinfectants, are required to reduce viral load and minimise transmission (Rao, 1995).

RV gastroenteritis, presenting after a short incubation period of 24 to 48 hours, is characterised by diarrhoea, vomiting and fever, occurring alone or in combination, and of variable severity (Davidson *et al*., 1975a; Desselberger and Gray, 2003). Vomiting is the prominent symptom and generally precedes the onset of diarrhoea by 1-2 days (reviewed in Clark and Offit, 2004). Other symptoms include nausea, anorexia, cramping, malaise and necrotising enterocolitis (Bass *et al*., 2007). In more severe cases, and in the absence of adequate therapeutic care, excessive fluid loss from vomiting and diarrhoea can result in shock, electrolyte imbalance, acidosis or death (Bernstein, 2009). Typically, gastrointestinal symptoms are resolved within 3 to 7 days post infection, although sporadic, longer term diarrhoeal disease has been reported in immunocompromised patients irrespective of age. The median duration of virus shedding of children hospitalised with rotaviral illness as determined by PCR was 10 days (range 4 to 57 days) (Richardson *et al*., 1998).

As the clinical symptoms of RV infection are non-specific and characteristic of other enteric pathogens, albeit with greater severity, definitive confirmation of RV as the causative agent can only be established by laboratory testing (ELISA, latex agglutination, EM, cell culture, flow cytometry and RT-PCR) (reviewed in Estes and Kapikian, 2007).

Oral rehydration therapy or intravenous rehydration (in more severe cases) are the main methods of treatment and are directed at symptom relief and the restoration of normal physiological function by re-establishing electrolyte and fluid balance. The use of antimotility drugs, although efficient in reducing fluid loss, is discouraged due to a risk of causing ileus damage or vomiting (Desselberger, 1999). Oral administration of human serum or milk, or chicken egg yolk preparations, containing immunoglobulins directed against RV have been successful in reducing the duration of diarrhoeal illness (reviewed in Davidson, 1996; Guarino *et al*., 1994; Kanfer *et al.*, 1994; Losonsky *et al*., 1985; Sarker *et al*., 2001). In contrast, the use of colostrum or milk obtained from cows

immunised with HRVs has generated conflicting results (reviewed in Davidson, 1996; Estes and Kapikian, 2007). Probiotics such as *L. acidophilus* demonstrate significant immunopotentiating effects, enhancing RV specific $CD8^+$ T and antibody secreting cell (ASC) responses and inducing serum IgM, IgA, IgG and virus neutralising antibodies in RV-infected animals and children (Majamaa *et al*., 1995; Zhang 2008). The use of antiviral agents, in concert with fluid replacement therapy needs to be investigated further. Preliminary studies have shown an association between the use of antiviral agents and a reduction in the duration of severe diarrhoeal illness in hospitalised children (reviewed in Farthing, 2006; Lanata and Franco, 2006; Salazar-Lindo *et al*., 2000). Drugs directed at the enteric nervous system (ENS) may provide alternative therapies in the treatment of diarrhoeal illness (Lundgren *et al*., 2000).

## 1.3 Rotavirus structure

RV is an icosohedral, non-enveloped, double-stranded RNA (dsRNA) virus, comprising a genus within the subfamily *Sedoreovirinae*, family *Reoviridae*. The mature virion is organised into three proteinaceous concentric layers (inner core, intermediate and outer layers), spanning 100 nm in diameter.

### 1.3.1 Rotavirus genome

The genome, embedded in the innermost core of the triple layered capsid, consists of 11 segments of double-stranded RNA, ranging in size from 667 (Segment 11) to 3,302 nucleotides (Segment 1) for the prototype RV strain, SA11 (Estes, 2001). All genes lack a polyadenylation signal, are A + U rich, and contain conserved consensus sequences at their 5' and 3' ends (Estes and Kapikian, 2007; Imai *et al*., 1983).

Most of the genome segments are monocistronic, typically encoding a single viral protein, inclusive of six structural proteins (VP1-4, VP6, VP7) and six non-structural proteins (NSP1-6). Genome segment 11 codes for both NSP5 (the primary product) and NSP6 from alternative long and short open reading frames (ORFs) in some RV strains (Mattion *et al.*, 1991; Torres-Vega *et al*., 2000). Figure 1.1 illustrates the gene coding assignments of the 11 segments of dsRNA with their respective protein(s).

### 1.3.2 Capsid architecture

The significant proteins of the three layers are VP2, the predominant inner core protein, VP6, the intermediate layer protein, and VP4 and VP7, the surface capsid proteins (Figure 1.1). Two forms of the virion exist, the infectious triple layered particles (TLPs) comprising the three concentric protein layers, and the non-infectious double layered particles (DLPs) in which the outermost layer has been removed.

#### 1.3.2.1 The surface layer

The smooth surface of the outermost layer consists of 780 copies of the VP7 glycoprotein organised as trimers. The protease-sensitive VP4 haemagglutinin forms 60 spike–like protuberances, existing as trimers (dimers detected by cryo-EM), extending 12 nm from the VP7 surface and positioned within type II channels (Estes and Kapikian, 2007; Prasad *et al.*, 1990). Each VP4 spike interacts with two VP7 molecules and six VP6 molecules (at the VP4 globular domain) surrounding the Type II Channels, implying a role in maintenance of the structural integrity between the inner and outer capsids (Estes and Kapikian, 2007).

Trypsin-activated cleavage of VP4 exposes the polypeptides VP5* (aa 248-776) comprising the body and base (β- and α-helical conformations respectively) and VP8* (aa 1-231) existing in a β-sheet conformation at the head of the VP4 protein (Tihova *et al*., 2001). VP8* contains a haemagglutination domain (aa 93 to 208) (Fuentes-Panana *et al*., 1995) and VP5* a hydrophobic fusogenic region capable of permeabilising lipid bilayers (Denisova *et al.*, 1999; Dowling *et al.*, 2000).

#### 1.3.2.2 Channels

The mature TLP is punctuated by three types of porous channels, designated I, II and III, approximately 140 Å deep (Estes and Kapikian, 2007). Of the 132 channels, 12 are Type I and the remaining 120 are of equal number of Types II and III. These channels, extending from VP7 into the inner core, permit the influx of NTPs and divalent cations into the interior of the capsid and the export of newly synthesised mRNA's (through

Type I channels) to the ribosomes for translation (Estes, 2001; Guglielmi *et al.,* 2010; Lawton *et al.*, 2000; Pesavento *et al.*, 2003).

#### 1.3.2.3 The intermediate layer

The intermediate layer is formed from 260 trimers of VP6, organised with the same T=13 *levo* icosahedral symmetry as the surface layer ensuring continuity of the aqueous channels. In the absence of an X-ray structure, a pseudo-atomic model has been proposed for VP6, comprising of two domains, a distal anti-parallel β-sandwich fold and a cluster of α-helices which interact with VP7 and VP2 respectively (Mathieu *et al.,* 2001). VP6 constitutes approximately 51% of the total protein content of the virion (Mattion *et al*., 1994).

#### 1.3.2.4 The inner core

The innermost core, encapsulating the viral genome, is of T=1 icosahedral symmetry and consists of 120 molecules (60 dimers) of VP2 and 12 molecules each of VP1 (an RNA-dependent RNA polymerase) and VP3 (a guanylyl and methyl transferase) (reviewed in Guglielmi *et al*., 2010). Twelve transcription enzyme complexes, consisting of a single copy of VP1 and VP3, are anchored to the amino terminal of VP2 at each of the twelve vertices, and are surrounded by an individual, highly condensed segment of genomic RNA (Prasad *et al*., 1996). Binding of RNA to VP2 occurs at the amino terminus, between aa 1-132 (Labbé *et al.,* 1994).

### 1.3.3 Non-structural proteins (NSPs)

All of the non-structural proteins are involved in virus replication, while NSP4 is also involved in viral morphogenesis. The functions of each are presented in Table 1.1 and, where appropriate, have been expanded in the text to illustrate these functions. The non-structural protein of interest within this report is NSP4, formerly NS28, which will be reviewed in considerable detail in proceeding sections.

a) b)

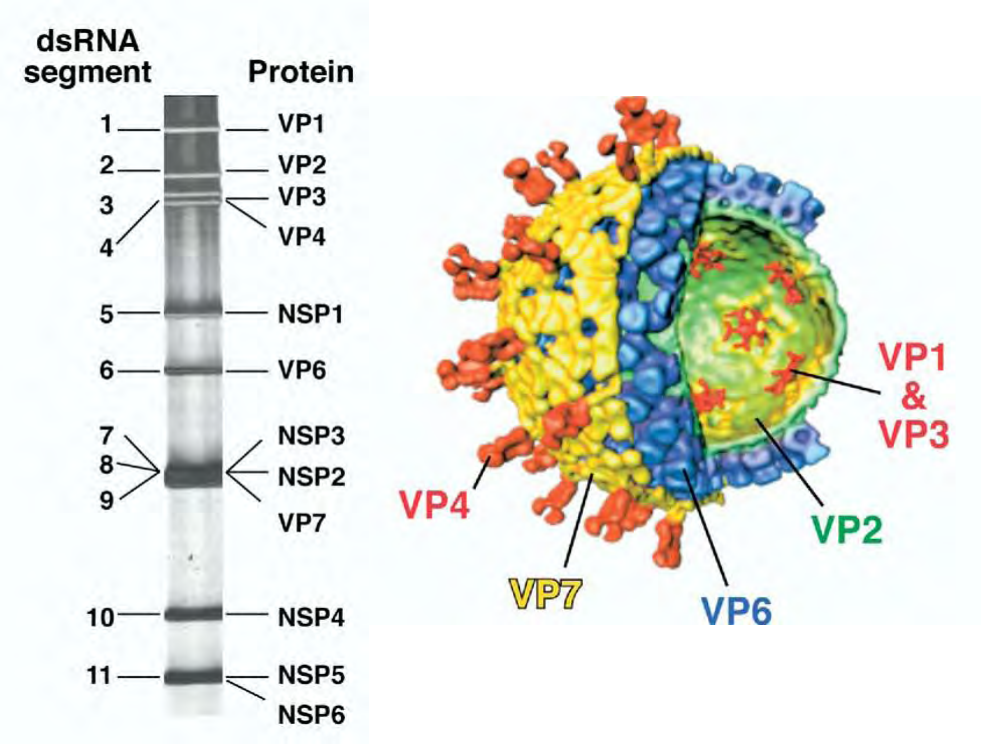


***Figure 1.1. Genome coding assignment and virion structure***. *a) Fractionation of the 11 segments of dsRNA of RV SA11 viral genome in a polyacrylamide gel. The identity of the viral genome segment is reported to the left of the electropherotype and the corresponding protein with which they encode to the right. b) Three-dimensional structure of the RV particle illustrating the outer, middle and inner capsid architecture. Figure adapted from Greenberg and Estes (2009).*

| Genome Segment[a] (size, bp) | Protein | Size aa (kDa) | Functional Properties |
|---|---|---|---|
| 1 (3302) | VP1 | 1088 (125) | RNA-dependent RNA polymerase, ssRNA binding, interacts with VP2 and forms a transcription complex withVP3 |
| 2 (2690) | VP2 | 880 (94) | Non-sequence-specific RNA binding activity, required for replicase activity of VP1 |
| 3 (2591) | VP3 | 835 (88) | Guanyly and methyl transferase, ss-RNA binding, forms a transcription complex with VP1 |
| 4 (2362) | VP4<br>VP5*<br>VP8* | 776 (86.7)<br>529 (60)<br>247 (28) | Hemagglutination, P-type-specific neutralisation antigen, virulence determinant, protease-enhanced infectivity, cell attachment protein, fusiogenic region |
| 5 (1611) | NSP1 | 495 (58.6) | RNA binding, antagonist of interferon (IRF-3) response, associates with the cytoskeleton, virulence (mice), zinc finger |
| 6 (1356) | VP6 | 397 (44.8) | Hydrophobic trimer, group and subgroup antigen, protection (intracellular neutralisation??) required for transcription |
| 7 1105) | NSP2 | 315 (36.7) | Helicase[1], possible molecular motor for packaging[1], viroplasm formation, nucleotide triphosphatase (NTPase), non-specific ssRNA binding, induces hyperphosphorylation of |
| 8 (1059) | NSP3 | 317 (34.6) | Viral mRNA translation, cellular poly(A) binding protein (PABP) homologue, mRNA binding, interacts with eIF4G, inhibits host translation, implicated in extraintestinal spread[2] |
| 9 (1062) | VP7c | 326 (37.4) | RER integral membrane glycoprotein, G-type neutralisation antigen, $Ca^{2+}$ binding |
| 10 (751) | NSP4 | 175 (20.2) | RER transmembrane glycoprotein, viral morphogenesis, enterotoxin, modulates $[Ca^{2+}]i$ and RNA replication, DLP intracellular receptor, viroplasm interactions, secreted cleavage product, |
| 11 (667) | NSP5 | 198 (21.7) | Viroplasm formation, interacts with NSP2 and NSP6, RNA binding (ss and ds), Protein kinase, essential for viral replication |
| | NSP6 | 92 (12) | Constituent of the viroplasm, interacts with NSP5 |

***Table 1.1. The properties of RV proteins.*** *The table was adapted from Estes (2001), Estes and Kapikian (2007), Angel et al. (2007) and Mertens (2004). Where indicated by enumerated superscript, the information was adapted from the following sources; (1) Patton et al. (2003), (2) Mossel and Ramig (2002). Where indicated by alphabetised superscript, the following information is applicable; (a) segments numbered based on migration of SA11 genome segments in SDS-PAGE gel, (b) protein size based on prototype strain, SA11, (c) depending on the strain, VP7 can be encoded by genome segments 7, 8 or 9.*

## 1.4 Rotavirus morphogenesis

*In vivo* RV replication occurs predominantly in the mature absorptive enterocytes of the villus epithelium of the proximal two thirds of the ileum (Widdowson *et al*., 2005). In cell culture, RV infection proceeds in a number of cell lines, but is most permissive in those of renal or intestinal epithelial origin (Ciarlet *et al*., 2002a; Estes, 2001). Somewhat refractory cell lines can replicate the virus efficiently when DLPs are delivered directly to the cytoplasm *via* transfection (Ciarlet *et al.*, 2002a).

### 1.4.1 Virus adsorption; binding and post-attachment receptors

RV-host cell interactions traditionally have been characterised as either neuraminidase (NA)-resistant (Sialic acid (SA)-independent) or NA-sensitive (SA-dependent) in accordance with the requirement for terminal SA on host cell receptors for the initial attachment of the virus. All human and most animal RV strains investigated to date are SA-independent (Ciarlet and Estes, 1999).

#### 1.4.1.1 Virus binding

The initial interaction between an NA-sensitive virus and a SA receptor (most probably a ganglioside, with terminal sialyl-galactose) occurs at the apical surface of polarised intestinal cells, is mediated *via* VP8* (aa 93-208) (Ciarlet *et al*., 2001; Iša *et al*., 1997) and potentially coincides with a conformational change in the VP4 protein in preparation for integrin-virus interactions (Ciarlet *et al*., 2001; Crawford *et al*., 2001). The interaction between the virus and the SA moiety is dependent on the VP4 genotype and not the species of origin (Ciarlet *et al*., 2002b).

The identity of the receptor, either a glycoconjugate or integrin, which is involved in the initial interaction between NA-independent strains and the host cell has not been resolved. The most widely accepted model is that the primary interaction of the virus occurs with a ganglioside (GM1a and GM3) or other SA-containing glycolipid which is impervious to NA cleavage, possibly due to internalisation of the SA moieties (Delorme *et al*., 2001; Guo *et al*., 1999; Iša *et al*., 2006). Conversely, studies using ligands

directed to the α2β1 sequence of the VP5* domain have identified its role in cell binding in both Caco-2 and MA104 cell lines (Graham *et al*., 2004). Zárate *et al.* (2000a) demonstrated the direct interaction between the VP5* domain of the RRV NA-independent variant nar3 and integrin α2β1 implicating its role in cell binding, although similar experiments conducted by Ciarlet *et al.* (2002a) with this variant did not present the same findings. Contrary to NA-sensitive viruses where entry is restricted to the apical surface, NA-resistant strains infect polarised cells at either the apical or basolateral surface (Ciarlet *et al*., 2001). More recent findings by Realpe *et al*. (2010) suggest that RVs infect both apical and basolateral domains, with a preference for the latter, and that this interaction is independent of NA sensitivity.

The generation of leaky tight junctions or receptor diffusion have been proposed as potential mechanisms by which the virus can infect cells basolaterally and may provide an explanation for the extraintestinal spread of RV and antigenemia (Lopez and Arias, 2006; Realpe *et al*., 2010).

The interaction of integrin α2β1 with the DGE recognition motif (aa 308 to 310) of VP5*, either as a binding or post-binding receptor, is strain dependent and precedes further virus-cell surface interactions as detailed below (Coulson *et al*., 1997; Graham *et al*., 2003; Hewish *et al*., 2000; Zárate *et al*., 2000a).

Lopez and Arias (2006) have proposed that this initial contact, irrespective of the receptor, allows the virus to "dock" onto the cells surface facilitating the initiation of more specific virus-cell interactions and resulting in virus penetration as described in the proceeding section.

#### 1.4.1.2 Post-attachment receptors

Interaction of the GPR sequence of VP7 (aa 253 to 255) with αxβ2 (Coulson *et al*., 1997; Graham *et al*., 2003), and an RGD-independent interaction of the virus with αvβ3 (Guerrero *et al*., 2000a) is believed to occur at a post-attachment step and is independent of NA-sensitivity (Graham *et al*., 2004). The interaction between αvβ3 and VP7 has been postulated to occur within the CNP region (aa 161-169) (López and Arias, 2004).

Work performed using small interfering RNAs (siRNAs) has reduced the relative importance of integrins α2 and β3 in virus entry (Iša *et al*., 2009). The role of integrin α4β1 is yet to be defined, with its ligand sequences LDV (aa 237 to 239) and IDA (aa 538 to 540) being identified on both VP7 and VP5* respectively (Coulson *et al*., 1997). The interaction between the KID sequence of VP5* and Hsc70 occurs post-attachment and is independent of NA sensitivity (Guerrero *et al*., 2002; López *et al*., 2006; Zárate *et al*., 2003). More recently Gualtero *et al.* (2007) identified a second Hsc70 binding domain on VP4 (aa 531-554), and a Hsc70 binding domain between aa 280-297 on VP6.

Glycosphingolipid and cholesterol enriched microdomains (or "lipid-rafts") within the cell membrane play a critical role in apical membrane trafficking (Simons and Ikonen, 1997), and have been implicated in cell entry, particle assembly and RV release. The existence of RV receptor complexes, embedded within lipid rafts of the plasma membrane and comprised of most, if not all of the receptors involved in virus attachment and entry, have been proposed to function as organising platforms facilitating RV-cell receptor interactions (Arias *et al*., 2002; Guerrero *et al*., 2000b; Iša *et al*., 2004; Lopez and Arias, 2006).

### 1.4.2 Virus entry and uncoating

The mechanism of viral entry, either $Ca^{2+}$-mediated endocytosis or direct penetration through the plasma membrane, has not yet been resolved (reviewed in Ciarlet and Estes, 2001). Initial studies into virus entry provided strong evidence to suggest that the mode of entry may be dependent on trypsin activation of the virus (Ruiz *et al*., 1994; Suzuki *et al*., 1985). Early studies on trypsin activated virus revealed that non-trypsinised virus entered the cell *via* endocytosis and was destined for lysosomal degradation, whilst trypsinised virus entered through direct membrane penetration resulting in a productive infection (Kaljot *et al*., 1988; Nandi *et al*., 1992; Suzuki *et al*., 1985). Trypsinised virus was also shown to enter cells more readily and rapidly than non-trypsinised virus (Clark *et al*., 1981; Crawford *et al*., 2001; Kaljot *et al*., 1988; Keljo *et al*., 1988).

*In vitro*, proteolytic cleavage of VP4 exposes VP5* and VP8*, and causes an increase in viral infectivity by facilitating cell penetration and virus entry (Arias *et al*., 1996; Clark *et al*., 1981; Espejo *et al*., 1981; Estes *et al*., 1981; Fukuhara *et al*., 1988). VP4 cleavage is not required for virus attachment (Clark *et al*., 1981; Crawford *et al*., 1994; 2001; Zárate *et al*., 2000b). *In vivo*, proteolytic cleavage occurs within the lumen of the small intestine of animal models and precedes enterocyte infection (Ludert *et al*., 1996).

#### 1.4.2.1 Direct membrane penetration

Trypsin cleavage of VP4 promotes membrane destabilising properties of the viral outer capsid proteins (Charpilienne *et al*., 1997; Denisova *et al*., 1999). Whether penetration is triggered by the generation of the cleavage products or a result of a conformational change in the spike protein is unresolved.

The direct penetration of the virus through the plasma membrane in association with VP4 has been well documented (Fukuhara *et al*., 1987; 1988; Kaljot *et al*., 1988). Trypsin cleavage of the three VP4 molecules constituting each spike results in conformational changes from a disordered state in which all three VP5* molecules are flexible, to a more highly ordered, rigid-bilobed spike protein (two VP5* molecules become rigid, the remainder flexible), which primes VP5* for cell entry and presents the VP8* core for cell-surface ligand binding (Crawford *et al*., 2001; reviewed in Dormitzer *et al*., 2004). The VP4 protein undergoes an additional conformational change, whereby the protein folds back on itself, forming a more stable umbrella-shaped trimer (all VP5* molecules are rigid) and translocating a hydrophobic region (potentially the VP5* fusogenic region) from one end of the spike to the other (Dormitzer *et al*., 2004). The ability of the VP5* fusogenic region (aa 385 to 404) to permeabilise model and bacterial membranes is highly suggestive of its role in cellular entry of the virus (Denisova *et al*., 1999, Dowling *et al*., 2000; Ruiz *et al*., 1994).

Solubilisation of the outer capsid proteins to produce transcriptionally competent DLPs requires a reduction in $[Ca^{2+}]_i$ below the critical $[Ca^{2+}]$ required for their stabilisation. The critical $[Ca^{2+}]$ is strain dependent and associated with VP7 (aa 134-146) (Estes and Cohen, 1989; Ruiz *et al*., 1996). Tihova *et al.* (2001) have proposed that reductions in

the $[Ca^{2+}]_i$, a consequence of calcium chelation by lipid headgroups, would result in the removal of the outer capsid protein as TLPs traverse the plasma membrane. Alternatively, the TLPs, upon entry into the cytoplasm, may utilise endosomes for transformation into DLPs as described below for calcium mediated endocytosis.

#### 1.4.2.2 Calcium mediated endocytosis

The classical endocytic pathway as a vehicle for cell entry is questionable, as the use of lysosomotropic drugs or the blocking of intracellular traffic for endocytic vesicles had no effect on RV infectivity (Fukuhara *et al*., 1987; Kaljot *et al*., 1988; Keljo *et al*., 1988). Membrane permeabilisation of RV-infected MA104 cells was demonstrated to occur independently of endocytosis, intraendosomal acidic pH or a proton gradient (Cuadras *et al*., 1997; Keljo *et al*., 1988).

RV particles are endocytosed into clathrin-coated vesicles containing mM concentrations of $Ca^{2+}$. The solubilisation of the outer capsid proteins is dependent on a reduction of endosomal $[Ca^{2+}]_i$ which is under the directive of the calcium gradient and possibly facilitated by the $H^+$-ATPase pump (Chemello *et al*., 2002; Ruiz *et al*., 2000). It has been proposed that VP5* may hasten the reduction in endosomal $[Ca^{2+}]$ by selectively permeabilising the early endosomal membrane (Dowling *et al*., 2000).

The activation of virus associated trypsin results in cleavage of VP7 and the induction of endosomal membrane permeabilisation with the concomitant release of DLPs to the cytoplasm of the host cell for virus replication initiation (Benureau *et al*., 2005; Charpilienne *et al*., 1997; Chemello *et al*., 2002; Cohen *et al*., 1979; Ruiz *et al*., 1997; 2000).

Sánchez-San Martin *et al.* (2004) described the entry of RV *via* raft-dependent endocytosis; a cholesterol-sensitive, caveolae- and clathrin-independent endocytosis, which is dependent on the functional GTPase protein, dynamin.

### 1.4.3 Transcription, replication and translation

Viroplasms, electron dense perinuclear cytoplasmic inclusions, visible 2 to 3 hours post infection, are formed by NSP5 and NSP2 and are the sites of virus transcription, replication, genome packaging and DLP assembly (Fabbretti *et al*., 1999; reviewed in Guglielmi *et al*., 2010). Each of the dsRNA segments are transcribed by VP1, the viral RNA-dependent-RNA polymerase (RDRP) within the virion core at one of twelve transcriptional complexes (Valenzuela *et al*., 1991). RDRP is latent in TLPs and can be activated *in vitro* by treatment with a chelating agent or by heat shock, consistent with the removal of the outer capsid proteins (Cohen *et al*., 1979; Spencer and Arias, 1981). VP1 polymerase activity is dependent on VP2 for its activation (Patton, 1996).

#### 1.4.3.1 Transcription

Transcription is asymmetric, and proceeds from the dsRNA negative strand to generate full length positive strands (McCrae and McCorquodale, 1983). Capping of the 5' end of the mRNA is performed by VP3 (Chen *et al*., 1999), and in the absence of polyadenylation, the nascent positive-stranded mRNA transcripts are extruded from the particle through Type 1 channels. The mRNA serves two functions: encoding of rotaviral proteins and as templates for the production of minus strand RNA for the generation of new dsRNA.

#### 1.4.3.2 Translation and synthesis of viral proteins

All viral proteins, with the exception of NSP4 and VP7, are produced on free ribosomes utilising the host cells translational machinery. NSP4 and VP7 are synthesised on the ER-associated ribosomes and are cotranslationally inserted into the ER membrane.

The concurrent interaction between the N-terminal and C-terminal domains of NSP3 with the 3'-consensus sequence of viral mRNA (Deo *et al*., 2002) and the initiation factor eIF4G (Groft and Burley, 2002) respectively, results in circularisation of mRNA, a concomitant impairment of cellular mRNA translation (due to PABP displacement from eIF4G) and the subsequent delivery of viral mRNA to ribosomes for protein synthesis (Padilla-Noriega *et al*., 2002; Piron *et al*., 1998; reviewed in Poncet, 2003;

Vende *et al*., 2000). The penultimate 5'-GACC-3' of the mRNA sequence functions as a translation enhancer (Chizhikov and Patton, 2000).

The binding of NSP3 to viral mRNA has also been proposed as a possible mechanism for transporting newly synthesised mRNA to viroplasms *via* the cytoskeleton for subsequent replication (Estes and Kapikian, 2007).

#### 1.4.3.3 Genomic RNA replication

The synthesis of dsRNA *in vitro* is an asymmetric process in which VP1 synthesises negative-stranded RNA from its nuclease-sensitive, positive stranded mRNA template (Patton, 1986). The production of negative stranded RNA is initiated upon the formation of a stable ternary complex between the 3' consensus sequence (3'-CC) of mRNA with VP1 and the G-dinucleotide (Chen *et al*., 2001).

It has been proposed that NSP2 provides the initial scaffolding for the organisation of the replicase complex (VP1/VP3) through its interaction with VP1 and NSP5 (Jayaram *et al*., 2004). NSP4 has been associated with the regulation of viral protein expression, mRNA synthesis and potentially, genome encapsidation (Berkova *et al*., 2006; Silvestri *et al*., 2005).

### 1.4.4 Genome packaging and DLP assembly

Several models for genome packing and subsequent DLP assembly have been proposed. The first, postulated by Gallegos and Patton (1989), assumes the successive addition of VP2 and VP6 to replication intermediates (RIs). Three species of RNA-RIs exist within infected cells: (i) the pre-core RI (containing viral mRNA, VP1 and VP3), (ii) the core RI (pre-core RI and VP2, NSP2 and NSP5), and (iii) the double-layered RI (VP6 added to the core RI), with the latter two species exhibiting replicase activity.

Pesavento *et al.* (2003) proposed an alternative model in which genome encapsidation and DLP assembly occur concurrently. Twelve functionally separate pentameric units, containing VP2 dimers complexed with a transcription enzyme complex (VP1/VP3) and

associated with a specific mRNA, self assemble to generate SLPs. Structural changes in VP2, may activate the RDRP and stimulate negative-stranded RNA synthesis to produce the genome (Guglielmi *et al*., 2010). The SLPs then provide the necessary scaffolding for VP6 assembly.

RV capsid proteins can self-assemble *in vitro* to generate empty virus-like particles (VLPs). Taken together with the knowledge of dsRNA bacteriophage phi6, the final model proposes that the viral mRNA is inserted into self assembled viral cores (reviewed in Estes and Kapikian, 2007).

The involvement of NSP5 and NSP2 in recruiting inner capsid proteins to viroplasms for core particle assembly was proposed by Patton *et al*., (2006). Studies using a mutant SA11 RV, *ts*E(1400), supported the role of the functionally active NSP2 octamer as a molecular motor, facilitating the packaging of mRNA into the core RI (Taraporewala *et al*., 2002) using energy derived from NTP hydrolysis (Schuck *et al*., 2001).

SiRNA studies have demonstrated a role for NSP4 in the localisation of VP6 at the periphery of viroplasms (López *et al*., 2005). The core particles, localised within the interior of the viroplasms migrate towards its exterior, acquiring VP6 and transpiring into DLPs at the ER membrane. The newly formed DLPs may either direct the synthesis of additional positive stranded mRNA transcripts or alternatively translocate across the ER to form infectious TLPs as detailed in the next section (reviewed in Patton *et al*., 2006).

### 1.4.5 Final stages of rotavirus maturation and release

DLPs synthesised in viroplasms, enter the dilated cisternae of the RER by budding (Suzuki *et al*., 1984). The budding process, mediated by the interaction between the ER resident NSP4 and VP6 of the DLP, results in the acquisition of a transient envelope, postulated to be an extension of the ER membrane and potentially punctated by NSP4 and VP7. Maturation of the DLP into infectious TLPs requires the loss of the lipid envelope, the exclusion of NSP4 and the assembly of the outer capsid proteins, VP7 and VP4. Removal of the ephemeral envelope has been attributed to VP7 (Arias *et al*., 2004;

Cuadras *et al*., 2006; Lopez *et al.*, 2005), VP4 (Denisova *et al*., 1999) and glycosylated NSP4 (reviewed in section 1.10.2), and in association with high ER luminal $Ca^{2+}$ concentrations (Poruchynsky *et al*., 1991; Shahrabadi *et al*., 1987).

The location and mechanisms by which the outer capsid proteins are assembled onto DLPs is still under investigation as studies using polarised Caco-2 cells is challenging the much held belief that the final stages of RV assembly, as evidenced in non-differentiated renal MA104 cells occurs solely within the ER. In addition, lipid raft microdomains of cell type specific heterogeneity have been identified as important components of viral morphogenesis in each of these cell lines (Delmas *et al*., 2007).

Substantial experimental data has been accumulated from studies performed with MA104 cells which lends credence to the acquisition of VP4 as a reticular event, most probably involving the endoplasmic reticulum golgi intermediate complex (ERGIC), and in which the addition of VP4 to DLPs occurs prior to, or simultaneously with VP7 assembly (Cuadras *et al*., 2006; Delmas *et al*., 2004a; 2004b; Gonzalez *et al*., 2000; Maas and Atkinson, 1990; Petrie *et al*., 1984; Poruchynsky and Atkinson, 1991; Trask and Dormitzer, 2006).

VP4 synthesised in monkey kidney cells was associated with microtubule β-tubulin and the authors proposed that the cytoskeleton was utilised for transport of the newly synthesised protein to the plasma membrane (Nejmeddine *et al*., 2000). VP4 in association with raft type membrane microdomains at the cell surface have been identified in MA104 cells and its projected role is as a "raft" receptor for RV particles or endogenously expressed NSP4 or its cleavage product (Cuadras *et al*., 2006; Delmas *et al*., 2007; Zhang *et al*., 2000). The infectious virions are released from the cells *via* lysis (Estes, 2001; Michelangeli *et al*., 1991).

Studies in polarised Caco-2 cells have indicated a much more complex process for VP assembly involving lipid rafts and the non-conventional targeting of the mature virus to the apical surface (Cuadras and Greenberg, 2003; Delmas *et al*., 2004b; Sapin *et al*., 2002). Immunofluorescence microscopy identified VP4 associated with lipid rafts and actin bundles at the external face of the apical plasma membrane of Caco-2 cells whilst

studies with tunicamycin demonstrated that VP4 assembly was a non-reticular event (Delmas *et al*., 2004a; Gardet *et al*., 2006; Sapin *et al*., 2002). These observations prompted the proposal of an alternative hypothesis whereby VP7-coated nascent particles acquire the terminal VP4 protein during transport from the ER to the apical surface (Cuadras and Greenberg, 2003; Delmas *et al*., 2004a; 2004b; Jourdan *et al*., 1997; Sapin *et al*., 2002).

The synthesis of rafts occurs in the Golgi apparatus and it is highly probable that raft/VP4 association occurs shortly thereafter. That VP4 assembly results from a fusion event between the ERGIC, in which neovirions reside, and a compartment containing the raft and its associated VP4 is supported by the co-localisation of VP4 and virion-assembled VP7 with ERGIC-53 (Cuadras and Greenberg, 2003; Cuadras *et al*., 2006; Delmas *et al*., 2004a; 2004b; 2007). The mature infectious TLPs encircled within specific raft containing vesicles are translocated to the apical membrane under the directive of an apical signal (most probably located on VP8*) where they are released in the absence of cell lysis (Cuadras and Greenberg, 2003; Delmas *et al*., 2007; Jourdan *et al*., 1997; Sapin *et al*., 2002).

The apical trafficking of RV particles in Caco-2 cells was attributed to their association with raft-type membrane microdomains until a similar relationship was observed in MA104 cells (Delmas *et al*., 2007). Gardet *et al*. (2006) proposed that apical targeting of VP4 to actin microfilaments and its subsequent reorganisation of actin bundles to actin bodies at the apical membrane is biphasic, and in concert with lipid raft microdomains, facilitates the final stages of virus assembly and non-lytic release of the infectious virion, respectively.

As to whether the apically located VP4 is assembled onto immature TLPs or functions as an intracellular receptor for virus particles has not been resolved, although the presence of NSP4 at these microdomains would support the former (Cuadras and Greenberg, 2003; Huang *et al*., 2001; reviewed in Pesavento *et al*., 2006; Sapin *et al*., 2002).

The acquisition of VP7 as a reticular event has not been unequivocally determined. It was widely believed that VP7 was acquired in the ER and terminally glycosylated within the ERGIC (Mirazimi *et al*., 1996). More recently, Delmas *et al*. (2004b) proposed that VP7 assembly may result from a fusion event between the ER and a post-Golgi compartment.

It is hoped that with the advent of a reverse genetics system for RV (Komoto *et al*., 2006) that the questions pertaining to virus morphogenesis, pathogenesis and immunity *in vivo*, may finally be elucidated.

## 1.5 Virus pathogenesis

### 1.5.1 Intestinal infection

The mechanism of RV diarrhoea induction in humans is incompletely understood and a direct relationship between disease severity and histopathological damage has not yet been established (reviewed in Franco *et al*., 2006). Limited studies of jejunal mucosal biopsy specimens of RV-infected infants have revealed villous shortening and atrophy, denudation of microvilli, mitochondrial swelling, distension of the ER, depressed disaccharidase concentrations, and mononuclear cell infiltration (Holmes *et al*., 1975; Davidson and Barnes, 1979).

A considerable contribution to the knowledge of RV pathogenesis has been accrued from studies performed with animal models using whole virus and virulent gene products. The following three mechanisms have been proposed as potential models of pathogenesis for the induction of diarrhoeal illness, but the outcome of disease is invariably dependent on a complicated interplay of host cell and viral factors, potentially involving more than one mechanism.

The first mechanism postulates that virus replication and shedding within the mature enterocytes of the small intestine results in villous atrophy and ischemia (in some animal models) promoting reactive crypt cell hyperplasia and the increased migration of immature cells defective in brush border associated hydrolases (sucrase-isomaltase, lactase) along the crypt-villus axis. These pathologic changes are observed 18-48 hours

post-infection, commencing in the duodenum and progressing distally to the ileum. Osmotic diarrhoeal illness is the outcome of the impairment of the digestive and absorptive functions of necrotic villous epithelia and is exacerbated by the compensatory hypersecretion of water from stimulated crypt cells (Collins *et al*., 1988; Davidson *et al*., 1977; Davidson and Barnes, 1979; Graham *et al*., 1984; Jourdan *et al*., 1998; reviewed in Lundgren and Svensson, 2001; Osborne *et al*., 1991; 1988; Servin, 2003; Stephen and Osborne, 1988).

The second mechanism, based on the findings of Ball *et al*. (1996), proposes that NSP4 or its peptide, $NSP4_{114-135}$, functions as an enterotoxin inducing secretory diarrhoea in mice. Early in the viral replication cycle (<24 h) diarrhoeal induction is due to the activation of a $Ca^{2+}$-dependent signal transduction pathway and proceeds in the absence of histopathological lesions. The properties of secreted NSP4 which may contribute to pathogenesis include its ability to alter transepithelial electrical resistance in polarised MDCK-1 cells (Tafazoli *et al*., 2001) and the inhibition of the $Na^{+}$-D-glucose symporter (SGLT1) activity in brush border membranes (Halaihel *et al*., 2000b). The role NSP4 plays in RV pathogenesis will be discussed in greater detail elsewhere.

Finally, RV activation of the ENS is mediated by a vasoactive intestinal peptide (potentially NSP4) which stimulates water and electrolyte secretion of intestinal crypts resulting in diarrhoeal illness in newborn mice (Kordasti *et al*., 2004; Lundgren *et al*., 2000; reviewed in Lundgren and Svensson, 2001). Lundgren *et al*. (2000) estimated that approximately two thirds of the fluid and electrolyte secretion observed in mice was attributed to activation of the ENS.

### 1.5.2 Systemic infection

Until recently it was believed that RV had an explicit tropism for the mature, differentiated absorptive enterocytes of the villus epithelium of the mid and upper regions of the small intestine (Bishop *et al*., 1973; Davidson *et al*., 1975a; 1975b) but increasing evidence is suggestive of RV hepatropism. Viremia, as determined by the detection of RV RNA in the cerebrospinal fluid of RV-infected children with seizures and in the liver and kidney sections of immunocompromised children, is most probably

accountable for the rare complications of extraintestinal disease (Gilger *et al*., 1992; Iturriza-Gomara *et al*., 2002a).

RV replication can proceed within tissues of extraintestinal organs (liver, lungs, spleen, kidneys, pancreas, thymus, brain and bladder) and macrophages of mice orally inoculated with RV (Crawford *et al*., 2006; Fenaux *et al*., 2006). RV particles were detected in the liver of severe combined immuno deficient (SCID) mice (Tatti *et al*., 2002; Uhnoo *et al*., 1990) and the extraintestinal spread of RV to the liver in the neonatal mouse model has been associated with NSP3 (Mossell and Ramig, 2002).

Immunohistochemical data demonstrated the presence of RV antigens (antigenemia) in the sera, liver and kidneys of immunocompetent children, implying the extraintestinal spread of the virus in the absence of enterocyte destruction, and providing an explanation for the induction of systemic immunity after infection (Blutt *et al*., 2003; 2007; Gilger *et al*., 1992).

## 1.6 Rotavirus classification

RVs are firstly classified into serological groups in accordance with the structure and immunological reactivity to the primary group antigen, VP6. Currently there are 7 serological groups, denoted A-G, of which groups A-C are infectious to both humans and animals whilst groups D-G exclusively infect animals.

RV strains of Group A are the major aetiological agents of endemic rotaviral infection in the young of mammalian species and consequently will be the focus of this discussion. Group B (adult diarrhoeal rotaviruses [ADR]) are the causative agents of waterborne outbreaks, resulting in severe cholera-like diarrhoeal disease in adults (epidemic infections in Asia and the subcontinent) and pigs (Krishnan *et al*., 1999; Tao *et al*., 1988). More recently, Group B RVs were associated with gastroenteritis in children (Barman *et al*., 2006). Group C RVs cause endemic infections, commonly associated with familial and community outbreaks, which frequently go unrecognised.

Within Group A there are four subgroups, SG (I, II, I+II, nonI-nonII), defined according to the specificity of VP6 for the monoclonal antibodies 255/60 and 631/9 (Arista *et al*., 1990; Greenberg *et al*., 1983). More recently, molecular characterisation of group A HRVs resulted in their assignment into two genogroups; genogroup I (SGI only) and genogroup II (SGII, SGI + II, SG nonI-nonII) (Iturriza Gómara *et al*., 2002b).

RVs are further subdivided within each group, according to a dual classification system based on neutralisation determinants to the protease-sensitive VP4 (defining P types) and the glycoprotein VP7 (G-types). Within group A there are currently 14 G serotypes (G1-14) and 14 P serotypes (Matthijnssens *et al*., 2008b).

RV strains are also classified according to their P and G genotypes which is determined by the nucleic acid sequence relatedness of VP4 and VP7 respectively. Currently 28 P genotypes (P[1]-P[28]) and 19 G genotypes have been identified within group A, of which 12 G and 12 P genotypes have been recognised in HRVs (reviewed in Greenberg and Estes, 2009; Matthijnssens *et al*., 2008a; 2008b). The relationship between P genotypes and serotypes is not absolute, and a distinction between the two typing systems in the nomenclature is achieved by the use of brackets for the former. P[8] and P[4] genotypes correspond to two subtypes, P1A and P1B, which share some cross-reactive epitopes of P1 serotype and is representative of more than 91% of circulating HRV strains (Gorziglia *et al*., 1990; Santos and Hoshino, 2004).

The existence of a considerable number of rotaviral strains can be attributed to the ability of the virus to undergo constant genetic variation: antigenic drift (point mutations), antigenic shift (genetic reassortment), and genetic rearrangement or intragenic recombination (reviewed in Desselberger *et al*., 2001). Genetic reassortment, whether a consequence of mixed infections with co-circulating human strains or interspecies transmission, demonstrates serogroup exclusivity and is the major contributor to the evolution of novel or atypical phenotypes (Franco *et al*., 2006; reviewed in Palombo, 2003; Ramig, 1997). There is increasing evidence (genetic relatedness of human G5, G6, G8, G9 and G10 to animal RVs) to support zoonotic transmission, predominantly through genetic reassortment (reviewed in Kobayashi *et al*., 2003; reviewed in Martella *et al*., 2009; Matthijnssens *et al*., 2006). Transmission of

whole virus to humans which culminates in disease, albeit a rare occurrence due to the natural attenuation of animal viruses in human hosts, has been reported (De Leener *et al*., 2004; Nakagomi and Nakagomi, 2000).

The complexity of RV nomenclature has prompted recommendations for a universal classification of group A RV to be based on all 11 genomic RNA segments (Matthijnssens *et al*., 2008a; 2008b).

## 1.7 Epidemiology

Group A RV infections cause age-dependent diarrhoeal illness. Primary infection typically occurs after 3 months of age, and causes illness of the greatest clinical severity until approximately 35 months of age. RV infections persist through to adulthood manifesting as mild to predominantly asymptomatic clinical disease (Bishop, 1996).

The absence of significant diarrhoeal illness in neonates has been attributed to transplacental antibodies whilst an increased incidence in the elderly has been associated with an age-dependent decrease in immune status and innate defence (Bernstein, 2009; Morris and Estes, 2001).

RV outbreaks exhibit a seasonal pattern in temperate climates where the incidence of infection peaks during the winter months. Conversely, in tropical countries (and developing nations) RV outbreaks are distributed more evenly throughout the year (reviewed in Midthun and Kapikian, 1996). Neonatal RV infections are generally endemic in nurseries.

The incidence and distribution of strains with differing G and P sero/genotypes varies geographically during a RV season and with consecutive seasons. The distribution of RV serotypes over time supports a role for a selective pressure of serotype specific antibodies (reviewed in Franco *et al*., 2006). There are at least 42 different G/P strains with different serotype combinations (Dennehy, 2008). Of global dominance are genotypes P[8]G1, P[4]G2, P[8]G3 and P[8]G4 which account for nearly 90% of HRV strains worldwide (>90% within Australia), with P[8]G1 the predominant genotype (60-

80% of strains annually, >80% Australia) (Gentsch *et al*., 2005; Santos and Hoshino, 2005). G9 (P[6, 8 or 11]) has established itself as a global serotype of clinical importance accounting for 4.1% of infections worldwide (24.3 % within Australia), whilst [P8]G5, [P4 & P6]G8 and [P8 & P6]G12 are of regional significance (India, Brazil and Africa, respectively) (reviewed in Angel *et al*., 2007; Kirkwood *et al*., 2009; reviewed in O'Ryan, 2009).

RV infection is generally species-specific but the cross-species barrier is not absolute. RV strains of animal origin, in particular porcine, have been detected in the stools of children and is indicative of either (a) the direct transmission of whole virus between species or (b) genetic reassortment between animal and human strains *in vivo* during mixed infections (Mascarenhas *et al*., 2007; Palombo, 2003; Santos and Hoshino, 2005; Varghese *et al*., 2004).

## 1.8 Immunity to rotavirus

An understanding of the immune mechanisms governing the control and prevention of RV disease is incomplete and much debate still surrounds the true correlates of protection against clinical disease. Studies on the protective role of serum antibodies has generated conflicting results with questions raised as to whether these antibodies are directly involved in protection or merely markers of a past infection (Johansen *et al*., 1994). The development of mucosal immunity is presumed to be the most important marker of RV infection (Grimwood *et al*., 1988). From the vast data collected from studies of animal models and humans, the importance of both a humoral (in particular mucosal IgA) and cell-mediated (T cells and cytokines) immune response in the resolution of infection and protection against subsequent infections has been indicated. Uncertainty still remains as to whether RV infection affords homotypic and/or heterotypic protection.

There is still doubt as to whether the level of serum IgA is reflective of mucosal IgA and, consequently, whether it is a reliable measure of protection against RV infection and illness. Faecal RV IgA antibody levels bear a direct relationship with duodenal IgA antibody levels (Grimwood *et al*., 1988) and rises in intestinal IgA levels demonstrate

an intestinal neutralising antibody response (Coulson and Masendycz, 1990). Investigation of intestinal biopsy samples and sera identified serum ASCs, and not circulating IgA, as correlates of an intestinal IgA response (Brown *et al*., 2000; Yuan *et al*., 1996). More recent studies by Rojas *et al*. (2008) using both a flow cytometry assay and limiting dilution assay demonstrated that RV IgA memory B cells, correlated with concentrations of RV plasma IgA, and more importantly, correlated with IgA serological memory. The presence of IgM in acute phase sera serves as a marker for acute RV infection (Yu *et al*., 2005).

The following is an overview of the immunological responses to RV infection in vaccinated and naturally infected humans and animals.

### 1.8.1 Evaluation of the immune response from human trials

Natural RV infection and vaccination with oral live vaccines elicits a humoral (serum and intestinal) response in children which reduces disease severity upon reinfection (reviewed in Jiang *et al*., 2002). The identity of the correlates of protection against reinfection and the specificity of the humoral response is still under investigation as the data collected is often conflicting, and may be dependent on the intrinsic properties of both the host and virus strain. These factors are confounded by insufficient patient information and differences in reagents and assays used to measure the immunological response.

#### 1.8.1.1 Correlates of protection after natural infection of children

Longitudinal studies of naturally infected and vaccinated children have demonstrated that the primary infection is most often of greatest severity, and a minimum of two natural infections, either asymptomatic or symptomatic, provides cumulative protection against clinically severe diarrhoeal illness upon reinfection (Bernstein *et al*., 1991; Bishop *et al*., 1983; Fischer *et al*., 2002b; Glass *et al*., 2005b; Moulton *et al*., 1998; Velázquez *et al*., 1996; 2000; Ward and Bernstein, 1994).

Serum isotypes IgG and IgA and mucosal IgA have been reported as predictors of clinical protection in children naturally infected with RV. Both serum IgG and IgA have been identified as correlates of protection against reinfection, whilst protection against moderate to severe diarrhoeal illness strongly correlated with serum or mucosal IgA titres (Coulson *et al*., 1992; González *et al*., 2005; Hjelt *et al*., 1987; Matson *et al*., 1993; O'Ryan *et al*., 1994a; Velázquez *et al*., 2000) or serum IgG titres (Clemens *et al*., 1992; Yu *et al*., 2005).

#### 1.8.1.2 Correlates of protection after vaccination of children

The immune responses to candidate animal and HRV strains and animal-human reassortment vaccines have been investigated in both children and adults. In general, the correlation between post-vaccination RV antibody titres, particularly to IgA, and protection against reinfection is weaker and less apparent than for natural RV infection (Barnes *et al*., 2002; Bernstein *et al*., 1995; González *et al*., 2005; Svensson *et al*., 1987; Ward and Bernstein, 1994; 1995; Ward, 2009). Vaccine trials for RotaShield® and RotaTeq® failed to identify a clear correlation between total serum RV IgA and serotype-specific neutralising antibody titres with protection from reinfection (González *et al*., 2005; Vesikari *et al*., 2006a; Ward and Bernstein, 1995; Ward *et al*., 1997a). The monovalent vaccine Rotarix® has demonstrated a correlation between serum IgA titres and protection, which is heterotypic (particularly against G9 strains) and incomplete; suggestive of the role of other immune effectors in protection, or as discussed previously, poor correlation between serum and mucosal IgA levels (De Vos *et al*., 2004; Salinas *et al*., 2005; Vesikari *et al*., 2004). Where animal-human reassortment vaccines (RotaShield® or WC3-QV) were used, the majority of children developed neutralising antibodies to antigens of the parental strain and not to the G- or P-type antigens of HRV (reviewed in Jiang *et al*., 2002).

Overall, seroconversion rates and the level of protection afforded are greater when higher vaccine titres are used and when administered in multiple doses. Higher antibody titres and seroconversion rates are observed in older children in the absence of maternal antibody (reviewed by Jiang *et al*., 2002).

#### 1.8.1.3 Adult human challenge studies

A correlation between serum antibodies and protection from diarrhoeal illness has been observed in adult volunteers. Pre-existing serum neutralising antibodies to VP4 or VP7, not jejunal neutralising antibodies, protected adult volunteers from diarrhoeal illness upon homologous challenge with a virulent HRV (strain D) (Green and Kapikian, 1992; Kapikian *et al*., 1983). Further analysis of these samples revealed that resistance to symptomatic infection correlated most strongly with homotypic VP4/VP7 serum IgG titres (Yuan *et al*., 2009).

A similar study with the HRV CJN strain demonstrated that serum RV IgG and jejunal neutralising antibody correlated with protection from infection and disease, respectively (Ward *et al*., 1989). These results were in disagreement with the earlier work of the authors, whereby no correlate of protection afforded by serum antibodies was established (Ward *et al*., 1986).

#### 1.8.1.4 The role of $CD4^+$ and $CD8^+$ T cells in HRV infections

The production of RV-specific $CD4^+$ and $CD8^+$ T lymphocytes is typically age dependent, correlated with previous exposure, and present after primary infection (Jaimes *et al*., 2002; Offit *et al*., 1992; 1993). RV-specific IFN-γ but not IL-13 or IL-4 T cells were detected in adults, and the IFN response was demonstrated to be both transient and significantly greater for respondents with previous RV exposure (Jaimes *et al*., 2002; Malik *et al*., 2008; Rojas *et al*., 2003). Both regulatory T cell (Treg $CD25^+$) and transforming growth factor-beta (TGF-β) mediated regulatory mechanisms were responsible for modulating the T cell (IFN-γ $CD4^+$ and $CD8^+$) immune response to RV in adults but not children (Mesa *et al*., 2010). The preferential expression of the intestinal homing receptor α4β7 on RV-specific IFN-γ-secreting $CD4^+$ cells in adults was characteristic of intestinally primed T cells (Rojas *et al*., 2003; Rott *et al*., 1997).

Typically, studies using flow cytometry have demonstrated low or undetectable levels of circulating cytokine secreting (IL-[2, 4, 10, 13, 17] and IFN-γ) RV-T cells in children with acute RV gastroenteritis (Jaimes *et al*., 2002; Mesa *et al*., 2010). IFN-γ secreting

RV-specific $CD8^+$ but not $CD4^+$ T cells were detected in an ELISPOT assay of RV-infected children, whilst both subsets of cells were detected in healthy adults (Rojas *et al*., 2003). A significant IFN-γ response to RV candidate vaccine strain 116E and to NSP4 was observed in peripheral blood mononuclear cells (PBMC) of naturally infected children and RV exposed adults (Malik *et al*., 2008).

### 1.8.2 Evaluation of the immune response from animal studies

Immunological studies of animal models is preferential to the use of human subjects as the viral exposure history is known and can be controlled in the former (Conner *et al*., 1991). Unfortunately, a significant drawback in the use of animal models is the inability to fully mimic the immunologic responses observed in humans.

The two most widely studied animal models are the neonatal gnotobiotic piglet and the mouse. The gnotobiotic piglet is superior to the mouse model due to its similarities with humans in regard to gastrointestinal physiology, mucosal immunity and susceptibility to HRV diarrhoea (reviewed in Gonzalez *et al*., 2008). Gnotobiotic piglets are also devoid of maternal antibodies but are immunocompetent, enabling the assessment of true primary immune responses (Yuan *et al*., 1996). As illustrated below, the main effectors in disease prevention varies between the two models. Neutralising intestinal IgA levels specific for VP4 and VP7 are important in disease prevention in neonatal pigs, whilst a number of immune effectors (IgA, IgG, $CD4^+$ and $CD8^+$ cells) have been associated with protection and clearance in the mouse model (reviewed in Ward, 2003; reviewed in Yuan and Saif, 2002).

RV-specific intestinal IgA correlates with protective active immunity in both animal models. The levels of intestinal IgA ASC, serum (IgA) and intestinal (IgA and IgG) antibody titres were associated with protection in gnotobiotic piglets challenged with virulent and attenuated HRV Wa (Tô *et al*., 1998; Yuan *et al*., 1996; 1998). Immunisation of gnotobiotic piglets with inactivated HRV Wa failed to be protected from diarrhoeal illness or virus shedding upon challenge with the virulent form of the virus (Yuan *et al*., 1998).

Orally immunised mice displayed a significant correlation between intestinal and serum IgA levels (but not IgG) with protection against homologous or heterologous RV infection (Burns *et al*., 1996; Feng *et al*., 1994; 1997; McNeal *et al*., 1994). Homologous infection was much more efficient in inducing mucosal and systemic immune responses than heterologous infection in both the mouse and rabbit models (Conner *et al*., 1991; Feng *et al*., 1994). Ishida *et al*. (1997) delineated that heterologous and homologous infections in the mouse model were more efficient at inducing systemic and local immune responses, respectively. Protection to heterologous RV infection in the mouse model was dose and strain dependent and was consistent with the attenuation of heterologous viruses in foreign hosts (Feng *et* al., 1994).

Homologous challenge in IgA knockout mice demonstrated the compensatory role for other antibody isotypes, particularly intestinal IgG, in mediating protection from diarrhoeal illness (O'Neal *et al*., 2000). Contradicting other studies, passively transferred RV IgG provided protection in calves (Besser *et al*., 1988) and in macaques (Westerman *et al*., 2005).

Studies performed in the mouse model have demonstrated (a) the role of $CD8^+$ T cells in resolving primary infection and providing partial short-term protection against reinfection and (b) the role of $CD4^+$ T and B cells in the production of RV-specific intestinal IgA, the fundamental effector of long-term protection (Franco and Greenberg, 1995; 1999; Franco *et al*., 1997; Jiang *et al*., 2008; McNeal *et al*., 1995; 1997). The adoptive transfer of $CD8^+$ splenic lymphocytes from RV-infected mice passively protected suckling mice against RV challenge and mediated the clearance of chronic virus shedding in SCID and Rag-1 knockout mice in the absence of virus-specific antibodies (Dharakul *et al*., 1990; Jiang *et al*., 2008; Offit and Dudzik, 1990). The intestinal production of IL-17 and IFN-γ in mice has been associated, either directly or indirectly, with protection against RV shedding (Smiley *et al*., 2007). RV-infected neonatal mice demonstrated a much lower T-cell response, particularly for $CD4^+$ T cells, and poor induction of neutralising antibodies (Jaimes *et al*., 2005). The distribution and trafficking of RV-specific $CD8^+$ T cells and the expression of effector markers (CD107a/b and IFN-γ) is affected by the route of RV infection in the mouse model (Jiang *et al*., 2008).

### 1.8.3 The importance of neutralising antibodies and serotype-specific immunity in protection

Longitudinal studies in vaccinated and naturally infected children have indicated that the primary response is both heterotypic and/or homotypic. These results are often conflicting and the heterotypic response has been attributed to previous RV exposure or to the presence of maternal antibodies (Green *et al*., 1989). Barnes *et al*. (2002) failed to find a correlation between immunity and maternally derived antibodies in phase II trials of HRV vaccine candidate RV3.

Serum-neutralising antibody affords titre dependent homotypic and/or heterotypic protection against RV disease in children (Chiba *et al*., 1986; 1993; O'Ryan *et al*., 1994a; Rojas *et al*., 1995; Ward *et al*., 1992). Following a primary RV infection VP4 is the immunodominant neutralisation protein and the response is predominantly homotypic, with subsequent infections resulting in a broadening of the cross-reactive VP7 neutralising antibody response (Barnes *et al*., 2002; Chiba *et al*., 1986; Gorrell and Bishop, 1999; Matson *et al*., 1992; O'Ryan *et al*., 1994a; 1994b; Richardson *et al*., 1993; Rojas *et al*., 1995; Ward *et al*., 1993; Velazquez *et al*., 1996; 2000).

Very few studies have investigated the immunogenicity of the "non-neutralising" structural proteins (VP1, 2, 3, 6) and the non-structural proteins (NSP1-6) during RV infections of humans. Serum IgG responses to RV structural (VP2, 3, 4, 6, 7) and non-structural (NSP2 and NSP5) proteins were detected in naturally infected children, with maximal IgG responses to VP2, VP4 and VP7 present in the convalescent-phase sera, and IgG to VP6 typically present in the acute sera and persisting for more than 4 months (Richardson *et al*., 1993). The presence of serum VP6-specific antibodies correlated with protection in RV-infected children and adults, and vaccinated (RRV-TV) children (Johansen *et al*., 1999; Vizzi *et al*., 2005).

The natural attenuation of heterologous viruses, a consequence of restricted virus replication in enterocytes, has been associated with the notable absence of antibodies directed to RV non-structural proteins in children vaccinated with candidate virus strains (Svensson *et al*., 1987). Heterotypic antibody responses to RV non-structural

protein NSP2 was observed for both primary infection and reinfection in children (Kirkwood *et* al., 2008). The role of NSP4 in protective immunity has been widely investigated and will be described elsewhere (Section 1.10.6).

Studies of RV infection in animal models has generated conflicting results regarding the degree to which neutralising antibodies contribute to protection; with some studies favouring the role of transcytosed IgA antibodies and intracellular neutralisation (reviewed in Bernstein, 2006; Feng *et al*., 1997). Neutralising antibodies to the outer capsid proteins have been shown to confer both heterotypic and/or homotypic immunity in several animal models (Conner *et al*., 1991; Hoshino *et al*., 1988; reviewed in Midthun and Kapikian, 1996; Offit *et al*., 1986). Modified Jennerian vaccines induced both heterotypic and homotypic immunity in mice (Feng *et al*., 1997). The highest serological response observed in several species of naïve animals occurred upon challenge with a homologous virus and heterotypic responses were dependent on the relatedness of VP4, and more specifically VP7 serotypes, to the primary virus (Snodgrass *et al*., 1991).

An immunocytochemical staining assay used to quantitate the systemic and local immune response of adult mice infected with homologous virus to recombinant RV proteins demonstrated the level of antigenicity to individual proteins to be in the order VP6, VP4 and VP3 (Ishida *et al*., 1996). The detection levels for IgA were considerably lower than for IgG for all proteins assayed and the response to VP7, NSP2 and NSP4 were very low in sera and undetectable in stool samples (Ishida *et al*., 1996). Similar results were obtained using the gnotobiotic piglet model (Chang *et al*., 2001b).

Non-neutralising VP6, the major viral immunogen, evokes a protective immune response in the adult mouse model after (a) DNA vaccination with recombinant plasmids carrying the VP6 gene (Chen *et al*., 1997) (b) passive administration of VP6-specific polymeric IgA monoclonal antibodies secreted from “backpack tumor” transplants or intraperitoneal delivery to BALB/C mice (Burns *et al*., 1996; Feng *et al*., 2002) (c) mucosal virus-like particle (VP2/VP6) immunisation (O’Neal *et al*., 1997; 1998) and (d) intranasal immunisation of mice with chimeric VP6 or adjuvants (McNeal *et al*., 2002; 2006). The mechanism of protection elicited by VP6 or VP6/VP2 VLPs

may be mediated by $CD4^+$ T lymphocytes, $CD8^+$ T cells and cytokines (McNeal *et al*., 2006; 2007a; 2007b; Smiley, 2007).

The immunisation of neonatal gnotobiotic pigs with either VP2/VP6 VLPs or VP6 DNA vaccines failed to induce protection unless preceded by priming with attenuated HRV. These results suggest that protective immunity to RV diarrhoea in pigs depends not only on the location, magnitude and antibody isotype, but also on VP4 and VP7 mucosal IgA neutralising antibodies, and is potentially mediated by cross-reactive T helper cells (Yuan *et al*., 2000; 2001; Yuan and Saif, 2002; Yuan *et al*., 2005).

## 1.9 Vaccine development

The development of a vaccine against RV was initiated in the early 1980's utilising a traditional Jennerian approach involving animal RVs. Vaccine development has since gravitated to the use of animal/human RV reassortants (modified Jennerian approach) or alternatively, live attenuated HRV strains (non-Jennerian). The most notable example of the former is the tetravalent Rhesus rotavirus vaccine (RRV-TV) (RotaShield®; Wyeth Lederdale, Collegeville, PA), constructed of single-gene reassortants encoding the VP7 gene of HRVs of serotypes G1, G2 and G4, in a RRV genome backbone contributing serotype G3. RotaShield® was licensed in the U.S. in August 1998 and subsequently withdrawn from use 11 months later due to a four-fold increase in the incidence of intussusception (invagination of a portion of the small intestine into a more distal region) 1 week post vaccination (Zanardi *et al*., 2001). It has been suggested that this initial figure was overestimated and that the truer value was one excess case in 32,000 or less and that the risk of intussusception correlated with an increase in age (> 3 months) (Murphy *et al*., 2003; Simonsen *et al*., 2001). To date, the mechanism by which the vaccine causes intussusception is unknown, with four theories (the unique strain, the bolus dose, viral replication and NSP4) proposed (Huppertz *et al*., 2006; Offit *et al*., 2003). No causal relationship has been established between natural RV infection and intussusception, but an evaluation of anatomic changes (increased distal ileum wall thickness and lymphadenopathy) indicates possible mechanisms by which RV may cause this condition (Chang *et al*., 2001a; Robinson *et al*., 2004).

Two live oral RV vaccines, RotaTeq® (Merck and Co. Ltd, Whitehouse Station, NJ) and Rotarix® (RIX4414, GlaxoSmithKline, Rixensart, Belgium) have been recently licensed and included in the childhood immunisation schedule. RotaTeq® is a pentavalent bovine/human reassortant vaccine comprising a bovine (WC-3) genome backbone and VP7 and VP4 genes of epidemiologically important human RV serotypes G1-4 and P1A[8]. Rotarix® is based on a live attenuated HRV strain (89-12) that bears specificity for one of the most widely circulating RV strains, P1A[8]G1. Data from Rotarix® clinical trials demonstrated the efficacy of the vaccine in not only protecting against homotypic strains, but also other strains sharing the P[8] genotype (G1, G3, G4 and G9) and to a lesser extent fully heterotypic strains (which share neither P or G epitopes with the vaccine strain, eg P[4]G2) (De Vos *et al*., 2004; Linhares *et al*., 2006; Ruiz-Palacios *et al*., 2006, Vesikari *et al*., 2007; Ward *et al*., 2006; Ward and Bernstein, 2009). Results from clinical trials in both developing and industrialised countries have shown both vaccines to be highly efficacious against severe RV disease; > 80% efficacy for Rotarix® (reviewed in Bernstein, 2006; Ruiz-Palacios *et al*., 2006; Ward and Bernstein, 2009) and 98% efficacy for Rotateq® (Vesikari *et al*., 2006a; 2006b; 2009), although neither vaccine affords protection from reinfection.

Other vaccines currently under development, in clinical trials or recently licensed include (a) Lanzhou lamb rotavirus (LLR) (P[12]G10) licensed as a live attenuated vaccine for humans in China (Lanzhou Institute of Biological Products) (b) naturally attenuated asymptomatic human neonatal strains are being investigated as potential vaccine candidates in Australia (strain RV3; P2A[6]G3) and India (strains 116E (P[11]G9) and I321 ([P11]G10)) (Barnes *et al*., 2002; Bishop *et al*., 1983; Glass *et al*., 2005b) and (c) development of a hexavalent human-bovine (UK) reassortant vaccine with VP7 G1, 2, 3, 4, 8 and 9 serotype specificity for use in developing countries (Kapikian *et al*., 2005).

The use of attenuated live vaccines is not recommended for the immunocompromised and alternatives such as antiviral agents which block RV binding, penetration or replication are being considered. The preincubation of RV with various sialylated glycoproteins inhibited RV replication in mice and, further to this, human milk mucinous glycoproteins prevented virus replication in tissue culture and experimental

gastroenteritis in the mouse model (reviewed in Isa *et al.*, 2006; Yolken *et al.*, 1992). Other approaches to vaccine development could include parenteral vaccines (developed from expressed proteins, VLPs or inactivated virus), DNA vaccines expressing RV genes, and the use of novel adjuvants (eg CTB or STB) or delivery systems (Glass *et al*., 2005a; reviewed in Palombo, 2003).

The experience with Rotashield® demonstrated the importance of conducting parallel clinical trials in both developing and developed countries, the inclusion of larger numbers of participants in Phase III clinical trials (>50,000) and the need for post-licensure surveillance (reviewed in Bines, 2005; Glass *et al*., 2005a).

## 1.10 The non-structural protein NSP4

The non-structural protein NSP4 (formerly NS28) encoded by genomic segment 10 of Group A RVs is a 175 residue, 28 kDa, doubly glycosylated, ER resident transmembrane protein (Ericson *et al*., 1983). NSP4 is a multifaceted protein with a myriad of roles both in virus morphogenesis and pathogenesis (reviewed in Ball *et al*., 2005; Estes, 2003).

Initial phylogenetic analysis of 100 available NSP4 amino acid sequences revealed the presence of six distinct NSP4 genotypes, A-F, identified within Group A (reviewed in Araújo *et al*., 2007). Genotypes A (KUN, I), B (Wa, II) and C (AU-1, III) include animal and human viruses, genotype D (EW) consists solely of murine strains, whilst genotypes E and F demonstrate exclusivity for avian strains (Ciarlet *et al*., 2000; Cunliffe *et al*., 1997; Horie *et al*., 1997; 1999; Kirkwood and Palombo, 1997; Lin and Tian, 2003; Mohan *et al*., 2003; Mori *et al*., 2002a). Genogroup A can be further divided into sub-genotypes, A1 and A2, dependent on the presence or absence respectively, of glycine at position 140 (Deepa *et al*., 2007). The more recent work of Matthijnssens (2008a) involved the analysis of 430 nucleotide sequences which revealed 11 NSP4 genotypes, which were designated E (enterotoxin) 1-11.

RV strains of NSP4 genotypes A and B generally cluster according to their species of origin, suggestive of a constant pattern of evolution within species (Ciarlet *et al*., 2000).

Typically, the genes encoding VP6 and NSP4 of HRVs co-segregate, with SGI and SGII clustering within NSP4 genotypes A and B, respectively (Iturriza-Gòmara *et al*., 2003; Kirkwood *et al*., 1999). More recently, discordance between NSP4 and VP6 genetic linkage has been identified for strains infecting adolescents and adults (Tatte *et al*., 2010) and for a group A porcine RV (Ghosh *et al*., 2006).

### 1.10.1 Structure and membrane topology of NSP4

Two models for NSP4 topology, differing in the proposed identity of the membrane spanning hydrophobic domain, have been proposed. Three hydrophobic domains (designated H1-H3) are located at the amino terminal half of the protein and predictions of the proteins secondary structure have indicated that the hydrophobic regions are predominantly β-sheet (Chan *et al*., 1988). Bergmann *et al.* (1989) deduced from protease protection assays of truncated NSP4 peptides of bovine RV strain NCDV that; H2 (aa 30-54) traverses the membrane and functions as a membrane anchor sequence, H1 (aa 7-25) is oriented toward the lumen of the ER and H3 (aa 63-80) is associated with the cytoplasmic face of the membrane. Similar studies performed by Chan *et al.* (1988) suggested that H3 (aa 67-85) of SA11 NSP4 is the membrane-spanning domain, and both H1 (aa 7-21) and H2 (aa 28-47) are partly embedded in lipid bilayers oriented toward the lumen of the ER.

Two N-linked high mannose oligosaccharide residues ($Man_9GlcNAc$ and $Man_8GlcNAc$), proposed to be critical for the assembly function of NSP4, are located at asparagine (Asn) 8 and 18, within the H1 domain (Both *et al*., 1983; Estes and Cohen, 1989; Kabcenell and Atkinson, 1985). Glycosylation of the 20 kDa primary translational product occurs within the ER to yield the 28 kDa polypeptide. Residues 28-40 within the H2 domain are essential for glycosylation (Bergmann *et al*., 1989).

The sensitivity of the carbohydrate moieties to endoglycosidase H is suggestive that NSP4 is not retrieved from the Golgi by retrograde transport and is localised to the ER (Bergmann *et al*., 1989; Both *et al*., 1983). The mechanism by which NSP4 is retained in the ER is still unknown. NSP4 contains an uncleaved signal sequence, preceding the three hydrophobic domains, which targets the protein to the ER, most probably to a pre-

Golgi compartment (Both *et al*., 1983; Kabcenell and Atkinson, 1985). ER retention of NSP4 may be associated with its interaction with the ER-resident molecular chaperone calnexin or through binding to microtubules (Mirazimi *et al*., 1998; Xu *et al*., 2000). Recent studies with truncated C-terminal peptides suggested the presence of a novel ER retention motif between residues 85-123 (Mirazimi *et al*., 2003).

The carboxy terminal half of approximately 131 residues resides within the cytoplasm and contains all of the known biological properties and critical binding domains which are involved in the multifactorial roles of this protein (Figure 1.2).

NSP4 oligomerises into homo-dimers, tetramers and higher-ordered multimeric structures (based on tetrameric subunits) (Jagannath *et al*., 2006; Maass and Atkinson, 1990; Poruchynsky *et al*., 1991; Taylor *et al*., 1996). The oligomerisation domain, comprising residues 95-137, self-associates into a parallel, tetrameric α-helical coiled-coil stalk structure, with the hydrophobic core interrupted by three polar layers occupying *a* and *d*-heptad positions (Bowman *et al*., 2000; Taylor *et al*., 1996). Computational and biochemical analyses indicated that an extended coiled-coil domain (aa 85-135) directed the formation of NSP4 tetramers, whilst cooperation between the amphipathic α-helical domain (aa 73-85), the enterotoxin domain and the extreme C terminus effected a unique conformational state within the oligomer which promoted the stabilisation of the coiled-coil region and multimerisation of the cytoplasmic tail, resulting in the formation of high molecular weight structures (Hyser *et al*., 2008; Jagannath *et al*., 2006). Studies performed on the crystal structure and secondary structure of $NSP4_{95-146}$ mutants of different genotypes have indicated that residues 138-146 may be unstructured (Deepa *et al*., 2007).

Within the hydrophobic core are divalent cation binding sites, two Glu120 and four Gln123 residues, reported to be involved in stabilisation of the tetrameric structure (Bowman *et al*., 2000). Several salt bridges and C-H…O bonds are also involved in stabilisation of the coiled coil (Deepa *et al*., 2007). NSP4 forms oligomeric complexes with VP4 and VP7 in enveloped particles (Maass and Atkinson, 1990).

The identification of at least three intracellular NSP4 pools (a) at the ER (b) within ERGIC and (c) distributed in cytoplasmic vesicular structures associated with viroplasms in RV-infected cells, may begin to explain the multifactorial properties of this protein in virus morphogenesis and pathogenesis (Berkova *et al*., 2006). The proceeding discussion will investigate the role of each of these pools of NSP4 in greater detail.

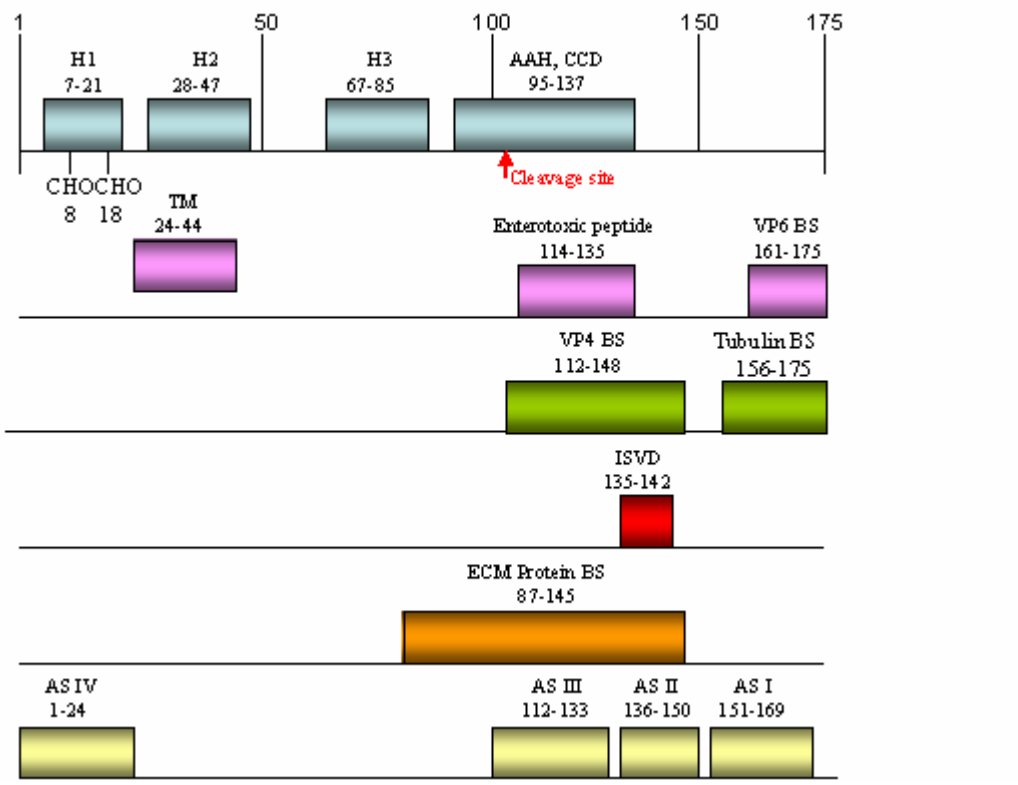


***Figure 1.2. Linear schematic of NSP4 functional domains.*** *Three hydrophobic domains, designated H1, H2 and H3, reside at the N terminus (Bergmann et al., 1989; Chan et al., 1988). Within the H1 domain are two glycosylation sites at Asn residues 8 and 18 (Both et al., 1983; Kabcenell and Atkinson, 1985). TM denotes the ER transmembrane domain. Cleavage at aa 112 generates a 7kDa NSP4 fragment (Zhang et al., 2000). BS denotes binding site. Within the cytoplasmic tail resides the majority of the NSP4 functional domains including; a coiled coil (CCD) amphipathic alpha helix (AAH) domain (Bowman et al., 2000; Taylor et al., 1996), enterotoxin domain (Ball et al., 1996), VP4 and VP6 BS (Au et al., 1993; O'Brien et al., 2000; Taylor et al., 1992; 1993; 1996), a tubulin BS (Xu et al., 2000), an interspecies variable domain (ISVD) (Horie et al., 1997; Lin and Tian, 2003) and an extracellular matrix protein BS (Boshuizen et al., 2004). Four antigenic sites (AS I-IV) were identified for NSP4 of avian RV strain PO-13 (Borgan et al., 2003). Figure adapted from Ball et al. (2005).*

### 1.10.2 Role of NSP4 in virus replication and morphogenesis

A unique step in RV morphogenesis is the budding of immature DLPs through the membrane of the ER. The binding of nascent DLPs, *via* VP6, to the ER membrane is mediated by NSP4, is enhanced in the presence of divalent cations ($Mg^{2+}$ and $Ca^{2+}$) and occurs with high affinity ($K_d$ of ~ 5 x $10^{-11}$ M) (Au *et al*., 1989; Meyer *et al*., 1989). Mutational analysis and direct binding experiments revealed that binding of VP6 to NSP4 occurred at the extreme carboxy terminus, between residues 156-175, in a conformation dependent manner, and that the integrity of the C-terminal methionine residue was critical for DLP binding (Au *et al*., 1993; Jagannath *et al*., 2006; O'Brien *et al*., 2000; Taylor *et al*., 1992; 1993; 1996). More recent studies have indicated that an additional binding site distant to the terminal carboxy region is required for DLP binding (Rajasekaran *et al*., 2008). Olivo and Streckert (1995) demonstrated that polymeric forms of the $NSP4_{160-169}$ synthetic peptide bound DLPs, whilst the monomeric form was inhibitory.

During the budding process, the DLPs, with associated NSP4, acquire an ephemeral envelope; proposed to be an extension of the ER membrane. Maturation of the virus particle requires the removal of the transient envelope and the concomitant addition of the outer capsid proteins VP4 and VP7. De-stabilisation of liposome membranes by full length NSP4 and $NSP4_{114-135}$ indicated a role for the protein in the removal of the envelope (Estes and Cohen, 1989; Tian *et al*., 1996a). Further to this, studies with the glycosylation-inhibitor tunicamycin demonstrated the requirement for glycosylation of NSP4 in envelope removal (Ericson *et al*., 1983; Petrie *et al*., 1983; Poruchynsky *et al*., 1991).

As discussed in Section 1.4.5, the location and mechanisms by which the outer capsid proteins are assembled onto DLPs is still under investigation. The presence of heteroligomers of NSP4, VP7 and VP4 within the ER of SA11-infected MA104 cells was suggestive that the final stages of maturation occurred as a reticular event (Maass and Atkinson, 1990; Poruchynsky and Atkinson, 1991).

Results obtained from studies on differentiated cell lines (Caco-2, HEK-293) are indicative of final RV assembly occurring as a post-reticular event; utilising a Golgi-independent pathway for NSP4 trafficking from the ER to lipid rafts at the PM. Several studies have demonstrated that newly synthesised RV infectious particles, NSP4 and VP4 interact with detergent-resistant lipid rafts at the PM (Cuadras and Greenberg, 2003; Cuadras *et al*., 2006; Sapin *et al*., 2002; Storey *et al*., 2007). Cuadras and Greenberg (2003) observed the presence of NSP4, in association with VP2, VP4, VP6 and VP7 at the lipid rafts of Caco-2 cells as early as 6 hours post infection, suggestive of a role for NSP4 as a transmembrane raft receptor for DLPs. Sapin *et al*. (2002) proposed that VP4 utilises rafts as a platform for virus assembly and that NSP4 is required for the final stages of virus maturation and release.

Circular dichroism revealed the association between NSP4 and $NSP4_{114\text{-}135}$ with cholesterol-rich model membrane vesicles which mimicked PM caveolae or caveolae-like microdomains (lipid rafts) (Huang *et al*., 2001; 2004). Further work by this group demonstrated that NSP4 associated with both the amino- and carboxyl-termini of the caveolae structural protein caveolin-1 (Mir *et al*., 2007; Parr *et al*., 2006). The binding of NSP4 to caveolin-1 was independent of glycosylation and occurred at the enterotoxin domain. The authors proposed that NSP4 may associate with cholesterol-caveolin-1 complexes, transporting NSP4 from the ER to the PM *via* caveolin-1 dependent cholesterol pathways, and bypassing the Golgi complex (Parr *et al*., 2006). ER trafficking of NSP4 or $NSP4_{114\text{-}135}$ to the PM may be required for the final stages of virus assembly and release, or secretion of the enterotoxin. The implications of the association between $NSP4_{114\text{-}135}$ and caveolin-1 in virus pathogenesis will be explained in further detail later (Section 1.10.3).

The association of NSP4 at the basolateral and/or apical membrane has been reported (Berkova *et al*., 2007; Boshuizen *et al*., 2004; Bugarcic and Taylor, 2006). The endogenous expression of EGFP-NSP4 in the inducible cell line HEK 293 caused a $Ca^{2+}$ dependent, sub-plasma membrane actin reorganisation through decreased phosphorylation of cofilin, an actin remodelling protein (Berkova *et al*., 2007). The authors proposed that stiffening of the basolateral sub-cortical network due to RV

infection provides a barrier which aids in directing nascent viral release from the apical membrane into the intestinal lumen.

Endogenously expressed NSP4 caused an increase in $[Ca^{2+}]_i$ which resulted in autophagosomal vesiculation of NSP4 and its subsequent association with viroplasms (Berkova *et al*., 2006). The vesicular form of NSP4 may (a) function as a lipid membrane scaffold for the formation of large viroplasms, (b) regulate the packaging of the RV genome and transcription through its association with VP6 or (c) trigger the budding process through the ER after VP6-NSP4 binding, and in association with the capping of viroplasms (Berkova *et al*., 2006; reviewed in Estes and Kapikian, 2009).

Silencing studies of RV proteins using siRNA is helping to elucidate the final stages of virus maturation. The silencing of NSP4 expression in RV-infected cells affects the intracellular distribution of viral proteins, mRNA synthesis, and viroplasm formation (Lopez *et al*., 2005; Silvestri *et al*., 2005). RNA silencing experiments have indicated a regulatory role for NSP4 in the expression of viral proteins (VP2, VP4, VP7, NSP2, NSP5 and NSP3) and the cellular redistribution of proteins VP7, VP4, VP2 and potentially VP6 (Lopez *et al*., 2005; Zambrano *et al*., 2008). With the exception of NSP3, which underwent a two-fold increase in expression levels, all other viral proteins experienced a reduction in expression levels upon silencing of NSP4 (Lopez *et al*., 2005). NSP4 has also been shown to indirectly contribute to RV particle-raft association by blocking the transit of particles in the ER and is required for the binding of viroplasms to the ER (Cuadras *et al*., 2006).

The formation of heterotrimeric complexes between NSP4, VP7 and VP4 had been associated with the budding of DLPs into the ER (Maas and Atkinson, 1990). But more recently, studies using siRNAs have demonstrated the sole requirement for NSP4 in the budding process (Lopez *et al*., 2005).

### 1.10.3 NSP4: the first identified viral enterotoxin

In 1996, Ball *et al.* identified NSP4 as the first viral enterotoxin. The intraperitoneal delivery of purified full-length NSP4 or a synthetic peptide, $NSP4_{114-135}$ (derived from strain SA11), induced dose- and age-dependent diarrhoea in CD-1 mice. Similarly, SA11 $NSP4_{112-175}$ caused diarrhoeal illness in mice; consistent with that of full-length NSP4 (Zhang *et al*., 1998; 2000). Higher doses of $NSP4_{114-135}$ and its derivatives were required to induce a diarrhoeal response equivalent to that of the full-length peptide; suggestive that this domain is either not representative of the complete active domain or that it fails to fold into the native conformation (Ball *et al*., 1996; Rajasekaran *et al*., 2008; Zhang *et al*., 2000).

NSP4 or peptides encompassing the enterotoxin domain of other Group A RVs (murine EW, porcine OSU and Gottfried, HRV Wa) have also elicited diarrhoeal illness in the mouse model (Horie *et al*., 1999; Hou *et al*., 2008; Sasaki *et al*., 2001; Zhang *et al*., 1998). $NSP4_{86-175}$ of HRV strain Wa administered at $DD_{50}$ evoked early (> 8 h.p.i.) onset diarrhoeal illness of a greater severity resulting in death of all ICR neonatal mice compared with mice inoculated with whole virus (onset of diarrhoeal illness > 24 h.p.i., no deaths) (Hou *et al*., 2008). NSP4 age-dependent induction of diarrhoeal illness in the mouse model has also been reported for Group B and C RVs (Ishino *et al*., 2006; Mori *et al*., 2001; 2002b; Sasaki *et al*., 2001).

The early onset of diarrhoea, prior to the detection of histologic changes within the mucosa following RV infection, has been associated with NSP4 and a number of pathways, as described below, have been proposed (Ball *et al*., 1996; reviewed in Estes *et al*., 2001; reviewed in Greenberg and Estes, 2009; Halaihel *et al*., 2000a; 2000b; Lundgren *et al*., 2000; Morris *et al*., 1999; Xu *et al*., 2000).

Ball *et al*. (1996) proposed that NSP4 was released from virus infected cells in a paracrine fashion, and bound to NSP4-specific cell membrane receptors on adjacent uninfected epithelial crypt cells. Integrins α1β1 and α2β1 have recently been identified as potential membrane receptors for the NSP4 enterotoxin (Seo *et al*., 2008). Electrophysiological analysis of intact mouse intestinal mucosa demonstrated that

$NSP4_{114-135}$ mobilisation of $Ca^{2+}$ from the ER potentiated cAMP-dependent chloride secretion with fluid loss (Ball *et al*., 1996). RV- or NSP4-induced diarrhoeal illness in cystic fibrosis transmembrane conductance regulator (CFTR) deficient mice demonstrated that calcium-mediated chloride secretion was distinct from the cAMP-dependent $Cl^-$ channel of crypt cells (Angel *et al*., 1998; Morris *et al*., 1999). The age-dependent induction of diarrhoeal illness by NSP4 or its active domain occurred through an age- and $Ca^{2+}$-dependent PM anionic halide permeability in intestinal epithelia *via* an as yet unidentified channel which is distinct from the CFTR (Morris *et al*., 1999). The absence of a direct, specific effect on chloride transport of $NSP4_{114-135}$ in rabbit brush border membranes provides further support for a signalling event which enhances net chloride secretion (Lorrot and Vasseur, 2006). Seo *et al.* (2008) demonstrated that integrin binding and signalling correlated with diarrhoea induction in neonatal mice. An NSP4 mutant ($E_{120}A$) which failed to bind to or signal through integrin α2 was attenuated in diarrhoea induction in neonatal mice.

Disruptions to $[Ca^{2+}]_i$ homeostasis may affect cell metabolism and/or gene expression, and activate signal transduction pathways which result in transactivation of genes regulated by a $Ca^{2+}$-responsive promoter element (Ball *et al*., 2005). NSP4 is known to alter intracellular $Ca^{2+}$ homeostasis by perturbing the plasma membrane and/or inducing $Ca^{2+}$ efflux from the ER to increase the cytosolic $[Ca^{2+}]$ in both mammalian and insect cells. The expression of NSP4 in COS-7 cells is responsible for the up-regulation of $Ca^{2+}$ binding proteins such as the ER-resident molecular chaperones (GRP, endoplasmin, BiP, calreticulun, ERP5) and the cytoplasmic translationally controlled tumour protein (TCTP) (Xu *et al*., 1998; 1999).

RV infection and $NSP4_{114-135}$ inhibit $Na^+$-D-glucose symporter (SGLT1) and $Na^+$-L-leucine transport into brush border membrane vesicles of rabbit enterocytes (Halaihel *et al*., 2000a; 2000b). Inhibition of the SGLT1 perturbs glucose and water absorption, resulting in a concomitant loss of fluid through the intestine. These results suggest another mechanism by which NSP4 could induce diarrhoea in the absence of histological damage to the intestinal mucosa following RV infection. Further to these studies, secreted NSP4 was shown to impair lactase enzymatic activity at the brush border membrane of RRV-infected Caco-2 cells (Beau *et al*., 2007). A reduction in

lactose digestive capacity was identified as an underlying cause, in addition to impaired villous morphology, for persistent diarrhoea following RV infection of colostrum deprived piglets (Mathai *et al*., 2008).

The binding of NSP4 to microtubules occurs at the extreme C-terminus (aa 120-175) and arrests ER-to-Golgi trafficking in a microtubule-dependent manner *in vivo* (Xu *et al*., 2000). The authors proposed that inhibition of the microtubule-mediated secretory pathway may decrease the activity of intestinal brush border disaccharidases in the PM and therefore contribute to the onset and/or persistence of diarrhoea.

Activation of the ENS by RV infection is mediated by a vasoactive intestinal peptide (presumptively NSP4) (Kordasti *et al*., 2004; Lundgren *et al*., 2000). The NSP4 associated increases in $[Ca^{2+}]_i$ may trigger the release of amines or peptides from endocrine cells of the gut which interact with dendrites or free nerve endings. The activation of nerve flexes ensues, resulting in the stimulation of water and electrolyte secretion of intestinal crypts, and culminating in diarrhoeal illness (Lundgren *et al*., 2000; reviewed in Lundgren and Svensson, 2001).

In contrast to the findings above which demonstrate diarrhoeal induction in the absence of significant histopathological damage, more recent studies by Hou *et al*. (2008) identified NSP4 ($NSP4_{86-175}$) associated histological changes (flattening and disorganisation of the villi, crypt cell proliferation and chronic inflammatory cell infiltrates) in the small intestine of neonatal mice with diarrhoeal illness. Similar histopathological changes, in the absence of appreciable crypt cell proliferation, were noted for mice infected with whole virus (Hou *et al*., 2008).

The activation of an NSP4-dependent signalling pathway which mobilises $Ca^{2+}$ from the ER resulting in chloride secretion, would require trafficking of endogenously expressed protein from the ER to the PM and/or release from the cell, in order to interact with surface signalling molecules on neighbouring uninfected cells.

A truncated form of NSP4 ($NSP4_{112-175}$) was detected in the supernatant of RV-infected mammalian and *Sf*-9 cells infected with recombinant NSP4 baculoviruses. This 7 kDa

cleavage product of NSP4 is most probably secreted into the extracellular medium of infected cells *via* a calcium-dependent, non-classical, Golgi-independent cellular secretory pathway utilising both the microtubule and actin microfilament networks, and in the absence of cell lysis (Zhang *et al*., 2000).

Both the apical and basolateral release of NSP4 from polarised, highly differentiated Caco-2 cells has been described (Boshuizen *et al*., 2004; Bugarcic and Taylor, 2006). Bugarcic and Taylor (2006) demonstrated that the secretion of a soluble form of NSP4 occurred preferentially at the apical surface of RV-infected Caco-2 cells and proceeded *via* a Golgi-dependent pathway which was distinct from that of virus release. It has been proposed that NSP4 may be secreted from cells in a complex with caveolin-1 (Bugarcic and Taylor, 2006; Estes and Kapikian, 2009; Parr *et al*., 2006).

Proteins or peptides released into the medium from RV-infected cells transiently mobilised the intracellular $Ca^{2+}$ of non-infected cells by a PLC-dependent efflux of $Ca^{2+}$ from the ER, and influx across the PM in association with microvillar F-actin disassembly (Brunet *et al*., 2000a). The apical, but not basolateral administration of NSP4 to polarised Madin-Darby canine kidney (MDCK-1) cells caused F-actin redistribution accompanied by a reduction in transepithelial electrical resistance (TER) and an increase in paracellular permeability (Tafazoli *et al*., 2001). The specificity of NSP4 for the apical membrane suggested the localisation of NSP4-specific receptors at this site. In contrast, the release of NSP4 from the basal side of infected enterocytes and its subsequent binding to extracellular matrix (ECM) proteins localised at the basement membrane of uninfected crypt cells could provide a mechanism by which NSP4 perturbs the calcium homeostasis in uninfected cells and induces fluid secretion (Ball *et al*., 2005; Boshuizen *et al*., 2004). Boshuizen *et al*. (2004) identified a region within the cytoplasmic domain of NSP4 (aa 87 to 145) which binds with the ECM proteins, laminin-β3 and fibronectin. Recent studies have demonstrated that NSP4 colocalises with integrin α2 at the basolateral surface of both RV-infected and neighbouring non-infected Caco-2 cells (Seo *et al*., 2008).

The association between NSP4 and caveolin-1 may help elucidate how extracellular NSP4 initiates intracellular signalling events. Caveolin-1 forms a scaffold to organise

key molecular components of $Ca^{2+}$ regulation and signalling ($Ca^{2+}$ ATPase, $IP_3$ receptors, G proteins and calmodulin) to the caveolae at the PM. Caveolae compartmentalise as much as 50% of cellular $PIP_2$ and is the site of $PIP_2$ hydrolysis (reviewed in Parr *et al*., 2006). An association between NSP4 and each of these molecules has already been established and all have been reported to be of integral importance in intracellular calcium mobilisation events. The authors have proposed that endogenously expressed NSP4 may transport to, and interact with, caveolae membranes and that exogenously added NSP4 may be targeted to G-proteins localised to caveolae (Parr *et al*., 2006).

Further support for the interaction between NSP4 and membrane receptors was provided by Huang *et al.* (2004) who demonstrated that $NSP4_{114-135}$ does not induce membrane disruption or disorganisation of model membranes at physiological concentrations. The association between model membranes and NSP4 or $NSP4_{114-135}$ resulted in an increase in the α-helical content for both NSP4 and its active domain. The authors proposed that structural conformational changes either exposed the receptor-binding domain of NSP4 or relocated the receptor-binding domain to a more advantageous position for binding to the cell receptor (Huang *et al*., 2004).

### 1.10.4 The cytopathic effects of NSP4 and its role in intracellular $Ca^{2+}$ mobilisation

Three defined stages of $Ca^{2+}$ mobilisation intimately associated with viral replication were identified and subsequently applied to explain the progressive increase in $[Ca^{2+}]_i$ due to RRV infection of Caco-2 cells (Brunet *et al*., 2000a). During the first hours of infection the increase in $[Ca^{2+}]_i$ is associated with an escalation in $Ca^{2+}$ permeability at the PM. At a late stage of infection, changes in $Ca^{2+}$ homeostasis is attributed to both extracellular $Ca^{2+}$ influx and a PLC-dependent efflux of $Ca^{2+}$ from the ER. Transient increases in the $[Ca^{2+}]_i$ of uninfected cells induced by peptides (presumptively identified as NSP4) released into the culture supernatant were associated with a PLC-mediated efflux of $Ca^{2+}$ from the ER and by $Ca^{2+}$ influx across the PM (Brunet *et al*., 2000a). The effects of whole virus and NSP4 on cellular calcium homeostasis will be discussed further in Chapter 4.

The mechanisms by which NSP4 mobilises intracellular $Ca^{2+}$ appears to be dependent on whether the protein is added exogenously to cells (enterotoxic effect) or transiently expressed in transfected cells (cytotoxic effect).

The exogenous addition of NSP4 or regions encompassing its active domain (114 to 135) to mammalian and *Sf*-9 cells elicits an increase in $[Ca^{2+}]_{i.}$ which is associated with a PLC-dependent release of calcium from the ER (Dong *et al*., 1997; Tian *et al*., 1995; Zhang *et al*., 1998; 2000). Dong *et al*. (1997) demonstrated that the application of NSP4 to fully differentiated HT29 cells initiated a PLC-dependent signalling pathway which elevated $IP_3$ production and induced $Ca^{2+}$ mobilisation *via* both intracellular $Ca^{2+}$ release from the ER and extracellular $Ca^{2+}$influx. The changes in calcium homeostasis upon the addition of truncated peptide to *Sf*-9 cells, in comparison with the full length protein was reduced because the peptide failed to (a) represent the functional domain in its entirety, (b) adopt the correct conformation or (c) incorporate other remote domains in NSP4 which may be critical for eliciting changes in $[Ca^{2+}]_i$ (reviewed in Tian *et al*., 1996b).

The endogenous expression of NSP4 or its functional domain has been associated with the cytotoxic properties of the protein. The expression of NSP4 (or truncated variants) in *Sf*-9 and mammalian (COS-7, HEK 293) cells caused an increase in $[Ca^{2+}]_i$; the result of a PLC-independent mobilisation of $Ca^{2+}$ from a subset of the thapsigargin-sensitive compartment (ER) (Berkova *et al*., 2003; Tian *et al*., 1994; 1995; Xu *et al*., 1999; Zhang *et al*., 1998; 2000).

As to whether the cytotoxic effect is solely due to changes in intracellular calcium homeostasis or changes to the PM integrity have not yet been resolved. The changes to $[Ca^{2+}]_i$ may be attributed to NSP4-associated mobilisation of calcium from the ER and/or activation of $Ca^{2+}$ channels at the plasma membrane. The expression of NSP4 in prokaryotic and eukaryotic cells has resulted in PM disruption and loss of cell viability (Browne *et al*., 2000; Guzman and McRae, 2005a; 2005b; Mohan *et al*., 2000; Newton *et al*., 1997; Tian *et al*., 1994). Newton *et al*. (1997) identified an amphipathic α-helical region (aa 55-72) in NSP4 which was associated with PM de-stabilising activity in MA104 cells. Similarly, Browne *et al.* (2000) demonstrated that NSP4 expression

disrupted bacterial membranes and the authors localised the membrane destabilising activity (MDA) domain to residues 48-91. NSP4 of Group B HRVs also exhibit cytotoxic effects, a consequence of membrane compromise, when expressed in *E. coli* or when added exogenously to MA104 or BHK cells (median cytotoxic concentration ($TC_{50}$) = 323 ng) (Guzman and McCrae, 2005a; 2005b).

Both NSP4 and $NSP4_{114-135}$ have been shown to possess membrane destabilisation activity which is specific for liposomes and ER vesicles, but not for PM vesicles (Halaihel *et al*., 2000b; Lorrot and Vasseur, 2006; Tian *et al*., 1996). NSP4 induced membrane destabilising activity at the ER caused an efflux of $Ca^{2+}$ into the cytosol and an elevation of intracellular calcium levels; the MDA was localised to the enterotoxin domain (Tian *et al*., 1995; 1996a). In contrast, $NSP4_{114-135}$ failed to cause membrane disruption of model membranes or bacterial membranes (Browne *et al*., 2000; Huang *et al*., 2004).

The mechanism(s) by which intracellular NSP4 alters ER permeability to $Ca^{2+}$ is still unknown and several models have been proposed. NSP4 may regulate or function as a $Ca^{2+}$ channel in the ER membrane (Greenberg and Estes, 2009; Tian *et al*., 1996b). Alternatively, the cytotoxic domain of NSP4 may cause ER membrane destabilisation or increase $Ca^{2+}$ leakage from the ER by co-translational insertion into the ER membrane (Greenberg and Estes, 2009; Tian *et al*., 1996a; 1996b).

### 1.10.5 Virus virulence

Studies of human and porcine reassortant RVs in the gnotobiotic pig model have demonstrated that genes encoding VP3, VP4, VP7 and NSP4 are virulence genes associated with diarrhoea induction (Hoshino *et al*., 1995). The correlation between mutations in the NSP4 sequence (particularly within the vicinity of the enterotoxigenic domain) and virulence phenotype is still under debate. Consequently, it is uncertain whether virulence is associated with a single protein or the concerted effort of more than one.

NSP4 sequence comparisons between genotypes A, B and C demonstrate that residues 1-130 are highly conserved and that variability increased towards the carboxy terminus of the enterotoxic peptide region (aa 114 to 135) (Horie *et al*., 1997). The interspecies-variable domain (ISVD) from aa 135 to 141 is the least conserved and shows species-specific divergence (Cunliffe *et al*., 1997; Horie *et al*., 1997; 1999; Mohan and Atreya, 2000; Mohan *et al*., 2000; Zhang *et al*., 1998).

Mutations within the N-terminus, ISVD, the enterotoxin domain and cytotoxic domain (aa 55-72) have been associated with (a) the attenuation or abrogation of cytotoxicity and diarrhoea-inducing ability of NSP4 (b) affected DLP binding and (c) altered virus virulence, *in vivo* (Ball *et al*., 1996; Huang *et al*., 2004; Jagannath *et al*., 2006; Kirkwood *et al*., 1996; Mohan *et al*., 2000; Newton *et al*.,1997; Rajasekaran *et al*., 2008; Zhang *et al*., 1998).

Single amino acid substitutions within the ISVD at residues 120, 131, 139 or 140 have been shown to reduce the diarrhoeagenic activity of NSP4 in the mouse model (Ball *et al*., 1996; Huang *et al*., 2004; Jagannath *et al*., 2006; Seo *et al*., 2008). The substitution Tyr131→Lys blocked the inhibitory effects of the $NSP4_{114-135}$ peptide on the SGLT1 (Halaihel *et al*., 2000b). Attenuation of the cytotoxic effects of endogenously expressed NSP4 (SA11) in *Sf*-9 cells was observed upon the replacement of His47, a highly conserved residue within all mammalian strains, with Asn (Tian *et al*., 2000).

Sequence comparisons of NSP4 of attenuated or avirulent strains and virulent parental strains afforded an opportunity to elucidate mutations which might alter viral phenotype. The results obtained have been conflicting and propose that structural changes rather than sequence variability may be of significance. Sequence and biological activities of NSP4 from virulent and attenuated porcine RV strains were compared and the results demonstrated that mutations within the region aa 131-140, potentially associated with residues 135 and 138, altered the virulence phenotype, including abrogation of the diarrhoea-inducing ability and calcium mobilisation of the protein (Zhang *et al*., 1998). Amino acid sequence comparisons of virulent and attenuated Group C porcine RV (Cowden strain) failed to identify mutations within this region (Chang *et al*., 1999). Similarly, sequence comparisons between virulent human,

feline and murine RV strains and their attenuated counterparts failed to demonstrate a correlation between virulence phenotype and mutations within residues 135-141 (Angel *et al*., 1998; Chang *et al*., 1999; Ciarlet *et al*., 2000; Mohan and Atreya, 2000; Oka *et al*., 2001; Ward *et al*., 1997b).

Mohan *et al*. (2000) stated that the mutations selected in NSP4 are dependent on whether NSP4 is expressed in the absence or presence of other viral mutations. The expression of Wa NSP4 in Caco-2 cells selects for mutations within the carboxyl domain of the protein, of which Pro138 has been implicated as an important determinant of cytotoxicity (Mohan *et al*., 2000). Further to this, Mohan *et al*. (2003) documented that the attenuation phenotype does not involve the NSP4 cytotoxic domain, perhaps due to the suppression of its cytotoxic activity by other rotaviral proteins.

The presence of asymptomatic strains in neonates also afforded an opportunity to investigate potential regions of NSP4 which might be involved in the abrogation of the pathogenic and virulent properties of the protein. Sequence studies of HRV strains of genotypes P[6]G3 and P[6]G4 demonstrated 1 (aa 135) and 4 (aa 82, 114, 138, 169) conserved substitutions respectively, between asymptomatic and symptomatic children (Kirkwood *et al*., 1996; Pager *et al*., 2000). Mascarenhas *et al*. (2007) identified the presence of isoleucine at aa residue 135 in both symptomatic and asymptomatic children infected with [P6] viruses. Additional data procured from NSP4 gene sequence analysis of RV strains obtained from asymptomatic neonates (nursery strains) and children afflicted with diarrhoea failed to identity changes which could account for differences in clinical outcome (Cunliffe *et al*., 2002; Horie *et al*., 1997; Lee *et al*., 2000). Taken together, these results could be suggestive of genotype specificity (VP4 or NSP4) in clinical outcome. In addition, the role of host, rather than viral factors, in asymptomatic disease has been proposed (Estes and Cohen, 1989).

Lin and Tian (2003) conducted a comprehensive analysis of all non-redundant NSP4 gene sequences entered into GenBank. They discovered that of the 284 sequences analysed, only fourteen residues are completely conserved across all five genogroups, inclusive of two glycosylation sites (Asn8, Thr10, Asn18, Thr20), a transmembrane segment (Leu40), the VP4 binding domain (Leu127, Glu147) and enterotoxin domain

(Lys55, Asn77, Ile113, Glu120, Glu122, Gln123, Leu126). Glu120 and Gln123 had previously been identified as $Ca^{2+}$ ligands within the tetrameric coiled-coil domain (Bowman *et al*., 2000). Overall, Lin and Tian (2003) failed to identify a specific amino acid or sequence motif within NSP4 that segregated with the virulence property of RV.

The diarrhoea-inducing and DLP-binding properties of NSP4 are dependent on a structurally and functionally overlapping conformational domain, formed by cooperation between the N- and C-terminal regions of the cytoplasmic tail (Jagannath *et al*., 2006). More recent studies by this group demonstrated that the flexible C terminus was a major determinant of the structural integrity (conformational and multimerisation) and biological properties (trypsin resistance, thioflavin binding, diarrhoea-induction and DLP binding) of the protein (Rajasekaran *et al*., 2008).

### 1.10.6 The immune response to NSP4 and a potential role in vaccine development

Antibody to NSP4 can reduce the severity and incidence of homotypic and heterotypic RV-induced diarrhoeal disease in neonatal mice (Ball *et al*., 1996; Choi *et al*., 2005; Hou *et al*., 2008; Yu and Langridge, 2001). Ball *et al*. (1996) demonstrated that antibodies to $NSP4_{114-135}$ reduced diarrhoeal disease in the mouse model. Dams vaccinated with SA11 $NSP4_{114-135}$ provided passive protection to pups from challenge with RV SA11 (Ball *et al*., 1996). The oral administration of $NSP4_{114-135}$-specific antibody to pups infected with SA11 greatly reduced subsequent diarrhoeal disease (Ball *et al*., 1996). NSP4-specific antibody administered prior to or during diarrhoeal illness prevented or reduced the severity of illness respectively, in neonatal mice challenged with either RV or $NSP4_{86-175}$ (Hou *et al*., 2008). Contrary to these results, Ishida *et al.* (1997) demonstrated that humoral immunity to NSP4 did not appear to play a major role in protection following both heterologous and homologous RV infection in the mouse model. Studies performed in the gnotobiotic piglet model demonstrated that antibodies to NSP4 did not play a significant role in protection against infection or diarrhoea upon challenge with RV (Yuan *et al*., 2004a).

Gut-associated lymphoid tissue (GALT)-targeted Toxin B (TB) subunits of Cholera (CTB), *S. dysenteriae* (STB) and *Ricinus communis* (RTB) possess strong mucosal adjuvant qualities for the stimulation of humoral antibody and cellular immune responses, making them ideal candidates for ligand-mediated delivery of immunodominant domains of viral enterotoxins/proteins. Immunisation of mice with GALT-NSP4 adjuvants evokes a protective humoral (systemic and mucosal) and cellular immune response (Choi *et al*., 2005; 2006a; 2006b; Kim *et al*., 2004; Yu and Langridge, 2001). The mucosal adjuvant properties of both full-length NSP4 and $NSP4_{112-175}$ have recently been recognised (Kavanagh *et al*., 2010).

The CTB-$NSP4_{114-135}$ antigen generated protective humoral and secretory antibodies against NSP4 in orally immunised mice challenged with RV (Yu and Langridge, 2001). A dominant Th1 response, as determined by cytokine levels (IL-2, IL-4, IFN-γ), Ab titres (IgG1 and IgG2a) and T-lymphocyte subpopulations, was observed for Toxin B-$NSP4_{86-175}$ and $NSP4_{114-135}$ fusion proteins (Choi *et al*., 2005; 2006b; Kim *et al*., 2004; Yu and Langridge, 2001). Higher serum IgG titres were reported for the $NSP4_{86-175}$ adjuvants suggesting that additional conformational or linear immunogenic epitopes beyond $NSP4_{114-135}$ were required to increase the protective efficacy of antibody responses (Kim *et al*., 2004). Immunisation of mice with the NSP4 fusion peptides generated greater anti-NSP4 IgG and IgA titres than immunisation with the peptide alone, demonstrative of the enhanced immunostimulatory capacity afforded by the subunit B peptide (Choi *et al*., 2005; 2006a; 2006b; Kim *et al*., 2004; Yu and Langridge, 2001). A reduction in the duration and severity of diarrhoeal illness was observed in RV-challenged pups born to dams orally inoculated with CTB-$NSP4_{114-135}$ or STB-$NSP4_{86-175}$ fusion antigens (Choi *et al*., 2005; Yu and Langridge, 2001). The effects were heterotypic and/or homotypic.

NSP4 and $NSP4_{114-135}$ elicit both humoral and cell-mediated immune responses in humans (Johansen *et al*., 1999; Ray *et al*., 2003; Rodríguez-Díaz *et al*., 2005). A Th-1 response, presenting as an increased production of IFN-γ or IL-2, to either NSP4 or a synthetic peptide $NSP4_{114-134}$ was detected in naturally infected children and adults (Johansen *et al*., 1999; Malik *et al*., 2008). The degree to which NSP4 elicits a humoral

response, in particular a significant mucosal response, in humans is still in contention and will be discussed further in Chapter 3.

As to whether antibodies directed against NSP4 afford heterotypic protection is still uncertain. Studies of naturally infected or vaccinated children demonstrated that the antibody response to NSP4 was homotypic and/or heterotypic. Monospecific sera raised against NSP4 of a Group B HRV were shown to be cross-reactive with Group A NSP4 and dependent on the conformational integrity of the epitope(s) (Guzman and McCrae, 2005a). IgA and IgG antibody responses to the NSP4 genotypes A, B and C were both heterotypic and/or homotypic in the sera of naturally infected and vaccinated children (Ray *et al*., 2003; Yuan *et al*., 2004b). Results obtained by Rodríguez-Díaz *et al*. (2005) suggested that IgG recognition of NSP4 of SA11 (genotype A) and Wa (genotype B) in adults and children convalescing from a RV infection was not always heterotypic.

Studies using gnotobiotic calves and piglets demonstrated that the antibody response to NSP4 was species-specific rather than genotype-specific (Yuan *et al*., 2004a). The heterotypic responses to NSP4 observed in naturally infected and vaccinated children may be attributable to maternal antibody interference and previous exposure to wild-type RV infection.

Little is known about the NSP4 antigenic epitopes. Borgan *et al.* (2003) demonstrated that MAbs directed against the avian strain PO-13 cross-reacted with avian but not mammalian NSP4s, despite the highly conserved sequence of the enterotoxin domains between the PO-13 and mammalian NSP4s (50-59%). The authors also identified two immunodominant regions, AS I (aa 151-169) and AS II (136-150) within the cytoplasmic tail of NSP4 of the avian RV strain, PO-13. Yuan *et al*. (2004a) identified the region between aa 131-141 as the immunodominant region.

## 1.11 Research aims

The major aims of this project are to investigate the immunological and biochemical characteristics of the RV non-structural protein NSP4 of two prototype HRV strains, RV4 and RV5.

To achieve these goals, recombinant NSP4 representative of each strain will need to be expressed and purified. General molecular biology techniques will be employed to produce recombinant baculovirus transfer vectors containing the NSP4 gene for each strain. The NSP4 gene will be inserted either upstream or downstream of a hexa-histidine ($His_6$) sequence.

The recombinant baculovirus transfer vectors will then be used to produce recombinant NSP4-baculoviruses *via* homologous recombination with linearised BacPAK 6 viral DNA in *Spodoptera frugiperda (Sf*-21) insect cells.

The Baculovirus Expression Vector System (BEVS) will be employed to produce C- and N- terminal $His_6$-NSP4 fusion proteins. The optimal conditions for generating high yields of the cytotoxic protein will be investigated. Immobilised metal affinity chromatography (IMAC) using an imidazole gradient will be used for the purification of the recombinant proteins.

The purified recombinant NSP4 proteins will be used as the coating antigen in the development of an indirect enzyme linked immunosorbent assay (ELISA) for the detection of NSP4-specific immunoglobulins (IgG and IgA). The ELISA will then be used to assess the isotype-specific responses to NSP4 in the sera of naturally infected and vaccinated children. The contribution of the proximal location of the $His_6$-tag in detecting NSP4-specific antibodies will also be investigated.

Spectrofluorimetric and microscopic methods will be developed for monitoring RV infection and NSP4-induced changes to the intracellular calcium homeostasis of single cells and mammalian cell populations. The efficacy of two distinct systems; (a) a calcium responsive synthetic dye (fluo-3) and (b) a calcium-sensitive fusion peptide

(flash pericam) for detecting changes to the intracellular calcium concentration will be investigated.

Human sera positive for α-NSP4 (as determined *via* ELISA) will be used to demonstrate whether neutralisation of NSP4 can reduce its cytotoxic effects.

# 2

# Production of recombinant-histidine tagged NSP4 proteins

## 2.1 Introduction

Baculoviruses (family *Baculoviridae*) are double-stranded circular DNA viruses, pathogenic to many invertebrate species, particularly those of the order *Lepidoptera*. Of relevance to this report is the baculovirus *Autographa californica* multiple nuclear polyhedrosis virus (AcMNPV) isolated from the alfalfa looper (Miller, 1988).

The baculovirus AcMNPV genome is 134 kbp in length and as a consequence of its size, it is not possible to directly clone foreign DNA within its sequence (Ayres *et al.*, 1994). The gene of interest is firstly cloned into a baculovirus transfer vector within the polyhedrin gene, and under the transcriptional control of the polyhedrin promoter. The introduction of foreign DNA into the baculovirus genome occurs *via* homologous recombination between the baculovirus genome and the baculovirus transfer vector. Co-transfection of *Spodoptera frugiperda* (*Sf*) cells enable the AcMNPV flanking sequences of the baculovirus transfer vector to recombine with the homologous sequences of the virus genome, allowing the transfer of the expression cassette to the polyhedrin locus, resulting in an occluded-negative (or polyhedrin-negative) virus containing the gene of interest (King and Possee, 1992; Kitts and Possee, 1993). Once the recombinant virus has been identified, expression of the recombinant protein, under the transcriptional control of the powerful polyhedrin promoter, is initiated.

The baculovirus expression vector system (BEVS) provides most of the post-translational processing events which occur in mammalian cells; inclusive of N-glycosylation required for NSP4 (Shuler *et al*., 1995). Native NSP4 proteins contain two high mannose glycosylation sites at amino acid residues 8 and 18 (Both *et al.*, 1983; Estes and Cohen, 1989; Kabcenell and Atkinson, 1985). The glycosylation process differs in insect cells from that of mammalian cells, with the former generating high mannose, unbranched sugar side-chains, devoid of terminal core oligosaccharide trimming and processing (most notably transferral of glucosamine-galactose and sialic acid residues) of the latter (reviewed in King and Possee, 1992; Miller, 1988). This difference is evidenced in denaturing polyacrylamide gels whereby the proteins produced in insect cells move with a greater mobility.

Four recombinant NSP4 baculoviruses bearing either N- or C- terminal hexa-histidine ($His_6$) sequences were produced using the BEVS in this study. The inclusion of a poly(histidine) tag at either the N- or C-termini of a protein, a method developed by Hochuli *et al.* (1988), enables the highly selective purification of the desired protein from cell lysates using immobilised metal affinity chromatography (IMAC). The antigenic recombinant N- and C-terminal $His_6$ NSP4 fusion proteins, of prototypic human rotavirus strains RV4 and RV5, were successfully expressed in *Sf*-21 cells and subsequently purified using nickel-nitrilotriacetic (Ni-NTA) immobilised metal-affinity chromatography. These proteins were then used in the development of an Enzyme Linked Immunosorbent Assay (ELISA) and in intracellular calcium mobilization studies.

## 2.2 Methods

### 2.2.1 General molecular biology techniques

All chemicals were of analytical grade and purchased from Sigma unless noted otherwise. Sterile MilliQ water purified with a MilliQ system to 18.2 MΩ·cm at 25°C was used exclusively in all buffer and media formulations and in enzyme reactions.

#### 2.2.1.1 DNA purification and cloning

DNA purification and general cloning techniques were performed in accordance with Sambrook and Russell (2001). Where commercial DNA purification kits were employed, the methodology was as per the manufacturer's specifications.

All enzymes (restriction endonucleases, T4 DNA ligase and Shrimp Alkaline Phosphatase (SAP)), were purchased from Promega unless reported otherwise, and used in accordance with the manufacturers guidelines.

#### 2.2.1.2 Polymerase Chain Reaction (PCR) of cDNA

With the exception of the primers and template DNA, all components of the PCR reaction were purchased from Promega.

A 50 µL standard reaction volume was used for all PCR reactions and comprised the following components; 2.5 mM $MgCl_2$, 1 X PCR Reaction Buffer, 0.2 mM dNTPs, 50 pmol of each primer, 2.5 U *Taq* DNA polymerase, 100 ng template DNA, made up to volume with MilliQ water. The amplification profile was customised for each reaction, and recorded in detail in the relevant sections of this chapter.

All PCR amplicons and endonuclease digested DNA were purified using the AppliChem DNA Isolation Kit (AppliChem GmbH) when used for cloning.

#### 2.2.1.3 Agarose gel electrophoresis

All DNA samples to be analysed were combined with 6 X gel loading buffer (0.25% (w/v) bromophenol blue, 40% (w/v) sucrose in Tris-EDTA [TE (10 mM Tris-HCl, 1 mM EDTA; pH 8.0)] and fractionated in a 1% (w/v) agarose gel containing 0.4 µg/mL ethidium bromide. The samples were electrophoresed at 120 V for approximately 90 minutes in a flat-bed gel apparatus (Bio-Rad Mini-sub®) in 1 X TBE (89 mM Tris, 89 mM Boric acid, 2 mM EDTA; pH 8) buffer.

The DNA bands were visualised under UV light and the quantity of DNA estimated by comparison of the relative intensities of sample DNA with the 1.6 Kb band of a 1 Kb DNA Standard Marker (Invitrogen).

#### 2.2.1.4 Transformation of competent *E. coli* JM109 cells

Competent *E.* coli JM109 cells were prepared using the rubidium chloride method provided by the Northwest Fisheries Science Centre (http://micro.nwfsc.noaa.gov/protocols/rbcl.html).

Ligation reactions were conducted at 4°C for 24 hours with T4 DNA ligase and 2 X Rapid Ligation Buffer (Promega). The protocol applied was as per the pGEM®-T Easy Vector System Manual (TM042, Promega).

JM109 cells were transformed with either plasmid DNA or ligation reactions using the method adapted from the *E. coli* Competent Cells Technical Bulletin (TB095, Promega). In brief, a volume not exceeding 10 µL of DNA was added to 100 µL of competent JM109 cells (>$10^6$ cfu/µg) within 15 mL polypropylene culture tubes (Falcon®). The cells were incubated on ice for 10 minutes, heat shocked for 45 seconds at 42°C and again held on ice for 2 minutes. The transformation components were added to 900 µL SOC complete medium (2% (w/v) Bacto®-tryptone, 0.5% (w/v) Bacto®-yeast extract, 10 mM NaCl, 2.5 mM KCl, 20 mM glucose and 20 mM $MgCl_2$; pH 7.0) and incubated at 37°C for 1 hour with constant agitation. Upon the completion of the incubation period, 100 µl of culture was plated onto LB/Agar plates (10% (w/v)

tryptone, 5% (w/v) yeast extract, 5% (w/v) NaCl and 15% (w/v) agar; pH 7.5) supplemented with ampicillin (100 µg/mL) and incubated overnight at 37°C. When blue/white screening was employed, the surface of the plates were overlaid with 0.5 mM IPTG and 80 µg/mL X-Gal.

Isolated colonies were inoculated into 5 mL LB medium (1% (w/v) Bacto®-tryptone, 0.5% (w/v) Bacto®-yeast extract and 0.5% (w/v) NaCl; pH 7.5) supplemented with 100 µg/mL ampicillin and incubated overnight, with agitation, at 37°C. Plasmid DNA was purified from cell pellets using the alkaline-lysis method (Sambrook and Russell, 2001) and subjected to restriction endonuclease analysis to confirm their identity.

### 2.2.2 Construction of baculovirus transfer vectors pHis-RV4N and pHis-RV5N

Prototype HRV strains RV4 and RV5 were selected for investigation in this study as they represent two globally dominant genotypes, P[8]G1 and P[4]G2, with NSP4 of differing genogroups.

The cDNA of NSP4 of human rotavirus strains RV4 (P1A[8]G1, II, NSP4 genogroup B) and RV5 (P1B[4]G2, I, NSP4 genogroup A) had been cloned previously into the mammalian transfer vector pIND/V5-His-TOPO® (Invitrogen), and were denoted as pTOPO-RV4 and pTOPO-RV5 respectively (Figure 2.1). These constructs were kindly provided by Rebecca Gorrell formerly of the Department of Gastroenterology and Clinical Nutrition, Royal Children's Hospital, Melbourne, Australia. The cDNA NSP4 gene sequences whilst retaining their START codon had been engineered for removal of their native termination codon (TCA).

As the construction of the baculovirus transfer vectors pHis-RV4N and pHis-RV5N proceeded through identical steps, there will be no differentiation between the two NSP4 genes, RV4-NSP4 and RV5-NSP4, in the following diagrams. The insert will be collectively referred to as "NSP4". Similarly, the use of the suffix "N" or "C" will be used to differentiate between plasmids destined for production of recombinant NSP4 proteins bearing the $His_6$ tag at the amino and carboxyl termini respectively.

All plasmid maps were generated using Bio-Log Plasm (Scientific Software; http://www.bio-log.biz/).

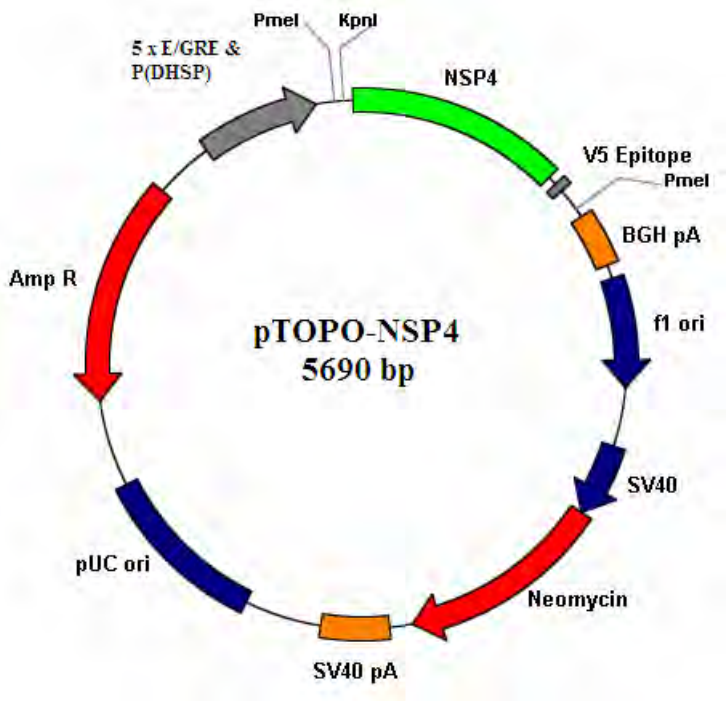


***Figure 2.1. Plasmid map of pTOPO-NSP4.*** *The cDNA of the NSP4 gene of rotavirus strains RV4 and RV5 was ligated within the MCS of pIND/V5-His-TOPO® (Invitrogen). The two PmeI sites are unique to the polylinker. A polyhistidine C-terminal tag is located within the MCS.*

PCR primers were designed (Table 2.1) to amplify the NSP4 gene from both pTOPO-RV4 and pTOPO-RV5. The sense primer (NSP4-N), containing a *Hin*dIII recognition sequence, was designed to bind to the NSP4 sequence downstream of the NSP4 start codon and was used for the amplification of NSP4 from both constructs. A *Bgl*II restriction site and termination codon, TCA, synonymous with the native NSP4 sequence, was designed into the anti-sense primers NSP4-CRV4 and NSP4-CRV5, specific for pTOPO-RV4 and pTOPO-RV5, respectively.

***Table 2.1. PCR primers for the amplification of the NSP4 gene from pTOPO-NSP4 - N-His-tag orientation.*** *The Hind*III *recognition sequence (red) and Bgl*II *recognition sequence (blue) are illustrated. The TCA termination codons are underlined. Primers were designed using Net Primer, PREMIER Biosoft International (www.premierbiosoft.com/netprimer) and synthesised by GeneWorks Pty Ltd.*

| **Primer** | **Sequence (5' → 3')** |
|---|---|
| **NSP4-N** | AAG CTT GCC GAG GTC AAC TAC |
| **NSP4-CRV4** | AGA TCT TCA CAT GGA TGC AGT CAC TTC |
| **NSP4-CRV5** | AGA TCT TCA CAT CGC TGC AGT CAC TTC |

The amplification profile consisted of an initial period of DNA denaturation at 95°C for 2 minutes, followed by 29 cycles of amplification (95°C for 30 seconds, 50°C for 30 seconds and 72°C for 1 minute) in a DNA Thermal Cycler (Minicycler™; Bio-Rad).

The 528 bp PCR product was visualised in a 1% (w/v) agarose gel as per 2.2.1.3 prior to gel purification and ligation with the pGEM®-T Easy Vector (TA-cloning kit; Invitrogen).

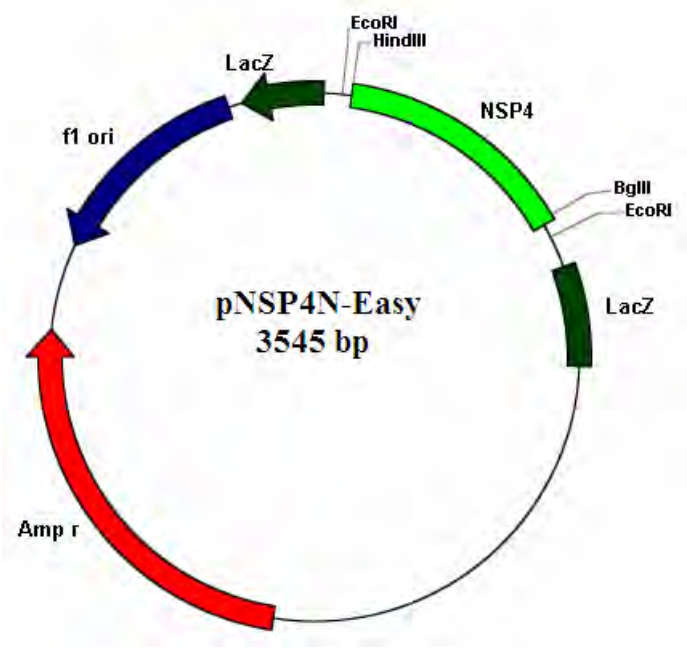


***Figure 2.2. Plasmid map of pNSP4N-Easy.*** *The 528 bp NSP4N amplicons were ligated with the pGEM®-T Easy vector to generate the recombinant plasmids pRV4N-Easy and pRV5N-Easy. Bgl*II *and Hind*III *restriction sites were engineered into the NSP4 amplicon. The Eco*RI *restriction sites are located on the parental vector pGEM®-T Easy.*

The pNSP4N-Easy plasmids were transformed into competent *E. coli* JM109 cells as detailed in Section 2.2.1.4. The purified plasmid DNA was digested with *Bgl*II and *Hin*dIII (Fermentas), fractionated in a 1% (w/v) agarose gel, and the 522 bp NSP4 fragment excised from the gel and purified using the AppliChem DNA Isolation Kit. The NSP4 fragment was directionally cloned, in frame, into pBacPAK-His 1 (Clontech) which had been similarly digested (*Bgl*II/*Hind*III), gel purified, and dephosporylated with SAP, to create the recombinant baculovirus transfer vectors pHis-NSP4N (Figure 2.3). The baculovirus transfer vector pBacPAK-His1, provides an initiating codon, ATG, proceeded by a $His_6$ tag and is located upstream from the MCS, facilitating the expression of recombinant proteins with an N-terminal $His_6$ tag.

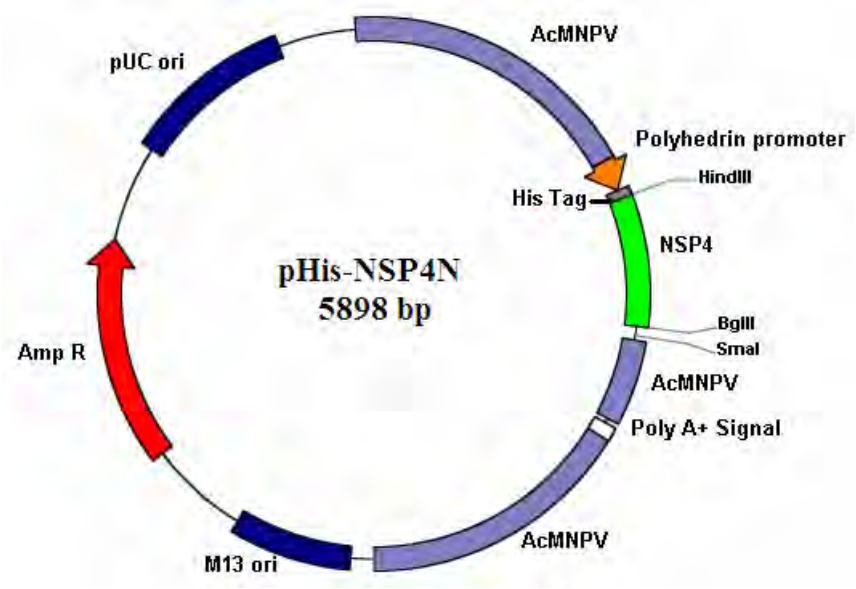


***Figure 2.3. Plasmid map of recombinant baculovirus transfer vector pHis-NSP4N.*** *The 522 bp Bgl*II*/Hind*III*-digested NSP4 amplicons were ligated with the baculovirus transfer vector pBacPAK-His1; downstream of the initiation codon, $His_6$ tag and the polyhedrin promoter. The NSP4 sequence is flanked either side by the AcMNPV sequence.*

### 2.2.3 Construction of baculovirus transfer vectors pBP8-RV4C and pBP8-RV5C

As outlined in Section 2.2.2, for the purpose of representing the constructs diagrammatically, no distinction between the NSP4 genes of RV4 and RV5 will be made. The suffix "C" (location of the $His_6$ sequence) will be applied to the names of the proceeding constructs, differentiating them from the former constructs ("N").

Primers were designed (using Net Primer) to amplify a nucleotide sequence inclusive of the NSP4 gene and a region coding for the hexa-histidine tag for both pTOPO-RV4 and pTOPO-RV5 (Figure 2.4). The primers were specific to the pIND/V5-His-TOPO® sequence and incorporated a *Bgl*II (red) restriction site (5'-CGAGCTCAGATCTACTAGTCCAGTGTG-3') upstream of the NSP4 sequence. In addition, the anti-sense primer (5'-AAACCCGGGATGGCTGGCAAC-3') was downstream of the polyhistidine region of the vector and engineered an *Xma*I (blue) restriction site within the sequence. The primers were synthesised by Sigma Genosys.

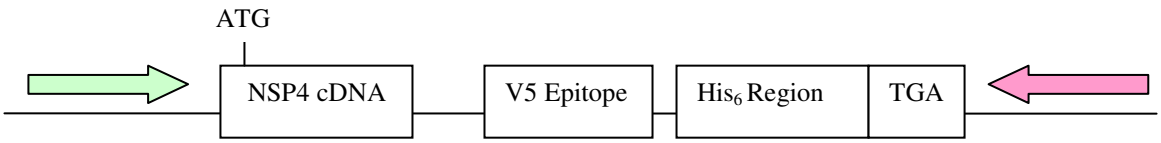


***Figure 2.4. Linear schematic of primer binding sites for amplification of NSP4C cDNA from pTOPO-NSP4.*** *The sense primer represented as the green arrow contains a Bgl*II *restriction site. The anti-sense primer (pink arrow) contains an Xma*I *restriction site. Additional key regions of interest; the V5 epitope, NSP4 sequence, polyhistidine ($His_6$) region and termination codon (TGA) have been identified.*

The amplification profile consisted of an initial period of DNA denaturation at 94°C for 2 minutes, annealing at 62°C for 2 minutes and extension at 72°C for 2 minutes, followed by 35 cycles of 94°C for 1 minute, 62°C for 1 minute and 72°C for 1 minute. The 804 bp amplicons were then ligated with the pGEM®-T Easy Vector using techniques described in Section 2.2.2.

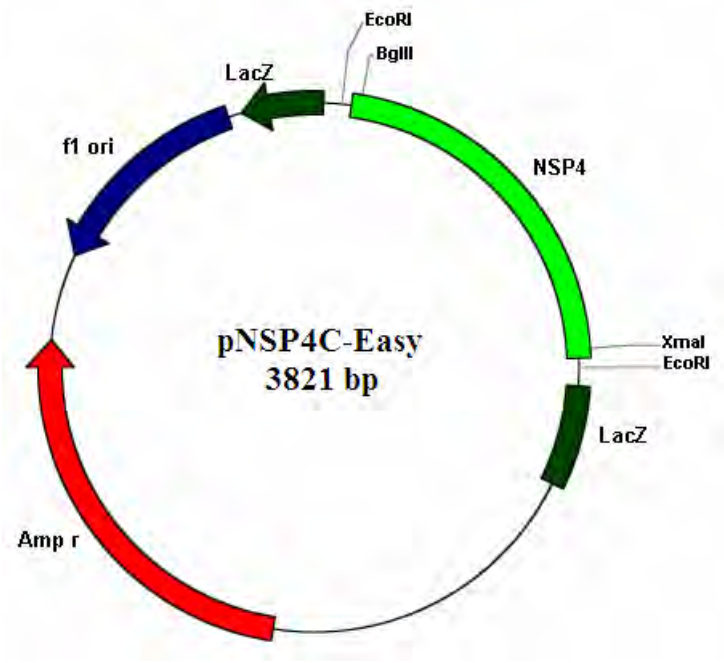


***Figure 2.5. Plasmid map of pNSP4C-Easy.*** *The 804 bp NSP4C amplicons of rotavirus strains RV4 and RV5 were ligated with the pGEM®-T Easy vector, yielding RV4C-Easy and RV5C-Easy respectively. Enzyme restriction sites (Eco*RI*, Bgl*II*, Xma*I*) utilised for further manipulation of the NSP4 cDNA or for diagnostic purposes have been identified.*

The pNSP4C-Easy plasmids were transformed into competent *E. coli* JM109 cells as previously described. The purified plasmid DNA was digested with *Bgl*II and *Xma*I, fractionated in a 1% (w/v) agarose gel and the NSP4 fragment purified from the gel using the AppliChem DNA Isolation Kit. The baculovirus transfer vector pBacPAK8 was digested with *Bgl*II and *Sma*I and gel purified. The ligation of the NSP4 fragment with dephosphorylated pBacPAK8 to yield the plasmid pBP8-NSP4C was as described for the construction of pHis-NSP4N.

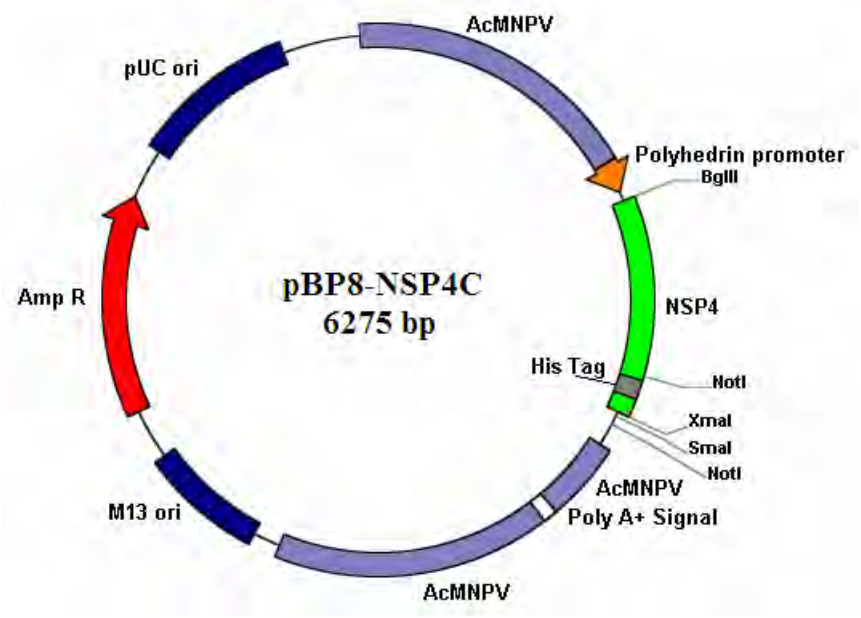


***Figure 2.6. Plasmid map of recombinant baculovirus transfer vector pBP8-NSP4C.*** *The 788 bp Bgl*II*/Xma*I *digested amplicons containing the NSP4 genes of rotavirus strains RV4 and RV5 were ligated with the baculovirus transfer vector pBacPAK8 downstream of the polyhedrin promoter and flanked by AcMNPV regions.*

The integrity of the recombinant baculovirus transfer vectors pHis-NSP4N and pBP8-NSP4C was confirmed by sequencing. Briefly, the baculovirus transfer vectors were purified from 5 mL overnight *E. coli* cultures using the AppliChem DNA Isolation Kit. The concentration of plasmid DNA was quantified by electrophoresis as detailed in Section 2.2.1.3 and 250-400 ng plasmid DNA submitted with 3.2 pmol of each primer (Bac1 and Bac2) for sequencing. Sequencing was performed using dye-terminator chemistry (Big Dye™ Terminator Version 2) and analysis with an ABI Prism® 377 DNA sequencer at either the Wellcome Trust sequencing centre or the Baker Institute sequencing facility. The primers Bac1 (5'-ACCATCTCGCAAATAAATAAG-3') and Bac2 (5'-ACAACGCACAGAATCTAGCG-3') were synthesised by GeneWorks and bind specifically to sequences flanking the MCS of the baculovirus transfer vectors, pBacPAK8 and pBacPAK-His1. The DNA sequence was analysed using Biology Workbench 3.2 software (http://workbench.sdsc.edu).

Once the integrity of the recombinant baculovirus transfer vector sequences had been confirmed, midi prep quantities of the transfer vectors were prepared from 200 mL cultures, as detailed in Sambrook and Russell (2001). This DNA was subsequently used for homologous recombination with linearised baculovirus DNA.

## 2.2.4 Construction of recombinant NSP4 baculoviruses

All works conducted using *Sf*-21 cells were performed in a Class II biological safety cabinet; using sterile reagents and media. The methodology for the construction of recombinant baculoviruses was in accordance with that published in King and Possee (1992).

### 2.2.4.1 Maintenance of *Sf*-21 cells

The *Sf*-21 insect cell line was originally established from pupal ovarian tissue of the Fall army worm (Vaughn *et al.,* 1977). *Sf*-21 cells (Invitrogen) were grown and maintained as 100 mL suspension cultures in *Sf*-900 II SFM (serum free-medium) (GIBCO®) at 28°C and 100 rpm. The cultures were routinely subcultured to a cell density of 3 x $10^5$ cells/mL once a density of ~ 2 x $10^6$ cells/mL had been reached.

### 2.2.4.2 Production of recombinant NSP4 baculoviruses

The recombinant NSP4 baculoviruses were generated by cationic liposome mediated co-transfection of the recombinant baculovirus transfer vector with linearised baculovirus DNA (*Bsu*361 digested BacPAK 6, Clontech Laboratories Inc.) into *Sf*-21 cells. Linearised BacPAK6, engineered to contain three *Bsu*361 restriction sites at the polyhedrin locus, was reported to increase the frequency of isolating recombinant baculoviruses after co-transfection by approximately 90%, compared with the low levels of recombinant viruses produced using wild type circular DNA (0.1-1%) (Kitts and Possee, 1993).

In brief, approximately 2 µg of the recombinant baculovirus transfer vector was ethanol precipitated with 400 ng BacPAK6 in the presence of 0.3 M sodium acetate for 30 minutes at -20°C. The DNA was recovered by centrifugation at high speed (13000 rpm)

for 10 minutes at 4°C and left to air dry, prior to its dissolution in 12 µL sterile MilliQ water.

The co-transfectin DNA was transferred to a polystyrene tube containing 8 µL Lipofectin® (Invitrogen) with 4 µL MilliQ water. DNA-liposome complexes were allowed to develop for 15 minutes prior to the addition to *Sf*-21 monolayers (3.5 x $10^5$ cells/mL) seeded within the wells of 6-well cell culture cluster plates (Costar). The cells were incubated at 28°C in a humid environment until CPE was observed. The viral supernatant was recovered and virus isolation achieved by performing a plaque assay adapted from King and Posse (1992) and described below.

#### 2.2.4.3 Isolation of recombinant NSP4 baculoviruses by plaque assay

*Sf*-21 cells were seeded at a density of 6 x $10^5$ cells/mL in 6-well plates. The cells were left to attach at 28°C for 30 minutes, after which the supernatant was removed by aspiration.

Ten-fold serial dilutions of the viral supernatant ($10^{-3}$ to $10^{-7}$) were prepared in *Sf*-900II SFM and 250 µL of each added, in duplicate, to each of the wells. Viral infection was allowed to proceed for 1 hour at 28°C.

The viral supernatant was aspirated from the cells and 2 mL of molten 1% SeaPlaque® Agarose (Cambrex) (w/v in *Sf*-900II SFM) added per well. Once the agarose had set, 1 mL of *Sf*-900II SFM was added to the agarose overlay. The cells were incubated at 28°C in a humid environment for between 4-10 days, until plaque formation was observed.

Plaques were stained with neutral red and were either excised from the agarose overlay for viral expansion or counted for viral titre determination (pfu/mL) as per King and Possee (1992).

The plaque-purified virus was subjected to two additional rounds of plaque purification and its identity confirmed by PCR analysis, prior to the establishment of a working stock.

#### 2.2.4.4 PCR screening of recombinant NSP4 baculoviruses

The use of PCR for confirming the identity of recombinant baculoviruses and verifying insert fidelity was reported by Webb *et al*. (1991). The method for purifying recombinant baculovirus DNA for PCR analysis was adapted from Clontech's "BacPAK™ Baculovirus Expression System User Manual" (PTI260-1; 1999).

*Sf*-21 cells were seeded at a cell density of 3 x $10^5$ cells/mL into 6-well plates. Once cell attachment had been achieved, 100 µL of the inoculum (plaque-purified virus) was added to the cells, and the virus left to infect for 2-3 days at 28°C. At the completion of the incubation period, the supernatant was recovered (P1 seed stock).

Cell detachment was achieved by streaming PBS (140 mM NaCl, 27 mM KCl, 8 mM $Na_2HPO_4$, 1.5 mM $KH_2PO_4$; pH 7.3) across the cell monolayer. The cells were pelleted by centrifugation at 1000 rpm for 1 minute prior to resuspension in 0.5 mL PBS and stored at 4°C for 24 hours.

The cells were pelleted and resuspended in 250 µL of TE buffer (10 mM Tris-HCl, 0.1 mM EDTA; pH 8.0) supplemented with RNAseA (100 µg/mL). Cell lysis was accomplished by incubation of the cell suspension in 250 µL Cell Lysis Buffer (50 mM Tris-HCl (pH 8.0), 10 mM EDTA, 5% (v/v) β-mercaptoethanol, 0.4% (w/v) SDS), 12.5 µL Proteinase K (10mg/mL in 50 mM Tris-HCl, 10 mM $CaCl_2$; pH 8) and 2 µL RNAse A (10mg/mL) at 37°C for 30 minutes.

The viral DNA was extracted with phenol:chloroform:isoamyl alcohol (25:24:1) thrice. The DNA was precipitated in the presence of 50 µL sodium acetate (3 M, pH 5.2) and 1 mL absolute ethanol at -20°C overnight. The viral DNA was collected by centrifugation at room temperature for 5 minutes, washed in excess 70% ethanol twice, and the DNA pellet air dried at room temperature under sterile conditions.

The pellet was resuspended in 50 µL TE buffer (pH 8.0) and incubated overnight at 4°C. A 10 µL aliquot of the purified viral DNA was used in the PCR reactions. The cycling parameters for the PCR amplification of viral DNA was adapted from Woo (2001) and modified to accommodate the optimum temperatures for the corresponding primer combinations.

In brief, the amplification profile for the Bac1/Bac2 primer combination consisted of an initial period of DNA denaturation at 94°C for minutes, annealing at 62°C for 2 minutes and extension at 72°C for 2 minutes, followed by 35 cycles of 94°C for 1 minute, 62°C for 1 minute and 72°C for 1 minute. At the completion of the cyclic step, a final denaturation step (94°C for 1 minute), annealing (62°C for 1 minute) and extension (72°C for 7 minutes) was undertaken. Amplification of the recombinant viral DNA using Bac1/NSP4 C-terminal specific primers was also performed using the cycling parameters outlined for the Bac1/Bac 2 primers.

#### 2.2.4.5 Expansion of recombinant NSP4 baculoviruses – seed stock (P2)

*Sf*-21 cells, seeded at a cell density of 5 x $10^5$ cells/mL in a 25 $cm^2$ T-flask, were inoculated with 250 µl plaque-purified recombinant baculovirus (P1) and the seed stock (P2) prepared as per King and Possee (1992).

Protein expression was established (Section 2.2.5.1) prior to the preparation of the recombinant baculovirus working stock (P3).

#### 2.2.4.6 Preparation of recombinant NSP4 baculovirus working stocks (P3)

*Sf*-21 suspension cultures (100 mL at a concentration of 5 x $10^5$ cells/mL) were inoculated with 500 µl recombinant virus seed stock (P2) and incubated at 28°C and 100 rpm. At 6 d.p.i. the supernatant containing the virus particles was harvested by centrifugation at 1500 rpm for 10 minutes.

Plaque assays were conducted using the working stock (P3) as inoculum to establish the viral titres.

## 2.2.5. Baculovirus expression of recombinant proteins $His_6$-NSP4

Four recombinant $His_6$-tagged NSP4 proteins were expressed using the BEVS; RV4C, RV5C, RV4N and RV5N. The suffixes C or N denote the location of the $His_6$ tag at the C or N-termini respectively of the NSP4 protein. RV4 and RV5 denotes the identity of the RV strain from which the NSP4 protein was derived. For simplicity, unless required otherwise, the recombinant NSP4 proteins will be referred to collectively as $His_6$-NSP4.

### 2.2.5.1 Confirmation of recombinant NSP4 protein expression

A small scale protein purification protocol (Mini Pull Down), adapted from the QIAexpressionist Handbook, was employed to ensure that the recombinant protein was being expressed in *Sf*-21 cells prior to committing to large scale protein purification.

*Sf*-21 cells were seeded into the wells of a 6-well plate at a cell density of 1 x $10^6$ cells/mL. Once the cell monolayer had been established, the medium was removed by aspiration and 300 µl of P2 seed stock added. The virus was allowed to adsorb for 1 hour, after which the inoculum was removed and 2 mL *Sf*-900II SFM added to the cell monolayer. The cells were incubated in a humid environment at 28°C for three days.

Upon completion of incubation, the cells were dislodged by streaming a minimal volume of supernatant across the surface of the monolayer. The cells were collected at low speed (1000 rpm) for 5 minutes and the supernatant discarded. The cells were lysed in 400 µl PBS-Tween-20 (at 4°C for 30 minutes) and the cellular debris separated from the supernatant (containing the soluble protein) by low speed centrifugation. The supernatant was added to 50 µl of pre-equilibrated IMAC resin and rotated end-over-end at 25°C for 30 minutes. The resin/protein complex was pelleted by centrifugation at low speed and extraneous proteins were removed from the resin by washing the complex in excess volumes of PBS thrice. The resin/protein complex was resuspended in 20 µl of 5 X SDS-PAGE-SRB (62.5 mM Tris-HCl; pH 6.8, 10% (v/v) glycerol, 2% (w/v) SDS, 5% (v/v) β-mercaptoethanol and 2.5% (v/v) bromophenol blue) and heated at 95°C for 3 minutes, prior to visualization of the $His_6$-NSP4 proteins in a polyacrylamide gel as described in Section 2.2.5.2.

#### 2.2.5.2 SDS-PAGE analysis of recombinant NSP4 proteins

The affinity purified $His_6$-NSP4 proteins were fractionated by electrophoresis at 200 V in a 12% (v/v) resolving and 5% (v/v) stacking SDS-polyacrylamide gel using a discontinuous buffering system as per Laemmli (1970). PageRuler™ prestained protein ladder (Fermentas) was run alongside the protein samples to monitor both the progress of the protein separation and to confirm the molecular weight (M.W.) of the NSP4 proteins. Proteins were visualized by staining with Coomassie brilliant blue R-250 (0.25% (w/v) in destaining solution) and subsequent destaining (50% methanol:10% glacial acetic acid). Where visibility of the protein band was poor, silver staining was performed as per Sambrook and Russell (2001).

Once the production of the recombinant protein had been verified, the viral stock was expanded (P3) and large scale production of the recombinant proteins undertaken.

#### 2.2.5.3 Expression of $His_6$-NSP4 proteins in *Sf*-21 cells

The recombinant baculoviruses were inoculated into 100 mL cultures of *Sf*-21 cells (cell density of 1 x $10^6$ cells/mL) at a multiplicity of infection (MOI) of 1.0 pfu/cell. The infected cells were harvested at 48 hours post-inoculation (h.p.i.). The optimum time of harvest and M.O.I., visualized as maximum NSP4 yield by SDS-PAGE, was determined empirically by time course analysis of *Sf*-21 cells infected with recombinant RV5N-His1 and RV4N-His1 baculoviruses. Briefly, the time course consisted of the purification of 3 mL aliquots of the NSP4 protein (as detailed in 2.2.5.1) from 100 mL of expression culture at 12 hour intervals for 72 hours. The time course experiment was conducted in triplicate.

## 2.2.6 Purification of $His_6$-NSP4

### 2.2.6.1 Affinity purification of $His_6$-NSP4

Nickel-nitrilotriacetic (Ni-NTA; Qiagen) immobilised metal-affinity chromatography was used for the batch purification of $His_6$-NSP4 under native conditions.

One of two pH-dependent buffering systems was used in the purification process to accommodate the differing isoelectric points of the recombinant NSP4 proteins. The $His_6$-NSP4 proteins (RV4C and RV4N) originating from the RV4 strain required a buffering capacity of pH 8.0, whilst $His_6$-NSP4 of RV5 (RV5C and RV5N) required pH 7.0. In the proceeding text, only instances where the pH was held constant for the purification of all constructs will be recorded. The methodology employed for the purification of the $His_6$-NSP4 proteins was adapted from Rodríguez-Díaz *et al.* (2003) and in compliance with The QIAexpressionist™ Handbook (Qiagen).

The recombinant NSP4 expression cultures were harvested at 48 h.p.i. and the cell pellet recovered by centrifugation at 4000 rpm for 20 minutes at room temperature. The cells were resuspended in cell lysis buffer (50 mM sodium phosphate, 10 mM imidazole, 300 mM NaCl, 1% (v/v) Triton® X-100) and lysed on ice for 30 minutes. The cell extract was centrifuged at 4000 rpm (10 minutes) to separate the clarified lysate from the insoluble material. The lysate was subjected to initial sterilization through Millipore 0.45 µm filters, prior to sterilisation through 0.22 µm filters.

The clarified cell lysate was incubated with 2 mL of 50% (w/v) Ni-NTA resin slurry (pre-equilibrated with 20 mM imidazole wash buffer) for 1 hour at room temperature and rotated end-over-end, prior to loading into a 2 mL (0.5 cm internal diameter x 5 cm) glass column (Bio-Rad). Chromatographic separation was conducted using the Econo-System (Bio-Rad) workstation. Removal of endogenous proteins was achieved by step-gradient application of 20 mM and 50 mM imidazole (diluent 50 mM sodium phosphate; 300 mM NaCl, 0.1% (v/v) Tween-20) to the resin/protein complex. The $His_6$-NSP4 protein was eluted in 0.5 mL fractions with 250 mM imidazole (50 mM sodium phosphate; 300 mM NaCl, 0.1% (v/v) Tween-20). The eluted protein was

monitored by absorbance at 280 nm, and Bradford's Reagent (0.05% (w/v) Coomassie Brilliant Blue G-250; 23.75% (v/v) Ethanol; 42.5% (v/v) Phosphoric Acid) was used to detect the presence of protein in the collected fractions.

#### 2.2.6.2 Post IMAC purification of $His_6$-NSP4

Affinity purified $His_6$-NSP4 proteins were subjected to an additional processing step using Amicon® Ultra-15 Centrifugal Filter Devices (Millipore), 5 kDa nominal M.W. limit. Protein samples for ELISA analysis (Chapter 3) were concentrated in fresh elution buffer. Samples to be used for intracellular calcium responses (Chapter 4), in addition to protein concentration, had to undergo buffer exchange to affect the removal of toxic imidazole. The protocol applied was as per the manufacturer's specifications.

Briefly, affinity purified $His_6$-NSP4 elution fractions were pooled, the volume made to 15 mL using the appropriate buffer, the samples added to the reservoir of the Amicon filtration device and the retentate collected by centrifugation at 6000 rpm for 20 minutes. The number of centrifugation steps was optimized for each of the purified samples.

#### 2.2.6.3 Quantitation of purified $His_6$-NSP4

The concentration of the affinity purified protein samples was estimated using the Bradford assay against a bovine serum albumin (Fraction V, Sigma) standard within the appropriate buffer (i.e. with or without imidazole).

### 2.2.7 Immunodetection of $His_6$-NSP4

The purified $His_6$-NSP4 proteins were fractionated by SDS-PAGE as outlined above (2.2.5.2). The proteins were then transferred to a nitrocellulose membrane (0.45 µm, Schleicher and Schuell or Hybond ECL) using the Trans-Blot® SD Semi-Dry Electrophoretic Transfer Cell (Bio-Rad). The protocol outlined below was adapted from both the Trans-Blot® SD Semi-Dry Electrophoretic Transfer Cell Instruction Manual and the ECL Western Blotting Detection Reagents and Analysis System Manual.

The optimum primary and secondary antibody concentrations were determined empirically via dot blot assays, prior to performing Western blot analysis of the Ni-NTA purified $His_6$-NSP4 proteins. The protocol for the dot blot assay was adapted from the ECL Western Blotting Manual. The primary antibody, rabbit α-SA11 polyclonal antibody, was kindly donated by Dr Carl Kirkwood of the Enteric Virus Research Group, Murdoch Children's Research Institute, Royal Children's Hospital (Parkville, Australia).

The membrane, SDS-polyacrylamide gel of fractionated proteins and Whatman 3MM filter paper were pre-equilibrated in Bjerrum and Schafer-Nielsen transfer buffer (48 mM Tris, 39 mM glycine, 20% (v/v) methanol, 1.3 mM SDS; pH 9.2) prior to protein transfer in the Trans Blot® apparatus at 10 V for 30 minutes.

Electrotransfer efficiency was verified by monitoring the transfer of PageRuler™ prestained protein ladder (Fermentas) from the gel to the membrane. On completion of electrotransfer, the membrane was incubated in 1% (w/v) blocking solution (ECL blocking agent dissolved in PBS-T (80 mM $Na_2HPO_4$, 20 mM $NaH_2PO_4.H_2O$, 100 mM NaCl, 0.1% (v/v) Tween-20; pH 7.5)) at room temperature on a rocking platform for 1 hour. At the completion of the incubation period the membrane was washed four times (twice for 5 minutes and twice for 15 minutes) in PBS-T. The membrane was then probed with rabbit α-SA11 antibody diluted 1000-fold in PBS-T overnight at room temperature on a rocking platform.

The membrane was washed as described previously with PBS-T, prior to development with horseradish-peroxidase (HRP)-conjugated donkey anti-rabbit IgG (GE Healthcare BioSciences) diluted 5000-fold in PBS-T, for 1 hour at room temperature. The membrane was washed as previously described, and the antibody-protein complex visualized with the ECL Plus Western Blotting Detection System (GE Healthcare BioSciences) and subjected to chemi illuminescence using Bio-Rad's Chemidoc XRS Documentation Station.

## 2.3 Results and Discussion

### 2.3.1 Generation of recombinant NSP4 baculoviruses

As the construction of the recombinant baculoviruses evolved through a series of intermediates, the identity of each construct had to be confirmed at each step. For the PCR vectors this simply involved performing presumptive restriction digestion reactions. The identification of the baculovirus transfer vectors proceeded through a more rigorous analysis involving restriction digestion, PCR and sequencing to verify the integrity of the nucleotide sequence. PCR was used to identify recombinant baculoviruses containing the NSP4 gene insert.

#### 2.3.1.1 Construction of N-His$_6$-tagged baculovirus transfer vectors; pHis-RV4N and pHis-RV5N

Initial attempts at direct ligation of the *Bg*lII/*Hin*dIII-digested PCR amplicon with the baculovirus transfer vector, pBacPAK-His1 were unsuccessful and consequently, the PCR products were cloned into the MCS of the pGEM® T Easy Vector. The MCS is located within the LacZ gene sequence, encoding the enzyme β-galactosidase, and imparts the ability to use blue/white screening for recombinant plasmid selection. In the presence of IPTG and X-Gal, deep blue colonies are indicative of an intact LacZ gene (no insert), whilst white colonies are suggestive of cells transformed with recombinant plasmids (insert). This assumption held true for the selection of pRV5N-Easy transformed cells, whilst the pRV4N-Easy transformants presented as pale blue colonies. Two possible causes of these blue colonies would be attributable to either the NSP4 sequence being cloned in frame with the LacZ gene or the introduction of mutations during amplification; although sequence analysis of the amplicon discounts the latter.

*Eco*RI restriction sites (native to the parental plasmid vector, pGem®-T Easy) flank the NSP4 sequence in the pNSP4N-Easy vectors (Figure 2.2). Consequently, the digestion of the recombinant vector with *Eco*RI should yield fragments of slightly greater size (bp) compared with the insert DNA (528 bp). *Eco*RI digestion of pRV5N-Easy released

a fragment consistent in length with the expected 548 bp product. The generation of three fragments (3018, 442 and 106 bp) for *Eco*RI digested pRV4N-Easy was consistent with an internal *Eco*RI site within the ORF of the NSP4 gene of RV4.

*Bgl*II and *Hin*dIII restriction sites were specific for the NSP4 amplicons and digestion of pNSP4N-Easy vectors with this double enzyme reaction resulted in the release of the 522 bp NSP4 sequence (Figure 2.2).

Confirmation of the identity of the baculovirus transfer vectors pHis-RV4N and pHis-RV5N involved two confirmative digestion reactions, *Bgl*II/*Hin*dIII and *Hin*dIII/*Sma*I, releasing fragments of 522 bp and 547 bp, respectively (Figure 2.3). Further to the restriction digest analysis of the recombinant baculovirus transfer vectors, PCR was also performed using combinations of AcMNPV specific (Bac1 and Bac2) and NSP4 specific primers. Once satisfied that the identity of the recombinant baculovirus transfer vectors had been confirmed, the DNA was submitted for DNA sequencing and the integrity of the nucleotide sequence confirmed (Biology Workbench 3.2).

#### 2.3.1.2 Construction of C-His$_6$-tagged baculovirus transfer vectors; pBP8-RV4C and pBP8-RV5C

Initial attempts to generate constructs which would produce C-terminal His$_6$-tagged proteins involved the direct cloning of *Kpn*I/*Pme*I (New England Biolabs) digested DNA sequences from pTOPO-NSP4 (Figure 2.1) into *Kpn*I/*Sma*I-digested pBacPAK8. This method was unsuccessful, either due to the release of fragments solely digested with *Pme*I and/or the inability to isolate *Kpn*I/*Pme*I-digested DNA from the former (17 bp size difference) on agarose gels.

The direct ligation of the *Bgl*II/*Xma*I-digested PCR amplicon with *Bgl*II/*Sma*I-digested pBacPAK8 was also unsuccessful and, consequently, the 804 bp PCR product was ligated with pGEM®-T Easy.

Blue/white screening was employed to isolate colonies transformed with recombinant pRV4C-Easy and pRV5C-Easy. The *Eco*RI restriction sites on the pGEM®T Easy

vector, as discussed previously, were utilised for the identification of pNSP4C-Easy constructs. *Eco*RI digestion of pRV5C-Easy released an 824 bp fragment, whilst similarly digested pRV4C-Easy released two fragments of 294 and 530 bp, consistent with the presence of a native *Eco*RI site within the ORF of this protein. The *Bgl*II/*Xma*I digestion of pNSP4C-Easy vectors released a fragment comparable in size with the expected 788 bp.

Confirmation of the identity of the baculovirus transfer vectors pBP8-RV4C and pBP8-RV5C involved two confirmative digestion reactions, *Bgl*II/*Xma*I and *Bgl*II/*Not*I. The latter digest reaction yielded two fragments, assuming complete digestion, of 632 and 182 bp (Figure 2.6). *Bgl*II/*Xma*I digestion yielded the 788 bp fragment (Figure 2.6). PCR analysis of the baculovirus transfer vectors using baculovirus specific (Bac1/Bac2) and NSP4-specific primer combinations were used to confirm the identity of the recombinant vectors prior to sequencing.

#### 2.3.1.3 Generation of recombinant NSP4 baculoviruses

Recombinant NSP4 baculoviruses were generated by co-transfection of the baculovirus transfer vectors with linearised BacPAK6 viral DNA into *Sf*-21 cells. The four recombinant baculoviruses were isolated by plaque assay and their identity confirmed by PCR analysis using baculovirus specific (Bac1/Bac2) primers and in combination with NSP4 amplicon specific primers. The following figure illustrates the screening process for RV5N-His1.

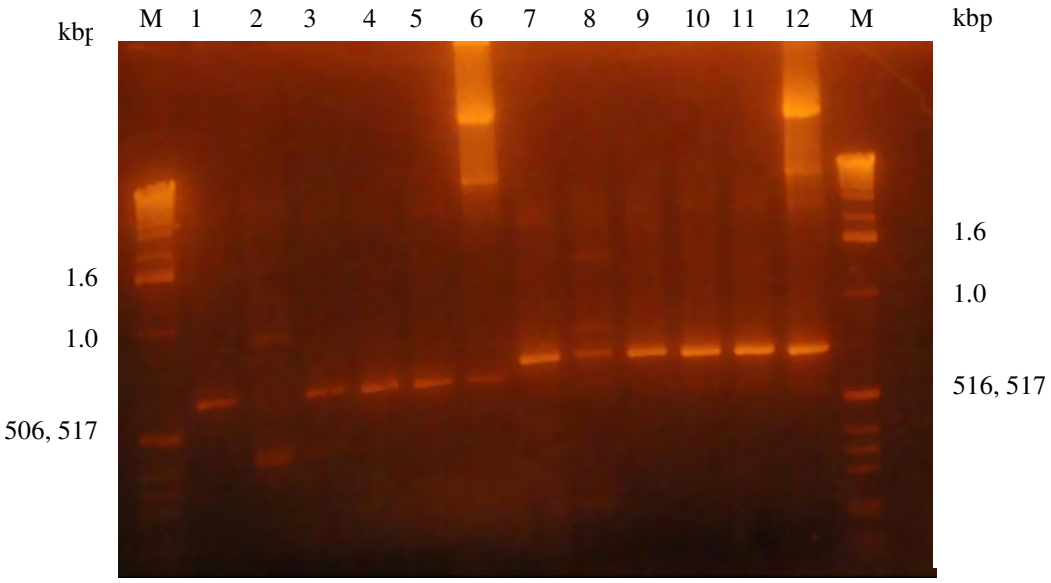


***Figure 2.7. PCR screening for RV5N-His1 baculovirus DNA.*** *Baculovirus DNA was isolated from plaque pick expansions and the DNA amplified with either AcMNPV specific primers (Bac1/Bac2) or a combination of NSP4 specific and AcMNPV primers (Bac1/CRV5). The viral DNA was run alongside the corresponding amplicons of the pHis-RV5N baculovirus transfer vectors on a 1% (w/v) agarose gel. $L_2$ - $L_6$ amplicons from Bac1/CRV5 PCR of RV5N-His1 viral isolates. $L_7$ amplicon of Bac1/CRV5 PCR of corresponding baculovirus transfer vector, pHis-RV5N. $L_8$ - $L_{12}$ amplicons from Bac1/Bac2 PCR of RV5N-His1 viral DNA. $L_{13}$ Bac1/Bac2 PCR of baculovirus transfer vector, pHis-RV5N. The standard 1Kb DNA marker is in $L_1$ and $L_{14}$. The molecular size (base pairs) of the M.W. marker are indicated ether side of the image.*

PCR of the recombinant baculovirus transfer vector pHis-RV5N using Bac1/Bac2 and Bac1/CRV5 primer combinations generate amplicons of 721 and 627 bp respectively. As illustrated in Figure 2.7, all viral isolates (with the exception of isolate 2) amplified sequences of comparable size.

PCR screening of baculovirus isolates using combinations of AcMNPV-specific and NSP4-specific primers proved to be an efficient method for identifying recombinant baculoviruses carrying the NSP4 gene. As demonstrated for isolate 2, the use of more

than one primer combination was required to unequivocally confirm the integrity of the recombinant virus.

The images obtained from the PCR screening of the three remaining recombinant baculoviruses (RV4N-His1, RV4C-BP8 and RV5C-BP8) have not been included in this report as the results mirror those presented for RV5N-His1.

#### 2.3.1.4 Determination of viral titre (pfu/mL)

The viral titre of the recombinant baculoviruses, as determined by plaque assay were as follows: RV5N-His1 (4.8 x $10^8$ pfu/mL), RV4N-His1 (3.6 x $10^8$ pfu/mL), RV5C-BP8 (4.4 x $10^8$ pfu/mL) and RV4C-BP8 (4.2 x $10^8$ pfu/mL).

### 2.3.2 The expression and purification of $His_6$-NSP4

#### 2.3.2.1 Optimisation of $His_6$-NSP4 expression

The BEVS has been used extensively by others for the expression of NSP4 in insect cells (Chang *et al*., 2001b; Ishida *et al*., 1996; 1997; Rodriguez-Diaz *et al*., 2003; 2005; Tian *et al*., 1994; 1996a; 2000; Yuan *et al*., 2004a; Zhang *et al*., 1998; 2000). The range of M.O.I.'s and the time of protein harvest used in these studies ranged from 2-10 pfu/mL and 36-72 h.p.i., respectively. Typically high M.O.I.'s, (5-10 pfu/mL), are routinely used for the expression of recombinant proteins using the BEVS (Summers and Smith, 1987).

The optimum time for harvesting the NSP4 expression culture in this study was established as 48 h.p.i.; determined empirically by harvesting cells at 12 hour intervals, for 72 hours, and assessing the protein yield by SDS-PAGE. In addition, the optimum expression of this protein was addressed at M.O.I.'s of 1 and 10 pfu/cell, across the same time course. A time of harvest of 48 h.p.i. and an M.O.I of 1 pfu/cell produced the greatest yield of the expressed protein and these parameters were applied in the expression of all the recombinant proteins.

Tian *et al*. (1994) observed NSP4 degradation products within *Sf*-9 cultures expressing the NSP4 protein of RV strain SA11 between 40 to 48 h.p.i. and they reported that maximal protein production was achieved at 36 h.p.i. No NSP4 degradation products were observed in the current study at >40 h.p.i. Such discrepancies between the two studies could be attributed to a number of factors including: (a) the relative toxicity of the NSP4 gene derived from different RV strains (HRV strains RV4 and RV5 versus SA11), (b) use of different insect cell lines (*Sf*21 versus *Sf*9) and (c) different M.O.I.'s (10 pfu/mL versus 1 pfu/mL).

The concentration of NSP4 produced beyond 48 h.p.i. decreased, coinciding with the demise of the expression culture; an effect attributable to NSP4-induced increases in $[Ca^{2+}]_i$, and the loss of NSP4 to the supernatant *via* cell lysis (Tian *et al*., 1994; 1995). Host cell death associated with increases in $[Ca^{2+}]_i$ of RV-infected cells, in conjunction with the accumulation of a viral protein(s), has been well documented, and NSP4 has been proposed as a potential candidate for this viral product (Brunet *et al.,* 2000a; del Castillo *et al*., 1991; Díaz *et al*., 2008; Dong *et al*., 1997; Michelangeli *et al*., 1991; 1995; Ruiz *et al*., 2000; 2005; Tian *et al*., 1994).

#### 2.3.2.2 Optimisation of IMAC purification of $His_6$-NSP4

The IMAC resin initially employed to purify the N-terminal $His_6$-NSP4 protein RV4N from the clarified insect cell lysate was TALON, a $Co^{2+}$-carboxylmethylaspartate matrix. Small scale purification of the protein demonstrated the efficacy of the TALON system in purifying RV4N from the insect cell lysate. Upon large scale purification of the protein, RV4N was absent from the elution fraction. Post purification SDS-PAGE analysis of all fractions and the resin demonstrated a notable absence of the $His_6$-tagged protein from all fractions, with the exception of the resin. This observation suggested that the interaction between the His-tag and the $Co^{2+}$ ion was sufficiently strong as to prevent displacement of RV4N under the elution conditions employed, or alternatively, that the protein was precipitating within the column. The latter seems the more appropriate conclusion, as the His-tagged protein was successfully purified using Ni-NTA, despite protein retention on $Ni^{2+}$ being reported to be three-fold that for $Co^{2+}$ (Arnold, 1991). The contribution of the matrix (i.e. carboxylmethylaspartate or

nitrilotriacetic) to protein retention has not been resolved as some investigators have claimed the superiority of the former, whilst others have noted no differences in protein retention (reviewed in Arnold, 1991).

Large-scale purification of the N-terminal $His_6$-tagged RV5 NSP4 protein (RV5N) presented with similar problems, but with the Ni-NTA resin. Analyses of the purification fractions illustrated the propensity for approximately half of the $His_6$-tagged protein to remain bound to the resin under pH 8 buffering conditions. This phenomenon was explained when the isoelectric points (pI) of the strain specific NSP4 proteins were determined. The pI of RV5N and RV5C, estimated using Biology Workbench 3.2, were 8.645 and 8.96, respectively. The use of the pH 8.0 buffering system would result in isoelectric precipitation of the protein. Consequently, a pH 7.0 buffering system was employed in the purification of these proteins. In addition, the precipitation of RV5N on the Ni-NTA resin may have been exacerbated by protein aggregation, a consequence of the formation of hydrogen bonds between $His_6$ residues and acidic amino acids, at pH's approaching the pI of the protein (Warwicker and O'Connor, 1995). The inclusion of 0.1% Tween-20 to the buffers would be expected to have prevented protein aggregation.

A buffering system of pH 8.0 was satisfactory for RV4N and RV4C with pI's of 6.884 and 6.932, respectively.

The use of the Bradford Assay for the detection of protein in the elution fractions was essential due to the high concentrations of imidazole included in the elution buffer and compounded by its absorbance, as with protein, at 280 nm. More often than not, the NSP4 elution peak was shielded by a broad imidazole peak on the chromatogram.

#### 2.3.2.3 Optimisation of protein concentration and buffer exchange

IMAC purified protein fractions were pooled and buffer exchange and/or concentration of the samples achieved using Amicon® Ultra-15 Centrifugal Filter Devices (Section 2.2.6.2).

The optimum number of centrifugation steps had to be determined for each of the recombinant protein samples, as after an initial increase in concentration, the concentration invariably decreased with additional centrifugation steps. The loss in protein concentration coincided with an increase in precipitant. The source of the precipitant could be attributed to a number of factors including; aggregation of the protein sample with leached nickel ions from the IMAC column, and/or micelle formation due to Tween-20 or, in the case of the samples to be used for calcium studies, protein aggregation due to the removal of imidazole from the buffer (Hamilton *et al.*, 2003). The histidine residues may also be contributing to protein aggregation through oxidation, the formation of salt bridges, or crosslinkages of metal, histidine and protein residues (reviewed in Hamilton *et al.*, 2003). Zhang *et al.* (1998) encountered difficulties in reconstituting NSP4, at concentrations exceeding 10µg, in PBS. Similar difficulties have been encountered in other laboratories, with NSP4 peptides demonstrating greater solubility (> 1000-fold) than their full-length counterpart (Halaihel *et al*., 2000b).

The most probable explanation for the presence of precipitant would be the formation of NSP4 "multimers", bound by a central $Ni^{+}$; a reaction exacerbated by the removal of imidazole from the buffer. When the precipitant was analysed alongside the soluble fraction by SDS-PAGE, high M.W. bands were notably absent from the latter, indicative of the precipitant being multimers of the NSP4 protein (results not shown).

#### 2.3.2.4 Confirmation of $His_6$-NSP4 expression and antigenicity

The M.W. of the 184 aa non-glycosylated N-terminal $His_6$-tagged RV4 NSP4 (RV4N) and RV5 NSP4 (RV5N) were approximately 21.2 and 21.5 kDa respectively; as estimated using Biology Workbench 3.2. The M.W. of the 220 aa non-glycosylated C-terminal $His_6$-tagged RV4 NSP4 (RV4C) and RV5 NSP4 (RV5C) were similarly determined and were calculated as 25 and 25.3kDa, respectively.

Singly- and doubly-glycosylated forms of the recombinant NSP4 proteins were observed for all constructs. The contribution to the overall M.W. of the incomplete

(singly) and complete (doubly) glycosylated forms of the NSP4 protein were 6 and 8 kDa, respectively (Both *et al.* 1983, Maas and Atkinson, 1990; Zhang *et al.*, 2000).

The size differences were visible by SDS-PAGE (Figure 2.8a) and confirmed the identification of the protein. In addition, Western Blotting demonstrated the antigenicity of the different forms of the protein to α-SA11 polyclonal antibody (Figure 2.8b).

The doubly glycosylated form of the NSP4 protein was most prevalent, with concentrations of the singly and non-glycosylated forms of the protein presenting in the order as listed. The reduced temperatures for *Spodoptera frugiperda* growth in culture is considered responsible for the decreased efficiency of glycosylation observed in insect cells (Tian *et al.*, 1996a).

Western blot analysis of the purified recombinant NSP4 protein fractions revealed the presence of high M.W. bands which were immunoreactive to α-SA11 (Figure 2.8). The source of these high M.W. bands could be credited to the copurification of host proteins; a consequence of disulfide bond formation between host and recombinant proteins. However, as reported elsewhere, the high M.W. proteins most probably resulted from oligomerisation of protein monomers due to native cysteine residues (aa 63 and 71) (Bergmann *et al.*, 1989; Rodriguez-Diaz *et al*., 2003; Tian *et al*., 1996a). Maass and Atkinson (1990) reported that tetramers of NSP4 were the dominant form and that dimers and higher-order structures also persisted. Iosef *et al.* (2002) reported on the elution of multimers of $His_6$-NSP4 at minimal imidazole concentrations of 0.6 M (dimers) and 0.8 M (trimers). The inclusion of β-mercaptoethanol in both the cell lysis buffer and SDS-PAGE-SRB (in association with heating at 100°C) should have reduced all disulphide bonds, eliminating the high M.W. bands; but the persistence of SDS-PAGE resistant oligomers has been reported elsewhere (Hyser *et al*., 2008).

Zhang *et al.* (2000) reported the presence of the 7 kDa enterotoxin, corresponding to aa 112-175 ($NSP4_{112-175}$), within the supernatant and cell lysate of *Sf*9cells expressing full-length SA11 NSP4. A protein of comparable size to the enterotoxin was not observed in the cell lysate in the current study; its absence most probably a consequence of the composition of polyacrylamide gels and electrophoresis conditions employed. Zhang *et*

*al.* (2000) also noted the presence of a 15 kDa cleavage product, consistent with the cytoplasmic domain of the NSP4 protein, resident within the cell lysate. A peptide comparable in size was detected in the cell lysate of *Sf*-21 cells expressing recombinant NSP4 proteins of RV4 and RV5 in this study.

a)

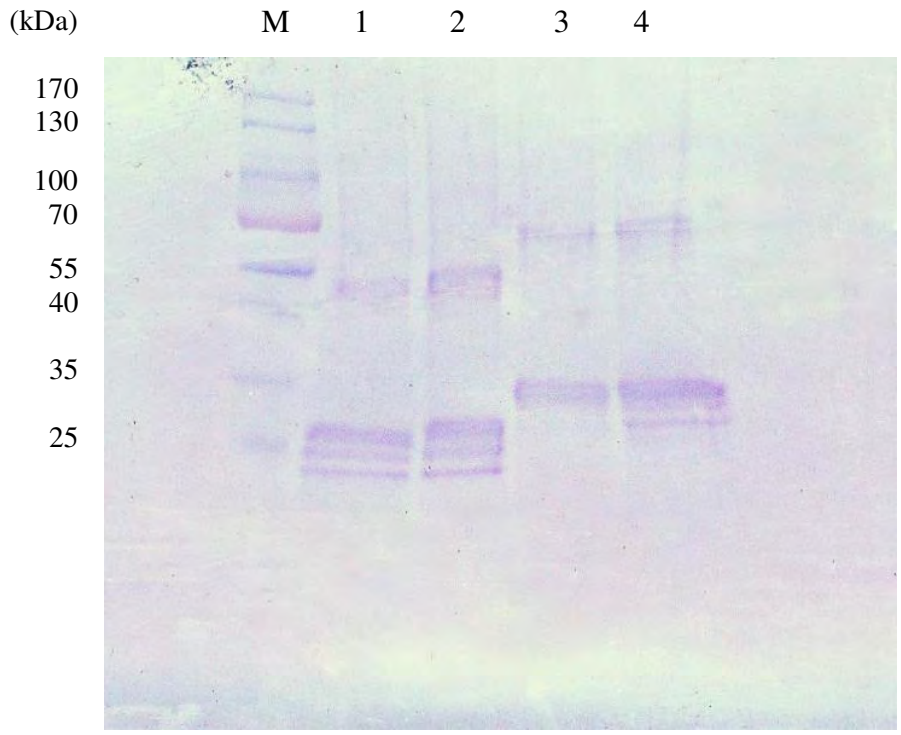

b)

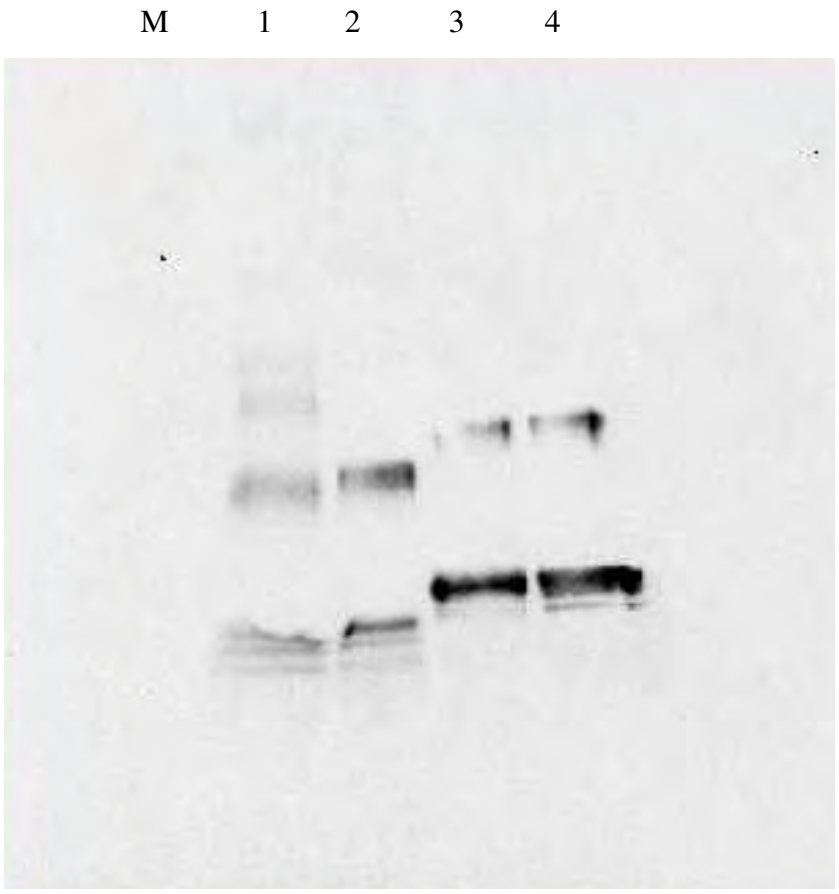


***Figure 2.8. SDS-PAGE (a) and Western blot (b) of $His_6$-NSP4 proteins.*** *Purified recombinant NSP4 proteins were analysed, alongside a prestained marker, by SDS-PAGE and Western blotting. Lane M corresponds to the protein marker (PageRuler™ Prestained Protein Ladder, Fermentas), $L_1$ RV4N, $L_2$ RV5N, $L_3$ RV4C, $L_4$ RV5C. The three bands detected for each recombinant protein corresponded to non-, single- and double-glycosylated forms of the protein. High MW proteins immunoreactive to α-SA11 polyclonal antibodies were also detected for each protein preparation.*

Quantitation of the purified proteins was achieved using the Bradford Assay against a BSA standard. The concentrations of the three glycosylation states, of both monomers and multimers, of the recombinant NSP4 protein contributed to the overall concentration of the protein samples. The estimated concentrations (mg/mL) of the pooled and concentrated (Amicon® ultrafiltration) protein samples have been recorded

in Table 2.2. Separate samples were prepared for use in ELISA development and calcium studies as per the reasons previously discussed (Section 2.2.6.2).

The ELISA fractions were approximately 10-fold less concentrated compared with the samples prepared for the $Ca^{2+}$ analysis component of this study. Such differences could be attributed to the differences in diluent in which the proteins were reconstituted, or may simply reflect the number of samples pooled for their preparation.

***Table 2.2. Quantitation of $His_6$-NSP4 concentration.*** *The concentration of the pooled and concentrated $His_6$-NSP4 proteins was quantitated with the Bradford Assay against a BSA standard. The $Ca^{2+}$ fractions had been reconstituted in imidazole free buffer, whilst the ELISA fractions had been concentrated in elution buffer (250mM imidazole). The concentrations as tabulated were the average of three independent measurements performed for each protein fraction.*

| | **$Ca^{2+}$ Fractions (mg/mL)** | **ELISA Fractions (mg/mL)** |
|---|---|---|
| **RV4C** | 0.48 | 0.06 |
| **RV4N** | 0.84 | 0.06 |
| **RV5C** | 1.01 | 0.14 |
| **RV5N** | 1.28 | 0.13 |

Clustal W sequence homology was performed for the recombinant NSP4 proteins against amino acid sequences of RV4 NSP4 (Accession number U59103.1) and RV5 NSP4 (Accession number U59108.1) imported from GenBank using Biology Workbench 3.2. This analysis confirmed no changes in the integrity of the sequences of the $His_6$-NSP4 proteins prepared in this study.

## 2.4 Summary

Recombinant baculovirus transfer vectors bearing the NSP4 gene of prototype HRV strains RV4 and RV5 were generated from intermediate plasmids using general molecular biology techniques. The NSP4 cassette was successfully transferred from the recombinant baculovirus transfer vectors to the baculovirus genome *via* homologous recombination in the insect cell line *Sf*-21. PCR screening of plaque purified isolates successfully identified the recombinant NSP4 baculoviruses.

The BEVS was employed to produce four recombinant $His_6$-tagged NSP4 proteins. For both strains investigated C- and N-terminal $His_6$-NSP4 fusion proteins were produced. Maximal production of the recombinant proteins was achieved when *Sf*-21 cells were inoculated at an M.O.I. of 1 pfu/mL and the protein harvested at 48 h.p.i.

Purification of the $His_6$-NSP4 proteins from endogenous insect cell lysate was achieved using Ni-NTA IMAC and an imidazole gradient (20 to 250 mM imidazole). The purification of RV4 and RV5 $His_6$-NSP4 proteins was achieved using a pH buffering system of 8 and 7 respectively due to differences in the isoelectric point (pI) of the proteins.

The $His_6$-tagged NSP4 proteins existed as three glycoforms (non-, singly- and doubly-glycosylated) as illustrated by SDS-PAGE and all forms of the protein were antigenic as determined by Western blotting. High M.W. and antigenic multimers of the NSP4 glycoforms were also detected.

The purified proteins were subsequently used for the development of an α-NSP4 specific ELISA (Chapter 3) and for calcium signalling studies (Chapter 4).

# 3

# Immunogenicity of NSP4

## 3.1 Introduction

The immune response to rotavirus (RV) infection is complex and suggestive of both humoral and cell-mediated involvement in disease clearance and protection. The development of mucosal immunity is considered to be the most important marker of RV infection.

The involvement of the RV non-structural protein NSP4 in protective immunity against disease and reinfection is still under investigation. Antibodies to NSP4 or to a synthetic peptide spanning the enterotoxin domain have provided protection from diarrhoeal illness upon virus challenge. Pups born to dams vaccinated with $NSP4_{114-135}$ or a plant-based multicomponent vaccine expressing $NSP4_{114-135}$ were passively protected from virus challenge, whilst oral administration of α-$NSP4_{114-135}$ antibodies reduced diarrhoeal illness in newborn mice (Ball *et al*., 1996; Yu and Langridge, 2001).

The extent to which NSP4 elicits a humoral immune response is still under debate as isotype-specific responses to NSP4 of children naturally infected with RV or to vaccine candidates have generated conflicting results: particularly in regards to the detection of NSP4-specific serum IgA (Johansen *et al*., 1999; Ray *et al*., 2003; Rodriguez-Diaz *et al*., 2005; Yuan *et al*., 2004b). Serum IgG directed towards NSP4, although detected in all published reports, has returned variable responses ranging from weak to very strong (Johansen *et al*., 1999; Ray *et al*., 2003; Rodriguez-Diaz *et al*., 2005; Yuan *et al*.,

2004b). The source of these anomalies may be attributed to differences in the sensitivity of the detection systems employed.

The question still remains as to whether NSP4 offers cross-reactive protection. Studies performed on gnotobiotic piglets and calves demonstrated that antibody responses to NSP4 were species-specific rather than genotype-specific (Yuan *et al*., 2004a) and that the heterotypic responses to NSP4 observed in the convalescent sera of naturally-infected (Ray *et al*., 2003; Richardson *et al*., 1993; Rodríguez-Díaz *et al*., 2005) and vaccinated children (Yuan *et al*., 2004b) may be attributable to maternal antibody interference and previous exposure to wild-type RV infection. Further investigation using immunologically naïve, colostrum-deprived gnotobiotic animals should help to elucidate the cross-reactivity of the NSP4 protein.

In addition to its ability to provoke a humoral response, NSP4 cellular-mediated immune responses have also been established. Johansen *et al*. (1999) demonstrated for the first time in adult humans, the ability of NSP4 to stimulate a cellular immune response involving IFN-γ and IL-2, and potentially cytolytic T-cells. Similar Th1 responses to NSP4 were observed in mice (Choi *et al*., 2006b; Kim *et al*., 2004; Yu and Langridge, 2001). More recently Malik *et al*. (2008) demonstrated that IFN-γ responses in humans were transient and higher in subjects previously exposed to RV.

The objective of this study was to develop and validate a sensitive and specific ELISA for the detection of antibodies to NSP4 in human sera. The patient samples analysed (acute and convalescent) were a subset from an extensive longitudinal study of children naturally infected with RV (Richardson *et al*., 1993; Grimwood *et al*., 1998). In addition, serum samples collected from children vaccinated with the Rotarix® vaccine were investigated. Unfortunately, very little information was available as to the history of the vaccine samples, albeit that they were positive for RV antibodies and collected after two doses of vaccine.

The ELISA would then be used to assess which recombinant protein configuration (N- or C-terminal $His_6$-tagged NSP4) was the most reactive such that the appropriate antigen could be used for the calcium signaling component of this research (Chapter 4).

In addition, the ELISA was used to identify a serum sample which contained high levels of α-NSP4 antibodies which could be utilised for studies of NSP4 neutralization and intracellular calcium mobilization effects.

## 3.2 Methods

### 3.2.1 ELISA development

#### 3.2.1.1 Generic ELISA format

The protocol outlined below was applied in the optimisation of the NSP4-specific ELISA and, when established, for the testing of α-NSP4 IgG and IgA within patient sera (Section 3.2.2).

Corning® high binding 96 well microtitre plates were coated with 100 µl of recombinant NSP4 (in 0.06 M sodium carbonate-bicarbonate buffer; pH 9.6), and the plates incubated overnight at 4°C. All test samples and controls were plated in triplicate unless noted otherwise.

Unbound antigen was removed by five washes with 0.05% (v/v) Tween-20 in PBS (PBS-T) (pH 7.4) and unbound sites blocked with 50 µl of blocking buffer at room temperature for 1 hour (or as specified). Plates were washed as described previously and 50 µl of the appropriately diluted primary antibody (1° Ab) added. The antibody diluent was blocking buffer unless reported otherwise. The plates were incubated for 1 hour at 37°C.

The plates were washed as described previously and 100 µl of the appropriately diluted conjugated antibody added. The plates were incubated for 1 hour at 37°C. The wash step was repeated and 100 µl of 3,3',5,5'-Tetramethylbenzidine (TMB; Sigma) substrate solution (0.1 mg/mL in 98.5 mM sodium acetate, 1.48 mM citric acid, containing 1.2 µl of 30% $H_2O_2$ per 10 mL) added to each well. The plates were incubated at room temperature for 10 minutes in the absence of light. The reaction was stopped with 2 M $H_2SO_4$ and the optical density (OD) measured at $\lambda_{450nm}$ using the EMax® Precision

Microplate Reader and SoftMax Pro 4.6 Software (Molecular Devices, Bio-Strategy Pty. Ltd., AUS).

#### 3.2.1.2 ELISA optimisation

The following parameters were investigated in the optimisation of an α-NSP4 ELISA in accordance with the guidelines proposed by Crowther (2001). All ELISA's were performed as directed in Section 3.2.1.1 and the appropriate parameters adjusted as follows.

- **Establishment of the saturating concentration of the coating antigen (NSP4)**

Recombinant $His_6$-NSP4 proteins (RV4C, RV5C, RV4N and RV5N) derived from prototype HRV strains RV4 and RV5 were used as coating antigen. The construction, expression and purification of these recombinant proteins was described in Chapter 2.

The saturation concentration was determined empirically for all recombinant protein samples using a standard checkerboard titration (CT) format. Briefly, serial two-fold dilutions of the coating antigen was assayed against the reference antibody, hyperimmune α-SA11-polyclonal antibody raised in rabbits (Richardson *et al*., 1998) diluted 500-fold. The concentration of the secondary antibody (2° Ab) HRP-conjugated donkey anti-rabbit IgG (GE Healthcare BioSciences) was held constant (1/5000).

- **Determination of the optimum HRP-conjugated antibody concentration**

A CT was performed to establish the optimum concentration of HRP-conjugated sheep anti-human IgG(γ) (Chemicon) and HRP-conjugated rabbit anti-human IgA(α) (DakoCytomation). Wells were coated with saturating concentrations of either C-terminal $His_6$-NSP4 of RV4 (RV4C) or RV5 (RV5C) (as determined previously). Patient sera (positive for anti-RV antibodies) was diluted 100-fold and used as the primary antibodies. For the IgG assay, dilutions of the order of 1:10,000, 1:15,000, 1:17,500, 1:20,000 and 1:25,000 were performed for the conjugate. For the IgA assay,

dilutions of the order of 1:200, 1:400, 1:800 and 1:16,000 were conducted for the conjugate.

The positive sera was selected from sample sets of individuals who had previously returned a positive response for the presence of anti-RV antibodies in an EIA (work performed by the Enteric Virus Research Group, Murdoch Children's Research Institute (MCRI), Parkville). These results were verified using saturating concentrations of RV4C or RV5C and HRP-conjugated sheep anti-human IgG(γ) and HRP-conjugated rabbit anti-human IgA(α) diluted 1:17,5000 and 1:800, respectively.

#### 3.2.1.3 Improvement of assay sensitivity – background noise reduction

- **Selection of blocking buffer and antibody diluent**

The effectiveness of the blocking agents, BSA (96.99% Albumin Fraction V; Sigma), Carnation Non-fat Dry Milk (NFDM) and Casein from bovine milk (Sigma), in background noise reduction and concomitant increase in signal strength was investigated. The inclusion of the blocking agents at variable concentrations in both the blocking buffer and antibody diluent was examined.

The following blocking buffer compositions (% (w/v) in PBS-T) were investigated for each of the blocking agents; BSA (1%), Casein (0.5, 1, 2 and 5%) and NFDM (0.5, 1, 5 and 10%). Similarly, the inclusion of these formulations as the antibody diluent was also investigated. The assay was conducted using positive patient sera as the 1°Ab and HRP-conjugated sheep anti-human IgG(γ) as the 2°Ab. Carbonate-coated wells were prepared as controls.

- **Effect of Tween-20 in the blocking buffer and antibody diluent**

The effect of Tween-20 in both the blocking buffer and antibody diluent was also explored using a modified method of Vogt *et al.* (1987). Briefly, wells of a microtitre plate were coated with differing compositions of blocking buffer (0.5, 1, 2, 5 and 10% NFDM (w/v)) in either PBS or PBS-T. The 2°Ab, rabbit α-human IgA-HRP was diluted

800-fold in the appropriate blocking buffer in the presence/absence of Tween-20. Refer to Table 3.2 for the various diluent and blocker configurations analysed.

- **Temperature**

The effect of temperature on assay precision was investigated. Plates were prepared in duplicate as described in the preceding section and incubated at either 25°C or 37°C for each incubation step.

#### 3.2.1.4 Assay validation

- **Feasibility of the assay**

Once the ELISA had been optimised, the feasibility of the method was determined by performing the assay on matched pairs of acute and convalescent sera obtained from children naturally infected with RV.

- **Inter- and intra-run assay variability**

The inter- and intra-run assay variability was investigated upon establishment of the optimal conditions for the ELISA. The coating antigen was recombinant RV4C (10 wells/plate) or coating buffer. The 1°Ab was sera previously determined to be positive for α-NSP4 IgG antibodies and the conjugate, HRP-conjugated sheep anti-human IgG(γ).

## 3.2.2 Indirect ELISA for the detection of NSP4-specific antibodies in human sera

### 3.2.2.1 Subjects and serum samples

The sera of children naturally infected with a primary RV infection were kindly provided by Dr Carl Kirkwood of the MCRI. The matched paired sera were obtained from children who presented at the Royal Children's Hospital, Parkville, with severe acute diarrhoea and RV was identified as the causative agent. The acute-phase sera were collected within 3-7 days (median 6 days) postinfection and the convalescent-phase sera within 28 to 43 days (median 34 days) postinfection (Grimwood *et al*., 1998). In addition a subset of samples (6 samples/candidate) procured from longitudinal studies of three children, sampled approximately every 3 months over a 2-3 year period were also investigated for the presence of α-NSP4 antibodies.

Vaccine samples were obtained after the administration of the second dose of Rotarix® and were provided by Glaxo-Smith Kline (GSK), Belgium.

### 3.2.2.2 ELISA for the detection of α-NSP4 IgG and IgA in sera

The protocol as outlined below was used for the detection of α-NSP4 IgG and IgA within patient sera.

Corning® high binding 96 well microtitre plates were coated with either 100 µl of (a) recombinant NSP4 diluted in coating buffer (0.06 M sodium carbonate-bicarbonate buffer; pH 9.6) at saturating concentration or (b) coating buffer (control wells), and the plates incubated overnight at 4°C. All test samples and controls were analysed in triplicate unless noted otherwise.

Unbound antigen was removed by five washes with PBS-T (pH 7.4) and unbound sites blocked with 50 µl of blocker, 0.5% (w/v) NFDM in PBS-T, at room temperature for 1 hour. Plates were washed as described previously and 50 µl of a 100-fold dilution of

patient serum diluted in blocker added to each well. The plates were incubated for 1 hour at 37°C.

The plates were washed as described above and 100 µl of the appropriately diluted conjugated antibody added. Secondary antibodies were: HRP-conjugated sheep anti-human IgG(γ) and HRP-conjugated rabbit anti-human IgA(α) used at 1:17,500 and 1:800 respectively. The plates were incubated for 1 hour at 37°C. The wash step was repeated and 100 µl of TMB substrate solution added to each well. The plates were incubated at room temperature for 10 minutes in the absence of light. The reaction was stopped with 2 M $H_2SO_4$ and the absorbance measured on a plate reader at $\lambda_{450nm}$ using SoftMax Pro 4.6 Software.

### 3.2.3 Statistical analysis

Data was analysed using the Excel Statistical Package, PHStat2 (Prentice Hall Inc, Australia, 2003). Paired student t-tests were used to assess the contribution of Tween-20 in both the blocking agents and antibody diluent at differing NFDM compositions and for comparisons of the antibody response to NSP4 in acute and convalescent sera of matched pairs. Statistical significance was determined at $p < 0.05$ for all analyses in this study.

## 3.3 Results and Discussion

### 3.3.1 Assay development

#### 3.3.1.1 Determination of the minimum saturating concentration of coating antigen

The determination of the minimum saturation concentration for each antigen was established using the reference 1°Ab, α-SA11, and HRP-conjugated donkey anti-rabbit IgG (2°Ab). This detection system was used in preference to the patient sera due to the limited volume of sample available.

The saturating concentration for each of the recombinant NSP4 proteins (per 100 µl) was determined to be 1.5 µg RV4C, 0.3 µg RV4N, 0.7 µg RV5C and 0.65 µg RV5N.

#### 3.3.1.2 Optimization of the ELISA: eliminating background interference

- **Selection of blocking buffer and antibody diluent**

Three different proteins, BSA (96.99% Albumin Fraction V), Carnation Non-fat Dry Milk (NFDM) and casein were investigated for their efficacy as blocking agents and antibody diluents in this assay.

An increase in casein concentration in both the blocking agent and antibody diluent resulted in an overall reduction in background, as measured by the OD of the carbonate coated wells. Unfortunately, this also coincided with a decline in the OD of the corresponding antigen coated wells, and consequently an overall loss in the net OD (OD test sample - OD corresponding control). Under the conditions investigated, the optimum combination of casein as antibody diluent and blocker was determined to be 0.5% (w/v) in PBS-T (data not shown).

BSA generated consistently high background, the source of which was either cross-reactivity to α-phosphotyrosine antibodies or to RV-specific immunoglobulins in human

sera (Gibbs, 2001). In the absence of coating antigen and sera, the background was comparable when 0.5% casein (PBS-T) and 1% BSA were used as the blocking agents, indicative of the background contribution of serum components.

NFDM, the superior blocking agent in these experiments, also contains phosphotyrosine, which would be expected to be cross-reactive with α-phosphotyrosine antibodies within sera. However, NFDM gave consistently lower background and greater signal for antigen coated wells compared with the other blocking agents investigated. When the concentration of NFDM was increased in both the antibody diluent and blocking buffer a decrease in signal strength (Table 3.1) or increase in background noise (Figures 3.1a and 3.1b) was observed. This phenomenon may be explained by the masking of antibody:antigen interactions and/or the inhibition of the enzyme conjugate by excessive amounts of blocking agent (Pierce ELISA and ELISPOT Products Handbook and Technical Guide).

The greater efficacy of both casein and NFDM (in comparison with BSA) as a blocking agent in immunoassays has been well documented (Kaur *et al*., 2002; Vogt *et al*., 1987). Vogt *et al*. (1987) demonstrated that both Casein and NFDM afforded greater than 90% blocking of non-specific binding to polystyrene microtitre plates.

***Table 3.1. Efficacy of casein, BSA and NFDM as antibody diluents and blocking agents.*** *The concentrations of casein and BSA were held constant at their previously determined optimal concentration. The concentration of NFDM was varied. The net OD value is the difference in OD between the experimental well (coated with RV4C) and the control well (carbonate buffer). The primary antibody was convalescent sera from a naturally infected child which was positive for α-RV antibodies. The secondary antibody was HRP-conjugated sheep anti-human IgG(γ).*

| | OD with | | | | | |
|---|---|---|---|---|---|---|
| **Blocking agent and antibody diluent** | Casein 0.5% | BSA 1% | NFDM 0.5% | NFDM 1% | NFDM 5% | NFDM 10% |
| **Coating: RV4C** | 0.494 | 1.079 | 0.699 | 0.582 | 0.702 | 0.776 |
| **Coating: Carbonate** | 0.210 | 0.938 | 0.274 | 0.211 | 0.377 | 0.560 |
| **Net OD** | 0.284 | 0.141 | 0.425 | 0.371 | 0.325 | 0.216 |

The contribution of patient sera to background noise varied for each test sample; a consequence of serum immunoglobulin-related interferences which could include (a) the presence of human α-human antibodies, (b) non-specific immunoglobulin interactions and (c) serum factors binding and interfering with Ig detection (Maple *et al*., 2004). A number of authors have reported similar effects and the methods employed to combat serum interference are extensive and varied. Of interest are the findings of Kenna *et al.* (1985) who noted that IgG of human sera (and not animal) adsorbed with greater affinity to the solid phase than casein and that the inclusion of the antimicrobial agent Thimersol in the buffering system reduced such background. They speculated that the inclusion of Thimersol reduced the binding of human antibodies to potential microbial contaminants in the buffer which would compete with casein for blocking sites.

- **The effect of Tween-20 in the blocking buffer and antibody diluent**

The use of Tween-20 in both the antibody diluent and blocking buffer was investigated, as it has been reported that its inclusion negates the effects of the proteinaceous blocking agent and should be restricted to the washing step proceeding the addition of the conjugate (Esser, 1997). Julián *et al.* (2001) reported that the inclusion of Tween-20 resulted in a loss of signal, presenting as false negatives, for ELISA's of four glycolipids of the cell wall of *Mycobacterium tuberculosis*. In the assays conducted in this research it was demonstrated that the inclusion of Tween-20 in NFDM blocking systems had very little effect on background noise when the composition of both the blocking agent and antibody diluent was at concentrations ≤ 2% for the assay performed at 25°C and at concentrations ≤ 1% when performed at 37°C. When the NFDM concentration in both the blocker and antibody diluent exceeded these concentrations, the inclusion of Tween-20 caused a significant increase in background noise ($p < 0.05$) irrespective of the operating temperatures of the assays. These results are presented in Figures 3.1a (assay performed at 25°C) and 3.1b (assay performed at 37°C).

- **Temperature**

The effects of blocking at 37°C and 25°C were investigated for NFDM using varying blocking buffer compositions (Table 3.2). When blocking was performed at 37°C a small number of erroneous high OD values, not observed for plates incubated at 25°C, were reported. Upon the exclusion of these outliers, there was no statistically significant difference ($p > 0.05$) in OD in performing the incubation steps at either of these temperatures when Tween-20 was included in the diluent and blocking buffer (Figures 3.1a and 3.1b). In the absence of Tween-20, all but two samples (1 and 4) returned differing OD values of statistical significance when incubated at the two different temperatures. Generally, the inclusion of Tween-20 and an increase in the NFDM composition of both the blocker and diluent at concentrations exceeding 2% (w/v) caused an increase in noise observed for both temperatures, but was greater when blocking was performed at the higher temperature. An association between background noise and increases in NFDM concentration had been demonstrated previously (Table 3.1). Despite contributing marginally to the background noise, the inclusion of Tween-20 in the antibody diluent and blocking buffer was considered necessary due to apparent temperature induced changes in OD in its absence.

a)

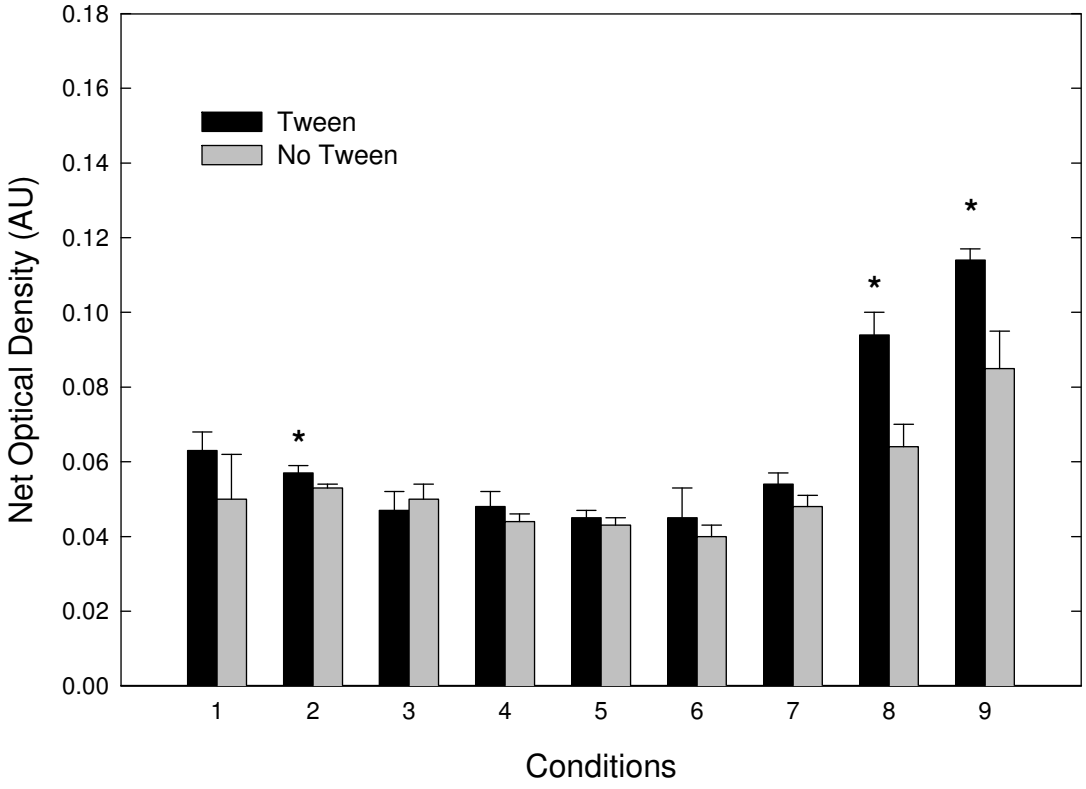
Tween
No Tween
Net Optical Density (AU)
0.18
0.16
0.14
0.12
0.10
0.08
0.06
0.04
0.02
0.00
1
2
3
4
5
6
7
8
9
Conditions
*
*
*

b)

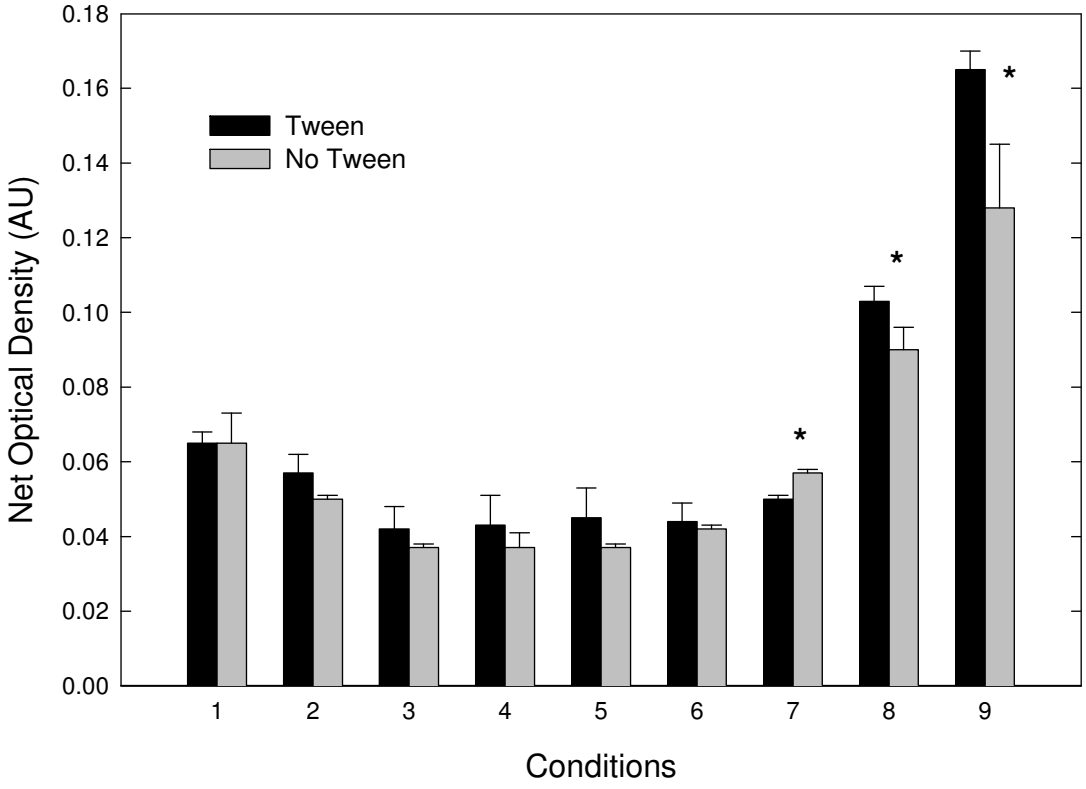


***Figure 3.1. The contribution to background noise by Tween-20 in an ELISA performed at (a) 25℃ and (b) 37℃.*** *The mean and standard deviation, as graphed, were calculated from triplicate measurements for each test sample investigated. A paired t-test was used to assess whether the presence of Tween-20 reduced the background noise when included in both the blocking buffer and antibody diluent. Differences at critical levels of $p<0.05$, were considered statistically significant and are represented by an asterisk (*). Statistical analysis was performed using the Excel Statistical Package PHStat2. The composition of blocking agent and antibody diluent for each condition (1, 2 etc, presented on the horizontal axis) have been tabulated (Table 3.2).*

***Table 3.2. The composition of NFDM in the antibody diluent and blocking buffer.*** *Each of these conditions was assayed in the investigation of the contribution of Tween-20 to background noise and assay performance at different operating temperatures (37℃ and 25℃).*

| Condition | Antibody Diluent (% NFDM) | Blocking Agent (% NFDM) |
|---|---|---|
| **1** | 0.5 | 10 |
| **2** | 0.5 | 5 |
| **3** | 0.5 | 2 |
| **4** | 0.5 | 1 |
| **5** | 0.5 | 0.5 |
| **6** | 1 | 1 |
| **7** | 2 | 2 |
| **8** | 5 | 5 |
| **9** | 10 | 10 |

Collectively, these results suggested that the optimum operating conditions for this ELISA would require the blocking step to be performed at 25°C with the inclusion of Tween-20 (0.05%) in both the blocking agent (0.5% NFDM) and antibody diluent (0.5% NFDM).

- **Extraneous effects**

On occasion, high background OD readings were observed for a single well in sample replicates which could not be accounted for by technique or experimental error. Rebeski *et al*. (1999) discussed the prevalence of high background, randomly distributed and associated with non-specific protein adsorption in γ-irradiated high binding polystyrene plates. They proposed that the irradiation procedure may not be uniform and reproducible, contributing to varying degrees of hydrophobic and hydrophilic binding sites across the wells. Gamma irradiation of polystyrene induces an increased polarity of the hydrophobic solid phase, generating additional binding sites relative to hydrophobic groups (Rasmussen, 1998).

#### 3.3.1.3 Assay validation

- **Feasibility of the assay**

The feasibility of the assay was determined by investigating matched serum pairs (acute and convalescent) and sera obtained from longitudinal studies of children naturally infected with RV. The results obtained from the assays were consistent with the information provided by the MCRI regarding the presence or absence of detectable RV antibodies where detected (Table 3.3).

- **Inter and intra run assay variability**

For repeatability data, the coefficient of variation (CV) for replicates should not exceed 10% (Crowther, 2001). The CV was calculated to be 0.22% for the intra and inter assay variability in this study.

### 3.3.2 Isotype-specific response to NSP4 in human sera

Plates were coated with either recombinant C terminal $His_6$-tagged NSP4 from RV strains RV4 (P1A[8]G1, II) or RV5 (P1B[4]G2, I). RV5 and RV4 belong to NSP4 genogroups A and B, respectively. The aims of this study were two-fold: firstly, to demonstrate whether NSP4 elicits a humoral response in children naturally infected with RV and secondly, to assess whether this response is homotypic and/or heterotypic. Once the isotype-specific response to NSP4 had been established the ELISA would be used to investigate whether two doses of an attenuated human vaccine elicited α-NSP4 IgG and IgA responses and whether these responses were cross-reactive.

#### 3.3.2.1 Isotype-specific response to NSP4 in the sera of children naturally infected with RV

Table 3.3 summarises the patient histories for the matched pairs of acute and convalescent sera for children naturally infected with RV. Using the ELISA developed in this study, the sera was identified as positive or negative to α-NSP4 IgG and IgA using RV4C and RV5C as the coating antigens. Test samples were considered positive if the OD in the experimental well (coated with antigen) was >0.1 OD unit and two-fold greater than the OD in the corresponding control well (carbonate buffer) (Moser *et al*., 1998; Rojas *et al*., 2007). The net OD (OD test sample - OD corresponding control) was calculated for each sample. Figure 3.2 summarises the ELISA results obtained for the detection of NSP4-specific IgG (3.2a) and NSP4-specific IgA (3.2b) for matched pairs of acute and convalescent sera of naturally infected children. All acute sera was negative for the presence of α-NSP4 antibodies, indicative that (a) the children had not had prior exposure to RV, or if exposed was of a serotype distinct from the strains assayed or (b) the α-NSP4 titre was below the sensitivity of the assay. Of the nine patient samples assayed, 89% seroconverted to NSP4.

a)

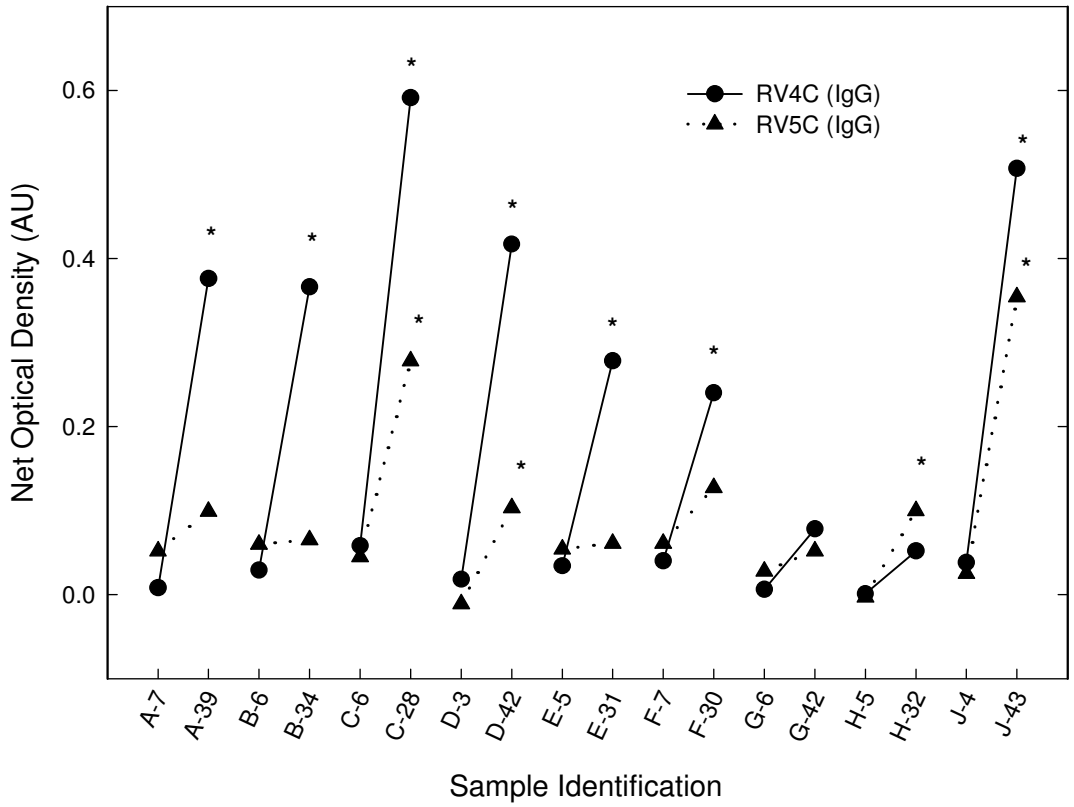
RV4C (IgG)
RV5C (IgG)
Net Optical Density (AU)
0.0
0.2
0.4
0.6
A-7
A-39
B-6
B-34
C-6
C-28
D-3
D-42
E-5
E-31
F-7
F-30
G-6
G-42
H-5
H-32
J-4
J-43
Sample Identification

b)

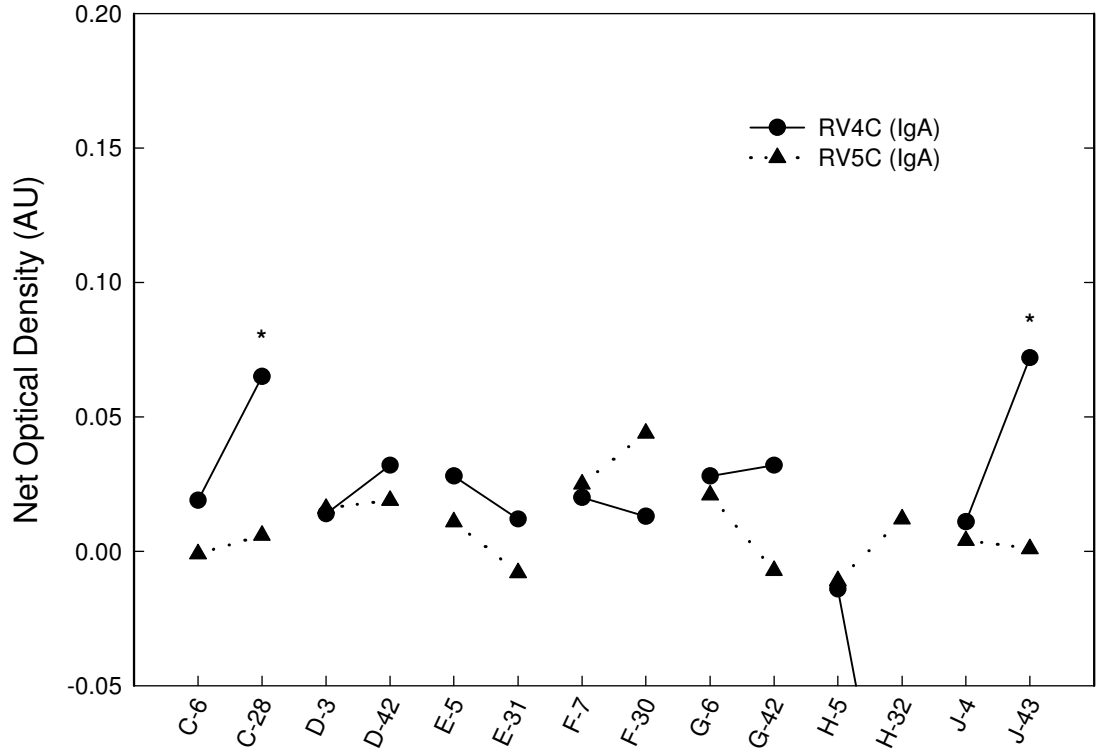


***Figure 3.2. α-NSP4 isotype-specific humoral response in children naturally infected with RV.*** *Figures (a) and (b) illustrate the α-NSP4 IgG and α-NSP4 IgA response respectively. The patient histories corresponding to all samples assayed are recorded in Table 3.3. The acute and convalescent sera for each sample are distinguished graphically by the assignment of a letter proceeded by a number denoting the days post infection in which the sera was obtained. The first value in each subset corresponds to the acute sera and the second value, the convalescent. The assay was conducted using either RV4C (●) or RV5C (▲) as the coating antigen. Serum samples were assigned as positive (*) if the OD in the experimental well was >0.1 OD unit and two-fold greater than the OD in the corresponding control well.*

***Table 3.3. Patient histories for children naturally infected with rotavirus.*** *This information was provided by Dr Carl Kirkwood of the MCRI. Where known, the serotype of the infecting RV strain was recorded. Days post infection refers to the number of days after infection when sera was taken.*

| Sample | Serotype of Infecting Rotavirus Strain | Days post infection | Days post infection |
|---|---|---|---|
| A | Serotype Unknown | Day 7 | Day 39 |
| B | G1 | Day 6 | Day 34 |
| C | G1/4 | Day 6 | Day 28 |
| D | G1 | Day 3 | Day 42 |
| E | G1 | Day 5 | Day 31 |
| F | Serotype Unknown | Day 7 | Day 30 |
| G | G4 | Day 6 | Day 42 |
| H | G1 | Day 5 | Day 32 |
| J | G1 | Day 4 | Day 43 |

Seroconversion has been defined as a ≥ 3-fold rise in α-NSP4-specific antibody titres between acute and convalescent sera of children naturally infected with RV, or pre and post vaccination sera in vaccine recipients (Ray *et al*., 2003; Vizzi *et al*., 2005). As the quantity of sera was limited in this study, the establishment of the antibody titre was not pursued. Therefore the absence of detectable α-NSP4 in the acute sera and the presence of NSP4-specific antibodies in the convalescent sera was considered to be indicative of "seroconversion".

***Table 3.4. Isotype-specific seroconversion to NSP4 for children naturally infected with RV.*** *The IgG and IgA seroconversion to NSP4 of prototype RV strains RV4 and RV5 of children naturally infected with RV was determined using the α-NSP4 ELISA. The serotypes of the infecting strains were provided by the MCRI. Both the absolute and percentile (brackets) values have been recorded for each test condition assayed.*

| | **Infecting Serotype (G1)** | | **Infecting Serotype (G4)** | | **Infecting Serotype (Nondefined)** | | **Dual Infection (G1/G4)** | |
|---|---|---|---|---|---|---|---|---|
| **Coating Antigen** | IgG | IgA | IgG | IgA | IgG | IgA | IgG | IgA |
| RV4C (G1) | 4/5 (80%) | 1/4 (25%) | 0/1 (0%) | 0/1 (0%) | 2/2 (100%) | 0/1 (0%) | 1/1 (100%) | 1/1 (100%) |
| RV5C (G2) | 3/5 (60%) | 0/4 (0%) | 0/1 (0%) | 0/1 (0%) | 0/2 (0%) | 0/1 (0%) | 1/1 100% | 0/1 0% |

The IgG response to NSP4 (60-80%) for G1 infections in the subset of patient sera analysed in this study is consistent with the findings (67-100%) of Richardson *et al*. (1993). The authors used radioimmunoprecipitation (RIP) to detect α-NSP4 IgG within these serum samples and found that the frequency of NSP4 (G1) and NSP4 (G2) which coprecipitated with G1-derived NSP4 antibodies was 80 and 60% respectively. Richardson *et al*. (1993) noted that NSP4 from a G2 strain failed to immunoprecipitate with serum samples of children infected with a G4 strain, but was recognized by 67% of serum samples of children infected with a G1 RV. In this study, NSP4 of both G1 and G2 origin failed to react with the serum sample of a G4 infected patient. Unfortunately, only a single G4 infection sample was available for this study.

As transplacentally acquired maternal Abs are typically of the IgG isotype, the presence of serum IgA Abs in infants is suggestive of an active humoral response to vaccination or natural exposure. Serum IgA levels are indicative of the IgA responses at the mucosal surface of the small intestine and consequently, indirectly correlate with protective immunity to RV disease in humans and animals (To *et al*., 1998; Velazquez *et al*., 2000; Yuan *et al*., 2004a; 2004b).

The response for α-NSP4 IgA was much lower than for IgG, with only 29% seroconversion observed across all samples analysed, and restricted to G1 NSP4 and a G1/G4 dual infection. This result was expected as IgG constitutes the dominant form of serum Ab and the absence of an NSP4-specific IgA response has been reported previously by others (Ishida *et al*., 1996; Johansen *et al*., 1999; Rodríguez-Díaz *et al*., 2005; Yuan *et al*., 2004a). Using full-length NSP4 of RV strains Wa (genotype B) and SA11 (genotype A) as antigens, Rodríguez-Díaz *et al*. (2005) failed to detect an α-NSP4 IgA response in the sera of convalescent children naturally infected with RV, whilst a weak NSP4-specific IgG response was detected. Johansen *et al*. (1999) reported similar responses in naturally-infected and RRV-TV-vaccinated children to both full-length SA11 NSP4 and a synthetic peptide ($NSP4_{114-134}$) corresponding to the enterotoxin domain. In contrast, a significant NSP4-specific IgA response in both post vaccination sera and convalescent sera of naturally children has been documented by others (Ray *et al*., 2003; Vizzi *et al*., 2005; Yuan *et al*., 2004b).

Studies performed on animal models also suggest that the α-NSP4 response is weak. An immunocytochemistry assay failed to detect IgA to NSP4 in the stool samples of adult mice infected with an homologous wild-type virus, and the corresponding IgG titres were low (Ishida *et al*., 1996). Infection of gnotobiotic calves with a homologous bovine RV (NCDV) yielded little to no detectable NSP4-specific IgA, despite performing the assay with limited dilutions of sera to the order of 1:4 (Yuan *et al*., 2004a). The inoculation of gnotobiotic piglets with either attenuated or virulent forms of the HRV strain Wa evoked only a small number of ASCs specific for NSP4 (Chang *et al*., 2001b).

Differences in assay design and reagents used have been associated with variances in the levels of detectable α-NSP4 antibodies due to apparent disparities in assay sensitivity. In two of the studies which demonstrated a significant NSP4-specific IgG and IgA response (Ray *et al*., 2003; Vizzi *et al*., 2005) the ELISA's were conducted using GST fusion peptides encompassing the cytoplasmic domain of NSP4 (~aa 85-175) as the coating antigen. The capturing of $NSP4_{85-175}$-GST fusion proteins by the immobilization of glutathione to the wells of a 96 well plate was suggested to preserve the antigen conformation in a more native fashion than observed by direct adsorption of

the antigen to 96 well plates (Vizzi *et al*., 2005). The immunocytochemistry assay conducted by Yuan *et al*. (2004b) returned significant IgA-specific antibody responses to full-length NSP4 and the authors reported that this assay is highly sensitive for the detection of antibodies to both conformation-dependent and independent epitopes. Ray *et al*. (2003) used biotin-conjugated α-human IgA and HRP-conjugated avidin-biotin for the detection of α-NSP4 IgA-specific antibodies, which may have improved the sensitivity of the assay.

A limiting factor in the sensitivity of the α-NSP4 ELISA's developed in this study may have been the high dilutions (1/100) performed for the patient sera, particularly for the α-NSP4 IgA ELISA. Yuan *et al*. (2004b) and Johansen *et al.* (1997) measured the titres of α-NSP4 IgA from the same serum samples (RRV-TV vaccine recipients) using an immunocytochemistry assay and ELISA respectively. Yuan and co-workers reported that the starting dilution of 1:100 for the IgA ELISA conducted by Johansen *et al.* may have been too high, as their investigation was performed with dilutions of 1:4. Yuan *et al.* (2004b) also reported that differences between the NSP4 genotype of the detecting antigen and that of the vaccine strain may also be responsible for variances in the level of detectable antibody titres. This statement is consistent with the results observed in this study, whereby ELISA's coated with the RV4 NSP4 antigen derived from a similar strain (G1) to the infecting viral strains elicited a higher rate of seroconversion in the samples analysed.

Overall, studies which detected IgA against NSP4, also reported moderate to significant titres of α-NSP4 IgG (Ray *et al*., 2003; Vizzi *et al*., 2005; Yuan *et al*., 2004b). For studies in which NSP4-specific IgA was not detected; the corresponding response to the IgG counterpart was low (Ishida *et al*., 1996; Johansen *et al*., 1999; Rodríguez-Díaz *et al*., 2005; Yuan *et al*., 2004a). These results suggest that the ability to detect NSP4-specific antibodies is highly dependent on the sensitivity of the assay employed for their detection.

The α-NSP4 IgA and IgG responses were also investigated for subsets of sera acquired from longitudinal studies of children conducted over a 2-3 year period. The results from one such study is presented in Figure 3.3. The increase in both an α-NSP4 IgG and IgA

response to NSP4 of genotypes A (RV5) and B (RV4) coincided with a primary (G1) RV infection at approximately 30 months. The magnitude of the net OD is reflective of the concentration of α-NSP4 antibodies present in the serum. Prior to RV infection, the quantity of NSP4-specific antibodies was at baseline level. Upon infection, the levels of α-NSP4-specific antibodies present in the sera increased, prior to returning to baseline levels at approximately 5 months post infection. Interestingly, a large IgA response was observed towards NSP4 of genotype B, which exceeded the response (as proposed by the net OD values) to IgG. The same trend was not observed for NSP4 of genotype A.

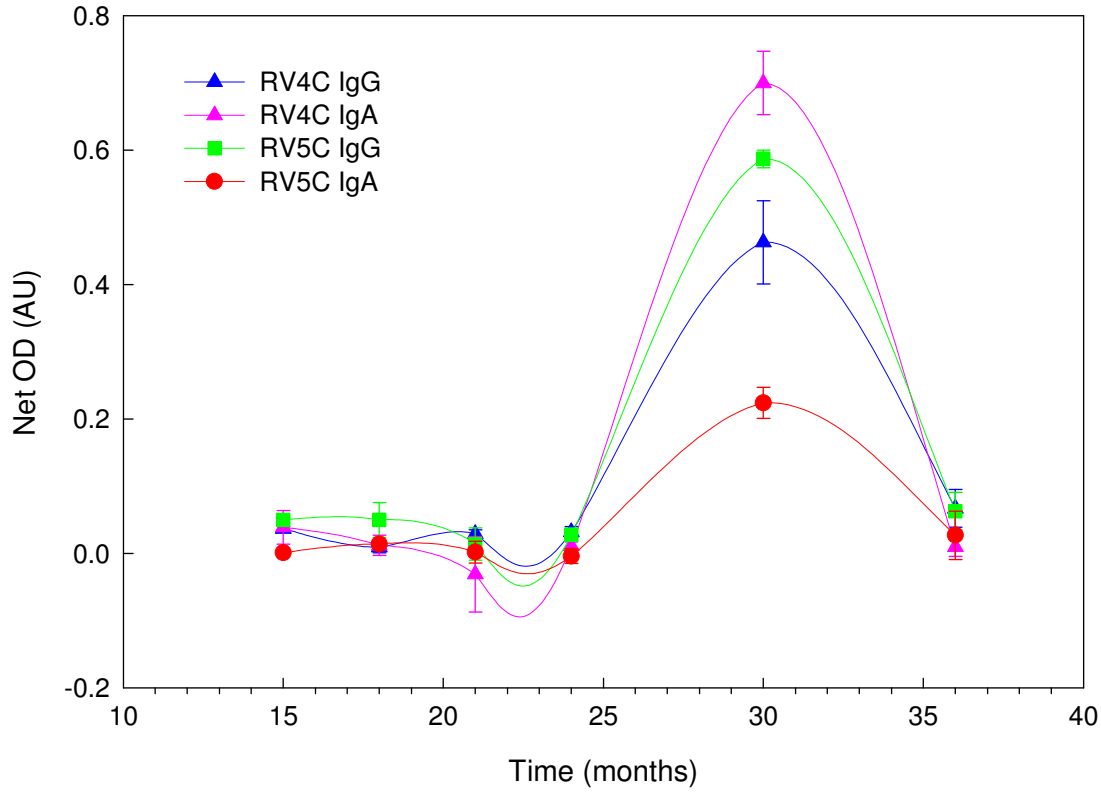


***Figure 3.3. Longitudinal analysis of α-NSP4 isotype-specific responses to RV4C and RV5C.*** *RV4C (1.5 µg/well) and RV5C (0.7 µg/well) were used as coating antigen for the detection of α-NSP4-specific IgG and IgA in patient sera. RV infection at approximately 30 months resulted in an increase in both an IgG and IgA response to NSP4 from basal levels. The infecting serotype was a G1 strain of HRV. Each sample was assayed in triplicate and the net OD plotted. Error bars apply to the standard deviation calculated for each data point.*

#### 3.3.2.2 NSP4-specific IgG response in the sera of children inoculated with 2 doses of an attenuated HRV vaccine

The serum samples were obtained from clinical trials of a 2 dose regimen of a live monovalent attenuated vaccine prepared from a human P1A[8]G1 strain (Rotarix®) and administered at 2 and 4 months of age.

The ELISA format used for the detection of NSP4-specific Ig isotypes was as described for the acute and convalescent sera of naturally infected children. The number of individuals that returned a positive response to NSP4 were reported (Table 3.5). For comparison, a similar treatment of results was performed for the convalescent sera obtained from children naturally infected with RV. The total number of vaccine recipients and naturally infected children analysed were 10 and 9 respectively. An α-NSP4 IgG response to NSP4 of Genotype A was observed for two of the vaccine recipients. These same samples also returned an α-IgG response to NSP4 of Genotype B. The response (as measured by net OD) was stronger for NSP4 of genotype B, the same genotype as the attenuated vaccine with which they were vaccinated. The number of naturally infected children which had α-NSP4 IgG antibodies was more than double that of the vaccine recipients. Anti-NSP4 IgA was not detected for any of the vaccine recipients.

***Table 3.5. Total α-NSP4 IgG response to NSP4 of Genotypes A and B in human sera.*** *The convalescent sera for naturally infected children (N=9) and post-vaccination sera from recipients of a 2-dose regimen for Rotarix® (N=10) were analysed. The percentile values represent the number of recipients who returned a positive response for NSP4-specific IgG from the total number of samples assayed. The values in brackets represent the absolute numbers.*

| | NSP4 RV5C (Genotype A) | NSP4 RV4C (Genotype B) |
|---|---|---|
| Natural Infection | 44% (4/9) | 78% (7/9) |
| Vaccinated | 20% (2/10) | 30% (3/10) |

In the absence of prevaccination sera it is not possible to draw conclusions regarding the rate of NSP4 "seroconversion" in response to vaccination. Table 3.5 illustrates that a greater proportion of children naturally infected with RV developed detectable levels of

α-NSP4 IgG compared with the vaccine recipients. These results are consistent with Vizzi *et al.* (2005) who reported that NSP4 evokes significantly higher seroconversion rates in children with naturally acquired RV infection (54%) compared with children inoculated with the RRV-TV vaccine (8%). In general, the correlation between post-vaccination RV antibody titres, particularly to IgA, and protection against reinfection is weaker and less apparent than for natural RV infection (Barnes *et al*., 2002; Bernstein *et al*., 1995; González *et al*., 2005; Svensson *et al*., 1987; Velazquez *et al*., 2000; Ward and Bernstein, 1994; 1995; Ward, 2009).

Antibodies directed against NSP4 after naturally acquired RV infection correlate with protection from rotaviral diarrhoea (Vizzi *et al*., 2005), but questions remain as to whether pre-existing antibodies to RV may limit viral replication and consequently affect the immune response to non-structural proteins. The answers to these questions would help to elucidate the contribution by NSP4-specific antibodies to the reduction of disease severity in vaccinated children.

Studies investigating the seroconversion rates to NSP4 upon reinfection have produced conflicting results. Ray *et al.* (2003) demonstrated that the seroconversion rate to NSP4 was lower upon reinfection compared to primary infection, whilst Vizzi *et al*. (2005) established that the NSP4 seroconversion rate was independent of the presence of pre-existing antibodies. Kirkwood *et al*. (2008) used RIP assays to detect NSP4-specific IgG antibodies in the sera of naturally infected children. The authors of this study observed boosts in NSP4 IgG antibody levels upon reinfection. They also reported that the levels of α-NSP4 IgG in the acute and convalescent sera declined rapidly and were not observed by 100 days post-primary infection.

To my knowledge, this is the only study which has investigated the NSP4 response to the Rotarix® vaccine. All other studies have investigated the immune responses to RV structural proteins (reviewed in Ward and Bernstein, 2009). In clinical trials, 61 to 96% of vaccinated infants developed RV-specific serum IgA or neutralizing antibody responses after two doses of the vaccine (Phua *et al*., 2005; Salinas *et al*., 2005; Vesikari *et al*., 2004; reviewed in Ward and Bernstein, 2009).

#### 3.3.2.3 Heterotypic and/or homotypic response to NSP4 of genotypes A and B

The humoral response to NSP4 appears to be heterotypic and independent of the NSP4 genotype. Significant IgG and IgA responses to homotypic and/or heterotypic NSP4 of genotypes A, B and C were reported in the sera of vaccinated children (Yuan *et al*, 2004b) and in the convalescent sera of naturally infected children (Ray *et al*., 2003). Vizzi *et al*. (2005) also reported homotypic and/or heterotypic responses to the $NSP4_{85-175}$ peptide of genotypes A, B and C for both naturally infected and RRV-TV vaccinated children.

The NSP4 genotypes of the infecting RV strains investigated in this study had not been determined, and consequently the conclusions drawn regarding NSP4 cross-reactivity was based on the assumption that G1 and G4 strains typically are of NSP4 genotype B and G2 of NSP4 genotype A (Kirkwood *et al*., 1999). The results obtained from the matched paired sera of children naturally infected with RV (Figure 3.2) demonstrated that the response to NSP4 of genotypes A and B is both homotypic and/or heterotypic. NSP4 of genotype A coprecipitated with sera obtained for a G1 virus in 60% of the data set, whilst IgG against NSP4 of genotype B was detected in all but 1 sample infected with a G1 virus, or G1/G4 virus. Data obtained from the longitudinal studies lend further support to the cross-reactivity of NSP4 genotypes, whereby NSP4 of genotypes A and B reacted with Ig's elicited from infection with strains G1 and G8 (arbitrarily assigned to NSP4 genotype B) (data not shown). What is of interest is the higher response observed for the NSP4 genotype A (RV5) antigen compared with the homotypic NSP4 genotype B (RV4) antigen for the IgG isotype (Figure 3.3). The difference in the immunological response was determined to be statistically significant (student's t test, $p < 0.05$).

The data obtained for the Rotarix® vaccine recipients indicated that the NSP4 response was heterotypic, although it is difficult to state in the absence of pre-vaccination sera, that NSP4 unequivocally elicits a cross-reactive immune response. The observed heterotypic response may be associated with the presence of pre-existing circulating NSP4 antibodies, indicative of previous exposure to RV.

### 3.3.3 NSP4 conformational dependence on the α-NSP4 response – influence of the $His_6$ tag position

Preliminary results indicated that the placement of the $His_6$ tag at the N-terminus of NSP4 generated a greater response compared with the corresponding C-terminal $His_6$-tagged protein; observed for NSP4 derived from strain RV4 only. These results could suggest that the presence of the $His_6$ tag at the carboxy terminus interferes with the binding of antibodies to epitopes located within the cytoplasmic domain of NSP4. These results are consistent with the identification of immunodominant epitopes located within the cytoplasmic domain of NSP4 (Borgan *et al*., 2003; Hyser *et al*., 2008; Kim *et al*., 2004; Rodríguez-Díaz *et al*., 2004; Yu and Langridge, 2001; Yuan *et al*., 2004a).

An NSP4-cholera toxin B subunit (CTB) fusion protein (CTB-$NSP4_{90}$) stimulated a greater IgG response in mice compared with CTB-$NSP4_{22}$ (immunodominant epitope of NSP4) indicating the presence of additional immunogenic epitopes on $NSP4_{90}$ (Kim *et al*., 2004; Yu and Langridge, 2001).

Borgan *et al*. (2003) identified three of four antigenic sites within the cytoplasmic domain of NSP4 of a group A avian RV strain (PO-13). Using MAbs directed against truncated NSP4s, the authors determined the presence of at least six epitopes within four spatially distinct antigenic sites (AS I-IV). AS I is located at aa 151-169, AS II at aa 136-150, AS III at aa 112-133 and AS IV at aa 1-24. Most of the MAbs were directed to AS I and II suggesting they were the major NSP4 epitopes. In addition, it was proposed that AS II is widely conserved among a variety of RVs (Borgan *et al*., 2003).

Hyser *et al*. (2008) identified four epitopes within the cytoplasmic tail of SA11 NSP4; three of which (aa 150-175, aa 120-147 and aa 114-135) are synonymous with AS, I II and III of the PO-13 strain identified by Borgan *et al*. (2003). A MAb B4-2/55 (produced against an attenuated Wa strain) mapped to a linear epitope within the amino acid domain 100-118; with residues E105, R108 and E111 critical for Ab binding. An anomalous binding domain was not identified by Borgan *et al*. (2003) for strain PO-13. Epitopes for α-$NSP4_{114-135}$ and $NSP4_{120-147}$ encompassing the enterotoxin domain were distinct. The α-$NSP4_{114-135}$ epitope mapped to the domain aa 114-125 and the residues

T117/T118, E120, and E122 were critical for binding of the antibody. The epitope for α-$NSP4_{120-147}$ was between amino acids 130-140 and residues Q137 and T138 were critical for its binding (Hyser *et al*., 2008). The third domain (aa 155-170) encompassed the DLP binding domain and specifically bound α-$NSP4_{150-175}$; residues E160 and E170 were critical for its binding (Hyser *et al*., 2008).

The contribution of the composition of the microtitre plates used in this study to the enhanced signal response observed for the N-terminal $His_6$-tagged NSP4 protein warrants further investigation. High binding microtitre plates favour interactions with cationic and hydrophobic regions of a peptide. The higher binding capacity of the N-terminal $His_6$-tagged protein may have been unduly influenced through binding of the hydrophobic domain to the plate, leaving the cytoplasmic domain exposed for greater interactions with α-NSP4 antibodies. The absence of an appreciable difference between the net OD of the C- and N-terminal $His_6$-NSP4 proteins derived from HRV strain RV5 would suggest that this phenomenon may not have an undue effect on protein binding.

## 3.4 Summary

An ELISA for the detection of α-NSP4-specific Ig isotypes (IgG and IgA) against HRV NSP4 of genotypes A and B was developed. The ELISA was employed for the detection of α-NSP4-specific antibodies in the sera of children naturally infected with RV and of recipients of the rotavirus vaccine, Rotarix®.

The results obtained are suggestive that an NSP4-specific humoral response is evoked both by natural RV infection and by vaccination with the live monovalent attenuated HRV vaccine. NSP4 seroconversion was reported for 89% of children naturally infected with RV, whilst only 30% of vaccine recipients returned a positive response for NSP4-specific Ig's. These results are consistent with the work of Vizzi *et al.* (2005) who reported that NSP4 evokes significantly higher seroconversion rates in children with naturally acquired RV infection (54%) compared with children inoculated with RRV-TV vaccine (8%).

An α-NSP4 IgG antibody response was the dominant isotype-specific serum response. The NSP4-specific IgG response to NSP4 of RV4 (G1, NSP4 genotype B) and RV5 (G2, NSP4 genotype A) in the sera of children infected with a G1 RV strain was 80% and 60% respectively. These results were consistent with the frequency (67-100%) reported by Richardson *et al*. (1993) who used RIP to detect α-NSP4-specific IgG's in the sera of children naturally infected with RV, and from which the sample subset assayed in this study originated.

Only 29% of the naturally infected children had seroconverted to detectable levels of α-NSP4 IgA, whilst no α-NSP4 IgA was detected in the sera of vaccine recipients. The lack of an α-NSP4 IgA response is consistent with the findings of others (Johansen *et al*., 1999; Rodríguez-Díaz *et al*., 2005).

The results demonstrate that the humoral response to NSP4 of genotypes A and B is both homotypic and heterotypic for naturally acquired RV infection and for Rotarix® vaccinated individuals. For the majority of samples analysed the α-NSP4 isotype-specific response was greatest for NSP4 of genotype B. This result is not entirely unexpected as RV4 shares the same serotype specificity (G1) and NSP4 genotype (B) as the majority of infecting strains assayed and of the vaccine strain. NSP4 of genotype A complexed with serum IgG's for a G1 infection in 60% of the data set, whilst NSP4 of genotype B reacted with IgG's of all but one sera infected with either G1 or G1/G4 viruses. Data obtained from the longitudinal studies lend further support to the cross-reactivity of NSP4, whereby NSP4 of genotypes A and B reacted with NSP4-specific IgG's for children infected with G1 and G8 (NSP4 genotype B) viruses. The α-NSP4 IgG response of vaccine sera to NSP4 of genotype A and B, was 20 and 30% respectively.

Preliminary data indicated that the N-terminal $His_6$-tagged NSP4 of strain RV4 yielded a greater response for serum NSP4-specific IgG than did its C-terminal counterpart. These results would be consistent with the preferential binding of the N-terminal to the high-binding polystyrene microtitre plates; allowing maximal interaction of the NSP4-specific antibodies with the immunodominant cytoplasmic tail of the protein. Alternatively, the fusion of the $His_6$-tag at the C-terminal may interfere with either the

direct binding of antibodies to linear epitopes or induce changes within the protein which alters conformation-dependent epitopes on the protein. This potential $His_6$ dependent response was not observed for recNSP4 of RV strain RV5, indicating potential differences in the immunodominant regions.

Serum samples returning a strong α-NSP4 response to all protein samples (RV4C, RV5C, RV4N and RV5N) were identified using the α-NSP4 ELISA and were selected for NSP4 neutralization studies in the proceeding chapter. Likewise, acute samples negative for α-NSP4 were selected as controls.

# 4

# Perturbation of cellular calcium homeostasis by rotavirus and NSP4

## 4.1 Introduction

Calcium is a vital intracellular second messenger responsible for controlling a vast array of cellular processes inclusive of gene transcription, muscle contraction, neurotransmitter release, oocyte fertilization, cell proliferation and differentiation, lymphocyte activation and cell death (Bootman *et al*., 2001; Moore *et al*., 1990; Winslow and Crabtree, 2005). Most, if not all changes to cellular function result from highly localised changes in calcium activity.

Calcium homeostasis within the cytosol of mammalian cells is maintained at approximately 100 nM by a complex interplay of mechanisms at the plasma membrane (PM) and involving intracellular organelles. The increases in cytosolic calcium concentration arise from the influx of calcium through calcium permeable channels at the PM and/or the release of calcium from intracellular stores such as the endoplasmic reticulum (ER) *via* 1,4,5-inositol triphosphate ($IP_3$) or ryanodine-sensitive channels. Sequestering of calcium by $Ca^{2+}$ pumps (e.g. sarcoplasmic endoplasmic reticulum ATPase (SERCA) pumps) into intracellular organelles (ER, sarcoplasmic reticulum, mitochondria) or extrusion by $Ca^{2+}$-ATPase and other transporters (e.g. $Na^{2+}/Ca^{2+}$ exchange) located at the PM serve to reduce excesses in cytosolic calcium concentration (Carafoli, 1987; 2002).

The basic building blocks of calcium signaling are spatially restricted "elementary" signals which remain localised at their point of origin and require the activation or recruiting of effector molecules to distribute their signal globally. Global calcium signals may traverse the entire cell (intracellular waves) or where gap junctions are present, pass to neighbouring cells (intercellular waves) to coordinate cellular responses within a tissue (Berridge *et al*., 1998; Thomas *et al*., 2000).

The dependence on the intrinsic calcium concentration for RV replication, morphogenesis and pathogenesis has been widely documented (reviewed in Ruiz *et al*., 2000). The solubilisation of the outer capsid layer and the activation of viral transcription is known to occur at low $[Ca^{2+}]_i$ (Benureau *et al*., 2005; Charpilienne *et al*., 1997; Chemello *et al*., 2002; Cohen *et al*., 1979; Ruiz *et al*., 1996; 1997; 2000); whilst the acquisition of the outer capsid layer and the integrity of the TLP is dependent on high ER $[Ca^{2+}]$ (Michelangeli *et al*., 1995; Poruchynsky *et al*., 1991; Ruiz *et al*., 2007). The formation of viroplasm-like structures and glycosylation of NSP4 and VP7 are also calcium regulated processes (Michelangeli *et al*., 1995; Sen *et al*., 2007).

The intracellular calcium homeostasis of cultured cells is altered by RV infection, is correlated with the synthesis of a glycosylated viral protein, and is most probably advantageous for virus replication (Brunet *et al*., 2000a; del Castillo *et al*., 1991; Díaz *et al*., 2008; Michelangeli *et al*., 1991; 1995; Pérez *et al*., 1998; Ruiz *et al*., 2000; 2005). The initial increase in $[Ca^{2+}]_i$ is attributable to the uncompensated increase in $Ca^{2+}$ permeability across the plasmalemma (Brunet *et al*., 2000a; Michelangeli *et al*., 1991; Pérez *et al*., 1998; Ruiz *et al*., 2000). The concomitant rise in the cytosolic calcium concentration triggers thapsigargin sensitive sequestering of $Ca^{2+}$ (Michelangeli *et al*., 1995). At a late stage of infection the increase in $[Ca^{2+}]_i$ is due to the influx of $Ca^{2+}$ across the PM and a PLC-dependent efflux of $Ca^{2+}$ from internal stores; which has a direct effect on F-actin and microtubule assembly (Brunet *et al*., 2000a; 2000b). RV associated increases in $[Ca^{2+}]_i$ are responsible for oncosis in MA104 cells (Michelangeli *et al*., 1991; 1995; Pérez *et al*., 1998).

Brunet *et al*. (2000a) demonstrated for the first time that viral proteins or peptides released into the culture medium at a late stage of RRV infection (18 h.p.i.) induced a

transient increase in $[Ca^{2+}]_i$ and was responsible for $Ca^{2+}$-dependent microvillar F-actin alteration in uninfected Caco-2 cells. The increase in $[Ca^{2+}]_i$ was attributable to both a PLC-dependent efflux of $Ca^{2+}$ from the ER and plasmalemma $Ca^{2+}$ influx.

NSP4 has been identified as a potential candidate for the viral product responsible for orchestrating changes to host cell $Ca^{2+}$ permeability (Diaz *et al*., 2008; Dong *et al*., 1997, Tian *et al*., 1994; Zambrano *et al*., 2008). NSP4-induced intracellular $Ca^{2+}$ mobilisation either *via* influx through the PM and/or efflux from the ER has been demonstrated in both mammalian and insect cell lines. The endogenous expression of NSP4 in insect (*Sf*9) and mammalian cells induced a PLC-independent increase in cytosolic calcium concentration, whilst the exogenous application of NSP4 or a peptide encompassing the enterotoxin domain ($NSP4_{114-135}$) elicited a PLC-dependent increase in $[Ca^{2+}]_i$ (Berkova *et al*., 2003; Tian *et al*., 1994; 1995; Xu *et al*., 1999; Zhang *et al*., 1998; 2000). The addition of NSP4 to human intestinal cells (HT29) induced intracellular $Ca^{2+}$ mobilisation through receptor-mediated PLC activation and $IP_3$ production (Dong *et al*., 1997). More recently, studies performed using siRNAs demonstrated that silencing of NSP4 expression completely ablated the increase in $Ca^{2+}$ permeability of the PM and the cytosolic $[Ca^{2+}]$ of renal cells (Zambrano *et al*., 2008).

Taken together these results are indicative of at least two mechanisms by which NSP4 may augment intracellular $Ca^{2+}$ homeostasis. The endogenous expression of NSP4 induces $Ca^{2+}$ efflux from the ER and is associated with the cytotoxic properties of the protein. The exogenous application of NSP4 is consistent with its functionality as an enterotoxin, whereby the extracellular form of NSP4 binds to host cell receptors ($\alpha1\beta1$ and $\alpha2\beta1$) on neighbouring uninfected cells were it effects intracellular $Ca^{2+}$ mobilisation (Ball *et al*., 1996; Dong *et al*., 1997; Seo *et al*., 2008).

As discussed in section 1.10.4, the true mechanisms by which NSP4 perturbs calcium homeostasis are still uncertain. The most contentious area of debate is whether NSP4 alters PM permeability to $Ca^{2+}$. The initial changes in $Ca^{2+}$ homeostasis of infected mammalian cells (COS-7, MA104, HT-29) was caused by glycosylated NSP4; which has been proposed to translocate to the cell membrane where it forms a $Ca^{2+}$ specific channel, enhancing membrane permeability to $Ca^{2+}$ (Diaz *et al*., 2008; Ruiz *et al*., 2005;

Zambrano *et al*., 2008). In contrast, a change in the ER membrane permeability to $Ca^{2+}$, and not plasma membrane permeability, was associated with the increase in $[Ca^{2+}]_i$ for *Sf*9 cells expressing NSP4 (Tian *et al*., 1995).

Figure 4.1 summarises the changes in $[Ca^{2+}]_i$ due to RV infection and to NSP4, and the associated models for diarrhoeal induction.

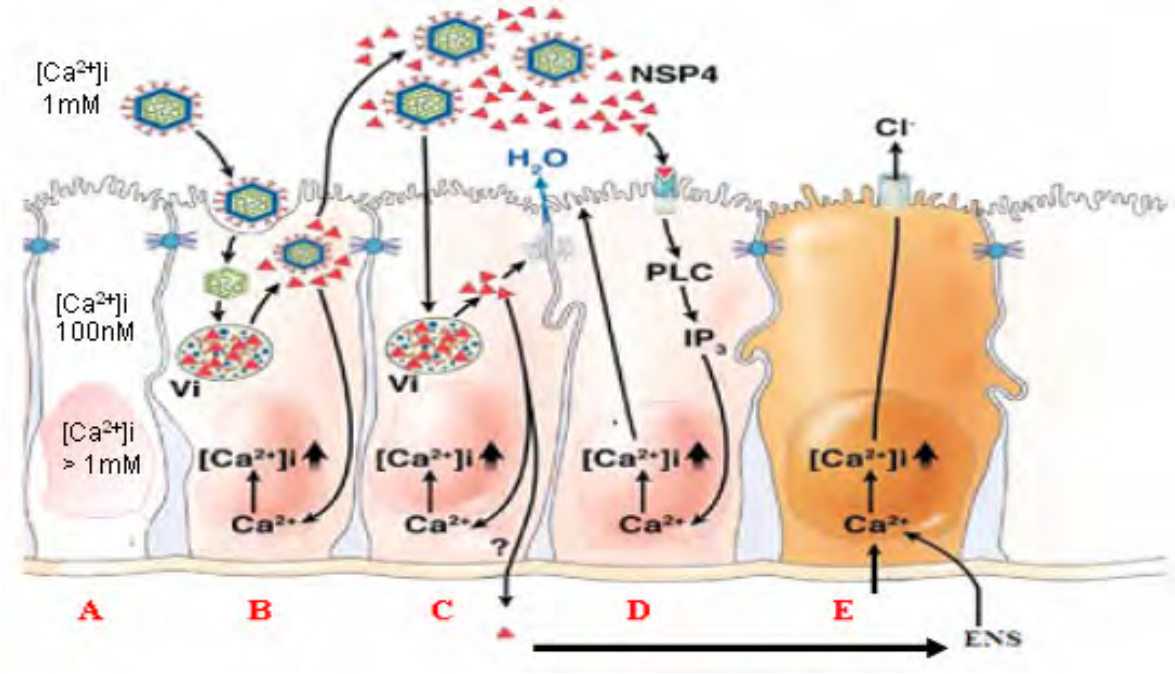


***Figure 4.1. RV and NSP4 associated changes to $[Ca^{2+}]_i$ – models for pathogenesis.*** *(A) represents the basal levels of $[Ca^{2+}]_i$ for uninfected enterocytes. (B) Infection of the initial cell by luminal virus results in virus entry, solubilisation of the outer capsid layer, activation of transcription, translation of viral proteins, the formation of viroplasms (Vi), and the apical release of infectious progeny virus and NSP4 by a nonclassical secretory pathway. Intracellular NSP4 induces $Ca^{2+}$efflux from internal stores, primarily the ER, resulting in an increase in the cytosolic $[Ca^{2+}]$. (C) Intracellular NSP4 disruption of tight junctions allows the paracellular flow of water and electrolytes (blue arrow). (D) NSP4 released to the extracellular medium from RV-infected cells, binds to cell receptors on adjacent uninfected cells, activating a PLC-dependent signaling pathway and mobilising calcium efflux from the ER to the cytosol. The increase in $[Ca^{2+}]_i$ causes disruption to the microvillar cytoskeleton. (E) Crypt cells (brown) can be acted on directly by NSP4 or via NSP4-induced activation of the ENS, which signals an increase in $[Ca^{2+}]_i$ resulting in $Cl^-$ secretion. Vi, viroplasm; ▲, NSP4. Image adapted from Greenberg and Estes, (2009).*

The major focus of this study was to investigate whether the exogenous application of NSP4 of prototype HRV strains RV4 and RV5 induced changes to the intracellular calcium homeostasis of mammalian cells. The effects of RV infection on calcium homeostasis would also be investigated.

Two independent methods for detecting changes in intracellular calcium flux, namely spectrofluorimetry and live cell imaging were to be developed. Spectrofluorimetric methods would enable the monitoring of global changes to the $[Ca^{2+}]_i$ of cell populations in suspension, whilst imaging would make possible the measurement of subcellular localised $[Ca^{2+}]_i$ responses in individual cells.

The responsiveness of two calcium sensitive fluorescent indicators (a) flash pericam; a GFP-derived protein and (b) fluo-3, AM (Invitrogen); a synthetic dye, to detect changes in $[Ca^{2+}]_i$ for each of the systems described above would be evaluated.

Once an NSP4-induced change in $[Ca^{2+}]_i$ had been demonstrated, serum NSP4-specific antibodies would be assayed to assess their ability to neutralise NSP4-associated calcium perturbations. NSP4 specific antibodies have been documented to reduce the severity and incidence of diarrhoeal illness in the mouse model (Ball *et al*., 1996; Choi *et al.*, 2005; Hou *et al.*, 2008; Yu and Langridge, 2001).

## 4.2 Methods

Unless mentioned otherwise, all tissue culture media and reagents were supplied by Invitrogen. All tissue culture work was performed using aseptic conditions in a Class II biohazard safety cabinet.

### 4.2.1 Mammalian cell lines

Two cell lines were routinely used for the intracellular calcium studies; a continuous embryonic epithelial kidney cell line (MA104) originating from the Macacus Rhesus monkey and a transformed fibroblast kidney cell line (COS-7) derived from the African Green monkey.

### 4.2.2 Maintenance of mammalian cell lines

Mammalian cells were grown as monolayers and were maintained in Dulbecco's Modified Eagle Medium (DMEM) supplemented with 10% foetal bovine serum (FBS) (Bovogen Biologicals Pty Ltd.), at 37°C in a humidified atmosphere, in the presence of 5% $CO_2$, unless noted otherwise.

The cells were routinely subcultured once they had attained 80-100% confluency. In brief, cells were washed once with PBS (137 mM NaCl, 2.7 mM KCl, 10 mM $Na_2HPO_4$, 2 mM $KH_2PO_4$; pH 7.4) prior to the addition of 1/10 culture volume of trypsin-ethylenediaminetetracetic acid (EDTA). Cell detachment was allowed to proceed at 37°C in the presence of 5% $CO_2$ for 5-15 minutes. The trypsinised cells were resuspended in 10 times the volume of media and an aliquot of the cell suspension was transferred to a fresh T-flask containing media.

### 4.2.3 Preparation of mammalian cell stock

Once the cell monolayer had approached 100% confluency, the cells were detached in the presence of trypsin-EDTA as detailed above. The trypsinised cell suspension was transferred to a 15 mL centrifugation tube (Falcon) and the cells pelleted at 750 rpm for

5 minutes. The supernatant was discarded and the cell pellet resuspended in 900 µL FBS and 100 µL dimethyl sulfoxide (DMSO). The cell suspension was transferred to a 1.5 mL cryogenic vial (Cellstar®; Greiner bio-one), incubated at -20°C for 1 hour prior to long-term storage at -87°C.

### 4.2.4 Recovery of mammalian cells from stock

Cells were rapidly thawed at 37°C and the cell suspension transferred to 5-10 mL of media in either a 25 $cm^2$ or 75 $cm^2$ T-flask (Falcon).

### 4.2.5 Propagation of rotavirus in mammalian cells

Stock viruses were tissue culture homogenates prepared by repeat freeze-thawing as described below. The viruses were propagated from aliquots of SA11, RV4 and RV5 kindly provided by Dr Carl Kirkwood (Murdoch Children's Research Institute).

Trypsin (10 µg/mL; 1:250 porcine pancreas; Type IX; Sigma) activation of the virus was conducted at 37°C for 30 minutes. The activated virus was added to monolayers of mammalian cells (80-90% confluency), prewashed twice with serum-free media, and the cells incubated under standard conditions. Virus adsorption was permitted to proceed for 1 hour, with gentle rocking at 15 minute intervals, after which the inoculum was removed and fresh serum-free media containing porcine trypsin (1 µg/mL) added. The cells were incubated at 37°C and 5% $CO_2$ until complete cytopathic effect (CPE) was observed.

The virus particles were released from the cells by subjecting the cells to three cycles of freeze-thawing (-87°C and 37°C for 15 minutes each). The supernatant was recovered, and the virus particles separated from the cellular debris by centrifugation at 750 rpm for 5 minutes. The supernatant was aliquoted into 1.5 mL microfuge tubes and stored at -20°C.

## 4.2.6 Viral titre determination

### 4.2.6.1 Plaque assay

The method as described below was adapted from Smith *et al.* (1979).

Mammalian cells were grown to 80-90% confluency in DMEM (10% FBS) within the wells of a 6 well plate. The supernatant was removed by aspiration and the cells washed twice with PBS (pH 7.4).

Two-hundred and fifty microlitres of serially diluted viral supernatant was added to the cell monolayers, in duplicate. Virus adsorption was allowed to proceed for 1 hour at 37°C, with gentle rocking at 15 minute intervals.

The inoculum was aspirated from the wells and 2 mL of molten 1% (w/v) SeaPlaque® Agarose (Cambrex) in serum-free DMEM, supplemented with 15 µg/mL porcine pancreatic trypsin and 100 µg/mL diethylaminoethyl (DEAE)-dextran (Sigma) added to each well.

The cells were incubated at 37°C and 5% $CO_2$ until plaques were observed. The plaques were visualised by neutral red staining as detailed in Section 2.2.4.3.

### 4.2.6.2 End point dilution assay

The endpoint dilution assay was adapted from King and Possee (1992).

Briefly, activated virus serially diluted in DMEM was added across the wells of a 96 well plate containing confluent monolayers of mammalian cells, in triplicate. The cells were incubated either at 37°C or 29°C with 5% $CO_2$ in a humidified environment until complete CPE was observed.

### 4.2.7 Rotavirus infection of mammalian cells for calcium studies

Aliquots of virus stock were activated with porcine trypsin (10 µg/mL) as previously described (4.2.5). Once activated, the virus was added to the prewashed cell monolayer, and the cells incubated under standard conditions. After 1 hour, the inoculum was removed and fresh serum-free media added. The infection was allowed to proceed for a nominated period of time post-infection.

### 4.2.8 The incorporation of calcium-sensitive fluorescent markers into mammalian cells

The measurement of changes to the $[Ca^{2+}]_i$ as a consequence of RV replication or the exogenous addition of NSP4 was addressed using two fundamental approaches; spectrofluorimetric analysis of mammalian cell populations or microscopic analysis of single cells. For each system investigated, flash pericam and fluo-3, AM were assessed for their potential use as calcium-sensitive fluorescent markers.

#### 4.2.8.1 Fluo-3, AM loading of mammalian cells

Fluo-3, AM loading of cells was performed when cells had either (a) reached 80-100% confluency (investigation of the effect of NSP4 on calcium homeostasis) or (b) the nominated RV incubation period was complete (effect of whole virus on intracellular calcium homeostasis).

- **Preparation for population studies**

The cell monolayer was washed with PBS prior to trypsin-EDTA assisted cell detachment as described previously (4.2.2). The cell suspensions were transferred to 15 mL centrifuge tubes and pelleted by centrifugation at 750 rpm for 5 minutes. The cells were washed twice by centrifugation with serum-free media prior to resuspension in a 2 mL volume of serum-free DMEM. Six to 12 µL (1 mg/ml) fluo-3, AM and an equivalent volume of Pluronic® F-127 (20% (w/v) in DMSO) were premixed prior to addition to the cell suspension and dye loading allowed to proceed for 1 hour at 37°C

with 5% $CO_2$. On completion of the incubation period, the cells were washed twice with extracellular buffer (ECB) (130 mM NaCl, 5 mM KCl, 1 mM $CaCl_2$, 1 mM $MgCl_2$, 20 mM HEPES; pH 7.4) (Ruiz *et al*., 2005), resuspended in 14 mL of ECB, and incubated for an additional 30 minutes to allow for complete de-esterification of intracellular AM esters.

The fluorescence intensity of the fluo-3, AM loaded cells, under the experimental conditions stipulated, were measured as described in Section 4.2.9.

- **Preparation for single cell studies**

Cells were seeded onto either single or double well concave slides and maintained in DMEM (10% FBS and 1% (v/v) Fungizone®) until required for fluo-3, AM loading and image analysis. The cells were washed twice by aspiration with serum-free DMEM. A 1:1 mixture of fluo-3, AM and Pluronic® F-127 in DMEM was added to the cell monolayer and incubated as per the population studies above. At the completion of the incubation period the dye was removed, the cells washed twice, and 250 µl DMEM added. The cells were incubated for an additional 30 minutes for de-esterification and fresh medium applied prior to visualisation of the cells as per Section 4.2.10.

#### 4.2.8.2 Transfection of mammalian cells with flash pericam DNA

The flash pericam/pcDNA3 plasmid was constructed by Nagai *et al*. (2001) and kindly donated by Dr Charles Cranfield (Swinburne University) for use in this work.

The flash pericam/pcDNA3 plasmid was purified from 200 mL of overnight *E. coli* culture using the PureLink™ HiPure Plasmid Maxiprep kit (Invitrogen). The plasmid DNA was eluted in 250 µl sterile MilliQ water.

Approximately 500 ng flash pericam plasmid DNA was ethanol precipitated in the presence of 0.3 M sodium acetate (pH 5.2) overnight at -20°C as described elsewhere (2.2.4.2).

The DNA was pelleted by centrifugation at 13,000 rpm for 10 minutes, the supernatant discarded and the DNA pellet air dried under aseptic conditions, prior to dissolution in serum-free DMEM.

Lipofectamine™ LTX reagent in conjunction with Plus™ reagent was used for the transfection of flash pericam DNA into mammalian cells. The protocol as outlined below, was adapted from the Invitrogen technical sheet, "Transfecting plasmid DNA into COS-7 cells using Lipofectamine™ LTX reagent".

The appropriate volume of Plus™ Reagent was added directly to the diluted DNA and incubated at room temperature for 15 minutes. The Lipofectamine™ LTX reagent was added to the diluted DNA and the formation of lipid-DNA complexes permitted to proceed for 1 hour at room temperature. The total volume of the reaction sample was added to the cell monolayer (pre-washed three times with serum-free medium) when cells had attained 50-80% confluency. The cells were incubated for four days at 29°C with 5% $CO_2$.

### 4.2.9 Changes to the calcium homeostasis of mammalian cell populations – a spectrofluorimetric approach to the effects of whole virus and NSP4

Changes to the intracellular calcium concentration of mammalian cells in response to infection with SA11 and upon the exogenous addition of the $His_6$-NSP4 fusion proteins derived from HRV strains RV4 and RV5 (Chapter 2) were investigated. The calcium ionophore calcimycin (1 mg/mL) was employed as a positive control.

The fluorescence (AU) of 3 mL aliquots of fluo-3, AM loaded or flash pericam transfected cell suspensions were measured on a Cary Eclipse Fluorescence Spectrophotometer (Varian Instruments, Australia). The appropriate excitation (Exλ) and emission (Emλ) wavelengths were selected for the detection of fluo-3, AM (Exλ = 506 nm, Emλ = 526 nm) and flash pericam (Exλ = 494 nm, Emλ = 514 nm), using a slit width of 5 nm.

- **Determination of $[Ca^{2+}]_i$**

The intracellular calcium concentration (nM) was determined as per the method of Tsien *et al.* (1982), whereby $[Ca^{2+}]_i = K_d[(f-f_{min})/(f_{max}-f)]$. The fluorescence maximum ($f_{max}$) and fluorescence minimum ($f_{min}$) for fluo-3, AM loaded cell suspensions was obtained by the sequential addition of 0.07% Triton X-100 and 33 mM ethylene glycol-bis (2-aminoethyl)-N,N,N',N'-tetraacetic acid (EGTA); pH 8.0 (Fluka BioChemika), respectively (Brunet *et al*., 2000a; Tian *et al*., 1994). The dissociation constant ($K_d$) of fluo-3, AM was taken as 390 nM (Haughland, 2005).

- **Effect of RV infection on plasma membrane permeability to $Ca^{2+}$**

The PM permeability to calcium of mock and RV-infected cells was assessed by imposing a step increase in the extracellular $Ca^{2+}$ concentration and monitoring the change in fluorescence intensity over a 2 minute interval (Brunet *et al*., 2000a; Michelangeli *et al*., 1991; 1995; Pérez *et al*., 1999; Ruiz *et al*., 2005; Zambrano *et al*., 2008). The results were presented graphically as a change in calcium concentration ($\Delta[Ca^{2+}] = (f-f_0)/f_0$) against time (Maravall *et al*., 2000). The basal fluorescence ($f_0$), is the fluorescence intensity (AU) prior to the application of the $Ca^{2+}$ pulse. Fluorescence ($f$) is the intensity (AU) measured in real time post addition of $Ca^{2+}$.

### 4.2.10 Changes to the calcium homeostasis of single cells – a microscopic approach to the effects of whole virus and NSP4

Mammalian cells were seeded onto glass concave well slides and either transfected with flash pericam DNA (4.2.8.2) or loaded with fluo-3, AM (4.2.8.1). Changes to the intracellular calcium homeostasis in response to the application of NSP4, calcimycin, and phosphate buffer (pH 8.0) was investigated.

Monitoring of the changes to the calcium permeability of SA11-infected cell monolayers upon the application of a 5 mM calcium pulse was also attempted.

The changes in fluorescence intensity was monitored on a Nikon Eclipse 50i epifluorescent microscope using a fluorescein isothiocyante (FITC) filter. Images were captured with a digital camera (Diagnostic Instruments, Inc.) using the associated software, RTke diagnostic SPOT advanced.

Image analysis was undertaken using Image J software (http://rsb.info.nih.gov/ij/). The mean gray value, as calculated by Image J for individual cells imaged within a single experiment, were background corrected and subsequently averaged to give an experimental observation of 1 (N=1). The $\Delta[Ca^{2+}]_i$ was calculated as described previously (Maravall *et al*., 2000).

### 4.2.11 NSP4 neutralisation assay

Human serum positive for NSP4-specific antibodies, as determined in Chapter 3, was incubated with recombinant $His_6$-NSP4 for 15 minutes prior to the addition to flash pericam transfected cell monolayers. The changes in fluorescence intensity were monitored as per 4.2.10.

### 4.2.12 Immunofluorescence analysis of rotavirus-infected cells

The methodology described below for the immunolabeling of RV-infected cells, was adapted from Maruri-Avidal *et al*. (2008) and performed in accordance with the manufacturer's recommendations for the Alexa Fluor® SFX Kit (Molecular Probes™). All incubation steps were conducted at 29°C with 5% $CO_2$ unless specified otherwise.

Before commencing immunolabeling, the cell monolayer was either mock or RV-infected. The cells were washed with prewarmed (37°C) PBS (pH 7.4) prior to fixing in 3.7% (v/v) formaldehyde (in PBS) for 20 minutes at room temperature. The cells were washed four times in PBS, permeabilised in 0.1% Triton X-100 for 15 minutes, and again washed four times with PBS. Approximately 200 µl of Image-iT™ FX signal enhancer was applied to the cells and incubated for 30 minutes. The cells were rinsed with PBS and 1 mL of RV-specific polyclonal antibody diluted 100-fold in PBS was added. After incubation for 1 hour, the cells were rinsed four times with PBS, and the

secondary antibody, goat α-rabbit IgG conjugated to Alexa Fluor® 488 was added. After a 1 hour incubation the cells were rinsed four times with PBS and visualised using an epifluorescence microscope with an FITC filter as described previously.

### 4.2.13 Statistical analysis

Results were analysed using the Excel Statistical Package, PHStat2. Student t-tests were performed at a significance level of $p < 0.05$.

## 4.3 Results and Discussion

### 4.3.1 Investigation of rotavirus and NSP4-induced changes to the calcium homeostasis of mammalian cell populations

Changes to the intracellular calcium homeostasis of mammalian cell populations exposed to RV infection and to NSP4 were measured using spectrofluorimetry. An appropriate fluorescent probe responsive to the induced changes in $[Ca^{2+}]_i$ for this system had to be established. Two calcium-sensitive fluorescent markers, fluo-3, AM and flash pericam were investigated for this purpose.

Fluo-3, AM is a cell permeant acetoxymethylester (AM) which, upon hydrolysation by intracellular esterases, produces a membrane impermeant calcium sensitive fluorochrome. Complexing of the dye with calcium results in little to no shift in the excitation and emission spectra (non-ratiometric). Consequently fluorescence intensity, and subsequently the estimation of $[Ca^{2+}]_i$ is unduly influenced by the concentration of fluo-3, AM, the cell volume and granularity (Rijkers *et al*., 1990).

The calcium sensitive fluorescent protein, flash pericam, was produced by Nagai *et al.* (2001) and its construction involved the fusion of genes encoding circularly permuted yellow fluorescent protein (cpYFP), a GFP variant, with calmodulin (CaM) and M13 (a 26-residue peptide derived from the CaM-binding region of the skeletal muscle myosin light-chain kinase). The binding of $Ca^{2+}$ to CaM and the subsequent association of the $Ca^{2+}$-CaM complex with M13 results in the ionization of cpYFP and an accompanying

8-fold increase in fluorescence intensity (Miyawaki *et al*., 2002; Nagai *et al*., 2001). The use of flash pericam is advantageous to that of synthetic $Ca^{2+}$ indicators such as fluo-3, AM, which are prone to dye leakage, organelle compartmentalisation, non-specific loading and photobleaching (reviewed in Hayashi and Miyato, 1994; Simpson, 2006; Takahashi *et al*., 1999). Unfortunately, a drawback of flash pericam is its sensitivity to pH and the necessity for temperatures within the range of 28-30°C for correct folding (Nagai *et al*., 2001).

The correlation between changes in the fluorescence intensity (AU) as detected spectrophotometrically and $\Delta[Ca^{2+}]_i$ was firstly addressed in fluo-3, AM loaded cells. The following parameters, as outlined below, were investigated using fluo-3, AM unless stated otherwise.

#### 4.3.1.1 Investigation of the integrity of the spectrofluorimetric system for detecting changes to $[Ca^{2+}]_i$

- **Establishing a correlation between the change in fluorescence intensity as a function of $\Delta[Ca^{2+}]_i$**

The sensitivity and specificity of the spectrofluorimetric system to detect changes in $[Ca^{2+}]_i$ was addressed by the application of (a) 33 mM EGTA; a calcium specific chelator (b) 0.07% Triton X-100; a nonionic surfactant for membrane permeabilisation and (c) 5 mM $Ca^{2+}$, to the extracellular medium of mock and RV-infected cells (Brunet *et al*., 2000a; Tsien *et al*., 1994). Triton X-100 and EGTA are routinely used for determining the fluorescence maximum ($F_{max}$) and fluorescence minimum ($F_{min}$) respectively (Moore *et al*., 1990). Saturating concentrations of $Ca^{2+}$ (5 mM) had been used by other investigators to evaluate PM permeability changes to $Ca^{2+}$ due to RV infection and to the exogenous application of NSP4 (Brunet *et al*., 2000a; Pérez *et al*., 1999; Tian *et al*., 1994; Zambrano *et al*., 2008).

As shown in Figure 4.2, an increase in the $\Delta[Ca^{2+}]_i$ was observed for both mock and RV-infected MA104 cells upon the addition of Triton X-100 (t=120 s); commensurate with membrane permeabilisation and calcium influx. The stepwise addition (t=130 s

and t=140 s) of 33 mM EGTA caused a reduction in the $\Delta[Ca^{2+}]_i$ which was coincident with the sequestering of $Ca^{2+}$ ions. The application of a 5 mM $Ca^{2+}$ pulse to the extracellular medium resulted in a rapid rise in the $\Delta[Ca^{2+}]_i$ for both RV and mock-infected cell populations. An increase in $[Ca^{2+}]_i$ was expected for RV-infected cells as cellular membrane perturbation to $Ca^{2+}$ and other cations is characteristic of RV infection (Brunet *et al*., 2000a; Diaz *et al*., 2008; Michelangeli *et al*., 1991; Pérez *et al*., 1998; 1999; Ruiz *et al*., 2005). The sizeable increase in signal intensity for the mock-infected cells was not anticipated and a change in osmolality, a consequence of the change to the environmental conditions undertaken for the spectrofluorimetric measurement, was investigated as a potential source for this erroneous result and will be described in greater detail in the proceeding section.

Alternative explanations for the rapid rise in fluorescence of mock (and invariably RV) infected cells to the $Ca^{2+}$ pulse may be associated with (a) the binding of calcium to extracellular fluo-3, AM (Schnetkamp *et al*., 1991), (b) alterations in cell membrane properties due to Pluronic® F-127 (Molecular Probes Manual, MP 03000) or (c) the presence of the pH sensitive indicator phenol red in the culture medium.

Pluronic® F-127 is a non-ionic surfactant polyol which aids in the solubilisation of water-insoluble dyes in physiological media and its use was critical in this study for the loading of fluo-3, AM into cells (Molecular Probes Manual, MP 03000). Phenol red indicator has been associated with the filtering of excitation and emission wavelengths, whilst the presence of another medium component riboflavin, contributes to autofluorescence and fluorescence quenching (Johnson, 2006; Kain *et al*., 1998; Moore *et al*., 1990; Slavik, 1998; Tsien *et al*., 1982). The contribution to background fluorescence from the cell culture medium was investigated in the proceeding section.

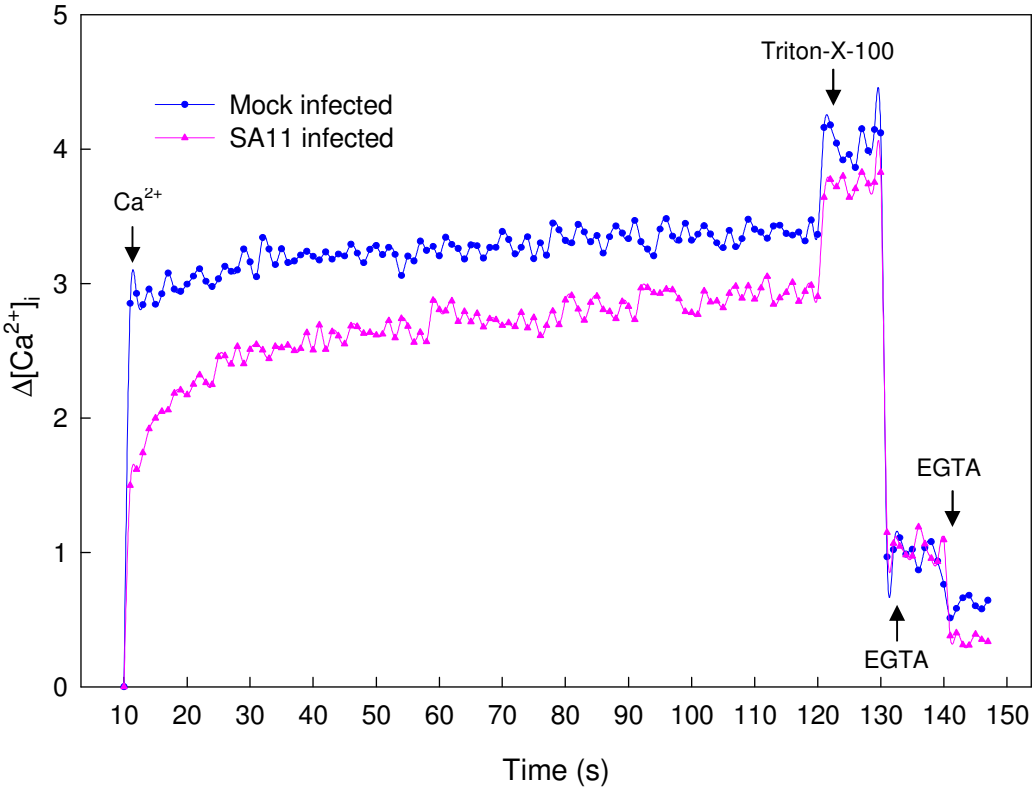


***Figure 4.2. Correlation between the $\Delta[Ca^{2+}]_i$ and fluorescence intensity.*** *Suspensions of SA11 or mock-infected fluo-3, AM loaded MA104 cells in DMEM were treated with 5 mM $Ca^{2+}$ (t=10 s), 0.07% Triton X-100 (t=120 s) and 33 mM EGTA (t=130 s and t=140 s) and the changes in fluorescence intensity measured on a spectrofluorimeter. The fluorescence intensity was converted to the $\Delta[Ca^{2+}]_i$ and plotted as a function of time. Representative traces of the mean value for each data point from two independent experiments (N=2) is presented.*

- **Selection of the appropriate extracellular medium**

Spectrofluorimetric analysis of cell populations was initially performed on fluo-3, AM loaded cells suspended in serum-free DMEM. The tightly regulated control of temperature (37°C), humidity and oxygen concentration (95%) optimal for cell growth and survival could not be adhered to when performing fluorescence measurements. The purpose of this study was two-fold; (a) to investigate the ability of the culture medium to resist changes to environmental conditions and (b) to assess the contribution of cell culture medium components (riboflavin and phenol red) to background fluorescence.

As illustrated in Figure 4.3, the application of a 5 mM $Ca^{2+}$ pulse to mock-infected MA104 cells loaded with fluo-3, AM and suspended in extracellular buffer (ECB) failed to induce a change in $[Ca^{2+}]_i$, whilst similarly treated cells suspended in DMEM returned a rapid $\Delta[Ca^{2+}]_i$. These observations suggested that cells suspended in DMEM may be more susceptible to the effects of environmental changes, such as temperature and osmolality, than were cells in HEPES-buffered ECB. The rapid increase in fluorescence upon the addition of the calcium pulse to cells in DMEM was indicative of a potential loss in cellular PM integrity.

The difference in basal fluorescence for fluo-3, AM loaded cells suspended in DMEM and ECB was determined to be statistically significant (Students t test; sig. level of $p < 0.05$). These results indicated that components within the culture media (e.g. phenol red and/or riboflavins) were contributing to the background fluorescence of the sample. In addition, these results preclude PM disruption by Pluronic® F-127 as a potential source of increased PM permeability to $Ca^{2+}$ as the cells suspended in ECB failed to respond to the applied $Ca^{2+}$ pulse.

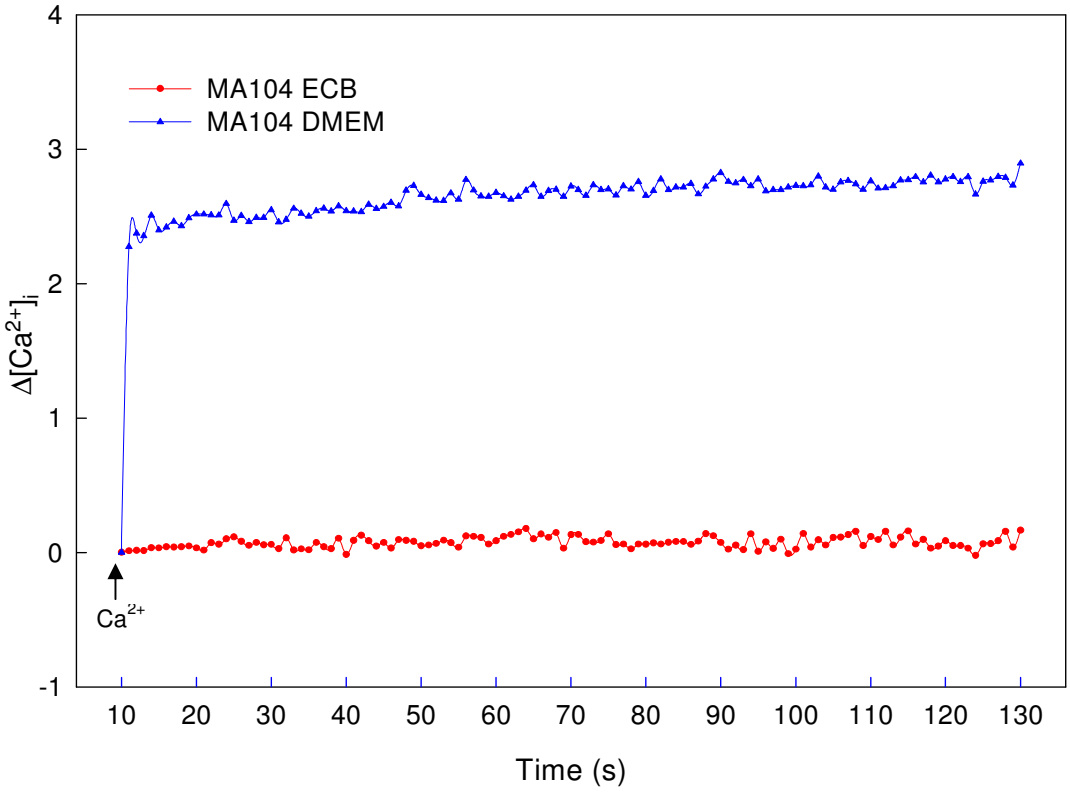


***Figure 4.3. Extracellular medium selection.*** *Fluo-3, AM loaded mock-infected MA104 cells were suspended in either culture medium (DMEM) or ECB. A 5 mM $Ca^{2+}$ pulse was applied to the extracellular medium at t=10 s. Fluorescence measurements were converted to $\Delta[Ca^{2+}]_i$ and plotted as a function of time. Representative traces of the mean value for each data point from two independent experiments (N=2) for cells suspended in DMEM and N=3 for cells suspended in ECB, are presented.*

- **Establishment of a positive control for the measurement of $Ca^{2+}$ influx**

The calcium ionophore calcimycin (also known as A23187) was chosen as a positive control to demonstrate the increase in fluorescence intensity associated with calcium influx across the PM of mammalian cells. Calcimycin is highly selective for $Ca^{2+}$, forming stable 2:1 complexes with the cation and greatly enhancing the ability of the ion to traverse biological membranes. At low ionophore concentrations, calcium flux across cellular membranes is typically *via* calcium-ionophore complexation, whilst at higher concentrations the ionophore behaves as a calcium channel (Jyothi *et al*., 1994).

As illustrated in Figure 4.4, the addition of increasing concentrations of calcimycin (6.5 µM to 26 µM) to mock-infected fluo-3, AM loaded MA104 cells caused a corresponding increase in the $\Delta[Ca^{2+}]_i$ which was commensurate with the applied dosage. The application of 5 mM $Ca^{2+}$ to the cell suspension (t = 10 s), in the absence of the ionophore, failed to induce a change in the fluorescence intensity.

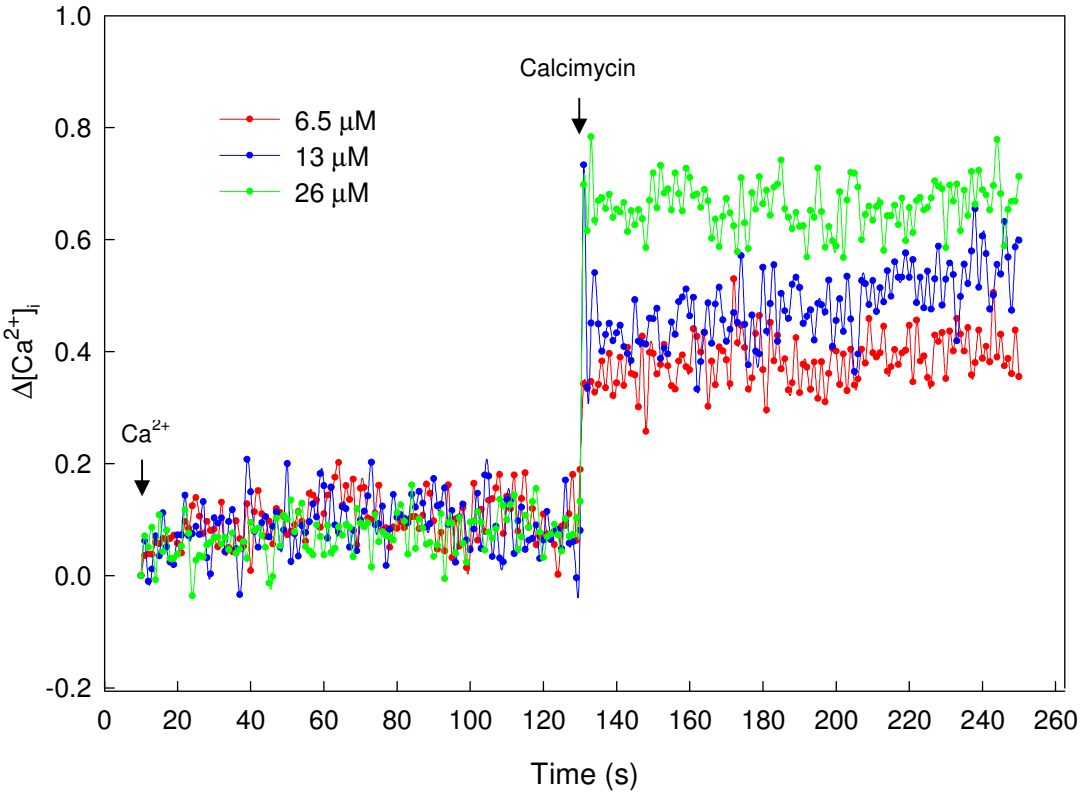


***Figure 4.4. Dose-dependent changes to the $[Ca^{2+}]_i$ induced by calcimycin.*** *Mock-infected fluo-3, AM loaded MA104 cells suspended in ECB were treated with calcimycin of varying concentrations (6.5 to 26 µM) at t = 131 s (N =3). At t= 10 s a 5 mM $Ca^{2+}$ pulse was applied.*

### ➢ Responsiveness of fluo-3, AM and flash pericam to $\Delta[Ca^{2+}]_i$

The sensitivities of fluo-3, AM and flash pericam to changes in intracellular calcium concentration were investigated in mock and SA11-infected mammalian cells. The detection system which demonstrated the greatest sensitivity to a $\Delta[Ca^{2+}]_i$ would be used exclusively for further population studies. The results for COS-7 infected cells are presented in Figure 4.5.

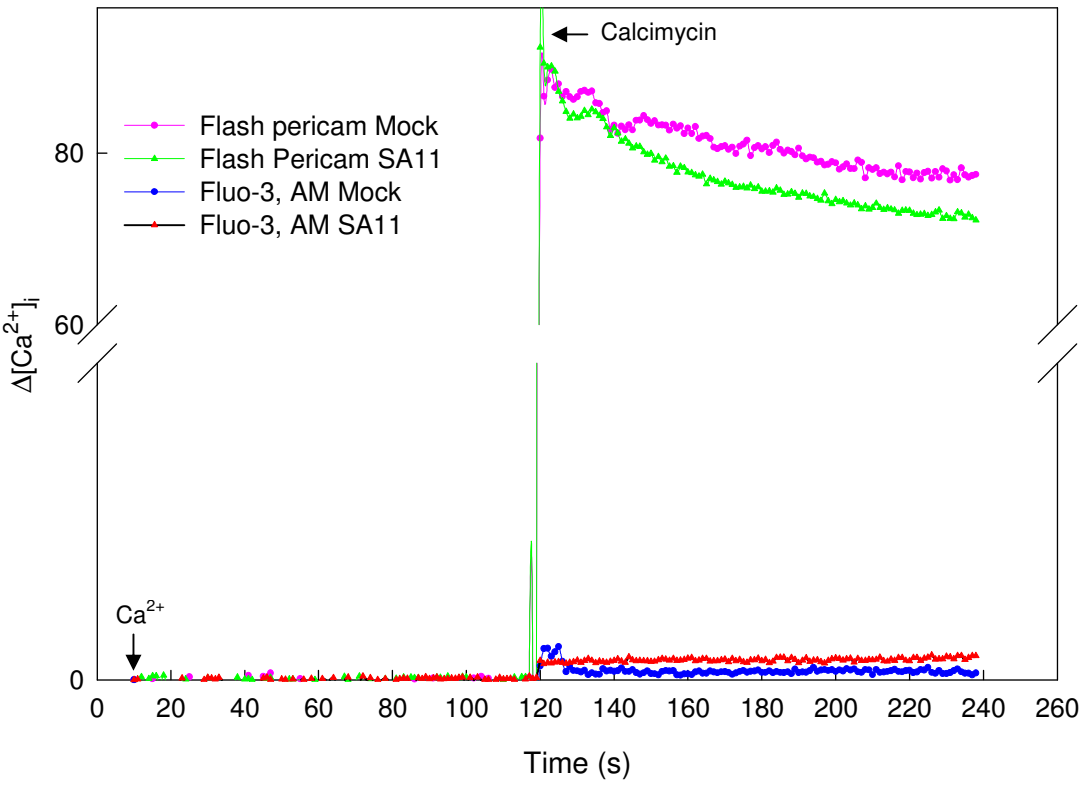


***Figure 4.5. Selection of a $Ca^{2+}$ sensitive probe: flash pericam versus fluo-3, AM.*** *The responsiveness of flash pericam and fluo-3, AM to changes in $[Ca^{2+}]_i$ was investigated by the application of a 5 mM $Ca^{2+}$ pulse at t=10 s and 12.3 µM calcimycin at t=120 s. Fluorescence intensity measurements for fluo-3 loaded COS-7 cells were performed at $\lambda_{Ex}$ and $\lambda_{Em}$ of 506 nm and 526 nm respectively. Fluorescence intensity measurements for flash pericam transfected COS-7 cells were performed at $\lambda_{Ex}$ and $\lambda_{Em}$ of 494 nm and 514 nm respectively. Each data point corresponds to the mean value from N=2 mock and SA11-infected samples.*

COS-7 cells transfected with flash pericam/pcDNA3 plasmid DNA exhibited a substantially greater $\Delta[Ca^{2+}]_i$ upon the application of 12.3 µM calcimycin to both mock and SA11-infected cell suspensions compared with fluo-3, AM loaded cells. These results indicated that flash pericam was more sensitive to changes in $[Ca^{2+}]_i$ than was fluo-3, AM. A review of the literature established that the expected increase in fluorescence intensity upon $Ca^{2+}$ binding for fluo-3, AM loaded cells would be within the order of 40-200-fold, whilst cells expressing flash pericam exhibited an approximate 8-fold increase (Nagai *et al*., 2001; reviewed in Takahashi *et al*., 1999).

As a general rule $Ca^{2+}$ sensitivity is most reliable in a $[Ca^{2+}]$ range below and very near the dissociation constant (Kd) of the fluorophore (Meyer *et al*., 1990). The Kd for flash pericam and fluo-3, AM are 700 nM and 390 nM respectively (Haughland, 2005; Nagai *et al.*, 2001). As the cytosolic $[Ca^{2+}]$ of mammalian cells is approximately 100 nM, it was expected that fluo-3, AM would be the more suitable dye. A possible explanation for the reduced response of fluo-3, AM to $Ca^{2+}$ may be the compartmentalisation of the dye into intracellular organelles. Of particular relevance would be its uptake into $Ca^{2+}$ storage vessels such as the ER, resulting in dye saturation and buffering of the calcium response (Takahashi *et al*., 1999).

Size exclusion prevents the 44 kDa flash pericam from becoming compartmentalised and it exhibits a uniform fluorescence throughout the cytosol and nucleus of HeLa cells (Miyawaki *et al*., 2002; Nagai *et al*., 2001).

Unfortunately, the use of flash pericam for the study of RV-induced changes to $[Ca^{2+}]_i$ was thwarted by an apparent caloric stress effect, as described in greater detail in Section 4.3.4. Consequently, despite its apparent lower sensitivity to changes in $[Ca^{2+}]_i$, fluo-3, AM was used as the calcium-sensitive indicator for all cell population studies.

Irrespective of the detection system used, the addition of 5 mM $Ca^{2+}$ consistently failed to induce a change in $[Ca^{2+}]_i$ for RV-infected cells. This discrepancy may be attributable to the extensive damage done to the host cell due to the protracted (18 h.p.i.) virus infections. The optimal time for $Ca^{2+}$ analysis of RV-infected cells was investigated further in Section 4.3.1.2.

- **Cellular autofluorescence**

The contribution to the total fluorescence signal by cellular autofluorescence was also investigated for each cell line (results not presented). The spectrofluorimetric measurement of basal fluorescence levels demonstrated that autofluorescence did not contribute appreciably to the fluorescence signal for fluo-3, AM loaded cells. The basal fluorescence level for cells transfected with flash pericam was substantially higher than for non-transfected cells; consistent with expression of the yellow fluorescent protein.

- **The spectrofluorimetric detection system for the measurement of changes to the $[Ca^{2+}]_i$ of cell populations**

Based on the data obtained from each of the experiments reported above, a spectrofluorimetric system using fluo-3, AM as the calcium-sensitive reporter was employed for the detection of NSP4 and RV-induced changes to the intracellular calcium homeostasis of mammalian cell lines MA104 and COS-7.

#### 4.3.1.2 Assessment of PM permeability to $Ca^{2+}$ of SA11-infected cells

The effect of RV infection on plasmalemma permeability to $Ca^{2+}$ has been investigated elsewhere using both polarised and non-polarised cell lines (Brunet *et al*., 2000a; Michelangeli *et al*., 1991; 1995; Pérez *et al*., 1999; Ruiz *et al*., 2005). In each of these studies a $Ca^{2+}$ pulse was applied to the extracellular medium and the change in $[Ca^{2+}]_i$ measured spectrofluorimetrically. The experimental design applied in this report has been adapted from these investigations.

RV-induced changes in PM permeability to $Ca^{2+}$ and to cytosolic $Ca^{2+}$ concentration were investigated in MA104 and COS-7 cell lines. The MA104 cell line is a model system routinely employed for RV studies and has been used extensively by others for investigating RV and NSP4-induced changes to intracellular calcium homeostasis (Cuadras *et al*., 1997; Michelangeli *et al*., 1991; 1995; Pérez *et al*., 1999; Ruiz *et al*., 2007). The COS-7 cell line although used less frequently (Diaz *et al*., 2008; Zambrano

*et al*., 2008) was included in this study primarily for the purpose of establishing high expression levels of flash pericam, as discussed in Section 4.3.2.1).

The RV strain SA11 was employed to establish the reliability of the spectrofluorimetric technique in detecting changes to $Ca^{2+}$ membrane permeability in response to RV infection. Once the detection system had been validated it would be used to monitor the changes to the intracellular calcium homeostasis of mammalian cells in response to infection with two HRV strains RV4 and RV5.

The data collected was plotted either as a function of the change in calcium concentration ($\Delta[Ca^{2+}]_i$) or of the absolute intracellular calcium concentration ($[Ca^{2+}]_i$) with time. The quantity $(f\text{-}f_0)/f_0$ is proportional to transient changes in the intracellular $Ca^{2+}$ concentration ($\Delta[Ca^{2+}]_i$) and for most analyses this value was sufficiently qualified to represent changes to $[Ca^{2+}]_i$ for real time measurements. The method of Tsien *et al.* (1982) was employed when absolute calcium concentrations were required for direct comparisons with published data.

The change in calcium concentration ($\Delta[Ca^{2+}]_i$) as a function of time was plotted for both mock and SA11-infected MA104 (Figure 4.6) and COS-7 (Figures 4.7a and b) cells in response to the application of a 5 mM $Ca^{2+}$ pulse to the extracellular medium.

As illustrated in Figure's 4.6 and 4.7a, the addition of 5 mM $Ca^{2+}$ (at t=10 s) to the extracellular medium caused an increase in the $\Delta[Ca^{2+}]_i$ for SA11-infected MA104 and COS-7 cells. Mock infected mammalian cells failed to demonstrate a similar change in calcium flux under the same experimental conditions. This is consistent with the observations of others (Brunet *et al*., 2000a; Michelangeli *et al*., 1991; 1995; Pérez *et al*., 1998; 1999; Ruiz *et al*., 2005). The initial increase in $[Ca^{2+}]_i$ within the first few seconds (~10 s) is representative of PM permeability to calcium and is attributable to the unidirectional flux of $Ca^{2+}$ across the PM from the extracellular medium into the cytosol (Brunet *et al*., 2000a; Pérez *et al*., 1998; 1999).

In this study, a succession of sharp peaks were observed for SA11-infected cells post application of the $Ca^{2+}$ pulse, rather than a single increase observed by other researchers

(Brunet *et al*., 2000a; Michelangeli *et al*., 1995; Pérez *et al*., 1998; Ruiz *et al*., 2005). This difference may be due to variances in the experimental protocol, particularly pertaining to the control of environmental parameters, the treatment of data and the use of the non-ratiometric calcium-sensitive fluorescent probe fluo-3, AM.

All published work consulted in the design of the spectrofluorimetric protocol reported that both temperature and sample homogeneity (continual stirring of suspension) were maintained throughout the duration of the recording of measurements. The spectrofluorimeter used in this research was not equipped for the control of either of these parameters, and it is possible that the absence of stirring may have had an undue influence on the measurements recorded. Morgan and Thomas (1999) reported that *"In populations, the initial response to submaximal concentrations of agonist is influenced by several factors, such as the latency prior to the initial* $[Ca^{2+}]_c$ *response (which may vary considerably from cell to cell), the percentage of responding cells and cell to cell differences in sensitivity (which in turn may affect the degree of synchronization and magnitude).*" Further to this they also noted the contribution to peak signals from both contaminating cell types and unhealthy cells.

Each peak may also be representative of a subpopulation ("clump") of cells which has experienced a change in $[Ca^{2+}]$ in response to the cation as it diffuses through the suspension at different time intervals post application. RV infection has been observed to cause clumping of cells (Michelangeli *et al*., 1991) and if not sufficiently dispersed in suspension, each peak may be representative of the interactions of $Ca^{2+}$ with these cell populations.

Fluo-3, AM was used to monitor the changes in PM permeability to $Ca^{2+}$ during virus infection. It is widely known that esterified $Ca^{2+}$ indicators can cross the membranes of other cellular organelles, either through passive diffusion or active uptake, resulting in compartmentalisation of the fluorescent dye (reviewed in Thomas *et al*., 2000). This effect was observed using fluorescence microscopy (Figure 4.8a) whereby punctate, highly fluorescent spots were visualised. Whether compartmentalisation was contributing to the atypical results obtained is unclear. One could surmise that the initial peak most probably coincided with the influx of exogenous calcium (5 mM) through the

plasma membrane, and each subsequent peak represents the influx of calcium from the cytosol into cellular organelles and *vice versa*. It can also be postulated that the presence of multiple peaks could be attributable to sample heterogeneity, exacerbated by the absence of a stirring mechanism to ensure uniformity in the presence of additives.

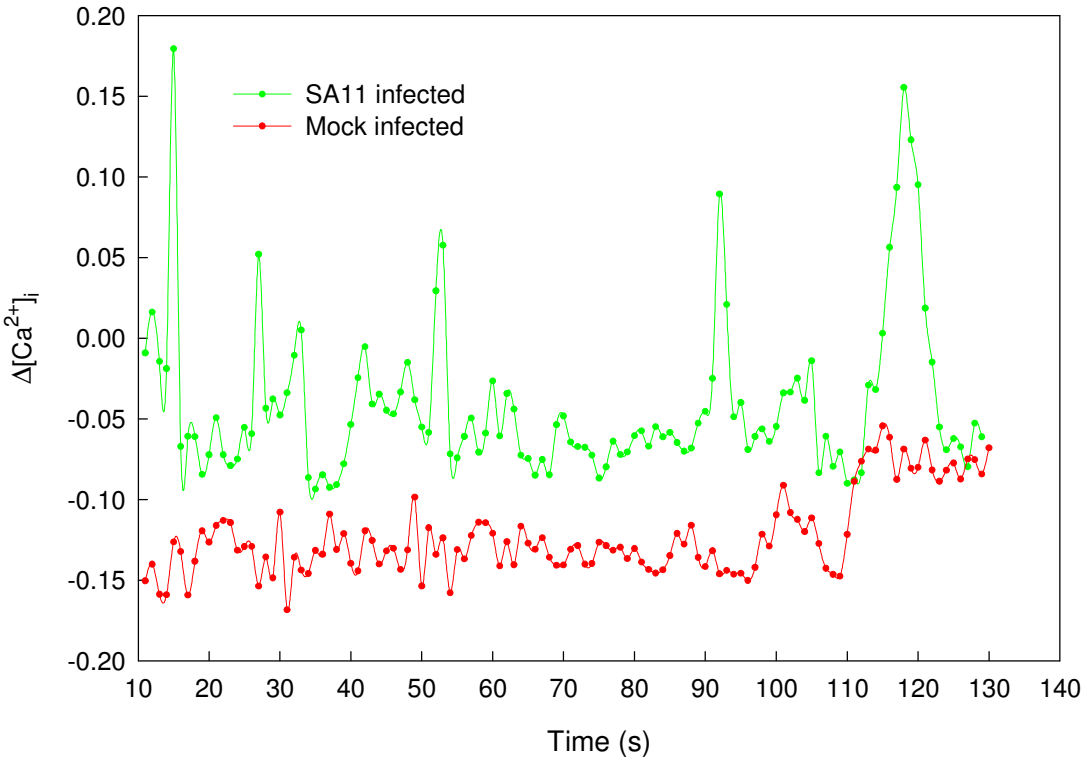


***Figure 4.6. The effect of SA11 infection on PM permeability to $Ca^{2+}$.*** *Both mock and SA11-infected MA104 cells loaded with fluo-3, AM were treated with 5 mM $Ca^{2+}$ at t=10 s. Virus replication was allowed to proceed for 18 h.p.i. prior to spectrofluorimetric analysis. Each data point corresponds to the mean of 4 independent experiments (measurements performed in duplicate) for mock and RV-infected MA104 cells.*

Another factor which needed to be addressed was the viability of the host cell, in particular the integrity of the PM, at the time of calcium measurement. The effects of membrane disruption to calcium measurements would be two-fold; (a) unregulated flux of $Ca^{2+}$ across the PM in response to the calcium pulse and (b) loss of fluo-3, AM to the extracellular medium. Michelangeli *et al.* (1991) observed a progressive increase in $[Ca^{2+}]_i$ from 5 h.p.i. with maximal values of the order of 500 nM attained at 8 h.p.i. in MA104 cells infected with the porcine RV strain OSU. They reported that

*"measurements beyond 9 hpi were not reliable due to clumping and decreased viability after trypsinisation".* A reduction in fura-2 accumulation due to a loss of PM integrity was observed 10 h.p.i. for OSU-infected MA104 and HT29 cells (Pérez *et al*., 1999).

A time course analysis was undertaken to address whether SA11-infected COS-7 cells, in which virus replication was allowed to proceed for a period greater than 18 h.p.i. was still feasible for measuring $\Delta[Ca^{2+}]_i$. Mock and virus infected cells were harvested at 6, 12, 18 and 24 h.p.i. The loading of cells with fluo-3, AM and the changes in fluorescence intensity in response to a 5 mM $Ca^{2+}$ pulse were measured for cells harvested at 6 and 12 h.p.i. only (Figures 4.7a-c) as per the reasons outlined below.

The initial stages of CPE i.e. cell contraction and rounding (Estes *et al*., 1979) were visible as early as 6 h.p.i. in SA11-infected COS-7 cells, and by 14 h.p.i. considerable detachment of the cell monolayer from the vessels surface was observed. Figures 4.12a and 4.13b, as captured for the caloric stress component of this research, are typical of the characteristic "balling up" of cell monolayers caused by RV infection observed throughout this study.

By 18 h.p.i. most of the cells were detached from the surface and consequently were not analysed further. These results are consistent with those observed by others. SA11 infection of MA104 cells at a low MOI (2-4 PFU/cell) resulted in CPE first visible within 8 to 10 h.p.i. and complete CPE observed by 48 h.p.i. (Estes *et al*., 1979). Similarly, oncosis in MA104 cells infected at a high MOI (20 FFU/cell) with the OSU strain commenced at 6-8 h.p.i. and was complete by 12-15 h.p.i. (Michelangeli *et al*., 1991; Pérez *et al*., 1998).

As illustrated in Figure 4.7a, at 6 h.p.i. an increased $\Delta[Ca^{2+}]_i$ was observed for SA11-infected cells only, whilst the reverse was observed for cells harvested at 12 h.p.i. (Figure 4.7b). The absence of a detectable $\Delta[Ca^{2+}]_i$ for virus infected cells at 12 h.p.i. may be due to deleterious alterations within the PM due to the progressive cytotoxic and lytic effects of the virus and consequently the inability to retain the fluorescent probe within the cell (Michelangeli *et al*., 1991; Pérez *et al*., 1999).

At 6 h.p.i. any $\Delta[Ca^{2+}]_i$ for mock-infected cells was most probably a result of capacitive $Ca^{2+}$ entry through the plasma membrane, whilst the increases in virus infected cells was attributable to both a virus-induced pathway and a capacitive component (Ruiz *et al*., 2005).

The absolute $[Ca^{2+}]_i$ was determined for both mock and virus-infected cells at each time point (Figure 4.7c) as per the method of Tsien *et al*. (1982). The $[Ca^{2+}]_i$ of SA11-infected cells at 6 h.p.i. was significantly greater than for the corresponding mock-infected cells; consistent with the results described above. No change in the $[Ca^{2+}]_i$ was observed between 6 and 12 h.p.i. for RV-infected cells (Students t-test; tested at a significance level, $p < 0.05$). Conversely, and quite unexpectedly the mock-infected cells demonstrated a 2-fold rise in $[Ca^{2+}]_i$ with time. The only conclusion drawn for this atypical result for mock-infected cells was the contribution of a greater cell density at 12 h.p.i. compared with 6 h.p.i. The contribution of cell density to estimates of $[Ca^{2+}]_i$ is questionable given that Banyard and Tellam (1985) found that neither cell density nor fluorescent dye concentration contributed to estimates of intracellular free calcium for quin-2 loaded human somatic cell hybrids. The notable absence of a change in $[Ca^{2+}]_i$ for RV-infected COS-7 cells between 6 and 12 h.p.i. was assumed to be associated with the loss of fluo-3, AM, a consequence of oncosis at the later time post infection as previously discussed.

a)

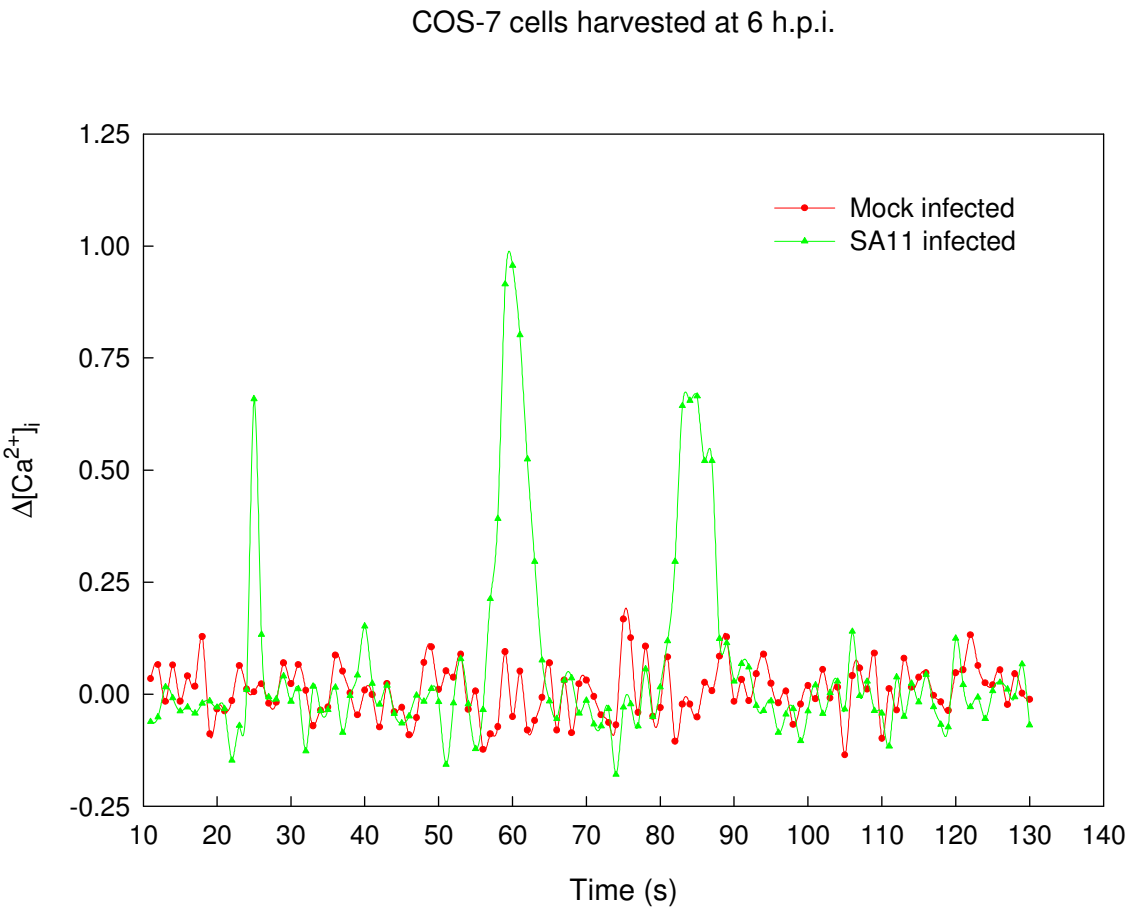
COS-7 cells harvested at 6 h.p.i.
Mock infected
SA11 infected
Δ[Ca2+]i
Time (s)
1.25
1.00
0.75
0.50
0.25
0.00
-0.25
10
20
30
40
50
60
70
80
90
100
110
120
130
140

b)

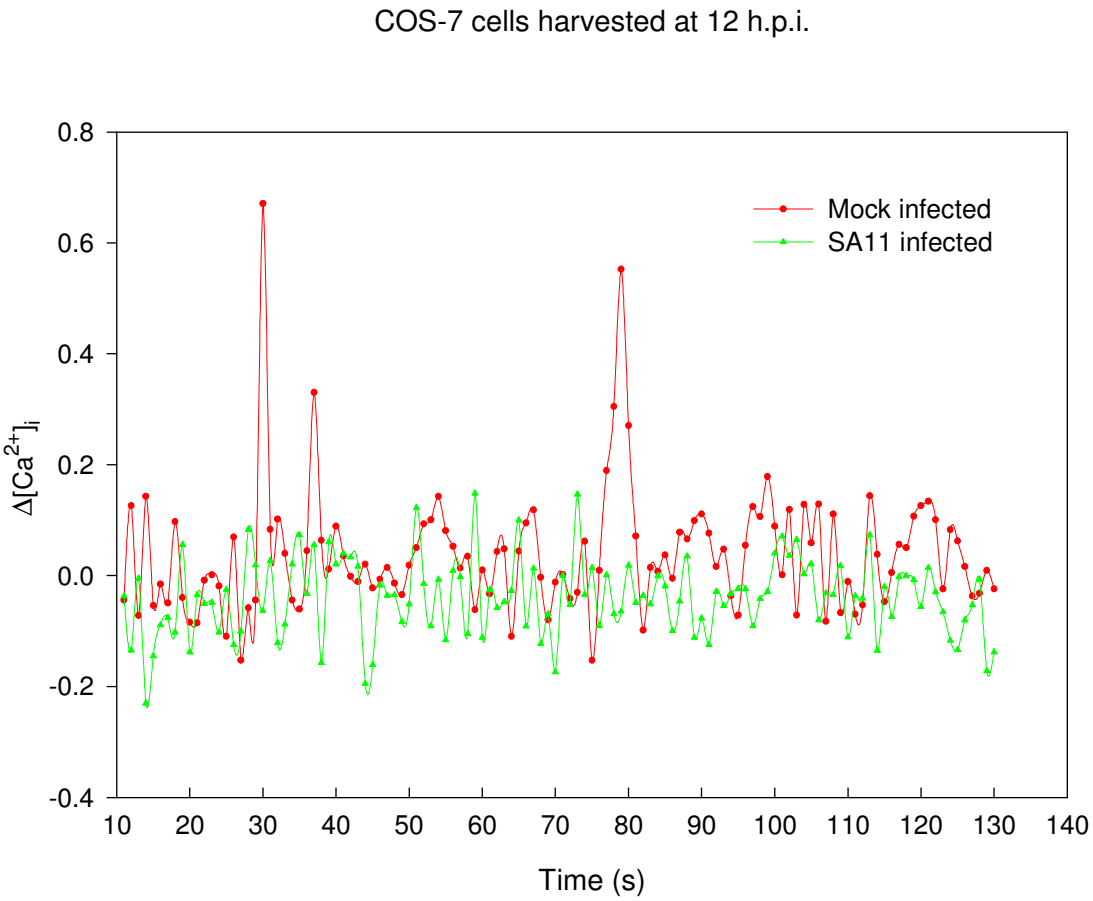
COS-7 cells harvested at 12 h.p.i.
Mock infected
SA11 infected
Δ[Ca2+]i
Time (s)
0.8
0.6
0.4
0.2
0.0
-0.2
-0.4
10
20
30
40
50
60
70
80
90
100
110
120
130
140

c)

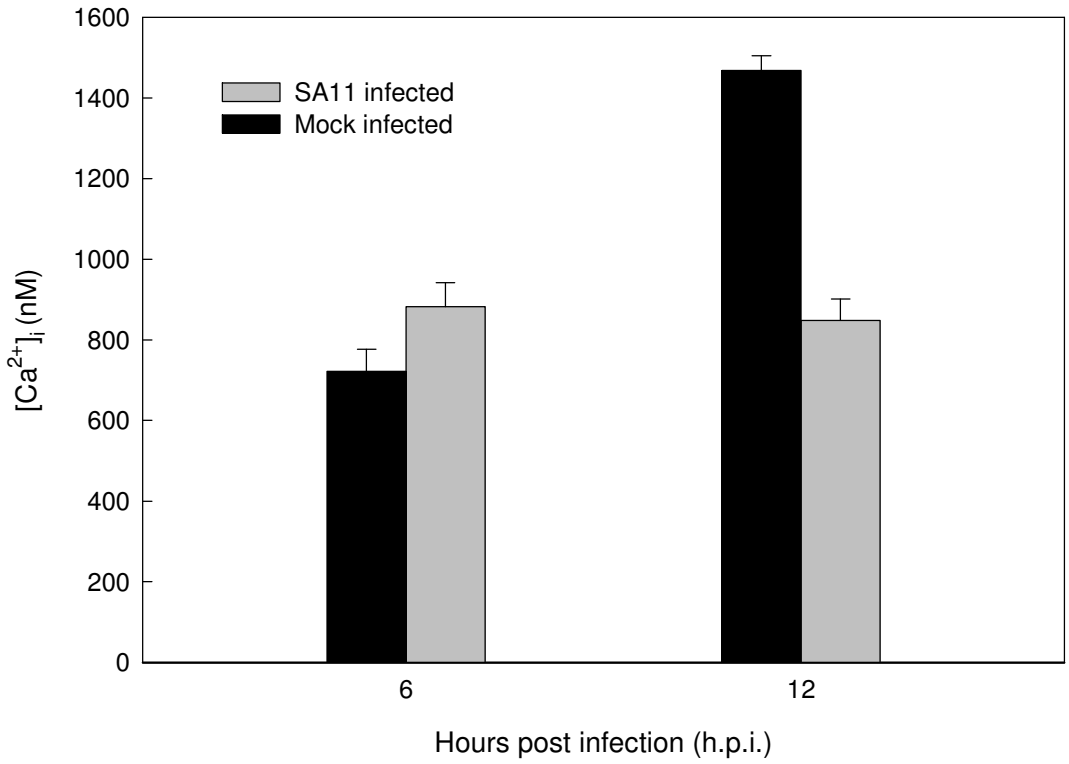


***Figure 4.7. Changes to the $[Ca^{2+}]_i$ of SA11-infected cells at (a) 6 h.p.i., (b) 12 h.p.i. and (c) as a function of absolute $[Ca^{2+}]_i$.*** *Mock and SA11-infected COS-7 cells were harvested at the indicated times (h.p.i.) and loaded with fluo-3, AM. The fluorescence intensity was monitored each second for 2 mins after the application of 5 mM $Ca^{2+}$ (t=10 s). Figures (a) and (b) are representative of the $\Delta[Ca^{2+}]_i$ as a function of real time. $[Ca^{2+}]_i$ was calculated as per Tsien et al. (1982) and is presented in (c) for mock and virus-infected cells at the two time points investigated. Calibration was performed for each sample after the sequential addition of Triton X-100 and EGTA to the cell suspension to obtain the respective maximum ($F_{max}$) and minimum ($F_{min}$). The dissociation constant of fluo-3, AM was taken as 390 nM. Statistical significance was determined at $p < 0.05$ for a Student's t-test. Error bars represent the standard deviation obtained from three independent measurements.*

Zambrano *et al*. (2008) also used the COS-7 cell line to investigate changes to the $[Ca^{2+}]_i$ evoked by a reassortant strain DxRRV. The authors performed their measurements at 7 h.p.i. and reported an increase from basal cytosolic calcium concentration from this time forward. Interestingly, they restricted their studies to COS-7 cells reporting that this cell line was more stable and resistant than MA104 cells under the experimental conditions performed.

Michelangeli and co-workers (1991) investigated the effect of calcium mobilisation in MA104 cells infected with the OSU strain. They determined that PM permeability to calcium occurred as early as 4 h.p.i.; in the absence of an accompanying change in $[Ca^{2+}]_i$, whilst increases to $[Ca^{2+}]_i$ within the cytosol and storage compartments was observed with the progression (> 5 h.p.i.) of the infection. Measurements of $[Ca^{2+}]_i$ beyond 9 h.p.i. were considered unreliable for both MA104 and HT29 cells as per the reasons disclosed previously (Michelangeli *et al*., 1991; Pérez *et al*., 1999). Brunet *et al.* (2000a) also demonstrated a progressive increase in $[Ca^{2+}]_i$ for fully differentiated and polarised intestinal Caco-2 cells infected with RRV; commencing at 7 h.p.i. and achieving maximal levels at 18 h.p.i. Measurements beyond 24 h.p.i. were considered unreliable due to alterations in the cell membrane. Any discrepancy between the experimental data presented here and that published may be due to differences in the infection kinetics of the virus strains, the cell lines and the M.O.I. used to infect the cells.

It is proposed that during the early stages of infection regulatory mechanisms for maintaining cytosolic calcium homeostasis, such as the $Ca^{2+}$-ATPase pump of the ER, are sufficient to compensate for the initial calcium influx across the PM. At later stages of infection, these mechanisms are overridden and the increase in $[Ca^{2+}]_i$ is attributed to the unregulated efflux of $Ca^{2+}$ from internal stores and influx across the PM (Brunet *et al*., 2000a; Michelangeli *et al*., 1991; Pérez *et al*., 1998; 1999).

In addition to the anomalies already discussed for the spectrofluorimetric analysis of cell populations, the magnitude of the absolute $[Ca^{2+}]_i$ calculated from the experimental data was inconsistent with the published values. The theoretical basal $[Ca^{2+}]_i$ of mammalian cells is approximately 100 nM (Carafoli, 1987), whilst the basal $[Ca^{2+}]_i$ of COS-7 cells calculated for this study (Figures 4.7c) was greater than 7-fold this value. A

potential reason for this deviation from the theoretical value may be attributed to the use of a published Kd value for fluo-3, AM in the determination of $[Ca^{2+}]_i$, rather than establishing the intracellular Kd value for the experimental system employed. The literature value for fluo-3, AM (Kd of 390 nM) was determined at 22°C in aqueous solution (Haughland, 2005). The determination of internal Kd values for fluo-3, AM is affected by temperature, pH, protein binding and dye compartmentalisation (reviewed in Rockwell and Storey, 1999). Consequently, the Kd value used for the determination of $[Ca^{2+}]_i$ may be markedly different from the true value for the experimental system and therefore no direct comparisons with published values of $[Ca^{2+}]_i$ could be made.

#### 4.3.1.3 Effects of NSP4 on PM permeability to $Ca^{2+}$

The addition of 5-10 nM of purified $His_6$-NSP4 directly to the cell suspension failed to induce a change in fluorescence intensity. The absence of a response may be due to the high dilution order imposed upon the protein using this experimental system. NSP4 has been reported to induce a dose-dependent mobilisation of intracellular calcium in *Sf*9 cells (Tian *et al*., 1995) and HT-29 cells (Dong *et al*., 1997). The smaller volumes of reagent required in the microscopic approach to changes in the intracellular calcium concentration of mammalian cells, as described in the proceeding section, should help to establish whether NSP4 perturbs calcium homeostasis and whether the response is dose-dependent.

### 4.3.2 Changes to calcium homeostasis – a microscopic approach to the effects of NSP4 and to whole virus

This section describes the development of a microscopic detection system for monitoring changes to the intracellular calcium homeostasis of single cells. Once established, the system was employed to monitor the $\Delta[Ca^{2+}]_i$ of mammalian cells in response to the exogenous addition of NSP4 or to RV infection. Epifluorescence microscopy, unlike the spectrofluorimetric technique described previously, would enable the quantification of the $\Delta[Ca^{2+}]_i$ to individual cells.

#### 4.3.2.1 Optimisation of the epifluorescent detection system

- **Selection of a calcium sensitive fluorescent probe**

The potential for fluo-3, AM or flash pericam to be used as indicators for detecting changes to the intracellular calcium homeostasis of individual cells was investigated. The specificity and sensitivity of each of the indicators to changes in $[Ca^{2+}]_i$ for this system had to be established.

Fluo-3, AM loaded MA104 and COS-7 cells exhibited the characteristic punctate staining associated with compartmentalisation of the synthetic dye. Figure 4.8a demonstrates the staining pattern of fluo-3, AM labeled cells observed in this study. Efforts to reduce the sequestering of fluo-3, AM into intracellular organelles was undertaken by manipulating the temperatures upon which dye loading and de-esterification were allowed to proceed. Reductions in dye loading temperature have been shown to produce a more uniform distribution of the dye within the cytoplasm and a decline in the rate of dye extrusion from the cell (reviewed in Hayashi and Miyato, 1994; Moore *et al*., 1990). The incubation of fluo-3 loaded HeLa cells at 37°C post dye loading was responsible for a substantial loss in cytoplasmic fluorescence and subsequent compartmentalisation of the dye to the mitochondria and ER (Thomas *et al*., 2000). Results from this work demonstrated that compartmentalisation of fluo-3, AM was reduced when dye-loading was allowed to proceed at 29°C rather than 37°C (results not presented).

Flash pericam produced a more uniform distribution of fluorescence throughout the cytoplasm and nuclear compartments (Figure 4.8b) and was thus considered a more suitable marker for the detection of intracellular $Ca^{2+}$ fluctuations in individual cells.

The responsiveness of fluo-3, AM loaded cells to the positive control calcimycin, was substantially lower when compared to that of cells expressing flash pericam (results not presented). This result was consistent with that previously demonstrated using the spectrofluorimetric technique (Figure 4.5).

a)

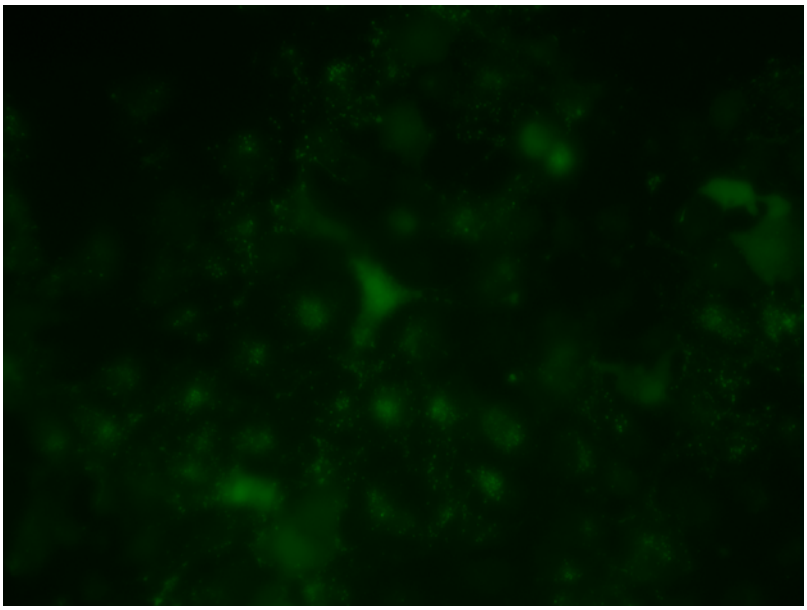

b)

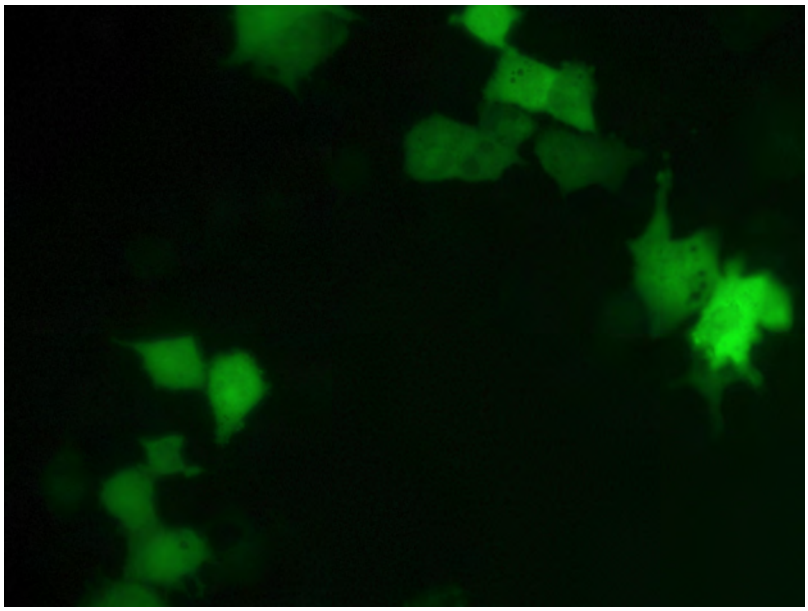

***Figure 4.8. The basal fluorescence profile of (a) fluo-3, AM and (b) flash pericam in COS-7 cells.*** *COS-7 cells were loaded with fluo-3, AM or transfected with flash pericam DNA prior to viewing under epifluorescence with an FITC filter. Magnification X 400.*

- **Choice of cell line**

The expression of flash pericam was comparatively more efficient in COS-7 cells than for the MA104 cell line; as evidenced by the higher basal fluorescence levels and ratio of cells expressing the protein for the former. This difference was not entirely unexpected given the properties of the cell lines used and the parent vector pcDNA3 into which flash pericam DNA was cloned.

The COS cell line was created by transforming an established monkey epithelial (CV-1) cell line with a mutated Simian virus SV40 genome (Gluzman, 1981; Jensen *et al*., 1964). The SV40 mutant contained a small deletion in the origin of replication (*ori*) preventing the replication of endogenous viral DNA.

COS cells express nuclear large T antigen and all of the proteins necessary for the replication of appropriate circular genomes, and the introduction of a plasmid containing an SV40 *ori* (e.g. flash pericam/pcDNA3 plasmid) results in replication of the plasmid to a high copy number (Hancock, 1991). Expression of flash pericam is driven by the immediate-early Cytomegalovirus promoter and although flash pericam expression can proceed in MA104 cells, the level of expression is greater in COS-7 cells due to the inability of plasmid DNA to be replicated to a high copy number in MA104 cells.

#### 4.3.2.2 NSP4-induced mobilisation of intracellular calcium in COS-7 cells

The effects of the C- and N-terminal $His_6$-NSP4 fusion proteins (RV4C, RV4N, RV5C and RV5N) on intracellular calcium mobilisation of flash pericam transfected COS-7 cells was investigated.

Calcimycin was chosen as the positive control for these studies as it had been used with success previously for demonstrating changes to the calcium homeostasis of mammalian cell populations (Section 4.3.1.1).

As illustrated in Figure 4.9, the addition of 38 µM calcimycin to COS-7 cells elicited an immediate and sustained increase in the $\Delta[Ca^{2+}]_i$ consistent with its role as an ionophore. The increase in fluorescence was associated with a calcimycin induced influx of $Ca^{2+}$ across the PM.

The addition of 60 nM RV5C (C-terminal $His_6$-tagged RV5 NSP4) to COS-7 cells induced an immediate rise in the $\Delta[Ca^{2+}]_i$ within the first few seconds, and a rapid return to baseline by approximately 25 seconds (Figure 4.9). This result is consistent with the work of others who demonstrated that the NSP4-induced mobilization of intracellular calcium is transient (Dong *et al*., 1997; Tian *et al*., 1996a; Zhang *et al.*, 1998; 2000). A rapid increase in $[Ca^{2+}]_i$ was observed within the first few seconds post application of 50 to 100 nM NSP4 to HT-29 cells, persisting for between 1-2 minutes, whereupon it returned to basal levels (Dong *et al*., 1997; Zhang *et al.*, 1998; 2000). A similar response was observed upon the addition of either NSP4 (6 µM) or $NSP4_{114-135}$ (100 µM) to *Sf*9 cells (Tian *et al*., 1996a). This transient, NSP4-induced rise in $[Ca^{2+}]_i$ is primarily associated with the release of $Ca^{2+}$ from intracellular stores (Dong *et al*., 1997).

The addition of 30 nM RV4C (C-terminal $His_6$-tagged RV4 NSP4) elicited an increase in $[Ca^{2+}]_i$ which was equivalent in rate to that observed for RV5C. The response to the exogenous application of RV4C was also transient but the decrease in the $\Delta[Ca^{2+}]_i$ was considerably more protracted than observed for RV5C, and failed to return to baseline level.

A decline in the fluorescence intensity below baseline level was observed at time points exceeding 25 s for the exogenous addition of RV5C. As the fluorescent indicator used was flash pericam, this loss in fluorescence could not be attributed to photobleaching. Morris *et al*. (1990) observed a similar trend in fura-2 loaded HT29 cells post application of neurotensin. They proposed that this "undershoot" was indicative of extrusion/reuptake in the recovery of $[Ca^{2+}]_i$. As this pattern was not observed for RV4C, it is plausible that this decline in intensity could be (a) commensurate with stage drift or (b) the two-fold higher concentration of RV5C used in this analysis. The dose-

dependency of NSP4 on intracellular calcium mobilisation will be discussed elsewhere (4.3.2.4).

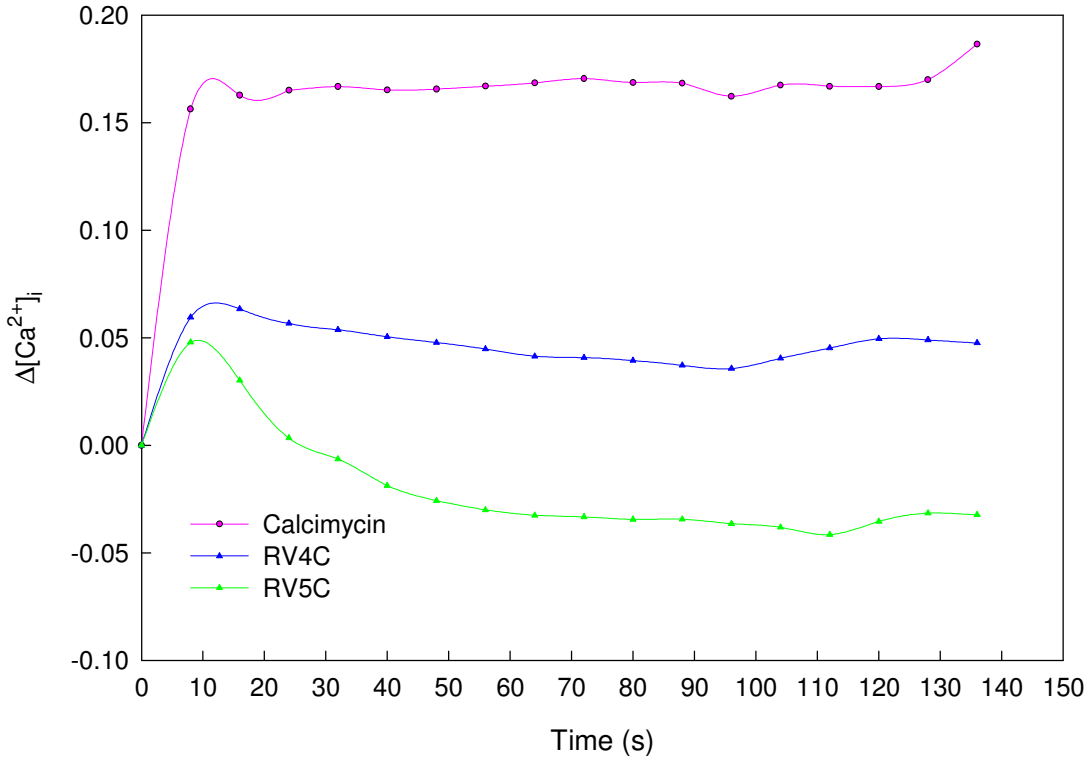


***Figure 4.9. NSP4-induced changes to the $[Ca^{2+}]_i$ of COS-7 cells.*** *Real time changes to the fluorescence intensity of flash pericam transfected COS-7 cells was monitored on an epifluorescence microscope in response to the application of 38 μM calcimycin (N=5), 60 nM RV5C (N=7) and 30 nM RV4C (N=5). The application of each of the agents was at t=0. Each data point represents the mean grey value averaged across the total number of independent experiments (N) for each agent as calculated from data acquired from Image J.*

#### 4.3.2.3 Proximal location of the $His_6$-tag on NSP4 and its influence on the $\Delta[Ca^{2+}]_i$

Preliminary data obtained from the studies of NSP4-specific antibody responses (Section 3.3.3) indicated that the position of the terminal $His_6$-tag may influence the immunological response to NSP4. It was postulated that the binding of the $His_6$-tag to the C-terminal of NSP4 may interfere with either the direct binding of antibodies to linear epitopes or induce changes within the protein which altered conformation-dependent epitopes. Based on these results, it was considered pertinent that the influence of the proximal location of the $His_6$-tag at both the C- and N-termini of NSP4 be investigated in response to the calcium mobilising properties of the protein.

As illustrated in Figure 4.10, the application of 60 nM RV4N to COS-7 cells resulted in an immediate increase in the $\Delta[Ca^{2+}]_i$ which was in agreement with the observations for RV4C. RV4N appeared to evoke a sustained increase to the $\Delta[Ca^{2+}]_i$ rather than the transient increase observed for RV4C.

Unfortunately, image sequences captured for RV5N (N-terminal $His_6$-tagged NSP4; RV5)-induced changes to the $[Ca^{2+}]_i$ of flash pericam transfected COS-7 cells were deemed unsuitable for further analysis due to the effects of focal shifts and stage drift. A consistent drawback of the microscopic method developed for this research was the shift in view field and/or focal drift associated with the application of reagents, or as a function of time. Another factor which also compromised the integrity of the real time imaging of cells was the movement of dead cells or cellular debris across the view field due to Brownian motion and the addition of reagents. Any image sequence which had been affected by any of these aberrations were discarded due to the subsequent changes in fluorescence intensity they incurred.

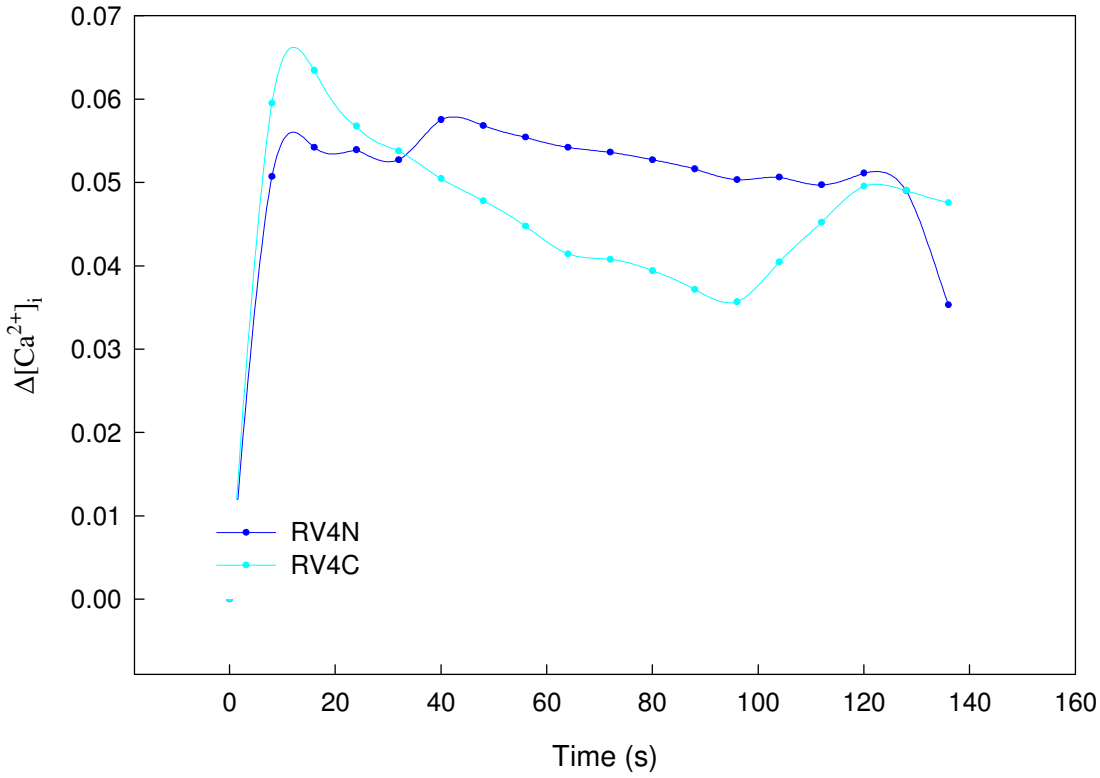


***Figure 4.10. Influence of $His_6$ tag location on NSP4-induced changes to $[Ca^{2+}]_i$.*** *Real time changes to the fluorescence intensity of flash pericam transfected COS-7 cells was monitored on an epifluorescence microscope in response to the application of 30 nM RV4C (N=5) and 60 nM RV4N (N=6). Zero time (t=0) was taken as the time of application for each of the agents. Each data point represents the mean grey value averaged across the total number of cells analysed for each independent experiment (N) as calculated from data acquired from Image J.*

#### 4.3.2.4 NSP4-induced changes in $[Ca^{2+}]_i$ is dose-dependent

NSP4-induced mobilisation of intracellular calcium in HT29 cells is dose-dependent, with concentrations as low as 4.6 nM NSP4 sufficient to elicit changes to the calcium homeostasis of 50% of the cell population ($ED_{50}$) (Dong *et al*., 1997). The authors of this study demonstrated that the $[Ca^{2+}]_i$ dose response curve, measured across an NSP4 concentration range of 0.1 nM to 10 mM, showed a saturable hyperbolic function. Figure 4.11 suggests the dose-dependency of RV4C on inducing changes to the intracellular calcium homeostasis of COS-7 cells. When the concentration of RV4C was reduced two-fold, from 30 nM to 15 nM, no change in fluorescent intensity was detected. These results are consistent with those obtained for the spectrofluorimetric

analysis of cell populations (4.3.1.3), whereby concentrations ≤ 10 nM NSP4 (RV4C and RV5C) failed to induce a change in $[Ca^{2+}]_i$. Taken together, these results imply that the minimum concentration required to elicit a change in intracellular calcium homeostasis for the C-terminal His-tagged form of the NSP4 protein would need to be greater than 15 nM.

Further investigation needs to be conducted over a greater concentration range to confirm unequivocally that NSP4 of HRV strains RV4 and RV5 induces a dose-dependent change to the $[Ca^{2+}]_i$ of COS-7 cells.

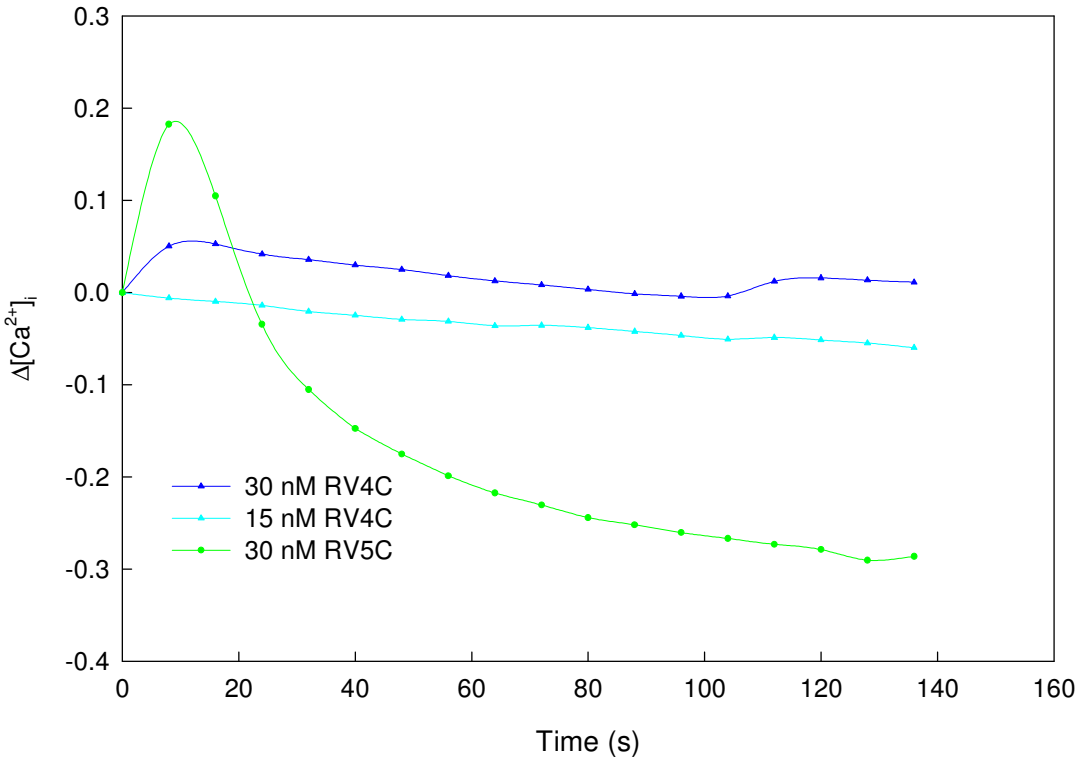


***Figure 4.11. NSP4 induces a dose-dependent $\Delta[Ca^{2+}]_i$.*** *Real time changes to the fluorescence intensity of flash pericam transfected COS-7 cells in response to the application of 30 nM RV5C, 30 nM RV4C and 15 nM RV4C were monitored on an epifluorescence microscope. Each data point represents the mean grey value averaged for two independent experiments for each agent as calculated from data acquired from Image J.*

#### 4.3.2.5 RV-induced changes to intracellular calcium homeostasis.

The evaluation of RV-induced changes to the intracellular calcium concentration of single cells was attempted with mammalian cells expressing flash pericam or labeled with fluo-3, AM. As previously described for the spectrofluorimetric analysis of cell populations, an apparent caloric stress effect prevented the use of flash pericam as the calcium sensitive probe for RV infections.

The use of fluo-3, AM for monitoring RV-induced changes to the intracellular calcium concentration of single cells also proved to be problematic. The excessive wash steps conducted pre- and post-dye loading often resulted in further damage to the RV-infected cell monolayer. In addition, the clumping of RV-infected cells prevented the monitoring of localised changes to the intracellular calcium concentration of single cells. Due to the sensitivity of the method to focal shifts upon the application of reagents, it was not possible to measure the absolute $[Ca^{2+}]_i$ in response to NSP4 or RV infection. Consequently, the study of RV-infected $\Delta[Ca^{2+}]_i$ of individual cells was aborted.

### 4.3.3 Neutralisation of NSP4 and its effect on the $\Delta[Ca^{2+}]_i$

Antibody to NSP4 has been shown to reduce the severity and incidence of RV-induced diarrhoeal disease in neonatal mice (Ball *et al*., 1996; Choi *et al*., 2005; Yu and Langridge, 2001). In contrast, studies performed using the gnotobiotic piglet model failed to demonstrate a correlation between NSP4-specific antibodies and protection against infection or diarrhoea upon challenge with RV (Yuan *et al*., 2004a).

To my knowledge this is the only study which has used direct neutralisation of NSP4 to address its ability to effectively block NSP4-induced changes to intracellular calcium homeostasis. De Marco *et al*. (2009) demonstrated that human serum Igs were able to block ion secretion and cell damage of RV-infected Caco-2 cells.

Preliminary experiments with flash pericam transfected COS-7 cells indicated that the preincubation of NSP4 with human sera positive for α-NSP4 antibodies (as determined in Chapter 3) did not inhibit changes to $[Ca^{2+}]_i$.

### 4.3.4 Caloric stress enhances the CPE of rotavirus-infected cells

An apparent thermal stress response which augmented the CPE of RV-infected cells was discovered by chance when performing infections on mammalian cells expressing flash pericam. When cells preincubated at the lower temperature for flash pericam expression (29°C for 3 to 4 days) were returned to 37°C for RV adsorption and replication, a marked increase in the CPE was observed as early as 2 h.p.i. In contrast, cells which had been maintained at 37°C exhibited an equivalent degree of CPE at > 8 h.p.i. Control cells which were mock infected with porcine trypsin and exposed to the same incubation conditions as per the virus infected cells failed to exhibit signs of CPE in the period of experimental investigation. An association between enhanced CPE and the expression of flash pericam was also investigated. Non transfected cells subjected to the same caloric stress as observed for flash pericam transfected cells exhibited enhanced CPE, thus precluding the contribution of the protein to cell death (Figure 4.12).

a)

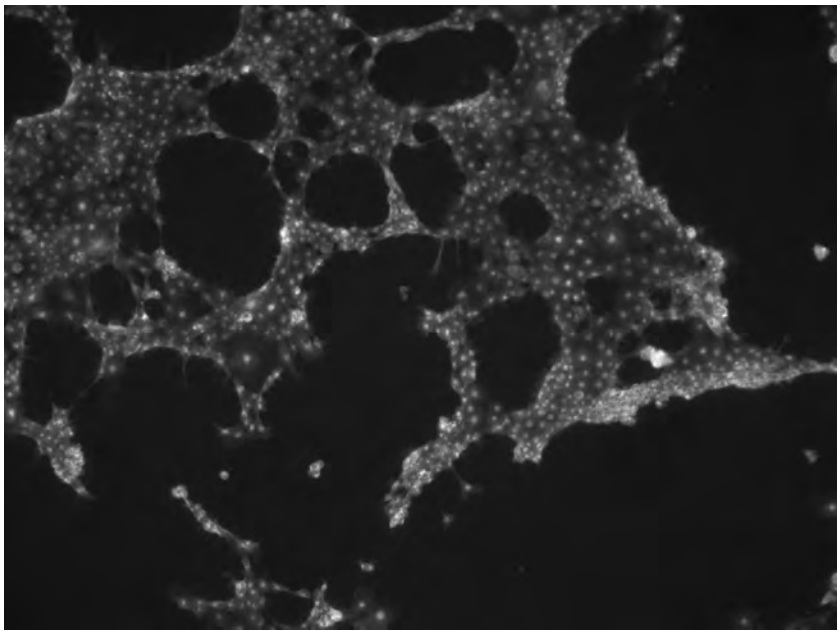

b)

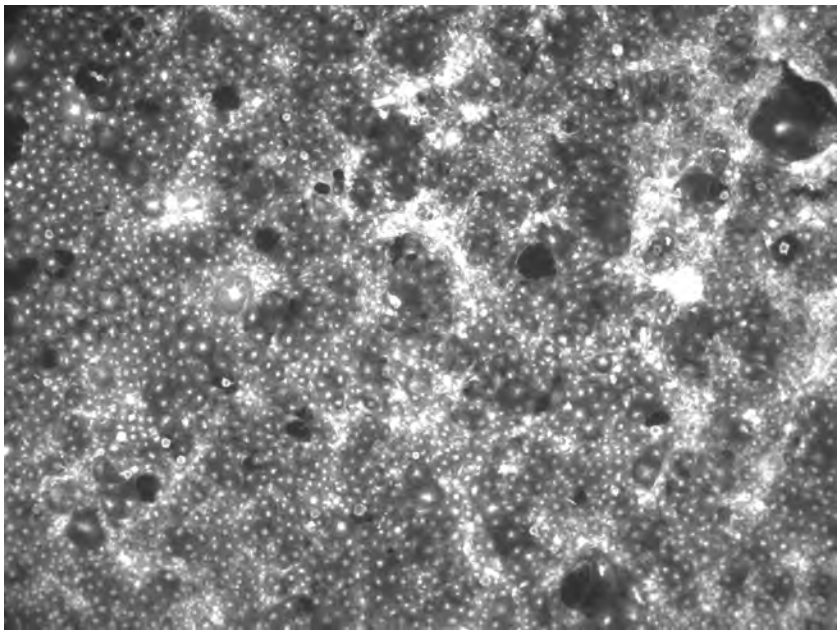

***Figure 4.12. Caloric stress effect on RV-infected mammalian cells.*** *COS-7 cells were infected with the HRV strain RV5 for 3.5 hours prior to fixation and immunofluorescence detection with the Alexa-Fluor 488 conjugate. Figure (a) illustrates the marked disruption to the cell monolayer for cells preconditioned at 29℃ prior to infection with RV5 at 37℃. Figure (b) is of RV5-infected COS-7 cells which had been maintained at 37℃. Cells were visualised on a Nikon Eclipse 50i epifluorescent microscope using a FITC filter. Magnification X 100.*

In this study, cells which had been maintained at the physiological temperature of 37°C were subjected to mild hypothermia (29°C) for 3-4 days, after which they were returned to 37°C for RV infection. The prewarming of cells to physiological temperatures following transient cold shock has been documented to induce a heat shock response (Liu *et al*., 1994; Sonna *et al*., 2010). As to whether the enhanced CPE observed for RV-infected cells cultivated at 29°C was due solely to a cold or heat shock effect, or a combination of both, was not determined and its elucidation was beyond the scope of this study.

Thermal stress, as demonstrated for mild hypothermia and hyperthermia, induces the expression of stress proteins including cold shock proteins (Csp's) and heat shock proteins (Hsp's). The induction or up-regulation of Hsp's in response to heat stress has been investigated widely for a large number of organisms and model cell systems. The Hsp's are a highly conserved group of proteins whose expression in cells is induced in response to low levels of stress (e.g. heat, heavy metals, oxidative stress, radiation and nitric oxide) (Samali and Orrenius, 1998). Hsp's are involved in many physiological processes, including cell cycle control, cell proliferation, development, organisation of the cytoarchitecture, and apoptosis (reviewed in Richter-Landsberg, 2009).

The level of constitutively expressed Hsp's (Hsc) is increased in response to stress, whilst other Hsp's are induced only after stress (Samali and Orrenius, 1998). The constitutively expressed Hsp's (e.g. Hsc70) function as molecular chaperones, regulating cellular processes such as protein synthesis, protein folding, transport and cell viability (Gething and Sambrook, 1992; Welch, 1991). Inducible Hsp's (e.g. Hsp70) assist in the repair of denatured and misfolded peptides, or target them for degradation by the ubiquitin/proteasome–dependent pathway (Richter-Landsberg, 2009; Samali and Orrenius, 1998). Hsp's are classified according to their molecular weights and the most extensively studied are the members of the Hsp70, Hsc70, Hsp60, Hsp90 and Hsp40 families.

Virus induction of heat shock proteins has been widely documented for a number of viruses (Newcastle, Sindbis, vesicular stomatitis, SV40 and polyomavirus) (Collins and Hightower, 1982; Garry *et al*., 1983; Khandjian and Türler, 1983; Nevins, 1982;

Notarianni and Preston, 1982) and has been demonstrated to enhance virus (adenovirus, cytomegalovirus, Epstein-Barr, HIV-1, HSV-1, measles, polyomavirus) replication (Burch and Weller, 2005; Chromy *et al*., 2003; Furlini *et al*., 1990; Glotzer *et al*., 2000; Vasconcelos *et al*., 1998; Zerbini *et al*., 1985; 1986).

RV infection is known to induce the expression of genes encoding Hsp40, Hsp70 and Hsp90, the translationally controlled tumour protein (TCTP) and ER-resident $Ca^{2+}$-binding molecular chaperones; which is both host cell and virus strain dependent (Broquet *et al*., 2007; Cuadras *et al*., 2002; Dutta *et al*., 2009; Xu *et al*., 1998; 1999).

The use of siRNA to down-regulate the expression of Hsp70 in Caco-2 cells was associated with an increase in the production of RV structural proteins (VP2, VP4, VP6) and progeny virus (Broquet *et al*., 2007). Given the protective role of Hsp70, it could be surmised that Hsp70 induction may afford a protective response to infection by negatively controlling RV protein bioavailability by directing viral proteins towards ubiquitin-dependent degradation (Broquet *et al*., 2007; Tavaria *et al*., 1996).

The heat shock cognate protein, Hsc70, has been identified as a potential post-attachment viral receptor and is present on the surface of MA104 cells (Guerrero *et al*., 2002). Binding of the RV particle with the peptide-binding domain of Hsc70, has been proposed to induce a conformational change of either host cell surface proteins or virus proteins which facilitates in either virus penetration or uncoating (Guerrero *et al*., 2002; López *et al*., 2006; Pérez-Vargas *et al*., 2006; Zárate *et al*., 2003). Two hsc70 binding domains (aa 642-658 and 531-554) have been identified on VP4 (Gualtero *et al*., 2007; Zárate *et al*., 2003). Gualtero *et al*. (2007) also discovered a Hsc70 binding domain (aa 280-297) on VP6, and they proposed that the Hsc70 induced conformational changes of VP4 resulted in the exposure of the VP6 domain, facilitating virus entry. It was postulated that the thermal stress imposed on the cells in this study may have caused the upregulation of Hsc70 and an associated increase in viral infectivity, but the results of Lopez *et al*. (2006) suggest otherwise. The authors demonstrated that the abundance of Hsc70 in MA104 and BHK cells was not modified in response to heat stress.

Hsp90 plays an integral role in the maintenance of cellular homeostasis; regulating the signal transduction pathways for cell cycle and survival. In the early stages of RV infection, Hsp90 positively regulates infection by modulating cellular signaling proteins or through direct interaction with viral proteins (Dutta *et al*., 2009).

Heat stress is also known to alter membrane permeability resulting in increases to intracellular $Na^+$, $H^+$, and $Ca^{2+}$ concentrations (reviewed in Sonna *et al*., 2002). Given the close association between $[Ca^{2+}]_i$ and RV replication, morphogenesis and pathogenesis, one could speculate that heat shock may induce changes to the calcium homeostasis of the host cell which is conducive to the survival and replication of the virus.

Changes to the intracellular calcium homeostasis of the host cell may also evoke an ER stress response. The upregulated expression of ER-resident proteins is a characteristic cellular response to-ER induced stress (Xu *et al*., 1999). NSP4 expression in COS-7 cells affected the up-regulation of the ER-resident $Ca^{2+}$ binding proteins GRP, endoplasmin, BiP, calreticulun, ERP5 and the cytoplasmic translationally controlled tumour protein (TCTP) (Xu *et al*., 1998; 1999). The authors proposed that the NSP4-associated reduction in ER $[Ca^{2+}]$ caused the induction of GRP78 expression, and subsequent translocation to the ER, in an effort to prevent protein aggregation and to restore $Ca^{2+}$ homeostasis. The depletion of ER calcium levels, in association with NSP4 expression, was also responsible for the increased transcription of the TCTP gene in COS-7 cells (Xu *et al*., 1999). Both GRP78 and GRP94 have been associated with RV maturation through the ER, potentially assisting in the correct folding of the outer capsid proteins (Xu *et al*., 1998).

Another dimension to the caloric stress imposed on the host cells in this study was that of mild hypothermia, or a cold shock effect. The induction of Hsp's in response to elevated temperatures has been studied widely in both prokaryotic and eukaryotic systems, but comparatively very little is known regarding the cold shock effects. The response of eukaryotes to cold stress has been implicated in adaptive thermogenesis and cold tolerance, and has been manipulated for sample (cells, tissues and organ) preservation and in the therapeutic treatment of brain damage (reviewed in Fujita, 1999).

More recently, the lowering of temperatures below sub-physiological levels (< 37°C) has been demonstrated to enhance adhesion of bacterial cells to the surface of host cells *in vitro* (Spaniol *et al*., 2009) and improve recombinant protein yield in mammalian cell culture (Al-Fageeh *et al*., 2006; Fujita, 1999).

The two-fundamental stressors of cold shock are related to changes in temperature and dissolved oxygen concentration. At the cellular level, cold shock elicits a coordinated response involving modulation of the cell cycle, metabolic processes, transcription, translation, and the cell cytoskeleton (Al-Fageeh *et al*., 2006). These responses are synonymous with those previously described for the heat shock effects. Growth arrest of prokaryotic and eukaryotic cells exposed to temperature downshifts is associated with the suppression of protein synthesis. Recent studies have shown that cold shock induces the expression of more than 20 genes in mammalian cells, and to date, two cold shock-induced proteins (CIRP and RBM3) have been identified in mammalian cells (Danno *et al*., 2000; Nishiyama *et al*., 1997; Sonna *et al*., 2002).

Cold shock is known to cause a reduction in F-actin and to initiate microtubule disassembly and associated actin filament disruption (reviewed in Al-Fageeh and Smale, 2006). RV is known to associate with, and cause disorganization of, the cell cytoskeleton in Caco-2 cells (Brunet *et al*., 2000b). It is possible that the enhanced CPE may be attributed to the cumulative disruption to the cellular architecture caused by both cold shock and RV infection. Cold shock is also known to change cellular membrane permeability resulting in a reduction in cellular pH (Al-Fageeh and Smale, 2006).

López *et al.* (2006) demonstrated that thermal stress enhanced the strain-dependent infectivity of the relatively refractory cell line (BMK) to RV, whilst offering little change to the highly permissive MA104 cell line. RV infection of both MA104 and COS-7 cells with each of the RV strains (SA11, RV4 and RV5) investigated in the present study, resulted in enhanced CPE for all cells exposed to thermal stress. Discrepancies between the results obtained in this study and that of López *et al.* (2006) may be associated with the marked differences in thermal stress conditions imposed on the cells. López *et al.* (2006) heat shocked the cells at 43-45°C for 20 minutes prior to

standard virus adsorption conditions. In addition, the cells were allowed to recover from heat shock at physiological temperatures prior to infection. In this research, cells were subjected to mild hyperthermia at 29-30°C for three days prior to virus adsorption and subsequent infection at 37°C. In addition, the cells were not acclimatised to 37°C prior to RV infection.

The viral titre had to be established in order to elucidate whether the enhanced CPE was associated with an increase in viral infectivity. Enumeration of the viral trite was attempted using three methods; an endpoint dilution assay, plaque assay and immunofluorescence focus assay. The latter two methods which are routinely used for establishing rotavirus titres proved to be unsuccessful in this study. Distinct and isolated plaques failed to develop for the plaque assay despite adopting published methods specific for RV titre determination (Ciarlet and Conner, 2000; Smith *et al*., 1979). The results from the immunofluorescence labeling of RV and mock-infected cells was inconclusive due to the non-specific reactivity of components of the mock-infected cell culture with either the anti-RV antibody or secondary antibody (Alexa-Fluor 488 conjugate) (Figure 4.13). What is apparent from these images is the distinct projections from the cell bodies of RV-infected cells. Berkova *et al*. (2007) demonstrated that endogenous expression of NSP4 or RV infection of mammalian cells (HEK-293 or MA104) resulted in the calcium-dependent re-organization of subcortical actin into ‘finger-like’ plasma membrane protrusions.

a)

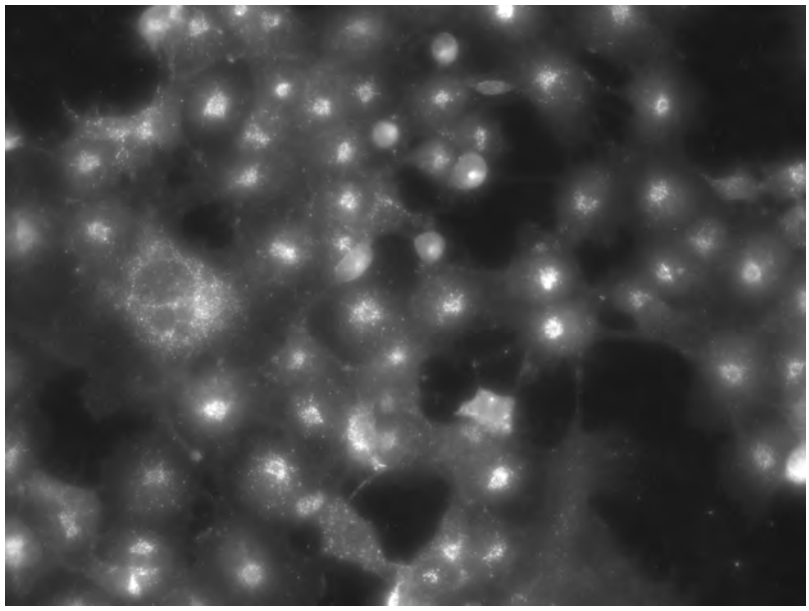

b)

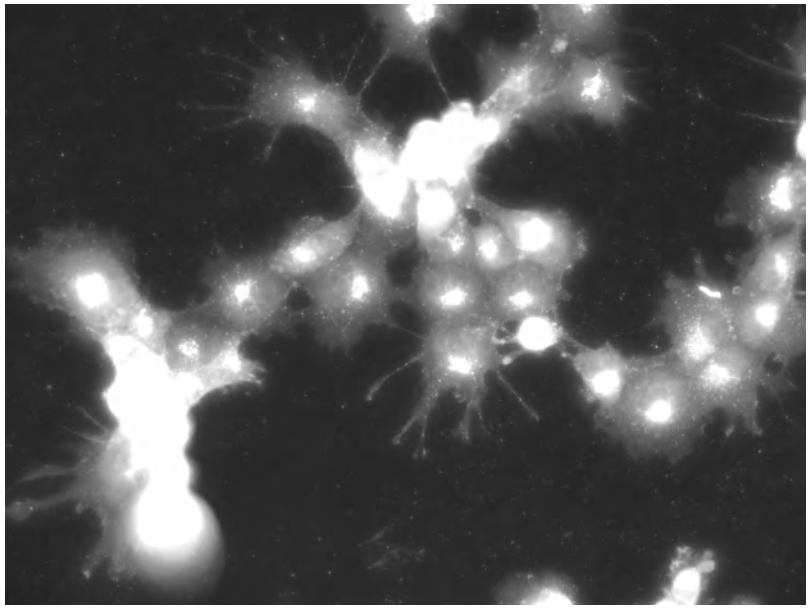

***Figure 4.13. Immunofluorescence labeling of COS-7 cells*** *The confluent monolayer of mock-infected COS-7 cells is observed in figure (a), whilst infection of this cell line for 7 hours with the HRV strain RV4 resulted in the characteristic rounding and detachment of cells from the vessel surface as illustrated in figure (b) Cells were visualised on a Nikon Eclipse 50i epifluorescent microscope using a FITC filter. Magnification X 400.*

The third method employed for the determination of viral titre was the end point dilution assay (King and Possee, 1992). Figure 4.14 illustrates the difference in viral titre, as determined for RV5-infected caloric stressed and non-stressed MA104 and COS-7 cells. The viral inoculum used for the thermal stress component of this study was the supernatant of caloric stressed cells which had exhibited complete CPE at 3.5 h.p.i. The supernatant for the non-stressed cells was obtained at 18 h.p.i. when complete CPE was observed. There was no apparent difference in viral titre for stressed and non-stressed COS-7 cells, whilst the viral titre for caloric stressed MA104 cells was significantly lower than for the corresponding control cells (Student's t-test; significance level of $< 0.05$).

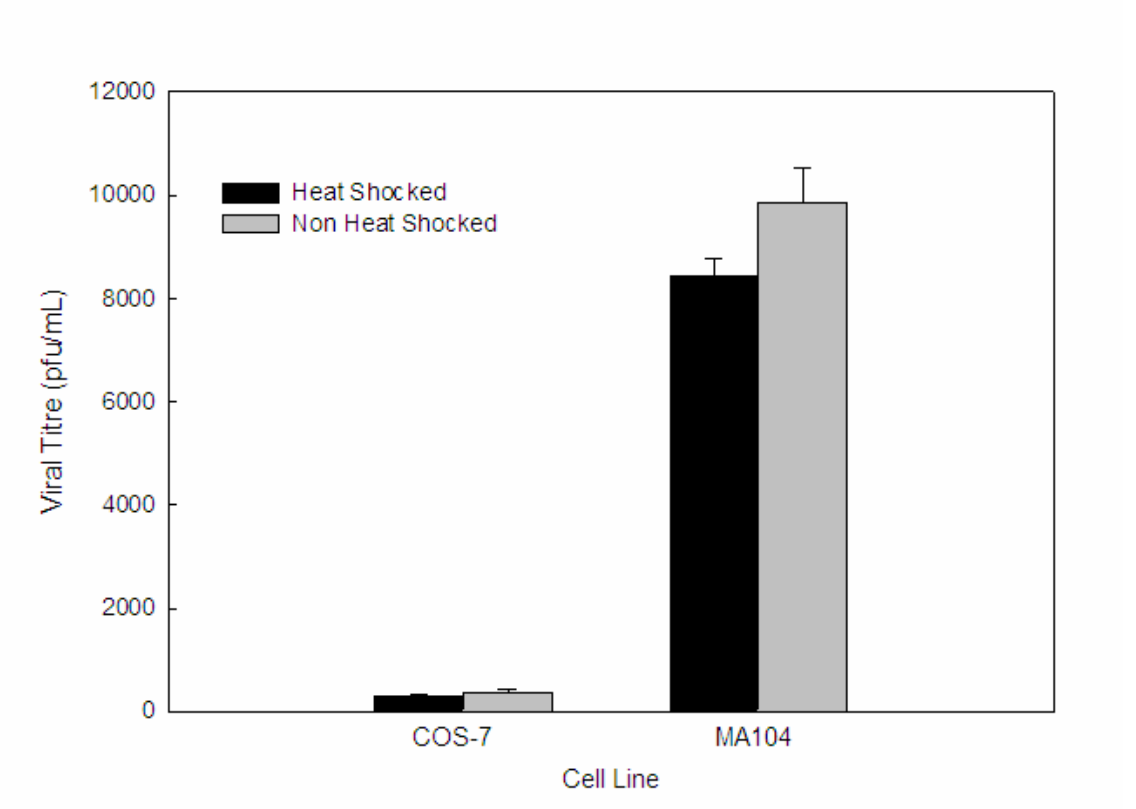


***Figure 4.14. Caloric stress effect on viral titre.*** *Thermal or non-thermal stressed cells were infected with RV5 and the supernatant collected when complete CPE was observed; 3.5 h.p.i. for thermal stressed cells and 18 h.p.i. for cells maintained at 37℃. The viral supernatant was serially diluted 2-fold and virus replication permitted to proceed in both MA104 and COS-7 cells at 37℃ until complete CPE was observed. The arithmetic mean and standard deviation of three independent experiments are presented.*

These results suggest that the viral titre of the starting inoculum for the caloric stressed cells may be equivalent to that of non-stressed cells. In order for this to be achieved viral replication must be upregulated and/or virus infectivity enhanced in caloric stressed cells. Lopez *et al*. (2006) demonstrated that heat stress facilitated strain-dependent RV infection of the relatively refractory cell line BHK at the penetration and post-penetration levels. The authors proposed that this effect was most probably attributed to enhanced penetration and/or uncoating of the virus. No corresponding increase in viral infectivity was observed for the highly permissive MA104 cell line.

Heat treatment has been shown to increase the production of viral transcripts; associated with the increased expression of a viral membrane glycoprotein and CPE in the measles virus (Vasconcelos *et al*., 1998). Applying these observations to RV infection of caloric stressed cells, it could be considered plausible that viral transcription is increased and that translation of nascent mRNA transcripts for the ER-resident glycoprotein NSP4 may be enhanced.

Under standard physiological conditions (37°C), RV replication in monkey kidney cells is known to be rapid, with maximal yields of virus observed 10-12 h.p.i. (reviewed in Estes and Cohen, 1989; Kitaoka *et al*., 1986). Viral protein synthesis has been observed as early as 2 h.p.i. for OSU-infected MA104 cells, with maximal rates of protein synthesis for viral strains SA11 and OSU reported between 3-5 h.p.i. (del Castillo *et al*., 1991; Ericson *et al*., 1982; Michelangeli *et al*., 1991). Progeny virion assembly occurred at approximately 2 h.p.i. in MA104 cells infected with the bovine RF strain (Delmas *et al*., 2007) and the lytic release of virus particles from this cell line was observed as early as 6 h.p.i. (Estes *et al*., 2001).

The upregulation of NSP4 synthesis and/or host NSP4-specific receptors, rather than whole virus replication, may be responsible for the enhanced CPE observed in cells exposed to thermal stress. NSP4 has been detected in the cell lysate of RV-infected Caco-2 cells as early as 1 h.p.i. (De Marco *et al*., 2009), and 2.5-3 h.p.i. in MA104 and HT29 cells (Kabcenell and Atkinson, 1985; Zhang *et al*., 2000). In addition, a peptide corresponding to the enterotoxin domain ($NSP4_{112-175}$) was observed within the culture media of SA11-infected MA104 cells at 4 h.p.i. (Zhang *et al*., 2000).

Given the known cytopathic and enterotoxigenic properties of NSP4 to perturbations in intracellular calcium homeostasis and PM integrity of mammalian and insect cells, and coincident with its early detection in the cell lysate and media of RV-infected cells, it would be worthwhile investigating the contribution of this protein to the enhanced CPE of RV-infected and caloric stressed cells.

Unfortunately, the results obtained from the viral titre assay has generated more questions, than answers. Future studies should focus on establishing whether RV infectivity is increased due to caloric stress and which proteins, host or viral, are upregulated in response to this stressor.

## 4.4 Summary

A spectrofluorimetric technique was developed and subsequently employed to monitor RV-induced changes to the intracellular calcium homeostasis of mammalian cell populations. The cellular response upon application of calcimycin, Triton X-100 and EGTA to fluo-3, AM loaded mammalian cells was consistent with the known properties of the reagents, and validated the technique for use in detecting changes to $[Ca^{2+}]_i$. A change in the intracellular calcium homeostasis of SA11-infected MA104 and COS-7 cell populations was observed using spectrofluorimetry, although the data did not completely emulate the changes reported by others.

The application of a 5 mM $Ca^{2+}$ pulse to the extracellular medium of RV-infected cells caused an increase in the $\Delta[Ca^{2+}]_i$ which was not observed for mock-infected cells, and was consistent with the work of others (Brunet *et al*., 2000a; Michelangeli *et al*., 1991; 1995; Perez *et al*., 1998; 1999; Ruiz *et al*., 2005). The initial increase in $[Ca^{2+}]_i$ was assumed to be associated with the unidirectional flux of extracellular calcium through the PM; a consequence of virus induced changes to the PM permeability to $Ca^{2+}$ (Brunet *et al*., 2000a; Perez *et al*., 1998; 1999). Rather than the single transient peak reported by these authors, a series of peaks were observed post application of the $Ca^{2+}$ pulse in the current study. A number of reasons were postulated to explain this observation, including the inability to maintain a homogenous sample and the clumping of RV-

infected cells within the suspension; either of which could have affected the synchronisation and magnitude of the response resulting in a series of peaks.

The $\Delta[Ca^{2+}]_i$ was also dependent on the time (h.p.i.) upon which the calcium response was measured. Progression of the virus induced a loss of PM integrity and consequently a loss of the synthetic dye from the cytosol.

The use of the calcium-sensitive fluorescent probe, flash pericam for the detection of RV-induced changes to the intracellular calcium concentration ($\Delta[Ca^{2+}]_i$) of cell populations was aborted due to an apparent caloric stress effect. Conversely, the compartmentalisation of fluo-3, AM and its lowered sensitivity to changes in calcium flux were responsible for its omission as the fluorescent probe for the microscopic studies of single cells.

The MA104 cell line is a model cell system which has been widely used to investigate changes to the $[Ca^{2+}]_i$ of NSP4 and whole virus infections. Due to the inability to express the flash pericam protein to high efficiency in this cell line, the transformed COS-7 cell line was used for microscopic cell signaling studies.

The exogenous application of NSP4 to flash pericam transfected COS-7 cells elicited an apparent dose-dependent response which was immediate and transient for both the C-terminal $His_6$-NSP4 proteins of prototype HRV strains RV4 and RV5. Preliminary results for the contribution of the proximal location of the $His_6$-tag on $\Delta[Ca^{2+}]_i$ although incomplete, suggest no disparities for NSP4 of RV4.

Caloric stress of both MA104 and COS-7 cells resulted in an enhanced CPE for all strains (SA11, RV4 and RV5) investigated in this study. Further research still needs to be conducted to determine whether the enhanced CPE is attributable to (a) an increase in the production of viral progeny, (b) the synthesis of specific viral proteins (in particular NSP4), (c) the upregulation of RV-specific cellular receptors or host cell effects, including the induction of thermal stress proteins or (d) the increased permeability of the PM to cations, in particular pertaining to the perturbation of calcium homeostasis.

# 5

# Summary and Future Directions

## 5.1 The expression and purification of recombinant $His_6$-NSP4 proteins derived from HRV strains RV4 and RV5

Recombinant NSP4 hexa-his-tagged ($His_6$) fusion proteins derived from NSP4 of prototype HRV strains RV4 and RV5 were produced using the baculovirus expression system (BEVS) and purified using immobilised metal affinity chromatography (IMAC). For each strain, recombinant proteins were produced with the $His_6$-tag resident at either the C- or N-terminus of NSP4. The purified proteins were then used for (a) the development of an ELISA for the detection of α-NSP4-specific antibodies in human sera and (b) the investigation of extracellular NSP4 and whole virus induced changes to the intracellular calcium homeostasis of mammalian cells.

Four recombinant baculovirus transfer vectors were constructed using general molecular biology techniques and the NSP4 cassette transferred to the baculovirus genome (linearised BacPAK 6) *via* homologous recombination in *Sf*-21 cells. The recombinant baculoviruses were isolated by plaque assay and their identity confirmed by PCR screening.

The recombinant $His_6$-NSP4 fusion proteins were expressed in suspension cultures of *Sf*-21 cells and the proteins purified from the cell lysate using Ni-NTA-IMAC against an imidazole gradient (20 mM to 250 mM). The optimum yield of the recombinant

proteins, as determined by time course analysis, was achieved when *Sf*-21 cells were inoculated at an M.O.I. of 1 pfu/mL and the protein harvested at 48 h.p.i.

The purification of $His_6$-NSP4 was shown to be pH dependent due to differences in the isoelectric point (pI) of NSP4 originating from the RV4 and RV5 strains. Bioinformatic analysis revealed the pI of NSP4 derived from the RV4 strain to be approximately pH 7, whilst that of RV5 NSP4 was pH 8. Consequently, the purification of the RV4 NSP4 proteins was performed at pH 8 and RV5 NSP4 performed at pH 7.

SDS-PAGE and Western blotting confirmed the expression of three antigenic glycoforms (non-, singly- and doubly-glycosylated) for each of the purified $His_6$-NSP4 proteins. In addition high M.W. proteins, assumed to be multimers of the NSP4 glycoforms and immunogenic to α-SA11 were also detected. Multimeric, SDS-PAGE resistant forms of NSP4 have been widely reported by others (Bergmann *et al.*, 1989; Hyser *et al*., 2008; Iosef *et al*., 2002; Maass and Atkinson, 1990; Rodriguez-Diaz *et al*., 2003; Tian *et al.*, 1996a). A peptide, consistent in size with the 15 kDa cleavage product reported by Zhang *et al*. (2000) was also detected in the cell lysate.

## 5.2 Immunogenicity of NSP4

An indirect ELISA, using recombinant $His_6$-NSP4 proteins as coating antigens, was developed for the detection of isotype (IgG and IgA) specific NSP4 antibodies in human sera.

### 5.2.1 Development of an α-NSP4-specific ELISA

The efficacy of three proteinaceous agents (BSA, casein and NFDM) routinely used in ELISA's as blocking agents and antibody diluents were evaluated for their use in the α-NSP4-specific antibody ELISA. NFDM was determined to be the superior agent and was most efficacious when used at 0.5% (w/v) in both the blocking buffer and diluent. The magnitude of the net OD was inversely proportional to the concentration of NFDM used in both the diluent and blocker for the concentration range explored (0.5% to 10% NFDM). Reasons postulated for this trend included (a) the masking of antigen:antibody

interactions and/or (b) the inhibition of the enzyme conjugate by an excessive concentration of blocking agent.

The inclusion of Tween-20 in ELISA reagents had been proposed to negatively affect the efficacy of proteinaceous blockers (Esser, 1997) and to reduce the signal response purporting false negatives (Julián *et al*., 2001). In the current research the inclusion of Tween-20 in NFDM blocking systems had a negligible effect on background noise when the composition of both the blocking agent and antibody diluent was at concentrations ≤ 2% (assays performed at 25°C) or ≤ 1% (assays performed at 37°C). When the NFDM concentration in both the blocker and antibody diluent exceeded these concentrations, the inclusion of Tween-20 caused a statistically significant increase in background noise which was independent of the incubation temperature. In contrast, the absence of Tween-20 from these reagents, although producing marginally less background noise, appeared to be temperature dependent.

The validity of the assay was undertaken by performing the perfunctory intra- and inter-run assays, yielding a coefficient of variation of 0.22%, within the limit of 10% suggested by Crowther (2001).

### 5.2.2 The α-NSP4-specific response evoked by natural rotavirus infection and vaccination of humans

The results obtained in this study were suggestive that natural RV infection or vaccination with an attenuated live HRV vaccine (Rotarix®) evoked an NSP4-specific humoral response, which was both heterotypic and/or homotypic. These findings emulate the work of others, whereby the humoral response to NSP4 has been shown to be both heterotypic and independent of the NSP4 genotype (Ray *et al*., 2003; Vizzi *et al*., 2005; Yuan *et al*., 2004b).

For both naturally infected children and vaccine recipients, the dominant isotype-specific serum response was to α-NSP4 IgG, and an α-NSP4 IgA response when detected, was consistently lower than for IgG. These results are consistent with the work of others (Johansen *et al*., 1999; Rodríguez-Díaz *et al*., 2005).

The NSP4 genotypes of the infecting RV strains investigated in this study had not been determined and consequently the conclusions drawn regarding NSP4 cross-reactivity was based on the assumption that G1 and G4 strains typically are of NSP4 genotype B and G2 of NSP4 genotype A (Kirkwood *et al*., 1999). The α-NSP4 IgG seroconversion rate for children naturally infected with a G1 RV strain to NSP4 of genotypes B (G1) and A (G2) was 80 and 60%, respectively. These results were in accordance with the findings of Richardson *et al*. (1993) who demonstrated that the IgG response to NSP4 for G1 infections for the population from which this sample subset was drawn was 67-100%. The α-NSP4 IgA seroconversion rate was considerably lower (29%) than for IgG, and was only detected when the infecting strain was homotypic to the coating antigen (RV4 NSP4; G1).

With respect to the serum samples obtained from recipients of the Rotarix® (P1A[8]G1) vaccine, the number of respondents who had detectable levels of α-NSP4 IgG was fewer (30%) than for children naturally infected with RV, whilst no α-NSP4 IgA was detected. The response to NSP4 was heterotypic, with the strongest response observed when the coating antigen was homotypic to the vaccine strain.

### 5.2.3 Conformational dependence of the immune response – influence of the $His_6$-tag position

Preliminary results indicated that the placement of the $His_6$-tag at the N-terminus of NSP4 from strain RV4 generated a greater response compared with the corresponding C-terminal $His_6$-NSP4 protein. These results suggest that the fusion of the $His_6$-tag at the carboxy terminus interferes with either the direct binding of antibodies to epitopes located within the cytoplasmic domain of NSP4 or induces changes within the protein which alters conformation-dependent epitopes on NSP4. These results are consistent with the identification of immunodominant epitopes located within the cytoplasmic domain of NSP4 (Borgan *et al*., 2003; Hyser *et al*., 2008; Kim *et al*., 2004; Rodríguez-Díaz *et al*., 2004; Yu and Langridge, 2001; Yuan *et al*., 2004a). The absence of a similar response for NSP4 derived from the RV5 strain may be indicative of differences in immunodominant regions and should be investigated further.

### 5.2.4 Future directions for the NSP4 immunological study

Published data on the levels of detectable α-NSP4 antibodies, particularly to IgA, in the sera of humans and animals are often conflicting and the disparities may be due to differences in assay sensitivity (Ishida *et al*., 1996; Johansen *et al*., 1999; Ray *et al*., 2003; Rodríguez-Díaz *et al*., 2005; Vizzi *et al*., 2005; Yuan *et al*., 2004a). Therefore, the general inability to detect serum α-NSP4 IgA responses for naturally infected children and vaccine recipients in this research may have been influenced by the sensitivity of the assay used. Studies which successfully detected NSP4 specific IgA used either (a) GST-fusion peptides encompassing the cytoplasmic domain of the NSP4 protein, and/or (b) an alternative detection system (biotin/avidin, immunocytochemistry) or (c) more concentrated serum samples (Ray *et al*., 2003; Vizzi *et al*., 2005: Yuan *et al*., 2004b). Future work may focus on the design of an assay which is more sensitive to the detection of NSP4 specific immunoglobulins.

It would also be interesting to investigate whether the rate of NSP4 seroconversion is enhanced with subsequent infections and if the NSP4 antibody response is age-dependent. Kirkwood *et al*. (2008) reported that RV reinfection resulted in a boost in NSP4-specific IgG antibodies, whilst Xu *et al*. (2010) documented that the antibody response to NSP4 is age-dependent, peaking at 12-23 months of age.

## 5.3 The effect of rotavirus infection and exogenous NSP4 on intracellular calcium homeostasis

Changes to the PM permeability to calcium or to the intracellular calcium concentration of mammalian cells in response to RV replication or to the exogenous application of recombinant $His_6$-NSP4 fusion proteins was evaluated using two independent methods; (a) spectrofluorimetric analysis of cell populations and (b) microscopic analysis of individual cells. For each system employed, the use of flash pericam and fluo-3, AM as potential calcium-sensitive fluorescent markers was investigated.

### 5.3.1 Changes to the calcium homeostasis of mammalian cell populations – a spectrofluorimetric approach to the effects of whole virus and to NSP4

The calcium sensitive fluorophores, flash pericam and fluo-3, AM, were evaluated for their responsiveness to changes to the intracellular calcium homeostasis of cell suspensions using spectrofluorimetry. The specificity and sensitivity of the fluorophores was determined by assessing the magnitude of the response (AU) to mock and RV-infected cell populations upon the application of (a) EGTA, a calcium-specific chelator, (b) Triton-X-100, (c) the calcium ionophore calcimycin and (d) a 5 mM calcium pulse. Despite flash pericam demonstrating a greater sensitivity to perturbations in calcium homeostasis compared with the synthetic dye fluo-3, AM its use in spectrofluorimetry had to be aborted due to an apparent thermal stress response for RV-infected cells.

#### 5.3.1.1 Assessment of RV-induced changes to PM permeability to $Ca^{2+}$

RV-induced changes to the $Ca^{2+}$ permeability of the PM and cytosolic calcium concentration were investigated in the monkey kidney cell lines, MA104 and COS-7. Both cell lines had been used previously by others for the investigation of RV or NSP4-induced changes to the $[Ca^{2+}]_i$ (Cuadras *et al*., 1997, Michelangeli *et al*., 1991; 1995; Pérez *et al*., 1999; Ruiz *et al*., 2007; Zambrano *et al*., 2008).

The application of saturating concentrations of calcium (5 mM) to the extracellular medium of cell suspensions had been used by other researchers to assess RV-induced changes to the $Ca^{2+}$ permeability of the PM (Brunet *et al*., 2000a; Pérez *et al*., 1999; Tian *et al*., 1994). The application of a 5 mM $Ca^{2+}$ pulse to the extracellular medium of fluo-3, AM loaded COS-7 and MA014 cell suspensions infected with RV SA11 elicited an immediate increase in fluorescence intensity, notably absent from mock-infected cells, and commensurate with an increase in $\Delta[Ca^{2+}]_i$. These results suggested that SA11 infection caused perturbation of the intracellular calcium homeostasis by increasing the PM permeability to $Ca^{2+}$ and emulated the observations of others (Brunet *et al*., 2000a; Michelangeli *et al*., 1991; 1995; Pérez *et al*., 1998; 1999; Ruiz *et al*., 2005). The initial increase in $[Ca^{2+}]_i$ within the first few seconds is representative of PM permeability to

$Ca^{2+}$ and is attributable to the unidirectional flux of $Ca^{2+}$ across the PM from the extracellular medium into the cytosol (Brunet *et al*., 2000a; Pérez *et al*., 1998; 1999).

One consistent disparity between the work presented here and that of others was the presence of multiple peaks rather than a single defined peak proceeding the application of the $Ca^{2+}$ pulse (Brunet *et al*., 2000a; Michelangeli *et al*., 1995; Pérez *et al*., 1998; Ruiz *et al*., 2005; Zambrano *et al*., 2008). It was postulated that the multiple peaks could have arisen from (a) the inability to control environmental parameters such as temperature and oxygen concentration, (b) sample heterogeneity, exacerbated by RV-induced cell clumping, (c) the use of a non-ratiometric dye and/or (d) differences in the treatment of data.

The viability of the host cells, in particular the integrity of the PM, at the time of calcium analysis was also investigated as a contributing factor to the atypical results obtained. The effects of PM disruption to calcium measurements would be two-fold; (a) unregulated flux of $Ca^{2+}$ across the PM in response to the calcium pulse and (b) loss of fluo-3, AM to the extracellular medium. The rate of RV-induced changes to the PM has been observed to proceed in a manner which is both strain and host cell dependent (Brunet *et al*., 2000a; Michelangeli *et al*., 1991: Pérez *et al*., 1999).

A time course analysis of SA11-infected COS-7 cells revealed that cells harvested at ≥ 18 h.p.i. could not be used for $Ca^{2+}$ studies due to excessive cell clumping and poor cell viability. An increase in the $\Delta[Ca^{2+}]_i$ was observed at 6 h.p.i., but was negated at 12 h.p.i. The decrease in the $\Delta[Ca^{2+}]_i$ for virus-infected cells at 12 h.p.i. may be due to deleterious alterations in the PM due to the progressive cytotoxic and lytic effects of the virus and the consequent inability to retain the fluorescent probe within the cell (Michelangeli *et al*., 1991; Pérez *et al*., 1999).

The absolute $[Ca^{2+}]_i$ concentration was calculated for both mock and virus-infected COS-7 cells at 6 and 12 h.p.i. (Tsien *et al*., 1982). The $[Ca^{2+}]_i$ of SA11-infected cells at 6 h.p.i. was significantly greater than for the corresponding mock-infected cells (tested at a significance level, $p < 0.05$). RV-infected cells harvested at 12 h.p.i. failed to show a change in $[Ca^{2+}]_i$ compared with cells harvested 6 hours prior. Such a notable absence

of a change in $[Ca^{2+}]_i$ for RV-infected COS-7 cells between 6 and 12 h.p.i. may be associated with oncosis at the later time post infection, as described for PM permeability to $Ca^{2+}$ studies. An unexpected 2-fold rise in $[Ca^{2+}]_i$ was observed between 6 and 12 h.p.i. for the mock-infected cells; no reason could be provided for this atypical result.

Michelangeli *et al*. (1991) determined that the increased PM permeability to $Ca^{2+}$ for MA104 cells infected with a porcine (OSU) RV occurred as early as 4 h.p.i., but in the absence of an accompanying change in $[Ca^{2+}]_i$. They and others have proposed that host cell regulatory mechanisms responsible for maintaining cytosolic calcium homeostasis can sufficiently compensate for the initial influx of $Ca^{2+}$ across the PM at the early stages of infection (Brunet *et al*., 2000a; Michelangeli *et al*., 1991; Pérez *et al*., 1998; 1999). Changes to the $[Ca^{2+}]_i$, a consequence of increased $Ca^{2+}$ in the cytosol and intracellular organelles was observed at > 5 h.p.i. The discrepancy between the experimental data presented here and that published may be due to differences in (a) the kinetics of the virus strains used, (b) the cell line used and (c) the M.O.I. used to infect the cells.

#### 5.3.1.2 Effects of NSP4 on PM permeability to $Ca^{2+}$

The exogenous application of $His_6$-NSP4 to mammalian cells in suspension failed to induce a change in intracellular calcium homeostasis. The absence of a response may be due to the high dilution order imposed upon the protein using this experimental system. NSP4 has been reported to induce a dose-dependent mobilization of intracellular calcium in *Sf*9 cells (Tian *et al*., 1995) and HT-29 cells (Dong *et al*., 1997).

## 5.3.2 Changes to the calcium homeostasis of single cells – a microscopic approach to the effects of whole virus and to NSP4

### 5.3.2.1 Effects of exogenous NSP4 on the intracellular calcium mobilization of COS-7 cells

Flash pericam was chosen as the calcium sensitive probe for monitoring changes to the intracellular calcium homeostasis of single cells in response to NSP4. Epifluorescence microscopy revealed the high propensity for fluo-3, AM to be sequestered into intracellular organelles, and a lowered responsiveness of the dye to detect changes in $[Ca^{2+}]_i$. Attempts to monitor changes to the intracellular calcium homeostasis of RV-infected cells was aborted due to an enhanced CPE, a consequence of the caloric stress imposed on the cells when performing both flash pericam expression and RV infection.

Both RV5C and RV4C elicited an increase in the $\Delta[Ca^{2+}]_i$ that was both immediate and transient in flash pericam transfected COS-7 cells and was consistent with the observations of others (Dong *et al*., 1997; Tian *et al*., 1996a; Zhang *et al.*, 1998; 2000). This transient, NSP4-induced rise in $[Ca^{2+}]_i$ is primarily associated with the release of $Ca^{2+}$ from intracellular stores (Dong *et al*.,1997).

### 5.3.2.2 Proximal location of the $His_6$-tag on NSP4 and its influence on the $\Delta[Ca^{2+}]_i$

Experiments conducted with the N- and C-terminal $His_6$-tagged NSP4 of RV4 demonstrated that the location of the $His_6$-tag did not unduly influence the rate of the intracellular calcium response. The exogenous application of the protein to flash pericam transfected COS-7 cells evoked an immediate increase in the $\Delta[Ca^{2+}]_i$ irrespective of the placement of the $His_6$-tag.

Unfortunately, insufficient data was accrued for the N-terminal $His_6$-tagged NSP4 of strain RV5 and consequently no conclusions could be drawn regarding the location of the tag for NSP4 of this strain. A consistent drawback of the microscopic method used in this study, and which could not be overcome, was either the change in view field

and/or focal drift upon the addition of the reagent or as a function of time. Therefore, any image sequence which presented with these aberrations was discarded from further analysis as the integrity of the cellular fluorescence was compromised.

The use of a perfusion circuit to ensure continuity in sample volume, particularly for reagent addition, may need to be addressed if the effects of NSP4 on intracellular calcium mobilization are to be investigated further; although the dose-dependency of NSP4 on calcium perturbation may render this method improbable.

#### 5.3.2.3 NSP4-induced changes in intracellular calcium concentration is dose-dependent

NSP4-induced changes to the intracellular calcium homeostasis of individual COS-7 cells was shown to be dose-dependent. The application of 30 nM, but not 15 nM of C-terminal $His_6$-tagged NSP4 (RV4C) induced an increase in the $\Delta[Ca^{2+}]_i$. Similarly, NSP4 administered at concentrations less than 10 nM failed to evoke a change in intracellular calcium concentration for fluo-3, AM loaded cell populations. Dong *et al*. (1997) demonstrated that NSP4 mobilization of intracellular calcium was dose-dependent and that concentrations as low as 4.6 nM were sufficient to elicit changes in $[Ca^{2+}]_i$.

### 5.3.3 Neutralization of NSP4 and its effect on the $\Delta[Ca^{2+}]_i$

Antibody to NSP4 has been shown to reduce the severity and incidence of RV-induced diarrhoeal disease in neonatal mice (Ball *et al*., 1996; Choi *et al*., 2005; Yu and Langridge, 2001) but not for the gnotobiotic piglet model (Yuan *et al*., 2004a).

This study hoped to establish whether NSP4-specific antibodies present in human sera could inhibit changes to the intracellular calcium homeostasis evoked by exogenous NSP4.

To my knowledge this is the only study which has used direct neutralization of NSP4 to address its ability to effectively block calcium perturbation by the protein. De Marco *et*

*al*. (2009) demonstrated that human serum immunoglobulins blocked ion secretion and cell damage of RV-infected Caco-2 cells.

Preliminary experiments with flash pericam transfected COS-7 cells indicated that the preincubation of NSP4 with human sera positive for α-NSP4 antibodies did not inhibit changes to $[Ca^{2+}]_i$.

## 5.4 Caloric stresses enhances CPE in RV-infected mammalian cells

A causal relationship between a thermal stress response and enhanced CPE for RV-infected mammalian cells was revealed when infections were performed on cells expressing flash pericam. When cells preconditioned at 29°C for 3 to 4 days during flash pericam expression were returned to 37°C for RV adsorption and replication, a marked increased in CPE was observed as early as 2 h.p.i. In contrast, cells which had been maintained at the physiological temperature (37°C) throughout the duration of the experiment exhibited an equivalent degree of CPE at a much later stage of infection (> 8 h.p.i.). This thermal stress response was observed for each of the RV strains (SA11, RV4 and RV5) investigated in this study and for both mammalian cell lines (MA104 and COS-7). The contribution to the enhanced CPE by the expression of flash pericam or porcine pancreatic trypsin was investigated and discounted.

A review of the literature has revealed that the cells in this study were subjected to both a cold shock and heat shock effect which may have potentiated the expression of host cell stress proteins (Liu *et al*., 1994; Sonna *et al*., 2010). As to whether the enhanced CPE was attributed to (a) the induction of heat or cold shock proteins or a combination thereof and/or (b) increased virus receptor expression and/or (c) an increase in viral transcriptional activity was not determined.

It is known that growth arrest in cells subjected to temperature downshifts (cold shock) is associated with the suppression of protein synthesis. Consequently, the subsequent rewarming of cells to physiological temperatures (heat shock) would ultimately result in the host reestablishing normal cell processes inclusive of an upregulation of protein

expression. It is possible that RV utilizes this heightened flux in the host cell translational machinery, mediating the reduction in cellular protein synthesis in favour of translation of viral proteins (Feigelstock *et al*., 2003).

RV infection is known to induce the expression of genes encoding heat shock proteins (Hsp40, Hsp70, Hsp90), the translationally controlled tumour protein (TCTP) and ER-resident $Ca^{2+}$-binding molecular chaperones (Broquet *et al*., 2007; Cuadras *et al*., 2002; Dutta *et al*., 2009; Xu *et al*., 1998; 1999).

Hsc70, has been identified as a potential post-attachment viral receptor and its enhanced expression in response to heat shock may have facilitated the entry of a greater number of virus particles into thermally stressed cells in contrast with cells maintained at standard physiological conditions (Gualtero *et al*., 2007; Guerrero *et al*., 2002; López *et al*., 2006; Pérez-Vargas *et al*., 2006; Zárate *et al*., 2003).

The upregulation of Hsp90, a known positive regulator of RV infection, in response to heat shock and preceding RV infection may have accelerated the early stages of infection either through the modulation of cellular signalling proteins or through direct interactions with viral proteins (Dutta *et al*., 2009).

In general Hsp70 induction affords a protective response to cellular stresses and is known to negatively control RV replication. Broquet *et al*. (2007) demonstrated that the overexpression of Hsp70 in Caco-2 cells was toxic. Therefore, it may be plausible that the enhanced CPE observed could be due to the overexpression of Hsp70 in response to both thermal stress and RV infection.

Heat stress is also known to alter membrane permeability resulting in increases in intracellular $Na^+$, $H^+$, and $Ca^{2+}$ concentrations (Reviewed in Sonna *et al*., 2002), whilst cold shock has been reported to cause microtubule and actin filament disassembly and associated permeability changes in the PM (Stapulionis *et al*., 1997). Given the close association between $[Ca^{2+}]_i$ and RV replication, morphogenesis and pathogenesis, one could speculate that either heat shock or cold shock may induce changes to the calcium

homeostasis of the host cell which is conducive to the survival and replication of the virus or to enhancing the enterotoxigenic effects of NSP4 (Brunet *et al*., 2000a).

It may also be possible that the increase in CPE is attributable to an increase in the synthesis of NSP4 or the up-regulation of host NSP4 specific-receptors, rather than replication of the whole virus. NSP4 has been detected in the cell lysate of RV-infected Caco-2 cells as early as 1 hour post-infection (De Marco *et al*., 2009) whilst a peptide corresponding to the enterotoxin ($NSP4_{112-175}$) domain was observed within the culture media of SA11-infected MA104 cells at 4 h.p.i. (Zhang *et al*., 2000).

Given the winter seasonality of RV infection it is appealing to speculate whether exposure to sub-physiologic temperatures enhances the infectivity of the virus. Transmission of RV *via* the respiratory route has been postulated and the associated reduction in temperature due to inhalation of cold air has been reported to reduce nasopharyngeal temperatures from 34°C to approximately 25°C (Rouadi *et al*., 1999). *Moraxella catarrhalis* a nasopharyngeal pathogen of the human respiratory tract displays seasonal variation with infections dominating in the winter months. Cold shock induction of *M. catarrhalis* at 26°C upregulated the expression of a major adhesion and putative virulence factor of the organism and enhanced its adherence to the ECM protein fibronectin of epithelial cells in culture (Spaniol *et al*., 2009). A region within the cytoplasmic domain of NSP4 (aa 87 to 145) has also been found to bind to the ECM proteins, laminin-β3 and fibronectin, although its fundamental role has been postulated to be as an enterotoxigenic agent, inducing changes to the intracellular calcium homeostasis of uninfected crypt cells within the gastrointestinal mucosa (Ball *et al*., 2005; Boshuizen *et al*., 2004).

As can be seen from the preceding discussion, a substantial number of viral and host cell factors could be contributing to the enhanced CPE observed for cells exposed to thermal stress. Future studies into the caloric stress response could involve the use of DNA microarray analysis and reverse-transcriptase quantitative PCR to assess whether there has been an increase in the up-regulation of the production of cellular or rotaviral proteins, and of particular interest to this report, that of NSP4 (Cuadras *et al*., 2002; Feigelstock *et al*., 2003; Peterson *et al*., 2006, Sonna *et al*., 2010; Wang *et al*., 2005). In

addition, it would be useful to determine whether the increase in CPE is associated with an increase in Hsp and/or Csp expression.

## 5.5 Close

The results from this study provided an insight into the immunological and biochemical properties of non structural protein 4 (NSP4) of two prototype HRV strains RV4 and RV5.

Using the indirect ELISA developed in this research it was established that natural RV infection or vaccination evoked an NSP4-specific humoral response, which was both heterotypic and/or homotypic. The prevalent isotype-specific serum response was to α-NSP4 IgG and was greatest for children exposed to natural RV infection. Preliminary results indicated that the placement of the $His_6$-tag at the N-terminus of NSP4 generated a greater response compared with the corresponding C-terminal $His_6$-NSP4 protein derived from strain RV4.

RV infection perturbed the intracellular calcium homeostasis of mammalian cells by increasing the PM permeability to $Ca^{2+}$. NSP4 elicited a dose-dependent increase in the $\Delta[Ca^{2+}]_i$ that was both immediate and transient in flash pericam transfected COS-7 cells. Preliminary experiments indicated that neutralization of NSP4 with human sera positive for α-NSP4 antibodies failed to inhibit changes to $[Ca^{2+}]_i$.

This study also identified a caloric stress response for RV-infected cells, which may be conducive for virus replication and pathogenesis and may invariably involve a complex interplay of host cell and virus responses.

# References


Adams, W.R. and Kraft, L.M. (1963). Epizootic diarrhea of infant mice: identification of the etiologic agent. *Science* **141**(3578), 359-360.

Al-Fageeh, M.B., Marchant, R.J., Carden, M.J. and Smales, C.M. (2006). The cold-shock response in cultured mammalian cells: harnessing the response for the improvement of recombinant protein production. *Biotechnol. Bioeng.* **93**(5), 829-835.

Al-Fageeh, M.B. and Smales, C.M. (2006). Control and regulation of the cellular responses to cold shock: the responses in yeast and mammalian systems. *Biochem. J.* **397**(Pt 2), 247-259.

Angel, J., Tang, B., Feng, N., Greenberg, H.B. and Bass, D. (1998). Studies of the role for NSP4 in the pathogenesis of homologous murine rotavirus diarrhea. *J. Infect. Dis.* **177**(2), 455-458.

Angel, J., Franco, M.A. and Greenberg, H.B. (2007). Rotavirus vaccines: recent developments and future considerations. *Nat. Rev. Microbiol* **5**, 529-539.

Ansari, S.A., Sattar, S.A., Springthorpe, V.S., Wells, G.A. and Tostowaryk, W. (1988). Rotavirus survival on human hands and transfer of infectious virus to animate and nonporous inanimate surfaces. *J. Clin. Microbiol.* **26**(8). 1513-1518.

Araújo, I.T., Heinemann, M.B., Mascarenhas, J. D'Arc P., Assis, R.M., Fialho, A.M. and Leite, J.P. (2007). Molecular analysis of the NSP4 and VP6 genes of rotavirus strains recovered from hospitalized children in Rio de Janeiro, Brazil. *J. Med. Microbiol*. **56**(Pt-6), 854-859.

Arias C.F., Romero, P., Alvarez, V., López, S. (1996). Trypsin activation pathway of rotavirus infectivity. *J. Virol.* **70**(9), 5832-5839.

Arias, C.F., Isa, P., Guerrero, C.A., Méndez, E., Zárate, S., López, T., Espinosa, R., Romero, P. and López, S. (2002). Molecular biology of rotavirus cell entry. *Arch. Med. Res.* **33**(4), 356-361.

Arias, C.F., Dector, M.A., Segovia, L., López, T., Camacho, M., Isa, P., Espinosa, R. and López, S. (2004). RNA silencing of rotavirus gene expression. *Virus Res.* **102**(1), 43-51.

Arista, S., Giovannelli, L., Pistoia, D., Cascio, A., Parea, M. and Gerna, G. (1990). Electropherotypes, subgroups and serotypes of human rotavirus strains causing gastroenteritis in infants and young children in Palermo, Italy, from 1985 to 1989. *Res. Virol.* **141**(4), 435-448.

Arnold, F.H. (1991). Metal-Affinity Separations: A New Dimension in Protein Processing. *Bio/Technology* **9**, 151-156.

Au, K.S., Chan, W.K., Burns, J.W. and Estes, M.K. (1989). Receptor activity of rotavirus nonstructural glycoprotein NS28. *J. Virol.* **63**(11), 4553-4562.

Au, K.S., Mattion, N.M., and Estes, M.K. (1993). A subviral particle binding domain on the rotavirus nonstructural glycoprotein NS28. *Virology* **194**(2), 665-673.

Ayres, M.D., Howard, S.C., Kuzio, J., Lopez-Ferber, M. and Possee, R.D. (1994). The complete DNA sequence of *Autographa californica* nuclear polyhedrosis virus. *Virology* **202**(2), 586-605.

Azevedo, M.S. Yuan, L., Jeong, K.-I., Gonzalez, A., Nguyen, T.V., Pouly, S., Gochnauer, M., Zhang, W., Azevedo, A. and Saif, L.J. (2005). Viremia and nasal and rectal shedding of rotavirus in gnotobiotic pigs inoculated with Wa human rotavirus. *J. Virol.* **79**(9), 5428-5436.

Ball, J.M., Tian, P., Zeng, C. Q.-Y., Morris, A.P. and Estes, M.K. (1996). Age-dependent diarrhea induced by a rotaviral nonstructural glycoprotein. *Science* **272**, 101-104.

Ball, J.M., Mitchell, D.M., Gibbons, T.F. and Parr, R.D. (2005). Rotavirus NSP4: a multifunctional viral enterotoxin. *Viral Immunol*. **18**(1), 27-40.

Banyard, M.R. and Tellam, R.L. (1985). The free cytoplasmic calcium concentration of tumorigenic and non-tumorigenic human somatic cell hybrids. *Br. J. Cancer* **51**(6), 761-766.

Barman, P., Ghosh, S., Samajdar, S., Mitra, U., Dutta, P., Bhattacharya, S.K., Krishnan, T., Kobayashi, N. and Naik, T.N. (2006). RT-PCR based diagnosis revealed importance of human group B rotavirus infection in childhood diarrhoea. *J. Clin. Virol*. **36**(3), 222-227.

Barnes, G.L., Lund, J.S., Mitchell, S.V., De Bruyn, L., Piggford, L., Smith, A.L., Furmedge, J., Masendycz, P.J., Bugg, H.C., Bogdanovic-Sakran, N., Carlin, J.B. and Bishop, R.F. (2002). Early phase II trial of human rotavirus vaccine candidate RV3. *Vaccine* **20**(23-24), 2950-2956.

Bass, E.S., Pappano, D.A. and Humiston, S.G. (2007) Rotavirus. *Pediatr. Rev.* **28**(5), 183-191.

Beau, I., Cotte-Laffitte, J., Géniteau-Legendre, M., Estes, M.K. and Servin, A.L. (2007). An NSP4-dependent mechanism by which rotavirus impairs lactase enzymatic activity in brush border of human enterocyte-like Caco-2 cells. *Cell. Microbiol*. **9**(9), 2254-2266.

Benureau, Y., Huet, J.C., Charpilienne, A., Poncet, D. and Cohen, J. (2005). Trypsin is associated with the rotavirus capsid and is activated by solubilization of outer capsid proteins. *J. Gen. Virol*. **86**(Pt 11), 3143-3151.

Bergmann, C.C., Maass, D., Poruchynsky, M.S., Atkinson, P.H. and Bellamy, A.R. (1989). Topology of the non-structural rotavirus receptor glycoprotein NS28 in the rough endoplasmic reticulum. *EMBO Journal* **8**, 1695-1703.

Berkova, Z., Morris, A.P. and Estes, M.K. (2003). Cytoplasmic calcium measurement in rotavirus enterotoxin-enhanced green fluorescent protein (NSP4-EGFP) expressing cells loaded with Fura-2. *Cell Calcium* **34**(1), 55-68.

Berkova, Z., Crawford, S.E., Trugnan, G., Yoshimori, T., Morris, A.P. and Estes, M.K. (2006). Rotavirus NSP4 induces a novel vesicular compartment regulated by calcium and associated with viroplasms. *J. Virol.* **80**(12), 6061-6071.

Berkova, Z., Crawford, S.E., Blutt, S.E., Morris, A.P. and Estes, M.K. (2007). Expression of rotavirus NSP4 alters the actin network organization through the actin remodeling protein cofilin. *J. Virol.* **81**(7), 3545-3553.

Bernstein, D.I., Sander, D.S., Smith, V.E., Schiff, G.M. and Ward, R.L. (1991). Protection from rotavirus reinfection: 2-year perspective study. *J. Infect. Dis.* **164**(2), 277-283.

Bernstein, D.I., Glass, R.I., Rodgers, G., Davidson, B.L. and Sack, D.A. (1995). Evaluation of rhesus rotavirus monovalent and tetravalent reassortant vaccines in U.S. children. US Rotavirus Vaccine Efficacy Group. *JAMA.* **273**(15), 1191-1196.

Bernstein, D.I. (2006). Live attenuated human rotavirus vaccine, Rotarix™. *Semin. Pediatr. Infect. Dis.* **17**(4), 188-194.

Bernstein, D.I. (2009). Rotavirus overview. *Pediatr. Infect. Dis. J*. **28**(Suppl 3), S50-S53.

Berridge, M.J., Bootman, M.D. and Lipp, P. (1998). Calcium – a life and death signal. *Nature* **395**(6703), 645-648.

Besser, T.E., Gay, C.C., McGuire, T.C. and Evermann, J.F. (1988). Passive immunity to bovine rotavirus infection associated with transfer of serum antibody into the intestinal lumen. *J. Virol.* **62**(7), 2238-2242.

Bines, J. (2006). Intussusception and rotavirus vaccines. *Vaccine* **24**(18), 3772-3776.

Bishop, R.F., Davidson, G.P., Holmes, I.H. and Ruck, B.J. (1973). Virus particles in epithelial cells of duodenal mucosa from children with acute non-bacterial gastroenteritis. *Lancet* **2**(7841), 1281-1283.

Bishop, R.F., Barnes, G.L., Cipriani, E. and Lund, J.S. (1983). Clinical immunity after neonatal rotavirus infection. A prospective longitudinal study in young children. *N. Engl. J. Med.* **309**(2), 72-76.

Bishop, R.F. (1996). Natural history of human rotavirus infection. *Arch. Virol. Suppl*. **12**, 119-128.

Blutt, S.E., Kirkwood, C.D., Parreňo, V., Warfield, K.L., Ciarlet, M., Estes, M.K., Bok, K., Bishop, R.F. and Conner, M.E. (2003). Rotavirus antigenaemia and viraemia: a common event? *Lancet* **362**(9394), 1445-1449.

Blutt, S.E., Matson, D.O., Crawford, S.E., Staat, M.A., Azimi, P., Bennett, B.L., Piedra, P.A. and Conner, M.E. (2007). Rotavirus antigenemia in children is associated with viremia. *PLoS Med*. **4**(4), 660-668.

Bootman, M.D., Lipp, P. and Berridge, M.J. (2001). The organisation and functions of local $Ca^{2+}$ signals. *J. Cell Sci*. **114**(Pt 12), 2213-2222.

Borgan, M.A., Mori, Y., Ito, N., Sugiyama, M. and Minamoto, N. (2003). Antigenic analysis of nonstructural protein (NSP)4 of group A avian rotavirus strain PO-13. *Microbiol. Immunol.* **47**(9), 661-668.

Boshuizen, J.A., Rossen, J.W., Sitaram, C.K., Kimenai, F.F, Simons-Oosterhuis, Y., Laffeber, C., Büller, H.A. and Einerhand, A.W. (2004). Rotavirus enterotoxin NSP4 binds to the extracellular matrix proteins laminin-β3 and fibronectin. *J. Virol.* **78**(18), 10045-10053.

Both, G.W., Siegman, L.J., Bellamy, A.R. and Atkinson, P.H. (1983). Coding assignment and nucleotide sequence of simian rotavirus SA11 gene segment 10: location of glycosylation sites suggests that the signal peptide is not cleaved. *J. Virol.* **48**(2), 335-339.

Bowman, G.D., Nodelman, I.M., Levy, O., Lin, S.L., Tian, P. Zamb, T.J., Udem, S.A., Venkataraghavan, B. and Schutt, C.E. (2000). Crystal structure of the oligomerization domain of NSP4 from rotavirus reveals a core metal-binding site. *J. Mol. Biol.* **304**(5), 861-871.

Broquet, A.H., Lenoir, C., Gardet, A., Sapin, C., Chwetzoff, S., Jouniaux, A.-M., Lopez, S., Trugnan, G., Bachelet, M. and Thomas, G. (2007). Hsp70 negatively controls rotavirus protein bioavailability in caco-2 cells infected by the rotavirus RF strain. *J. Virol.* **81**(3), 1297-1304.

Brown, K.A., Kriss, J.A., Moser, C.A., Wenner, W.J. and Offit, P.A. (2000). Circulating rotavirus-specific antibody-secreting cells (ASCs) predict the presence of rotavirus-specific ASCs in the human small intestinal lamina propria. *J. Infect. Dis.* **182**(4), 1039-1043.

Browne, E.P., Bellamy, A.R. and Taylor, J.A. (2000). Membrane-destabilizing activity of rotavirus NSP4 is mediated by a membrane-proximal amphipathic domain. *J. Gen. Virol.* **81**(8), 1955-1959.

Brunet, J.-P., Cotte-Laffitte, J., Linxe, C., Quero, A.-M., Géniteau-Legendre, M. and Servin, A. (2000a). Rotavirus infection induces an increase in intracellular calcium concentration in human intestinal epithelial cells: role in microvillar actin alteration. *J. Virol.* **74**(5), 2323-2332.

Brunet, J.P., Jourdan, N., Cotte-Laffitte, J., Linxe, C., Géniteau-Legendre, M., Servin, A.L. and Quéro, A.M. (2000b). Rotavirus infection induces cytoskeleton disorganization in human intestinal epithelial cells: implication of an increase in intracellular calcium concentration. *J. Virol.* **74**(22), 10801-10806.

Bugarcic, A. and Taylor, J.A. (2006). Rotavirus nonstructural glycoprotein NSP4 is secreted from the apical surfaces of polarized epithelial cells. *J. Virol.* **80**(24), 12343-12349.

Burch, A.D. and Weller, S.K. (2005). Herpes simplex virus type I DNA polymerase requires the mammalian chaperone hsp90 for proper localization to the nucleus. *J. Virol.* **79**(16), 10740-10749.

Burns, J.W., Siadat-Pajouh, M., Krishnaney, A.A. and Greenberg, H.B. (1996). Protective effect of rotavirus VP6-specific IgA monoclonal antibodies that lack neutralizing activity. *Science* **272**(5258), 104-107.

Carafoli, E. (1987). Intracellular calcium homeostasis. *Ann. Rev. Biochem.* **56**, 395-433.

Carafoli, E. (2002). Calcium signaling: a tale for all seasons. *Proc. Natl. Acad. Sci. U.S.A.* **99**(3), 1115-1122.

Chan, W.K., Au, K.S. and Estes, M.K. (1988). Topography of the simian rotavirus nonstructural glycoprotein (NS28) in the endoplasmic reticulum membrane. *Virology* **164**(2), 435-442.

Chang, H.G.H., Smith, P.F., Morse, D.L., Ackelsberg, J. and Glass, R.I. (2001a). Intussuseption, rotavirus diarrhea, and rotavirus vaccine use among children in New York state. *Pediatrics* **108**(1), 54-60.

Chang, K.O., Kim, Y.J. and Saif, L.J. (1999). Comparisons of nucleotide and deduced amino acid sequences of NSP4 genes of virulent and attenuated pairs of group A and C rotaviruses. *Virus Genes* **18**(3), 229-233.

Chang, K.O., Vandal, O.H., Yuan, L., Hodgins, D.C. and Saif, L.J. (2001b). Antibody-secreting cell responses to rotavirus proteins in gnotobiotic pigs inoculated with attenuated or virulent human rotavirus. *J. Clin. Microbiol.* **39**(8), 2807-2813.

Charpilienne, A., Abad, M.J., Michelangeli, F., Alvarado, F., Vasseur, M., Cohen, J. and Ruiz, M.C. (1997). Solubilized and cleaved VP7, the outer glycoprotein of rotavirus, induces permeabilization of cell membrane vesicles. *J. Gen. Virol*. **78**(Pt 6), 1367-1371.

Cheever, F.S. and Mueller, J.H. (1947). Epidemic diarrheal disease of suckling mice: I. Manifestations, epidemiology, and attempts to transmit the disease. *J. Exp. Med.* **85**(4), 405-416.

Chemello, M.E., Aristimuño, O.C., Michelangeli, F. and Ruiz, M.C. (2002). Requirement for vacuolor $H^+$-ATPase activity and $Ca^{2+}$ gradient during entry of rotavirus into MA104 cells. *J. Virol.* **76**(24), 13083-13087.

Chen, D., Luongo, C.L., Nibert, M.L. and Patton, J.T. (1999). Rotavirus open cores catalyze 5'-capping and methylation of exogenous RNA: evidence that VP3 is a methyl-transferase. *Virology* **265**(1), 120-130.

Chen, D., Barros, M., Spencer, E. and Patton, J.T. (2001). Features of the 3'-consensus sequence of rotavirus mRNAs critical to minus strand synthesis. *Virology* **282**(2), 221-229.

Chen, S.C., Fynan, E.F., Robinson, H.L., Lu, S., Greenberg, H.B., Santoro, J.C. and Herrmann, J.E. (1997). Protective immunity induced by rotavirus DNA vaccines. *Vaccine* **15**(8), 899-902.

Chiba, S., Yokoyama, T., Nakata, S. Morita, Y., Urasawa, T., Taniguchi, K., Urasawa, S. and Nakao, T. (1986). Protective effect of naturally acquired homotypic and heterotypic rotavirus antibodies. *Lancet* **2**(8504), 417-421.

Chiba, S., Nakata, S., Ukae, S. and Adachi, N. (1993). Virological and serological aspects of immune resistance to rotavirus gastroenteritis. *Clin. Infect. Dis.* **16**(Suppl 2), S117-121.

Chizhikov, V. and Patton, J.T. (2000). A four-nucleotide translation enhancer in the 3'-terminal consensus sequence of the nonpolyadenylated mRNAs of rotavirus. *RNA*. **6**(6), 814-825.

Choi, N.W., Estes, M.K. and Langridge, W.H. (2005). Oral immunization with a shiga toxin B subunit::rotavirus $NSP4_{90}$ fusion protein protects mice against gastroenteritis. *Vaccine* **23**(44), 5168-5176.

Choi, N.W., Estes, M.K. and Langridge, W.H. (2006a). Ricin toxin N subunit enhancement of rotavirus NSP4 immunogenicity in mice. *Viral Immunol.* **19**(1), 54-63.

Choi, N.W., Estes, M.K., Langridge, W.H. (2006b). Mucosal immunization with a ricin toxin B subunit-rotavirus NSP4 fusion protein stimulates a Th1 lymphocyte response. *J. Biotechnol.* **121**, 272-283.

Chromy, L.R., Pipas, J.M. and Garcea, R.L. (2003). Chaperone-mediated in vitro assembly of Polyomavirus capsids. *Proc. Natl. Acad. Sci. U.S.A.* **100**(18), 10477-10482.

Ciarlet, M. and Estes, M.K. (1999). Human and most animal rotavirus strains do not require the presence of sialic acid on the cell surface for efficient infectivity. *J. Gen. Virol*. **80**(Pt 4), 943-948.

Ciarlet, M. and Conner, M.E. (2000). Evaluation of Rotavirus Vaccines in Small Animal Models. *In* "Rotaviruses; Methods and Protocols" (J. Gray, and U. Desselberger, Eds.), pp 147-187. Humana Press, New Jersey.

Ciarlet, M., Liprandi, F., Conner, M.E. and Estes, M.K. (2000). Species specificity and interspecies relatedness of NSP4 genetic groups by comparative NSP4 sequence analyses of animal rotaviruses. *Arch. Virol.* **145**(2), 371-383.

Ciarlet, M., Crawford, S.E. and Estes, M.K. (2001). Differential infection of polarized epithelial cell lines by sialic acid-dependent and sialic acid-independent rotavirus strains. *J. Virol.* **75**(23), 11834-11850.

Ciarlet, M. and Estes, M.K. (2001). Interactions between rotavirus and gastrointestinal cells. *Curr. Opin. Microbiol*. **4**(4), 435-441.

Ciarlet, M., Crawford, S.E., Cheng, E., Blutt, S.E., Rice, D.A., Bergelson, J.M. and Estes, M.K. (2002a). VLA-2 (α2β1) integrin promotes rotavirus entry into cells but is not necessary for rotavirus attachment. *J. Virol.* **76**(3), 1109-1123.

Ciarlet, M., Ludert, J.E., Iturriza-Gómara, M., Liprandi, F., Gray, J.J., Desselberger, U. and Estes, M.K. (2002b). Initial interaction of rotavirus strains with N-acetylneuraminic (sialic) acid residues on the cell surface correlates with VP4 genotype, not species of origin. *J. Virol.* **76**(8), 4087-4095.

Clark, H.F. and Offit, P.A. (2004). Vaccines for rotavirus gastroenteritis universally needed for infants. *Pediatr. Ann.* **33**(8), 536-543.

Clark, S.M., Roth, J.R., Clark, M.L., Barnett, B.B. and Spendlove, R.S. (1981). Trypsin enhancement of rotavirus infectivity: mechanism of enhancement. *J. Virol.* **39**(3), 816-822.

Clemens, J.D., Ward, R.L., Rao, M.R., Sack, D.A., Knowlton, D.R., van Loon, F.P., Huda, S., McNeal, M., Ahmed, F. and Schiff, G. (1992). Seroepidemiologic evaluation of antibodies to rotavirus as correlates of the risk of clinically significant rotavirus diarrhea in rural Bangladesh. *J. Infect. Dis.* **165**(1), 161-165.

Cohen, J., Laporte, J., Charpilienne, A. and Scherrer, R. (1979). Activation of rotavirus RNA polymerase by calcium chelation. *Arch. Virol*. **60**(3-4), 177-186.

Collins, J, Starkey, W.G., Wallis, T.S., Clarke, G.J., Worton, K.J., Spencer, A.J., Haddon S.J., Osborne, M.P., Candy, D.C. and Stephen, J. (1988). Intestinal enzyme profiles in normal and rotavirus-infected mice. *J.Pediatr. Gastroenterol. Nutr.* **7**(2), 264-272.

Collins, P.L. and Hightower, L.E. (1982). Newcastle disease virus stimulates the cellular accumulation of stress (heat shock) mRNAs and proteins. *J. Virol*. **44**(2), 703-707.

Conner, M.E., Gilger, M.A., Estes, M.K. and Graham, D.Y. (1991). Serologic and mucosal immune response to rotavirus infection in the rabbit model. *J. Virol.* **65**(5), 2562-2571.

Coulson, B.S. and Masendycz, P.J. (1990). Measurement of rotavirus-neutralizing coproantibody in children by fluorescent focus reduction assay. *J. Clin. Microbiol.* **28**(7), 1652-1654.

Coulson, B.S., Grimwood, K., Hudson, I.L., Barnes, G.L. and Bishop, R.F. (1992). Role of coproantibody in clinical protection of children during reinfection with rotavirus. *J. Clin. Microbiol.* **30**(7), 1678-1684.

Coulson, B.S., Londrigan, S.L. and Lee, D.J. (1997). Rotavirus contains integrin ligand sequences and a disintegrin-like domain that are implicated in virus entry into cells. *Proc. Natl. Acad. Sci. USA* **94**(10), 5389-5394.

Crawford, S.E., Labbé, M., Cohen, J., Burroughs, M.H., Zhou, Y.J. and Estes, M.K. (1994). Characterization of virus-like particles produced by the expression of rotavirus caspid proteins in insect cells. *J. Virol.* **68**(9), 5945-5952.

Crawford, S.E., Mukherjee S.K., Estes, M.K., Lawton, J.A., Shaw, A.L., Ramig, R.F. and Prasad, B.V. (2001). Trypsin cleavage stabilizes the rotavirus VP4 spike. *J. Virol.* **75**(13), 6052-6061.

Crawford, S.E., Patel, D.G., Cheng, E., Berkova, Z., Hyser, J.M., Ciarlet, M., Finegold, M.J., Conner, M.E. and Estes, M.K. (2006). Rotavirus viremia and extraintestinal viral infection in the neonatal rat model. *J. Virol.* **80**(10), 4820-4832.

Crowther, J.R. (2001). The ELISA guidebook, Methods in molecular biology, vol, 149, Humana Press, Totowa, New Jersey.

Cuadras, M.A., Arias, C.F. and López, S. (1997). Rotaviruses induce an early membrane permeabilization of MA104 cells and do not require a low intracellular $Ca^{2+}$ concentration to initiate their replication cycle. *J. Virol.* **71**(12), 9065-9074.

Cuadras, M.A., Feigelstock, D.A., An, S. and Greenberg, H.B. (2002). Gene expression pattern in Caco-2 cells following rotavirus infection. *J. Virol.* **76**(9), 4467-4482.

Cuadras, M.A. and Greenberg, H.B. (2003). Rotavirus infectious particles use lipid rafts during replication for transport to the cell surface in vitro and in vivo. *Virology* **313**(1), 308-321.

Cuadras, M.A., Bordier, B.B., Zambrano, J.L., Ludert, J.E. and Greenberg, H.B. (2006). Dissecting rotavirus particle-raft interaction with small interfering RNAs: insights into rotavirus transit through the secretory pathway. *J. Virol.* **80**(8), 3935-3946.

Cunliffe, N.A., Woods, P.A., Leite, J.P., Das, B.K., Ramachandran, M., Bhan, M.K., Hart, C.A., Glass, R.I. and Gentsch, J.R. (1997). Sequence analysis of NSP4 gene of human rotavirus allows classification into two main genetic groups. *J. Med. Virol.* **53**(1), 41-50.

Cunliffe, N.A., Rogerson, S., Dove, W., Thindwa, B.D., Greensill, J., Kirkwood, C.D., Broadhead, R.L. and Hart, C.A. (2002). Detection and characterization of rotaviruses in hospitalized neonates in Blantyre, Malawi. *J. Clin. Microbiol.* **40**(4), 1534-1537.

Danno, S., Itoh, K., Matsuda, T. and Fujita, J. (2000). Decreased expression of mouse Rbm3, a cold-shock protein, in sertoli cells of cryptorchid testis. *Am. J. Pathol.* **156**(5), 1685-1692.

Davidson, G.P., Bishop, R.F., Townley, R.R and Holmes, I.H. (1975a). Importance of a new virus in acute sporadic enteritis in children. *Lancet* **1**(7901), 242-246.

Davidson, G.P., Goller, I., Bishop, R.F., Townley, R.R., Holmes, I.H. and Ruck, B.J. (1975b). Immunofluorescence in duodenal mucosa of children with acute enteritis due to a new virus. *J. Clin. Pathol.* **28**(4), 263-266.

Davidson, G.P., Gall, D.G., Petric, M., Butler, D.G. and Hamilton, J.R. (1977). Human rotavirus enteritis induced in conventional piglets. Intestinal structure and transport. *J. Clin. Invest.* **60**(6), 1402-1409.

Davidson, G.P. and Barnes, G.I. (1979). Structural and functional abnormalities of the small intestine in infants and young children with rotavirus enteritis. *Acta. Paediatr. Scand.*. **68**(2), 181-186.

Davidson, G.P. (1996). Passive protection against diarrheal disease. *J. Pediatr. Gastroenterol. Nutr.* **23**(3), 207-212.

De Leener, K., Rahman, M., Matthijnssens, J., Van Hoovels, L., Goegebuer, T., van der Donck, I. and Van Ranst, M. (2004). Human infection with a P[14], G3 lapine rotavirus. *Virology* **325**(1), 11-17.

De Marco, G., Bracale, I., Buccigrossi, V., Bruzzese, E., Canani, R.B., Polito, G., Ruggeri, F.M. and Guarino, A. (2009). Rotavirus induces a biphasic enterotoxic and cytotoxic response in human-derived intestinal enterocytes, which is inhibited by human immunoglobulins. *J. Infect. Dis.* **200**(5), 813-819.

De Vos, B., Vesikari, T., Linhares, A.C., Salinas, B., Pérez-Schael, I., Ruiz-Palacios, G.M., Guerrero, M.L., Phua, K.B., Delem, A. and Hardt, K. (2004). A rotavirus vaccine for prophylaxis of infants against rotavirus gastroenteritis. *Pediatr Infect Dis J.* **23**(Suppl 10): S179-S182.

Deepa, R., Durga Rao, C. and Suguna, K. (2007). Structure of the extended diarrhea-inducing domain of rotavirus enterotoxigenic protein NSP4. *Arch. Virol.* **152**(5), 847-859.

del Castillo, J. R., Ludert, J.E., Sanchez, A., Ruiz, M.-C., Michelangeli, F. and Liprandi, F. (1991). Rotavirus infection alters $Na^+$ and $K^+$ homoestasis in MA104 cells. *J. Gen. Virol.* **72**, 541-547.

Delmas, O., Durand-Schneider, A.M., Cohen, J., Colard, O. and Trugnan, G. (2004a). Spike protein VP4 assembly with maturing rotavirus requires a postendoplasmic reticulum event in polarized Caco-2 cells. *J. Virol.* **78**(20), 10987-10994.

Delmas, O., Gardet, A., Chwetzoff, S., Breton, M., Cohen, J., Colard, O., Sapin, C. and Trugnan, G. (2004b). Different ways to reach the top of a cell. Analysis of rotavirus assembly and targeting in human intestinal cells reveals an original raft-dependent, Golgi-independent apical targeting pathway. *Virology* **327**(2), 157-161.

Delmas, O., Breton, M., Sapin, C., Le Bivic, A., Colard, O. and Trugnan, G. (2007). Heterogeneity of raft-type membrane microdomains associated with VP4, the rotavirus spike protein, in Caco-2 and MA 104 cells. *J. Virol.* **81**(4), 1610-1618.

Delorme, C., Brüssow, H., Sidoti, J., Roche, N., Karlsson, K.A., Neeser, J.R. and Teneberg, S. (2001). Glycosphingolipid binding specificities of rotavirus: identification of a sialic acid-binding epitope. *J. Virol.* **75**(5), 2276-2287.

Denisova, E., Dowling, W., LaMonica, R., Shaw, R., Scarlata, S., Ruggeri, F. and Mackow, E.R. (1999). Rotavirus capsid protein VP5* permeabilizes membranes. *J. Virol.* **73**(4), 3147-3153.

Dennehy, P.H. (2008). Rotavirus vaccines: an overview. *Clin. Microbiol. Rev.* **21**(1), 198-208.

Deo, R.C., Groft, C.M., Rajashankar, K.R. and Burley, S.K. (2002). Recognition of the rotavirus mRNA 3'consensus by an asymmetric NSP3 homodimer. *Cell* **108**(1), 71-81.

Desselberger, U. (1999). Rotavirus Infections: guidelines for treatment and prevention. *Drugs* **58**(3), 447-452.

Desselberger, U., Iturriza-Gómara, M. and Gray, J.J. (2001). Rotavirus epidemiology and surveillance. *Novartis Found. Symp.* **238**, 125-147.

Dharakul, T., Rott, L. and Greenberg, H.B. (1990). Recovery from chronic rotavirus infection in mice with severe combined immunodeficiency: virus clearance mediated by adoptive transfer of immune $CD8^+$ lymphocytes. *J. Virol.* **64**(9), 4375-4382.

Diaz, Y., Chemello, M.E., Peña, F., Aristimuño, O.C., Zambrano, J.L., Rojas, H., Bartoli, F., Salazar, L., Chwetzoff, S., Sapin, C., Trugnan, G., Michelangeli, F. and Ruiz, M.C. (2008). Expression of non structural rotavirus protein mimicks $Ca^{2+}$ homeostasis changes induced by rotavirus infection in cultured cells. *J. Virol.* **82**(22), 11331-11334.

Dong, Y., Zeng, C. Q.-Y., Ball, J.M. and Estes, M.K. (1997). The rotavirus enterotoxin NSP4 mobilizes intracellular calcium in human intestinal cells by stimulating phospholipase C-mediated insoitol 1,4,5-triphosphate production. *Proc. Natl. Acad. Sci. U.S.A.* **94**(8), 3960-3965.

Dormitzer, P.R., Nason, E.B., Prasad, B.V. and Harrison, S.C. (2004). Structural rearrangements in the membrane penetration protein of a non-enveloped virus. *Nature* **430**(7003), 1053-1058.

Dowling, W., Denisova, E., LaMonica, R. and Mackow, E.R. (2000). Selective membrane permeabilization by the rotavirus VP5* protein is abrogated by mutations in an internal hydrophobic domain. *J. Virol.* **74**(14), 6368-6376.

Dutta, D., Bagchi, P., Chatterjee, A., Nayak, M.K., Mukherjee, A., Chattopadhyay, S., Nagashima, S., Kobayashi, N., Komoto, S., Taniguchi, K. and Chwla-Sarkar, M. (2009). The molecular chaperone heat shock protein-90 positively regulates rotavirus infections. *Virology* **391**(2), 325-333.

Ericson, B.L., Graham, D.Y., Mason, B.B. and Estes, M.K. (1982). Identification, synthesis, and modifications of simian rotavirus SA11 polypeptides in infected cells. *J. Virol.* **42**(3), 825-839.

Ericson, B.L., Graham, D.Y., Mason, B.B., Hanssen, H.H. and Estes, M.K. (1983). Two types of glycoprotein precursors are produced by the simian rotavirus SA11. *Virology* **127**(2), 320-332.

Espejo, R.T., López, S. and Arias, C. (1981). Structural polypeptides of simian rotavirus SA11 and the effect of trypsin. *J. Virol.* **37**(1), 156-160.

Esser, P. (1997). Blocking agent and detergent in ELISA. *Nunc Technical Bulletin*, No.9, 337-340.

Estes, M.K., Graham, D.Y., Gerba, C.P. and Smith, E.M. (1979). Simian rotavirus SA11 replication in cell cultures. *J. Virol.* **31**(3), 810-815.

Estes, M.K., Graham, D.Y. and Mason, B.B. (1981). Proteolytic enhancement of rotavirus infectivity: molecular mechansims. *J. Virol.* **39**(3), 879-888.

Estes, M.K. and Cohen, J. (1989). Rotavirus gene structure and function. *Microbiol. Rev.* **53**(4), 410-449.

Estes, M.K. (2001). Rotaviruses and their replication. *In* "Fields Virology" 4th Edn. (D.M. Knipe, P.M. Howley, D.E. Griffin, R.A. Lamb, M.A. Martin, B. Roizman and S.E. Straus, Eds.), pp. 1747-1785. Lippincott Williams and Wilkins, Philadelphia.

Estes, M.K., Kang, G., Zeng, C. Q., Crawford, S.E. and Ciarlet. (2001). Pathogenesis of rotavirus gastroenteritis. *Novartis Found. Symp.* 238, 82-100.

Estes, M.K. (2003). The rotavirus NSP4 enterotoxin: current status and challenges. *In* "Viral Gastroenteritis" (U. Desselberger and J. Gray, Eds.), pp. 207-224. Elsevier Science B.V., Amsterdam, The Netherlands.

Estes, M.K. and Kapikian, A.Z. (2007). Rotaviruses. *In* "Fields Virology" 5th Edn. Vol. 2. (D.M. Knipe, P.M. Howley, D.E. Griffin, R.A. Lamb, M.A. Martin, B. Roizman and S.E. Straus, Eds.), pp. 1917-1974, Wolters Kuwer Health, Lippincott, Williams and Wilkins, Philadelphia, P.A.

Fabbretti, E., Afrikanova, I., Vascotto, F. and Burrone, O.R. (1999). Two nonstructural rotavirus proteins, NSP2 and NSP5, form viroplasm-like structures in vivo. *J. Gen. Virol.* **80**(Pt 2), 333-339.

Farthing, M.J. (2006). Antisecretory drugs for diarrheal disease. *Dig. Dis.* **24**(1-2), 47-58.

Feigelstock, D.A., Cuadras, M.A. and Greenberg, H.B. (2003). Microarrays and host-virus interactions: a transcriptional analysis of Caco-2 cells following rotavirus infection. *In* "Viral Gastroenteritis" (U. Desselberger and J. Gray, Eds.), pp. 255-289. Elsevier Science B.V., Amsterdam, The Netherlands.

Fenaux, M., Cuadras, M.A., Feng, N., Jaimes, M. and Greenberg, H.B. (2006). Extraintestinal spread and replication of a homologous EC rotavirus strain and a heterologous rhesus rotavirus in BALB/c mice. *J. Virol.* **80**(11), 5219-5232.

Feng, N., Burns, J.W., Bracy, L. and Greenberg, H.B. (1994). Comparison of mucosal and systemic humoral immune responses and subsequent protection in mice orally inoculated with a homologous or a heterologous rotavirus. *J. Virol*. **68**(12), 7766-7773.

Feng, N., Vo, P.T., Chung, D., Vo, T.V., Hoshino, Y. and Greenberg, H.B. (1997). Heterotypic protection following oral immunization with live heterologous rotaviruses in a mouse model. *J. Infect. Dis.* **175**(2), 330-341.

Feng, N., Lawton, J.A., Gilbert, J., Kuklin, N., Vo, P., Prasad, B.V. and Greenberg, H.B. (2002). Inhibition of rotavirus replication by a non-neutralizing, rotavirus VP6-specific IgA mAb. *J. Clin. Invest.* **109**(9), 1203-1213.

Fischer, T.K., Steinsland, H. and Valentiner-Branth, P. (2002a). Rotavirus particles can survive storage in ambient tropical temperatures for more than 2 months. *J. Clin. Microbiol*. **40**(12), 4763-4764.

Fischer, T.K. Valentiner-Branth, P., Steinsland, H., Perch, M., Santos, G., Aaby, P., Mølbak, K. and Sommerfelt, H. (2002b). Protective immunity after natural rotavirus infection: a community cohort study of newborn children in Guinea-Bissau, West Africa. *J. Infect. Dis.* **186**(5), 593-597.

Fischer, T.K., Bresee, J.S. and Glass, R.I. (2004). Rotavirus vaccines and the prevention of hospital-acquired diarrhea in children. *Vaccine* **22**(Suppl. 1), S49-S54.

Flewett, T.H., Bryden, A.S. and Davies, H. (1973). Letter: Virus particles in gastroenteritis. *Lancet* **2**(7844), 1497.

Flewett, T.H. (1983). Rotavirus in the home and hospital nursery. *Br. Med. J. (Clin. Res. Ed.)* **287**(6392), 568-569.

Franco, M.A. and Greenberg, H.B. (1995). Role of B cells and cytotoxic T lymphocytes in clearance of and immunity to rotavirus infection in mice. *J. Virol.* **69**(12), 7800-7806.

Franco, M.A., Tin, C. and Greenberg, H.B. (1997). $CD8^+$ T cells can mediate almost complete short-term and partial long-term immunity to rotavirus in mice. *J. Virol.* **71**(5), 4165-4170.

Franco, M.A. and Greenberg, H.B. (1999). Immunity to rotavirus infection in mice. *J. Infect. Dis.* **179(**Suppl 3), S466-S469.

Franco, M.A., Angel, J. and Greenberg, H.B. (2006). Immunity and correlates of protection for rotavirus vaccines. *Vaccine* **24**(15), 2718-2731.

Fuentes-Panana, E.M., López, S., Gorziglia, M. and Arias, C.F. (1995). Mapping the hemagglutination domain of rotaviruses. *J. Virol*. **69**(4), 2629-2632.

Fujita, J. (1999). Cold shock response in mammalian cells. *J. Mol. Microbiol. Biotechnol.* **1**(2), 243-255.

Fukuhara, N., Yoshie, O., Kitaoka, S., Konno, T. and Ishida, N. (1987). Evidence for endocytosis-independent infection by human rotavirus. *Arch. Virol*. **97**(1-2), 93-99.

Fukuhara, N., Yoshie, O., Kitaoka, S. and Konno, T. (1988). Role of VP3 in human rotavirus internalization after target cell attachment via VP7. *J. Virol.* **62**(7), 2209-2218.

Furlini, G., Re, M.C., Musiani, M., Zerbini, M.L. and La Placa, M. (1990). Enhancement of HIV-1 marker detection in cell cultures treated with mild heat-shock. *Microbiologica* **13**(1), 21-26.

Galati, J.C., Harsley, S., Richmond, P. and Carlin, J.B. (2006). The burden of rotavirus-related illness among young children on the Australian health care system. *Aust. N.Z. J. Publ. Heal*. **30**(5), 416-421.

Gallegos, C.O. and Patton, J.T. (1989) Characterization of rotavirus replication intermediates: a model for the assembly of single-shelled particles. *Virology* **172**(2), 616-627.

Gardet, A., Breton, M., Fontanges, P., Trugnan, G. and Chwetzoff, S. (2006). Rotavirus spike protein VP4 binds to and remodels actin bundles of the epithelial brush border into actin bodies. *J. Virol.* **80**(8), 3947-3956.

Garry, R.F., Ulug, E.T. and Bose Jr, H.R. (1983). Induction of stress proteins in Sindbis virus- and vesicular stomatitis virus-infected cells. *Virology* **129**(2), 319-332.

Gentsch, J.R., Laird, A.R., Bielfelt, B., Griffin, D.D., Bányai, K., Ramachandran, M., Jain, V., Cunliffe, N.A., Nakagomi, O., Kirkwood, C.D., Fischer, T.K., Parashar, U.D., Bresee, J.S., Jiang, B. and Glass, R.I. (2005). Serotype diversity and reassortment between human and animal rotavirus strains: implications for rotavirus vaccine programs. *J. Infect. Dis.* **192**(Suppl 1), S146-S159.

Gething, M.J. and Sambrook, J. (1992). Protein folding in the cell. *Nature* **355**(6355), 33-45.

Ghosh, S., Varghese, V., Samajdar, S., Bhattacharyha, S.K., Kobayashi, N. and Naik, T.N. (2006). Evidence for independent segregation of the VP6- and NSP4-encoding genes in porcine group A rotavirus G6P[13] strains. *Arch. Virol.* **152**(2), 423-429.

Gibbs, J. (2001). Effective blocking procedures, ELISA Technical Bulletin No. 3; Corning Life Sciences.

Gilger, M.A., Matson, D.O., Conner, M.E., Rosenblatt, H.M., Finegold, M.J. and Estes, M.K. (1992). Extraintestinal rotavirus infections in children with immunodeficiency. *J. Pediatr.* **120**(6), 912-917.

Glass, R.I., Bresee, J.S., Parashar, U., Turcios, R., Fischer, T., Jiang, B., Widdowson, M.A. and Gentsch. J. (2005a). Rotavirus vaccines: past, present, and future. *Arch. Pediatr.* **12**(6), 844-847.

Glass, R.I., Bhan, M.K., Ray, P., Bahl, R., Parashar, U.D., Greenberg, H., Rao, C.D., Bhandari, N., Maldonado, Y., Ward, R.L., Bernstein, D.I. and Gentsch, J.R. (2005b). Development of candidate rotavirus vaccines derived from neonatal strains in India. *J. Infect. Dis.* **192**(Suppl 1), S30-S35.

Gleizes, O., Desselberger, U., Tatochenko, V., Rodrigo, C., Salman, N., Mezner, Z., Giaquinto, C. and Grimprel, E. (2006). Nosocomial rotavirus infection in European countries: a review of the epidemiology, severity and economic burden of hospital-acquired rotavirus disease. *Pediatr. Infect. Dis. J.* **25**(Suppl 1): S12-S21.

Glotzer, J.B., Saltik, M., Chiocca, S., Michou, A.I., Moseley, P. and Cotton, M. (2000). Activation of the heat-shock response by an adenovirus is essential for viral replication. *Nature* **407**(6801), 207-211.

Gluzman, Y. (1981). SV40-transformed simian cells support the replication of early SV40 mutants. *Cell* **23**(1), 175-182.

González, A.M., Azevedo, M.S.P. and Saif, L.J. (2008). Intestinal and systemic immunity to rotavirus in animal models and humans. *In* "Immunity against mucosal pathogens" (M. Vajdy, Ed.), pp. 263-297. Springer, USA.

González, R.A., Espinosa, R., Romero, P., López, S. and Arias, C.F. (2000). Relative localization of viroplasmic and endoplasmic reticulum-resident rotavirus proteins in infected cells. *Arch. Virol.* **145**(9), 1963-1973.

González, R., Franco, M., Sarmiento, L., Romero, M. and Schael, I.P. (2005). Serum IgA levels induced by rotavirus natural infection, but not following immunization with the RRV-TV vaccine (Rotashield), correlate with protection. *J. Med. Virol.* **76**(4), 608-612.

Gorrell, R.J. and Bishop, R.F. (1999). Homotypic and heterotypic serum neutralizing antibody response to rotavirus proteins following natural primary infection and reinfection in children. *J. Med. Virol.* **57**(2), 204-211.

Gorziglia, M., Larralde, G., Kapikian, A.Z. and Chanock, R.M. (1990). Antigenic relationships among human rotaviruses as determined by outer capsid protein VP4. *Proc. Natl. Acad. Sci. U S A.* **87**(18), 7155-7159.

Graham D.Y., Sackman, J.W. and Estes, M.K. (1984). Pathogenesis of rotavirus-induced diarrhea. Preliminary studies in miniature swine piglet. *Dig. Dis. Sci.* **29**(11), 1028-1035.

Graham, K.L., Halasz, P., Tan, Y., Hewish, M.J., Takada, Y., Mackow, E.R., Robinson, M.K. and Coulson, B.S. (2003). Integrin-using rotaviruses bind α2β1 integrin α2 I domain via VP4 DGE sequence and recognize αxβ2 and αvβ3 by using VP7 during cell entry. *J. Virol.* **77**(18), 9969-9978.

Graham, K.L., Zeng, W., Takada, Y., Jackson, D.C. and Coulson, B.S. (2004). Effects on rotavirus cell binding and infection of monomeric and polymeric peptides containing α2β1 and αxβ2 integrin ligand sequences. *J. Virol.* **78**(21), 11786-11797.

Green, K.Y., Taniguchi, K., Mackow, E.R. and Kapikian, A.Z. (1990). Homotypic and heterotypic epitope-specific antibody responses in adult and infant rotavirus vacinees: implications for vaccine development. *J. Infect. Dis.* **161**(4), 667-679.

Green, K.Y. and Kapikian, A.Z. (1992). Identification of VP7 epitopes associated with protection against human rotavirus illness or shedding in volunteers. *J. Virol.* **66**(1), 548-553.

Greenberg, H., McAuliffe, V., Valdesuso, J., Wyatt, R., Flores, J., Kalica, A., Hoshino, Y, and Singh, N. (1983). Serological analysis of the subgroup protein of rotavirus, using monoclonal antibodies. *Infect. Immun.* **39**(1), 91-99.

Greenberg, H.B. and Estes, M.K. (2009). Rotaviruses: from pathogenesis to vaccination. *Gastroenterology* **136**(6), 1939-1951.

Grimwood, K., Lund, J.C.S., Coulson, B.S., Hudson, I.L., Bishop, R.F. and Barnes, G.L. (1988). Comparison of serum and mucosal antibody responses following severe acute rotavirus gastroenteritis in young children. *J. Clin. Microbiol.* **26**(4), 732-738.

Groft, C.M. and Burley, S.K. (2002). Recognition of eIF4G by rotavirus NSP3 reveals a basis for mRNA circularization. *Mol. Cell.* **9**(6), 1273-1283.

Gualtero, D.F., Guzmán, F., Acosta, O, and Guerrero, C.A. (2007). Amino acid domains 280-297 of VP6 and 531-554 of VP4 are implicated in heat shock cognate protein hsc70-mediated rotavirus infection. *Arch. Virol.* **152**(12), 2183-2196.

Guarino, A., Canani, R.B., Russo, S., Albano, F., Canani, M.B., Ruggeri, F.M., Donelli, G. and Rubino, A. (1994). Oral immunoglobulins for treatment of acute rotaviral gastroenteritis. *Pediatrics* **93**(1), 12-16.

Guerrero, C.A., Méndez, E., Zárate, S., Isa, P., López, S. and Arias, C.F. (2000a). Integrin αvβ3 mediates rotavirus cell entry. *Proc. Natl. Acad. Sci. USA* **97**(26), 14644-14649.

Guerrero, C.A., Zárate, S., Corkidi, G., López, S. and Arias, C.F. (2000b). Biochemical characterization of rotavirus receptors in MA104 cells. *J. Virol.* **74**(20), 9362-9371.

Guerrero, C.A., Bouyssounade, D., Zárate, S., Isa, P., López, T., Espinosa, R., Romero, P., Méndez, E., López, S. and Arias, C.F. (2002). Heat shock cognate protein 70 is involved in rotavirus cell entry. *J. Virol.* **76**(8), 4096-4102.

Guglielmi, K.M., McDonald, S.M. and Patton, J.T. (2010). Mechanism of intra-particle synthesis of the rotavirus double-stranded RNA genome. *J. Biol. Chem.* E. pub. Accessed April 26th 2010 (http://www.jbc.org/cgi/doi/10.1074/jbc.R110.117671)

Guo, C.T., Nakagomi, O., Mochizuki, M., Ishida, H., Kiso, M., Ohta, Y., Suzuki, T., Miyamoto, D., Hidari, K.I. and Suzuki, Y. (1999). Ganglioside GM1a on the cell surface is involved in the infection by human rotavirus KUN and MO strains. *J. Biochem.* **126**(4), 683-688.

Guzman, E. and McCrae, M.A. (2005a). Molecular characterization of the rotavirus NSP4 enterotoxin homologue from group B rotavirus. *Virus Res*. **110**(1-2), 151-160.

Guzman, E. and McCrae, M.A. (2005b). A rapid and accurate assay for assessing the cytotoxicity of viral proteins. *J.Virol. Methods* **127**(12), 119-125.

Halaihel, N., Liévin, V., Alvarado, F. and Vasseur, M. (2000a). Rotavirus infection impairs intestinal brush border membrane $Na^+$-solute cotransport activities in young rabbits. *Am. J. Physiol*. *Liver Physiol*. **279**(3), G587-596.

Halaihel, N., Lievin, V., Ball, J.M., Estes, M.K., Alvarado, F. and Vasseur, M. (2000b). Direct inhibitory effect of rotavirus NSP4(114-135) peptide on the $Na^+$-D-glucose symporter of rabbit intestinal brush border membrane. *J. Virol.* **74**(20), 9464-9470.

Hamilton, S., Odili, J., Pacifico, M.D., Wilson, G.D. and Kupsch, J.-M. (2003). Effect of imidazole on the solubility of a His-tagged antibody fragment. *Hybridoma and Hybridom.* **22**(6), 347-355.

Hancock, J.F. (1991). COS cell expression. *Methods. Mol. Biol.* **8**, 153-159.

Haughland, R.P. (2005). The Handbook – A guide to fluorescent probes and labeling technologies. 10th Ed., Molecular Probes, San Diego, U.S.A.

Hayashi, H. and Miyata, H. (1994). Fluorescence imaging of intracellular $Ca^{2+}$. *J. Pharmacol. Toxicol. Methods* **31**(1), 1-10.

Hewish, M.J., Takada, Y. and Coulson, B.S. (2000). Integrins α2β1 and α4β1 can mediate SA11 rotavirus attachment and entry into cells. *J. Virol.* **74**(1), 228-236.

Hjelt, K., Grauballe, P.C., Paerregard, A., Nielsen, O.H. and Krasilnikoff, P.A. (1987). Protective effect of preexisting rotavirus-specific immunoglobulin A against naturally acquired rotavirus infection in children. *J. Med. Virol.* **21**(1), 39-47.

Hochuli, E., Bannwarth, W., Dobeli, H., Gentz, R. and Stuber, D. (1988). Genetic approach to facilitate purification of recombinant proteins with a novel metal chelate absorbent. *Bio/Technology* **6**, 1321-1325.

Holmes, I.H., Ruck, B., Bishop, R. and Davidson, G. (1975). Infantile enteritis; morphogenesis and morphology. *J. Virol.* **16**(4), 937-943.

Hopkins, R.S., Gaspard, G.B., Williams, F.P. Jr., Karlin, R.J.., Cukor, G. and Blacklow, N.R. (1984). A community waterborne gastroenteritis outbreak: evidence for rotavirus as the agent. *Am. J. Public Health* **74**(3), 263-265.

Horie, Y., Masamune, O. and Nakagomi, O. (1997). Three major alleles of rotavirus NSP4 proteins identified by sequence analysis. *J. Gen. Virol.* **78**(Pt-2), 2341-2346.

Horie, Y., Nakagomi, O., Koshimura, Y., Nakagomi, T., Suzuki, Y., Oka, T., Sasaki, S., Matsuda, Y. and Watanabe, S. (1999). Diarrhea induction by rotavirus NSP4 in the homologous mouse model system. *Virology* **262**(2), 398-407.

Hoshino, Y., Saif, L.J., Sereno, M.M., Chanock, R.M. and Kapikian, A.Z. (1988). Infection immunity of piglets to either VP3 or VP7 outer capsid protein confers resistance to challenge with a virulent rotavirus bearing the corresponding antigen. *J. Virol*. **62**(3), 744-748.

Hoshino, Y., Saif, L.J., Kang, S.Y., Sereno, M.M., Chen, W.K. and Kapikian, A.Z. (1995). Identification of group A rotavirus genes associated with virulence of a porcine rotavirus and host range restriction of a human rotavirus in the gnotobiotic piglet model. *Virology* **209**(1), 274-280.

Hou, Z., Huang, Y., Huan, Y., Pang, W., Meng, M., Wang, P., Yang, M., Jiang, L., Cao, X. and Wu, K.K. (2008). Anti-NSP4 antibody can block rotavirus-induced diarrhea in mice. *J. Pediatr. Gastroenterol. Nutr.* **46**(4), 376-385.

Huang, H., Schroeder, F., Zeng, C., Estes, M.K., Schoer, J.K. and Ball, J.M. (2001). Membrane interactions of a novel viral enterotoxin: rotavirus nonstructural glycoprotein NSP4. *Biochemistry* **40**(13), 4169-4180.

Huang, H., Schroeder, F., Estes, M.K., McPherson, T. and Ball, J.M. (2004). The interaction(s) of rotavirus NSP4 C-terminal peptides with model membranes. *Biochem. J.* **380**(Pt 3), 723-733.

Huppertz, H.I., Soriano-Gabarró, M., Grimprel, E., Franco, E., Mezner, Z., Desselberger, U., Smit, Y., Wolleswinkel-van den Bosch, J., De Vos, B. and Giaquinto, C. (2006). Intussusception among young children in Europe. *Pediatr. Infect. Dis. J.* **25**(Suppl 1), S22-S29.

Hyser, J.M., Zeng, C.Q.-Y., Beharry, Z., Palzkill, T. and Estes, M.K. (2008). Epitope mapping and use of epitope-specific antisera to characterize the VP5* binding site in rotavirus SA11 NSP4. *Virology* **373**(1), 211-228.

Imai, M., Akatani, K., Ikegami, N. and Furuichi, Y. (1983). Capped and conserved terminal structures in human rotavirus genome double-stranded RNA segments. *J. Virol*. **47**(1), 125-136.

Iosef, C., Chang, K.-O., Azevedo, M.S. and Saif, L. J. (2002). Systemic and intestinal antibody responses to NSP4 enterotoxin of Wa human rotavirus in a gnotobiotic pig model of human rotavirus disease. *J. Med. Virol.* **68**(1), 119-128.

Iša, P., López, S., Segovia, L. and Arias, C.F. (1997). Functional and structural analysis of the sialic acid-binding domain of rotaviruses. *J. Virol.* **71**(9), 6749-6756.

Iša, P., Realpe, M., Romero, P., López, S. and Arias, C.F. (2004). Rotavirus RRV associates with lipid membrane microdomains during cell entry. *Virology* **322**(2), 370-381.

Iša, P., Arias, C.F. and López, S. (2006). Role of sialic acids in rotavirus infection. *Glycoconj. J.* **23**(1-2), 27-37.

Iša, P., Sánchez-Alemán, M.A., López, S. and Arias, C.F. (2009). Dissecting the role of integrin subunits α2 and β3 in rotavirus cell entry by RNA silencing. *Virus Res.* **145**(2), 251-259.

Ishida, S.-I., Feng, N., Tang, B., Gilbert, J. M. and Greenberg, H. B. (1996). Quantification of systemic and local immune responses to individual rotavirus proteins during rotavirus infection in mice. *J. Clin. Microbiol.* **34**(7), 1694-1700.

Ishida, S.-I.., Feng, N., Gilbert, J.M., Tang, B. and Greenberg, H.B. (1997). Immune responses to individual rotavirus proteins following heterologous and homologous rotavirus infection in mice. *J. Infect. Dis.* **175**(6) 1317-1323.

Ishino, M., Mise, K., Takemura, H., Ahmed, M.U., Alam, M.M., Naik, T.N. and Kobayashi, N. (2006). Comparison of NSP4 protein between group A and B human rotaviruses: detection of novel diarrhea-causing sequences in group B NSP4. *Arch. Virol.* **151**(1), 173-182.

Iturriza-Gòmara, M., Auchterlonie, I.A., Zaw, W. Molyneaux, P., Desselberger, U. and Gray, J. (2002a). Rotavirus gastroenteritis and central nervous system (CNS) infection: characterization of the VP7 and VP4 genes of rotavirus strains isolated from paired fecal and cerebrospinal fluid samples from a child with CNS disease. *J. Clin. Microbiol*. **40**(12), 4797-4799.

Iturriza-Gòmara, M., Wong, C., Blome, S., Desselberger, U. and Gray, J. (2002b). Molecular characterization of VP6 genes of human rotavirus isolates: correlation of genogroups with subgroups and evidence of independent segregation. *J. Virol.* **76**(13), 6596-6601.

Iturriza-Gòmara, M., Anderton, E., Kang, G., Gallimore, C., Phillips, W., Desselberger, U. and Gray, J. (2003). Evidence for genetic linkage between the gene segments encoding NSP4 and VP6 proteins in common and reassortant human rotavirus strains. *J. Clin. Microbiol*. **41**(8), 3566-3573.

Jagannath, M.R., Kesavulu, M.M., Deepa, R., Sastri, P.N., Kumar, S.S, Suguna, K. and Rao, C.D. (2006). N- and C-terminal cooperation in rotavirus enterotoxin: novel mechanism of modulation of the properties of a multifunctional protein by a structurally and functionally overlapping conformational domain. *J. Virol.* **80**(1), 412-425.

Jaimes, M.C., Rojas, O.L., González, A.M., Cajiao, I., Charpilienne, A., Pothier, P., Kohli, E., Greenberg, H.B., Franco, M.A. and Angel, J. (2002). Frequencies of virus-specific $CD4^+$ and $CD8^+$ T lymphocytes secreting gamma interferon after acute natural rotavirus infection in children and adults. *J. Virol.* **76**(10), 4741-4749.

Jaimes, M.C., Feng, N. and Greenberg, H.B. (2005). Characterization of homologous and heterologous rotavirus-specific T-cell responses in infant and adult mice. *J. Virol.* **79**(8), 4568-4579.

Jayaram, H., Estes, M.K. and Prasad, B.V. (2004). Emerging themes in rotavirus cell entry, genome organization, transcription and replication. *Virus Res.* **101**(1)**,** 67-81.

Jensen, F.C., Girardi, A.J., Gilden, R.V. and Koprowski, H. (1964). Infection of human and simian tissue cultures with Rous sarcoma virus. *Proc. Natl. Acad. Sci. U.S.A.* **52**, 53-59.

Jiang, B, Gentsch, J.R. and Glass, R.I. (2002). The role of serum antibodies in the protection against rotavirus disease: an overview. *Clin. Infect. Dis.* **34**(10), 1351-1361.

Jiang, J.Q., He, X.S., Feng, N. and Greenberg, H.B. (2008). Qualitative and quantitative characteristics of rotavirus-specific CD8 T cells vary depending on the route of infection. *J. Virol.* **82**(14), 6812-6819.

Johansen, K., Granqvist, L., Karlén, K., Stintzing, G., Uhnoo, I. and Svensson, L. (1994). Serum IgA immune response to individual rotavirus polypeptides in young children with rotavirus infection. *Arch. Virol.* **138**(3-4), 247-259.

Johansen, K., Hinkula, J., Espinoza, F., Levi, M., Zeng, C., Rudén, U., Vesikari, T., Estes, M. and Svensson, L. (1999). Humoral and cell-mediated immune responses in humans to the NSP4 enterotoxin of rotavirus. *J. Med. Virol.* **59**(3), 369-377.

Johnson, I.D. (2006). Practical considerations in the selection and application of fluorescent probes. *In* "Handbook of biological confocal microscopy, 3rd Ed." (J. B. Pawley, Ed.), pp. 353-364. Springer Science + Business Media, New York.

Jourdan, N., Maurice, M., Delautier, D., Quero, A. M., Servin, A.L. and Trugnan, G. (1997). Rotavirus is released from the apical surface of cultured human intestinal cells through nonconventional vesicular transport that bypasses the Golgi apparatus. *J. Virol.* **71**(11), 8268-8278.

Jourdan, N., Brunet, J.P., Sapin, C., Blais, A., Cotte-Laffitte, J., Forestier, F., Quero, A.M., Trugnan, G. and Servin, A.L. (1998). Rotavirus infection reduces sucrase-isomaltase expression in human intestinal cells by perturbing protein targeting and organization of microvillar cytoskeleton. *J. Virol.* **72**(9), 7228-7236.

Julián, E., Cama, M., Martínez, P. and Luquin, M. (2001). An ELISA for five glycolipids from the cell wall of *Mycobacterium tuberculosis:* Tween 20 interference in the assay. *J. Immunol. Methods* **251**(1-2), 21-30.

Jyothi, G., Surolia, A. and Easwaran, K.R.K. (1994). A23187 – Channel behaviour: fluorescence study. *J. Biosci*. **19**(3), 277-282.

Kabcenell, A.K. and Atkinson, P.H. (1985). Processing of the rough endoplasmic reticulum membrane glycoproteins of rotavirus SA11. *J. Cell Biol.* **101**(4), 1270-1280.

Kain, S.R., Zhang, G., Gurtu, V. and Kitts, P.A. (1998). Microscopic imagery of mammalian cells expressing an enhanced green fluorescent protein gene. *Methods Mol. Biol.* **102**, 33-42.

Kaljot, K.T., Shaw, R.D., Rubin, D.H. and Greenberg, H.B. (1988). Infectious rotavirus enters cells by direct cell membrane penetration, not by endocytosis. *J. Virol.* **62**(4), 1136-1144.

Kanfer, E.J., Abrahamson, G., Taylor, J., Coleman, J.C. and Samson, D.M. (1994). Severe rotavirus-associated diarrhoea following bone marrow transplantation: treatment with oral immunoglobulin. *Bone Marrow Transplant* **14**(4), 651-652.

Kapikian, A.Z., Wyatt, R.G., Levine, M.M., Yolken, R.H., VanKirk, D.H., Dolin, R., Greenberg, H.B. and Chanock, R.M. (1983). Oral administration of human rotavirus to volunteers: induction of illness and correlates of resistance. *J. Infect. Dis*. **147**(1), 95-106.

Kapikian, A.Z., Simonsen, L., Vesikari, T., Hoshino, Y., Morens, D.M., Chanock, R.M., La Montagne, J.R. and Murphy, B.R. (2005). A hexavalent human rotavirus-bovine rotavirus (UK) reassortant vaccine designed for use in developing countries and delivered in a schedule with the potential to eliminate the risk of intussusception. *Journal Infect. Dis.* **192**(Suppl 1), S22-S29.

Kaur, R., Dikshit, K.L. and Raje, M. (2002). Optimization of immunogold labeling TEM: An ELISA-based method for evaluation of blocking agents for quantitative detection of antigen. *J. Histochem. and Cytochem.* **50**(6), 863-873.

Kavanagh, O.V., Ajami, N.J., Cheng, E., Ciarlet, M., Guerrero, R.A., Zeng, C.Q.Y., Crawford, S.E. and Estes, M.K. (2010). Rotavirus enterotoxin NSP4 has mucosal adjuvant properties. *Vaccine* **28**(18), 3106-3111.

Keljo, D.J., Kuhn, M. and Smith, A. (1988). Acidification of endosomes is not important for the entry of rotavirus into the cell. *J. Pediatr. Gastroenterol. Nutr.* **7**(2), 257-263.

Kenna, J.G., Major, G.N. and Williams, R.S. (1985). Methods for reducing non-specific antibody binding in enzyme-linked immunosorbent assays. *J. Imunol. Methods* **85**(2), 409-419.

Khandjian, E.W. and Türler, H. (1983). Simian virus 40 and polyoma virus induce synthesis of heat shock proteins in permissive cells. *Mol. Cell. Biol.* **3**(1), 1-8.

Kim, T.-G., Befus, N. and Langridge, W.H.R. (2004). Co-immunization with an HIV-1 Tat transduction peptide-rotavirus enterotoxin fusion protein stimulates a Th1 mucosal immune response in mice. *Vaccine* **22**(3-4), 431-438.

King, L.A. and Possee, R.D. (1992). *The Baculovirus Expression System. A Laboratory Guide*, London, Chapmann and Hall.

Kirkwood, C.D., Coulson, B.S. and Bishop, R.F. (1996). G3P2 rotaviruses causing diarrhoeal disease in neonates differ in VP4, VP7 and NSP4 sequence from G3P2 strains causing asymptomatic neonatal infection. *Arch. Virol*. **141**(9), 1661-1676.

Kirkwood, C.D. and Palombo, E.A. (1997). Genetic characterization of the rotavirus nonstructural protein, NSP4. *Virology* **236**(2), 258-265.

Kirkwood, C.D., Gentsch, J.R. and Glass, R.I. (1999). Sequence analysis of the NSP4 gene from human rotavirus strains isolated in the United States. *Virus Genes* **19**(2), 113-122.

Kirkwood, C.D., Boniface, K., Richardson, S., Taraporewala, Z.F., Patton, J.T. and Bishop, R.F. (2008). Non-structural protein NSP2 induces heterotypic antibody responses during primary rotavirus infection and reinfection in children. *J. Med. Virol*. **80**(6), 1090-1098.

Kirkwood, C.D., Boniface, K., Bogdanovic-Sakran, N., Masendycz, P., Barnes, G.L. and Bishop, R.F. (2009). Rotavirus strain surveillance – an Australian perspective of strains causing disease in hospitalized children from 1997 to 2007. *Vaccine* **27**(Suppl 5), F102-F107.

Kitaoka, S., Suzuki, H., Numazaki, Y., Konno, T. and Ishida, N. (1986). The effect of trypsin on the growth and infectivity of human rotavirus. *Tohoku J. Exp. Med.* **149**(4), 437-447.

Kitts, P.A. and Possee, R.D. (1993). A method for producing recombinant baculovirus expression vectors at high frequency. *Biotechniques* **14**(5), 810-817.

Kobayashi, N., Alam, M.M., Kojima, K., Mise, K., Ishino, M. and Sumi, A. (2003). Genomic diversity and evolution of rotaviruses: An overview. *In* "Genomic diversity and molecular epidemiology of rotaviruses" (N. Kobayashi, Ed.). pp. 75-89.

Komoto, S., Sasaki, J. and Taniguchi, K. (2006). Reverse genetics system for introduction of site-specific mutations into the double-stranded RNA genome of infectious rotavirus. *Proc. Natl. Acad. Sci. USA*. **103**(12), 4646-4651.

Kordasti, S., Sjövall, H., Lundgren, O. and Svensson, L. (2004). Serotonin and vasoactive intestinal peptide antagonists attenuate rotavirus diarrhoea. *Gut* **53**(7), 952-957.

Krishnan, T., Sen, A., Choudhury, J.S., Das, S., Naik, T.N. and Bhattacharya, S.K. (1999). Emergence of adult diarrhoea rotavirus in Calcutta, India. *Lancet* **353**(9150), 380-381.

Labbé, M., Charpilienne, A., Crawford, S.E., Estes, M.K. and Cohen, J. (1991). Expression of rotavirus VP2 produces empty corelike particles. *J. Virol.* **65**(6), 2946-2952.

Labbé, M., Baudoux, P., Charpilienne, A., Poncet, D. and Cohen, J. (1994). Identification of the nucleic acid binding domain of the rotavirus VP2 protein. *J. Gen. Virol.* **75**(Pt 12), 3423-3430.

Laemmli, U.K. (1970). Cleavage of structural proteins during the assembly of the head of bacteriophage T4. *Nature* **227**(5259), 680-685.

Lanata, C.F. and Franco, M. (2006). Nitazoxanide for rotavirus diarrhea? *Lancet* **368**(9530), 100-101.

Lawton, J.A., Estes, M.K. and Prasad, B.V. (2000). Mechanism of genome transcription in segmented dsRNA viruses. *Adv. Virus Res.* **55**, 185-229.

Lee, C.N., Wang, Y.L., Kao, C.L., Zao, C.L., Lee, C.Y. and Chen, H.N. (2000). NSP4 gene analysis of rotaviruses recovered from infected children with and without diarrhea. *J. Clin. Microbiol.* **38**(12), 4471-4477.

Lin, S.L. and Tian, P. (2003). Detailed computational analysis of a comprehensive set of group A rotavirus NSP4 proteins. *Virus Genes* **26**(3), 271-282.

Linhares, A.C., Ruiz-Palacios, G.M., Guerrero, M.L., Salinas, B., Perez-Schael, I., Costa Clemens, S.A., Innis, B., Yarzabal, J.P., Vespa, G., Cervantes, Y., Hardt, K. and De Vos, B. (2006). A short report on highlights of world-wide development of RIX4414: A Latin American experience. *Vaccine* **24**(18), 3784-3785.

Liu, A.Y., Bian, H., Huang, L.E. and Lee, Y.K. (1994). Transient cold shock induces the heat shock response upon recovery at 37 degrees C in human cells. *J. Biol. Chem.* **269**(20), 14768-14765.

López, S. and Arias, C.F. (2004). Multistep entry of rotavirus into cells: a Versaillesque dance. *Trends Microbiol.* **12**(6), 271-278.

Lopez, S. and Arias, C.F. (2006). Early steps in rotavirus cell entry. *Curr. Top. Microbiol. Immunol.* **309**, 39-66.

López, T., Camacho, M., Zayas, M., Nájera, R., Sánchez, R., Arias, C.F. and López, S. (2005). Silencing the morphogenesis of rotavirus. *J. Virol.* **79**(1), 184-192.

López, T., López, S. and Arias, C.F. (2006). Heat shock enhances the susceptibility of BHK cells to rotavirus infection through the facilitation of entry and post-entry virus replication steps. *Virus Res.* **121**(1), 74-83.

Lorrot, M. and Vasseur, M. (2006). Rotavirus $NSP4_{114-135}$ peptide has no direct, specific effect on chloride transport in rabbit brush-border membrane. *Virol. J.* **3**:94.

Losonsky, G.A., Johnson, J.P., Winkelstein, J.A., and Yolken, R.H. (1985). Oral adminstration of human serum immunoglobulin in immunodeficient patients with viral gastroenteritis. A pharmacokinetic and functional analysis. *J. Clin. In*vest. **76**(6), 2362-2367.

Ludert, J.E., Krishnaney, A.A., Burns, J.W., Vo, P.T. and Greenberg, H.B. (1996). Cleavage of rotavirus VP4 in vivo. *J. Gen. Virol.* **77**(Pt 3), 391-395.

Lundgren, O., Peregrin, A.T., Persson, K., Kordasti, S., Uhnoo, I. and Svensson, L. (2000). Role of the enteric nervous system in the fluid and electrolyte secretion of rotavirus diarrhea. *Science* **287**(5452), 491-495.

Lundgren, O. and Svensson, L. (2001). Pathogenesis of rotavirus diarrhea. *Microbes Infect.* **3**(13), 1145-1156.

Maass, D.R. and Atkinson, P.H. (1990). Rotavirus proteins VP7, NS28, and VP4 form oligomeric structures. *J. Virol.* **64**(6), 2632-2641.

Majamaa, H., Isolauri, E., Saxelin, M. and Vesikari, T. (1995). Lactic acid bacteria in the treatment of acute rotavirus gastroenteritis. *J. Pediatr. Gastroenterol. Nutr.* **20**(3), 333-338.

Malik, J., Gupta, S.K., Bhatnagar, S., Bhan, M.K. and Ray, P. (2008). Evaluation of IFN-γ response to rotavirus and non-structural protein NSP4 of rotavirus in children following severe rotavirus diarrhea. *J. Clin. Virol*. **43**(2)**,** 202-206.

Maple, L., Lathrop, R., Bozich, S., Harman, W., Tacey, R., Kelley, M. and Danilkovitch-Miagkova, A. (2004). Development and validation of ELISA for herceptin detection in human serum. *J. Immunol. Methods* **295**(1-2), 169-182.

Maravall, M., Mainen, Z.F., Sabatini, B.L., and Svoboda, K. (2000). Estimating intracellular calcium concentrations and buffering without wavelength ratioing. *Biophys. J.*, **78**(5), 2655-2667.

Martella, V., Bányai, K., Matthijnssens, J., Buonavoglia, C. and Ciarlet, M. (2009). Zoonotic aspects of rotaviruses. *Vet. Microbiol.* **140**(3-4), 246-255.

Maruri-Avidal, L., López, S. and Arias, C.F. (2008). Endoplasmic reticulum chaperones are involved in the morphogenesis of rotavirus infectious particles. *J. Virol.* **82**(11), 5368-5380.

Mascarenhas, J.D., Linhares, A.C., Gabbay, Y.B., Lima, C.S., Guerra Sde, F., Soares, L.S., Oliveira, D.S., Lima, J.C., Macêdo, O. and Leite, J.P.G. (2007). Molecular characterization of VP4 and NSP4 genes from rotavirus strains infecting neonates and young children in Belém, Brazil. *Virus Res.* **126**(1-2), 149-158.

Mathai, R.A., Andres, A., Helregel, B.A., Kuhlenschmidt, T.B., Kuhlenschmidt, M.S. and Donovan, S.M. (2008). Gastrointestinal structural and functional responses to rotavirus infection in the neonatal piglet. *FASEB J.* **22**(1), 896.6.

Mathieu, M., Petitpas, I., Navaza, J., Lepault, J., Kohli, E., Pothier, P., Prasad, B.V., Cohen, J. and Rey, F.A. (2001). Atomic structure of the major capsid protein of rotavirus: implications for the architecture of the virion. *EMBO J.* **20**(7), 1485-1497.

Matson, D.O., O'Ryan, M.L., Pickering, L.K., Chiba, S., Nakata, S., Raj, P. and Estes, M.K. (1992). Characterization of serum antibody responses to natural rotavirus infections in children by VP7-specific epitope-blocking assays. *J. Clin. Microbiol.* **30**(5), 1056-1061.

Matson, D.O., O'Ryan, M.L., Herrera, I., Pickering, L.K. and Estes, M.K. (1993). Fecal antibody response to symptomatic and asymptomatic rotavirus infections. *J. Infect. Dis.* **167**(3), 577-583.

Matthijnssens, J., Rahman, M., Martella, V., Xuelei, Y., De Vos, S., De Leener, K., Ciarlet, M., Buonavoglia, C. and Van Ranst, M. (2006). Full genomic analysis of human rotavirus strain B4106 and lapine rotavirus strain 30/96 provides evidence for interspecies transmission. *J. Virol.* **80**(8), 3801-3810.

Matthijnssens, J., Ciarlet, M., Heiman, E., Arijs, I., Delbeke, T., McDonald, S.M., Palombo, E. A., Iturriza-Gómara, M., Maes, P., Patton, J.T., Rahman, M. and Van Ranst, M. (2008a). Full genome-based classification of rotaviruses reveals a common origin between human Wa-like and porcine rotavirus strains and human DS-1-like and bovine rotavirus strains. *J. Virol.* **82**(7), 3204-3219.

Matthijnssens, J., Ciarlet, M., Rahman, M., Attoui, H., Bányai, K., Estes, M.K., Gentsch, J.R., Iturriza-Gómara, M., Kirkwood, C.D., Martella, V., Mertens, P.P., Nakagomi, O., Patton, J.T., Ruggeri, F.M., Saif, L.J., Santos, N., Steyer, A., Taniguchi, K., Desselberger, U. and Van Ranst, M. (2008b). Recommendations for the classification of group A rotaviruses using all 11 genomic RNA segments. *Arch. Virol.* **153**(8), 1621-1629.

Mattion, N.M., Mitchell, D.B., Both, G.W. and Estes, M.K. (1991). Expression of rotavirus proteins encoded by alternative open reading frames of genome segment 11. *Virology* **181**(1), 295-304.

Mattion, N.M., Cohen, J. and Estes, M.K. (1994). The rotavirus proteins. *In* "Viral infections of the gastrointestinal tract" 2nd Edn. (A.Z. Kapikian, Eds.), pp. 169-249. Marcel Dekker, N.Y.

McCrae, M.A. and McCorquodale, J.G. (1983). Molecular biology of rotaviruses. V. Terminal structure of viral RNA species. *Virology* **126**(1), 204-212.

McNeal, M.M., Broome, R.L. and Ward, R.L. (1994). Active immunity against rotavirus infection in mice correlated with viral replication and titers of serum rotavirus IgA following vaccination. *Virology* **204**(2), 642-650.

McNeal, M.M., Barone, K.S., Rae, M.N. and Ward, R.L. (1995). Effector functions of antibody and $CD8^+$ cells in resolution of rotavirus infection and protection against reinfection in mice. *Virology* **214**(2), 387-397.

McNeal, M.M., Rae, M.N. and Ward, R.L. (1997). Evidence that resolution of rotavirus infection in mice is due to both CD4 and CD8 cell-dependent activities. *J. Virol.* **71**(11), 8735-8742.

McNeal, M.M., VanCott, J.L., Choi, A.H.-C., Basu, M., Flint, J.A., Stone, S.C., Clements, J.D. and Ward, R.L. (2002). CD4 T cells are the only lymphocytes needed to protect mice against rotavirus shedding after intranasal immunization with a chimeric VP6 protein and the adjuvant LT(R192G). *J. Virol.* **76**(2), 560-568.

McNeal, M.M., Stone, S.C., Basu, M., Bean, J.A., Clements, J.D., Hendrickson, B.A., Choi, A.H.-C. and Ward, R.L. (2006). Protection against rotavirus shedding after intranasal immunization of mice with a chimeric VP6 protein does not require intestinal IgA. *Virology* **346**(2), 338-347.

McNeal, M.M., Basu, M., Bean, J.A., Clements, J.D., Choi, A.H. and Ward, R.L. (2007a). Identification of an immunodominant $CD4^+$ T cell epitope in the VP6 protein of rotavirus following intransasal immunization of BALB/c mice. *Virology* **363**(2), 410-418.

McNeal, M.M., Stone, S.C., Basu, M., Clements, J.D., Choi, A.H. and Ward, R.L. (2007b). IFN-gamma is the only anti-rotavirus cytokine found after in vitro stimulation of memory CD4+ T cells from mice immunized with a chimeric VP6 protein. *Viral Immunol*. **20**(4), 571-584.

Mesa, M.C., Gutiérrez, L., Duarte-Rey, C., Angel, J. and Franco, M.A. (2010). A TGF-β mediated regulatory mechanism modulates the T cell immune response to rotavirus in adults but not in children. *Virology* **399**(1), 77-86.

Meyer, J.C., Bergmann, C.C. and Bellamy, A.R. (1989). Interaction of rotavirus cores with the nonstructural glycoprotein NS28. *Virology* **171**(1), 98-107.

Meyer, T., Wensel, T. and Stryer, L. (1990). Kinetics of calcium channel opening by inositol 1,4,5-triphosphate. *Biochemistry* **29**(1), 32-37.

Michelangeli, F., Ruiz, M.-C., del Castillo, J.R., Ludert, J.E. and Liprandi, F. (1991). Effect of rotavirus infection on intracellular calcium homeostasis in cultured cells. *Virology* **181**(2), 520-527.

Michelangeli, F., Liprandi, F., Chemello, M.E., Ciarlet, M. and Ruiz., M.-C. (1995). Selective depletion of stored calcium by thapsigargin blocks rotavirus maturation but not the cytopathic effect. *J. Virol.* **69**(6), 3838-3847.

Midthun, K. and Kapikian, A.Z. (1996). Rotavirus vaccines: an overview. *Clin. Microbiol. Rev.* **9**(3), 423-434.

Miller, L.K. (1988). Baculoviruses as gene expression vectors. *Ann Rev Microbiol* **42**, 177-199.

Mir, K.D., Parr, R.D., Schroeder, F. and Ball, J.M. (2007). Rotavirus NSP4 interacts with both the amino- and carboxyl-termini of caveolin-1. *Virus Res*. **126**(1-2), 106-115.

Mirazimi, A., von Bonsdorff, C.H. and Svensson, L. (1996). Effect of brefeldin A on rotavirus assembly and oligosaccharide processing. *Virology* **217**(2), 554-563.

Mirazimi, A., Nilsson, M. and Svensson, L. (1998). The molecular chaperone calnexin interacts with the NSP4 enterotoxin of rotavirus in vivo and in vitro. *J. Virol.* **72**(11), 8705-8709.

Mirazimi, A., Magnusson, K.E. and Svensson, L. (2003). A cytoplasmic region of the NSP4 enterotoxin of rotavirus is involved in retention in the endoplasmic reticulum. *J. Gen. Virol.* **84**(Pt-4), 875-883.

Miyawaki, A., Nagai, T., Shimozono, S., Fukano, T. and Mizuno, H. (2002). Circularly permuted green fluorescent proteins engineered to sense $Ca^{2+}$ and their application to imaging of subcellular $Ca^{2+}$ dynamics. *RIKEN Review: Focused on Ultrafast Optical Sciences* **49**, 55-59.

Mohan, K.V. and Atreya, C.D. (2000). Comparative sequence analysis identified mutations outside the NSP4 cytotoxic domain of tissue culture-adapted ATCC-Wa strain of human rotavirus and a novel inter-species variable domain in its C-terminus. *Arch Virol.* **145**(9), 1789-1799.

Mohan, K.V., Dermody, T.S. and Atreya, C.D. (2000). Mutations selected in rotavirus enterotoxin NSP4 depend on the context of its expression. *Virology* **275**(1), 125-132.

Mohan, K.V., Kulkarni, S., Glass, R.I., Zhisheng, B. and Atreya, C.D. (2003). A human vaccine strain of lamb rotavirus (Chinese) NSP4 gene: complete nucleotide sequence and phylogenetic analyses. *Virus Genes* **26**(2), 185-192.

Moore, E.D., Becker, P.L., Fogarty, K.E., Williams, D.A. and Fay, F.S. (1990). $Ca^{2+}$ imaging in single living cells: theoretical and practical issues. *Cell Calcium* **11** (2-3), 157-179.

Moreira, L.L., Netto, E.M. and Nascimento-Carvalho, C.M. (2009). Risk factors for nosocomial rotavirus infection in a paediatric hospital: the potential role for vaccine use. *Vaccine* **27**(3), 416-420.

Morgan, A.J. and Thomas, A.P. (1999). Single cell and subcellular measurement of intracellular $Ca^{2+}$ concentration ($[Ca^{2+}]i$]. *Methods Mol. Biol.* **114**, 93-123.

Mori, Y., Sugiyama, M., Takayama, M., Atoji, Y., Masegi, T. and Minamoto, N. (2001). Avian-to-mammal transmission of an avian rotavirus: analysis of its pathogenicity in a heterologous mouse model. *Virology* **288**(1), 63-70.

Mori, Y., Borgan M.A., Ito, N., Sugiyama, M. and Minamoto, N. (2002a). Sequential analysis of nonstructural protein NSP4s derived from Group A avian rotaviruses. *Virus Res*. **89**(1), 145-151.

Mori, Y., Borgan, M.A., Ito, N., Sugiyama, M. and Minamoto, N. (2002b). Diarrhea-inducing activity of avian rotavirus NSP4 glycoproteins, which differ greatly from mammalian rotavirus NSP4 glycoproteins in deduced amino acid sequence, in suckling mice. *J. Virol.* **76**(11), 5829-5834.

Morris, A.P., Kirk, K.L. and Frizzell, R.A. (1990). Simultaneous analysis of cell $Ca^{2+}$ and $Ca^{2+}$-stimulated chloride conductance in colonic epithelial cells (HT29). *Cell Regul.* **1**(12), 951-963.

Morris, A.P., Scott, J.K., Ball, J.M., Zeng, C.Q., O'Neal, W.K. and Estes, M.K. (1999). NSP4 elicits age-dependent diarrhea and $Ca^{2+}$ mediated $I^-$ influx into intestinal crypts of CF mice. *Am. J. Physiol.* **277**(2 Pt 1), G431-G444.

Morris, A.P. and Estes, M.K. (2001). Microbes and microbial toxins: paradigms for microbial-mucosal interactions. VIII. Pathological consequences of rotavirus infection and its enterotoxin. *Am. J. Physiol.* **281**(2), G303-G310.

Moser, C.A., Cookinham, S., Coffin, S.E., Clark, H.F. and Offit, P.A. (1998). Relative importance of rotavirus-specific effector and memory B cells in protection against challenge. *J. Virol.* **72**(2), 1108-1114.

Mossel, E.C. and Ramig, R.F. (2002). Rotavirus genome segment 7 (NSP3) is a determinant of extraintestinal spread in the neonatal mouse. *J. Virol.* **76**(13), 6502-6509.

Moulton, L.H., Staat, M.A., Santosham, M. and Ward, R.L. (1998). The protective effectiveness of natural rotavirus infection in an American Indian population. *J. Infect. Dis*. **178**(6), 1562-1566.

Murphy, B.R., Morens, D.M., Simonsen, L., Chanock, R.M., La Montagne, J.R. and Kapikian, A.Z. (2003). Reappraisal of the association of intussusception with the licensed live rotavirus vaccine challenges initial conclusions. *J. Infect. Dis.* **187**(8), 1301-1308.

Nagai, T., Sawano, A., Park, E.S. and Miyawaki, A. (2001). Circularly permuted green fluorescent proteins engineered to sense $Ca^{2+}$. *Proc. Natl. Acad. Sci. U.S.A.*, **98**(6), 3197-3202.

Nakagomi, T. and Nakagomi, O. (2000). Human rotavirus HCR3 possesses a genomic RNA constellation indistinguishable from that of feline and canine rotaviruses. *Arch. Virol.* **145**(11), 2403-2409.

Nandi, P., Charpilienne, A. and Cohen, J. (1992). Interaction of rotavirus particles with liposomes. *J. Virol.* **66**(6), 3363-3367.

Nejmeddine, M., Trugnan, G., Sapin, C., Kohli, E., Svensson, L., Lopez, S. and Cohen, J. (2000). Rotavirus spike protein VP4 is present at the plasma membrane and is associated with microtubules in infected cells. *J. Virol.* **74**(7), 3313-3320.

Nevins, J.R. (1982). Induction of the synthesis of a 70,000 dalton mammalian heat shock protein by the adenovirus EIA gene product. *Cell* **29**(3), 913-919.

Newton, K., Meyer, J.C., Bellamy, A.R. and Taylor, J.A. (1997). Rotavirus nonstructural glycoprotein NSP4 alters plasma membrane permeability in mammalian cells. *J. Virol.* **71**(12), 9458-9465.

Nishiyama, H., Higashitsuji, H., Yoko, H., Itoh, K., Danno, S., Matsuda, T. and Fujita, J. (1997). Cloning and characterization of human CIRP (cold-inducible RNA-binding protein) cDNA and chromosomal assignment of the gene. *Gene* **204**(1-2), 115-120.

Notarianni, E.L. and Preston, C.M. (1982). Activation of cellular stress protein genes by herpes simplex virus temperature-sensitive mutants which overproduce immediate early polypeptides. *Virology* **123**(1), 113-122.

O'Brien, J.A., Taylor, J.A. and Bellamy, A.R. (2000). Probing the structure of rotavirus NSP4: a short sequence at the extreme C terminus mediates binding to the inner capsid particle. *J. Virol.* **74**(11), 5388-5394.

Offit, P.A., Clark, H.F., Blavat, G. and Greenberg, H.B. (1986). Reassortant rotaviruses containing structural proteins VP3 and VP7 from different parents induce antibodies protective against each parental serotype. *J. Virol.* **60**(2), 491-496.

Offit, P.A. and Dudzik, K.I. (1990). Rotavirus-specific cytotoxic T lymphocytes passively protect against gastroenteritis in suckling mice. *J. Virol.* **64**(12), 6325-6328.

Offit, P.A., Hoffenberg, E.J., Pia, E.S, Panackal, P.A. and Hill, N.L. (1992). Rotavirus-specific helper T cell responses in newborns, infants, children and adults. *J. Infect. Dis.* **165**(6), 1107-1111.

Offit, P.A., Hoffenberg, E.J., Santos, N. and Gouvea, V. (1993). Rotavirus-specific humoral and cellular immune response after primary, symptomatic infection. *J. Infect. Dis.* **167**(6), 1436-1440.

Offit, P.A., Clark, H.F. and Ward, R.L. (2003). Current state of development of human rotavirus vaccines. *In* "Viral Gastroenteritis" (U. Desselberger and J. Gray, Eds.), .pp. 345-356. Elsevier Science B.V., Amsterdam, The Netherlands.

Oka, T., Nakagomi, T. and Nakagomi, O. (2001). A lack of consistent amino acid substitutions in NSP4 between rotaviruses derived from diarrheal and asymptomatically-infected kittens. *Microbiol. Immunol*. **45**(2), 173-177.

Olivo, M. and Streckert, H.J. (1995). Studies on the single-shelled rotavirus receptor with a synthetic peptide derived from the cytoplasmic domain of NS28. *Arch. Virol.* **140**(12), 2151-2161.

O'Neal, C.M., Crawford, S.E., Estes, M.K. and Conner, M.E. (1997). Rotavirus virus-like particles administered mucosally induce protective immunity. *J. Virol*. **71**(11), 8707-8717.

O'Neal, C.M., Clements, J.D., Estes, M.K. and Conner, M.E. (1998). Rotavirus 2/6 viruslike particles administered intranasally with cholera toxin, *Escherichia coli* heat-labile toxin (LT), and LT-R192G induce protection from rotavirus challenge. *J. Virol*. **72**(4), 3390-3393.

O'Neal, C.M., Harriman, G.R. and Conner, M.E. (2000). Protection of the villus epithelial cells of the small intestine from rotavirus infection does not require immunoglobulin A. *J. Virol.* **74**(9), 4102-4109.

O'Ryan, M.L., Matson, D.O., Estes, M.K. and Pickering, L.K. (1994a). Anti-rotavirus G type-specific and isotype-specific antibodies in children with natural rotavirus infections. *J. Infect. Dis.* **169**(3), 504-511.

O'Ryan, M.L., Matson, D.O., Estes, M.K. and Pickering, L.K. (1994b). Acquisition of serum isotype-specific and G type specific antirotavirus antibodies among children in day care centres. *Pediatr. Infect. Dis. J.* **13**(10), 890-895.

O'Ryan, M.L. (2009). The ever-changing landscape of rotavirus serotypes. *Pediatr. Infect. Dis. J.* **28**(Suppl 3), S60-S62.

Osborne, M.P., Haddon, S.J., Spencer, A.J., Collins, J., Starkey, W.G., Wallis, T.S., Clarke, G.J., Worton, K.J., Candy, D.C. and Stephen, J. (1988). An electron microscopic investigation of time-related changes in the intestine of neonatal mice infected with murine rotavirus. *J. Pediatr. Gastroenterol. Nutr.* **7**(2), 236-248.

Osborne, M.P., Haddon, S.J., Worton, K.J., Spencer, A.J., Starkey, W.G., Thornber, D. and Stephen, J. (1991). Rotavirus-induced changes in the microcirculation of intestinal villi of neonatal mice in relation to the induction and persistence of diarrhea. *J. Pediatr. Gastroenterol. Nutr.* **12**(1), 111-120.

Padilla-Noriega, L., Paniagua, M. and Guzmán-León, S. (2002). Rotavirus protein NSP3 shuts off host cell protein synthesis. *Virology* **298**(1), 1-7.

Pager, C.T., Alexander, J.J. and Steele, A.D. (2000). South African G4P[6] asymptomatic and symptomatic neonatal rotavirus strains differ in their NSP4, VP8*, and VP7 genes. *J. Med. Virol.* **62**(2), 208-216.

Palombo, E.A. (2003). Genetic reassortment and interspecies transmission of rotaviruses. *In* "Genomic Diversity and Molecular Epidemiology of Rotaviruses" (N. Kobayashi, Ed.), pp. 1-12.

Parashar, U.D., Gibson, C.J., Bresee, J.S. and Glass, R.I. (2006). Rotavirus and severe childhood diarrhea. *Emerg. Infect. Dis.* **12**(2), 304-306.

Parr, R.D., Storey, S.M., Mitchell, D.M., McIntosh, A.L., Zhou, M., Mtir, K.D. and Ball, J.M. (2006). The rotavirus enterotoxin NSP4 directly interacts with the caveolar structural protein caveolin-1. *J. Virol.* **80**(6), 2842-2854.

Patton, J.T. (1986). Synthesis of simian rotavirus SA11 double-stranded RNA in a cell-free system. *Virus. Res.* **6**(3), 217-233.

Patton, J.T. (1996). Rotavirus VP1 alone specifically binds to the 3'-end of viral mRNA but the interaction is not sufficient to initiate minus-strand synthesis. *J. Virol.* **70**(11), 7940-7947.

Patton, J.T., Kearney, K. and Taraporewala, Z. (2003). Rotavirus genome replication: role of the RNA-binding proteins. *In* "Viral Gastroenteritis" (U. Desselberger and J. Gray, Eds), pp. 165-183, Elsevier Science B.V., Amsterdam, The Netherlands.

Patton, J.T., Silvestri, L.S., Tortorici, M.A., Vasquez-Del Carpio, R. and Taraporewala, Z.F. (2006). Rotavirus genome replication and morphogenesis: role of the viroplasm. *Curr. Top. Microbiol. Immunol.* **309**, 169-187.

Pérez, J.F., Chemello, M.E., Liprandi, F., Ruiz, M.-C. and Michelangeli, F. (1998). Oncosis in MA104 cells is induced by rotavirus infection through an increase in intracellular $Ca^{2+}$ concentration. *Virology* **252**(1), 17-27.

Pérez, J.F., Ruiz, M.-C. Chemello, M.E. and Michelangeli, F. (1999). Characterization of a membrane calcium pathway induced by rotavirus infection in cultured cells. *J. Virol.* **73**(3), 2481-2490.

Pérez-Vargas, J., Romero, P., López, S. and Arias, C.F. (2006). The peptide-binding and ATPase domains of recombinant hsc70 are required to interact with rotavirus and reduce its infectivity. *J. Virol.* **80**(7), 3322-3331.

Pesavento, J.B., Estes, M.K. and Venkataram Prasad, B.V. (2003). Structural organization of the genome in rotavirus. *In* "Viral Gastroenteritis" (U. Desselberger and J. Gray, Eds.), pp. 115-127. Elsevier Science B.V., Amsterdam, The Netherlands.

Pesavento, J.B., Crawford, S.E., Estes, M.K. and Prasad, B.V. (2006). Rotavirus proteins: structure and assembly. *Curr. Top. Microbiol. Immunol*. **309**, 189-219.

Petrie, B.L., Estes, M.K. and Graham, D.Y. (1983). Effects of tunicamycin on rotavirus morphogenesis and infectivity. *J. Virol.* **46**(1), 270-274.

Petrie, B.L., Greenberg, H.B., Graham, D.Y. and Estes, M.K. (1984). Ultrastructural localization of rotavirus antigens using colloidal gold. *Virus Res.* **1**(2), 133-152.

Phua, K.B., Quak, S.H., Lee, B.W., Emmanuel, S.C., Goh, P., Han, H.H., De Vos, B. and Bock, H.L. (2005). Evaluation of RIX4414, a live, attenuated rotavirus vaccine, in a randomized, double-blind, placebo-controlled phase 2 trial involving 2464 Singaporean infants. *J. Infect. Dis.* **192**(Suppl. 1), S6-S16.

Piron, M., Vende, P., Cohen, J. and Poncet, D. (1998). Rotavirus RNA-binding protein NSP3 interacts with eIF4GI and evicts the poly(A) binding protein from eIF4F. *EMBO J.* **17**(19), 5811-5821.

Poncet, D. (2003). Translation of rotavirus mRNAs in the infected cell. *In* "Viral Gastroenteritis" (U. Desselberger and J. Gray, Eds.), pp. 185-205. Elsevier Science B.V., Amsterdam, The Netherlands.

Poruchynsky, M.S. and Atkinson, P.H. (1991). Rotavirus protein rearrangements in purified membrane-enveloped intermediate particles. *J. Virol.* **65**(9), 4720-4727.

Poruchynsky, M.S., Maass, D.R. and Atkinson, P.H. (1991). Calcium depletion blocks the maturation of rotavirus by altering the oligomerization of virus-encoded proteins in the ER. *J. Cell Biol*. **114**(4), 651-661.

Prasad, B.V., Burns, J.W., Marietta, E., Estes, M.K. and Chiu, W. (1990). Localization of VP4 neutralization sites in rotavirus by three-dimensional cryo-electron microscopy. *Nature* **343**(6257), 476-479.

Prasad, B.V., Rothnagel, R., Zeng, C.Q., Jakana, J., Lawton, J.A., Chiu, W., and Estes, M.K. (1996). Visualization of ordered genomic RNA and localization of transcriptional complexes in rotavirus. *Nature* **382**(6590), 471-473.

Rajasekaran, D., Sastri, N.P., Marathahalli, J.R., Indi, S.S., Pamidimukkala, K., Sugana, K. and Rao, C.D. (2008). The flexible C terminus of the rotavirus non-structural protein NSP4 is an important determinant of its biological properties. *J. Gen. Virol*. **89**, (Pt-6), 1485-1496.

Ramig, R.F. (1997). Genetics of the rotaviruses. *Ann. Rev. Microbiol.* **51**, 225-255.

Rao, G.G. (1995). Control of outbreaks of viral diarrhoea in hospitals: a practical approach. *J. Hosp. Infect.* **30**(1), 1-6.

Rasmussen, S.E. (1998). Solid phases and chemistries. *In* "Complementary Immunoassays" (W.P. Collins, Ed.), pp. 43-55, Wiley, Chichester.

Ray, P., Malik, J., Singh, R.K., Bhatnagar, S., Bahl, R., Kumar, R. and Bhan, M.K. (2003). Rotavirus nonstructural protein NSP4 induces heterotypic antibody responses during natural infection in children. *J. Infect. Dis.* **187**(11), 1786-1793.

Realpe, M., Espinosa, R., López, S. and Arias, C.F. (2010). Rotaviruses require basolateral molecules for efficient infection of polarized MDCKII cells. *Virus Res.* **147**(2), 231-241.

Rebeski, D.E., Winger, E.M., Shin, Y.-K., Lelenta, M., Robinson, M.M., Varecka, R. and Crowther, J.R. (1999). Identification of unacceptable background caused by non-specific protein adsorption to the plastic surface of 96-well immunoassay plates using a standardized enyme-linked immunosorbent assay procedure. *J. Immunol. Methods* **226**(1-2), 85-92.

Richardson, S.C., Grimwood, K. and Bishop, R.F. (1993). Analysis of homotypic and heterotypic serum immune responses to rotavirus proteins following primary rotavirus infection by using the radioprecipitation technique. *J Clin. Microbiol.* **31**(2), 377-385.

Richardson, S.C., Grimwood, K., Gorrell, R., Palombo, E.A., Barnes, G.L., and Bishop, R.F. (1998). Extended excretion of rotavirus after severe diarrhoea in young children. *Lancet* **351**(9119), 1844-1848.

Richter-Landsberg, C. (2009). Heat Shock Proteins: Expression and functional roles in nerve cells and glia. *In*. "Heat shock proteins in neural cells" (C. Richter-Landsberg, Ed.), pp 1-12. Springer, N.Y.

Rijkers, G.T., Justement, L.B., Griffioen, A.W. and Cambier, J.C. (1990). Improved method for measuring intracellular $Ca^{2+}$ with fluo-3. *Cytometry* **11**(8), 923-927.

Robinson, C.G., Hernanz-Schulman, M., Zhu, Y., Griffin, M.R., Gruber, W. and Edwards, K.M. (2004). Evaluation of anatomic changes in young children with natural rotavirus infection: is intussusception biologically plausible? *J. Infect. Dis.* **189**(8), 1382-1387.

Rockwell, P.L. and Storey, B.T. (1999). Determination of the intracellular dissociation constant, $K_D$, of the fluo-3 $Ca^{2+}$ complex in mouse sperm for use in estimating intracellular $Ca^{2+}$ concentrations. *Mol. Reprod. Dev.* **54**(4), 418-428.

Rodríguez-Díaz, J., López-Andújar, P., García-Díaz, A., Cuenca, J, Montava, R. and Buesa, J. (2003). Expression and purification of polyhistidine-tagged rotavirus NSP4 proteins in insect cells. *Protein Expres. Purif.* **31**(2), 207-212.

Rodríguez-Díaz, J., Monedero, V., Pérez-Martínez, G. and Buesa, J. (2004). Single-chain variable fragment (scFv) antibodies against rotavirus NSP4 enterotoxin generated by phage display. *J. Virol. Methods* **121**(2), 231-238.

Rodríguez-Díaz, J., Montava, R., García-Díaz, A. and Buesa, J. (2005). Humoral immune response to rotavirus NSP4 enterotoxin in Spanish children. *J. Med. Virol.* **77**(2), 317-322.

Rojas, A.M., Boher, Y., Guntiňas, M.J. and Pérez-Schael, I. (1995). Homotypic immune response to primary infection with rotavirus serotype G1. *J. Med. Virol.* **47**(4), 404-409.

Rojas, O.L., González, A.M., González, R., Pérez-Schael, I., Greenberg, H.B., Franco, M.A. and Angel, J. (2003). Human rotavirus specific T cells: quantification by ELISPOT and expression of homing receptors on CD4+ T cells. *Virology* **314**(2), 671-679.

Rojas, O.L., Caicedo, L., Guzmán, C., Rodríguez, L.-S., Castañeda, J., Uribe, L., Andrade, Y., Pinzón, R., Narváez, C.F., Lozano, J.M., De Vos, B., Franco, M.A. and Angel, J. (2007). Evaluation of circulating intestinally committed memory B cells in children vaccinated with attenuated human rotavirus vaccine. *Viral Immunol.* **20**(2), 300-311.

Rojas, O.L., Narváez, C.F., Greenberg, H.B., Angel, J. and Franco, M.A. (2008). Characterization of rotavirus specific B cells and their relation with serological memory. *Virology*, **380**(2), 234-242.

Rott, L.S., Rosé, J.R., Bass, D., Williams, M.B., Greenberg, H.B. and Butcher, E.C. (1997). Expression of mucosal homing receptor alpha4beta7 by circulating $CD4^+$ cells with memory for intestinal rotavirus. *J. Clin. Invest.* **100**(5), 1204-1208.

Rouadi, P., Baroody, F.M., Abbott, D., Naureckas, E., Solway, J., Naclerio, R.M. (1999). A technique to measure the ability of the human nose to warm and humidify air. *J. Appl. Physiol.* **87**(1), 400-406.

Ruiz, M.C., Alonso-Torre, S.R., Charpilienne, A., Vasseur, M., Michelangeli, F., Cohen, J. and Alvarado, F. (1994). Rotavirus interaction with isolated membrane vesicles. *J. Virol.* **68**(6), 4009-4016.

Ruiz, M.C., Charpilienne, A., Liprandi, F., Gajardo, R., Michelangeli, F. and Cohen, J. (1996). The concentration of $Ca^{2+}$ that solubilizes outer capsid proteins from rotavirus particles is dependent on the strain. *J. Virol.* **70**(8), 4877-4883.

Ruiz, M.C., Abad, M.J., Charpilienne, A., Cohen, J. and Michelangeli, F. (1997). Cell lines susceptible to infection are permeabilized by cleaved and solubilized outer layer proteins of rotavirus. *J. Gen. Virol*. **78**(Pt 11), 2883-2893.

Ruiz, M.C., Cohen, J. and Michelangeli, F. (2000). Role of $Ca^{2+}$ in the replication and pathogenesis of rotavirus and other viral infections. *Cell Calcium* **28**(3), 137-149.

Ruiz, M.C., Díaz, Y., Peña, F., Aristimuño, O.C., Chemello, M.E. and Michelangeli, F. (2005). $Ca^{2+}$ permeability of the plasma membrane induced by rotavirus infection in cultured cells is inhibited by tunicamycin and brefeldin A. *Virology* **333**(1), 54-65.

Ruiz, M.C., Aristimuño, O.C., Díaz, Y., Peña, F., Chemello, M.E., Rojas, H., Ludert, J.E. and Michelangeli, F. (2007). Intracellular disassembly of infectious rotavirus particles by depletion of $Ca^{2+}$ sequestered in the endoplasmic reticulum at the end of virus cycle. *Virus Res*. **130**(1-2), 140-150.

Ruiz-Palacios, G.M., Pérez-Schael, I., Velázquez, F.R., Abate, H., Breuer, T., Clemens, S.C., Cheuvart, B., Espinoza, F., Gillard, P., Innis, B.L., Cervantes, Y., Linhares, A.C., López, P., Macías-Parr, M., Ortega-Barria, E., Richardson, V., Rivera-Medina, D.M., Rivera, L., Salinas, B., Pavía-Ruz, N., Salmerón, J., Rüttimann, R., Tinoco, J.C., Rubio, P., Nuñez, E., Guerrero, M.L., Yarzábal, J.P., Damasco, S., Tornieporth, N., Sáez,-Llorens, X., Vergara, R.F., Vesikara, T., Bouckenooghe, A., Clemens, R., De Vos, B. and O'Ryan, M. (2006). Safety and efficacy of an

attenuated vaccine against severe rotavirus gastroenteritis. *N. Engl. J. Med.* **354**(1), 11-22.

Salazar-Lindo, E., Santisteban-Ponce, J., Chea-Woo, E. and Gutierrez, M. (2000). Racecadotril in the treatment of acute watery diarrhea in children. *N. Engl. J. Med.* **343**(7), 463-467.

Salinas, B., Pérez Schael, I., Linhares, A.C., Ruiz Palacios, G.M., Guerrero, M.L., Yarzábal, J.P., Cervantes, Y., Costa Clemens, S., Damaso, S., Hardt, K. and De Vos, B. (2005). Evaluation of safety, immunogenicity and efficacy of an attenuated rotavirus vaccine, RIX4414: A randomized, placebo controlled trial in Latin American infants. *Pediatr. Infect. Dis. J.* **24**(9), 807-816.

Samalia, A. and Orrenius, S. (1998). Heat shock proteins: regulators of stress response and apoptosis. *Cell Stress Chaperones* **3**(4), 228-236.

Sambrook, J. and Russell, D.W. (2001). *Molecular Cloning. A laboratory manual* (3rd ed), Cold Spring Harbor Laboratory Press, USA.

Sánchez-San Martin, C., López, T., Arias, C.F. and López, S. (2004). Characterization of rotavirus cell entry. *J. Virol.* **78**(5), 2310-2318.

Santos, N. and Hoshino, Y. (2005). Global distribution of rotavirus serotypes/genotypes and its implication for the development and implementation of an effective rotavirus vaccine. *Rev. Med. Virol.* **15**(1), 29-56.

Sapin, C., Colard, O., Delmas, O., Tessier, C., Breton, M., Enouf, V., Chwetzoff, S., Ouanich, J., Cohen, J., Wolf, C. and Trugnan, G. (2002). Rafts promote assembly and atypical targeting of a nonenveloped virus, rotavirus, in caco-2 cells. *J. Virol.* **76**(9), 4591-4602.

Sarker, S.A., Casswall, T.H., Juneja, L.R., Hoq, E., Hossain, I., Fuchs, G.J. and Hammarström, L. (2001). Randomized, placebo-controlled, clinical trial of hyperimmunized chicken egg yolk immunoglobulin in children with rotavirus diarrhea. *J. Pediatr. Gastroenterol. Nutr.* **32**(1), 19-25.

Sasaki, S. Horie, Y., Nakagomi, T., Oseto, M. and Nakagomi, O. (2001). Group C rotavirus NSP4 induces diarrhea in neonatal mice. *Arch. Virol.* **146**(4), 801-806.

Sattar, S.A., Springthorpe, V.S., Karim, Y. and Loro, P. (1989). Chemical disinfection of non-porous inanimate surfaces experimentally contaminated with four human pathogenic viruses. *Epidemio. Infect.* **102**(3), 493-505.

Schnetkamp, P.P., Li, X.-B., Basu, D.K. and Szerencsei, R.T. (1991). Regulation of free cytosolic $Ca^{2+}$ concentration in the outer segments of bovine retinal rods by Na-Ca-K exchange measured with fluo-3. I. Efficiency of transport and interactions between cations. *J. Biol. Chem.* **266**(34), 22975-22982.

Schuck, P., Taraporewala, Z., McPhie, P. and Patton, J.T. (2001). Rotavirus nonstructural protein NSP2 self-assembles into octamers that undergo ligand-induced conformational changes. *J. Biol. Chem.* **276**(13), 9679-9687.

Sen, A., Sen, N. and Mackow, E.R. (2007). The formation of viroplasm-like structures by the rotavirus NSP5 protein is calcium regulated and directed by a C-terminal helical domain. *J. Virol.* **81**(21), 11758-11767.

Seo, N.S., Zeng, C.Q.Y., Hyser, J.M., Utama, B., Crawford, S.E., Kim, K.J., Höök, M. and Estes, M.K. (2008). Inaugural article: integrins α1β1 and α2β1 are receptors for the rotavirus enterotoxin. *Proc. Natl. Acad. Sci. USA*. **105**(26), 8811-8818.

Servin, A.L. (2003). Effects of rotavirus infection on the structure and functions of intestinal cells. *In* "Viral Gastroenteritis" (U. Desselberger and J. Gray Eds.), pp. 237-254. Elsevier Science B.V., Amsterdam, The Netherlands.

Shahrabadi, M.S., Babiuk, L.A. and Lee, P.W. (1987). Further analysis of the role of calcium in rotavirus morphogenesis. *Virology* **158**(1), 103-111.

Shuler, M.L., Hammer, D.A., Granados, R.R. and Wood, H.A. (1995). Overview of Baculovirus – Insect culture system. *In* "Baculovirus expression systems and biopesticides" (M.L. Shuler, M.L., H.A. Wood, R.R. Granados, D.A. Hammer, Eds.) pp. 1-9. Wiley-Liss, New York.

Silvestri, L.S., Tortorici, M.A., Vasquez-Del Carpio, R. and Patton, J.T. (2005). Rotavirus glycoprotein NSP4 is a modulator of viral transcription in the infected cell. *J. Virol.* **79**(24), 15165-1574.

Simons, K. and Ikonen, E. (1997). Functional rafts in cell membranes. *Nature* **387**(6633), 569-572.

Simonsen, L., Morens, D., Elixhauser, A., Gerber, M., Van Raden, M. and Blackwelder, W. (2001). Effect of rotavirus vaccination programme on trends in admission of infants to hospital for intussusception. *Lancet* **358**(9289), 1224-1229.

Simpson, A.W. (2006). Fluorescent measurement of $[Ca^{2+}]c$: basic practical considerations. *Methods Mol. Biol.* **312**, 3-36.

Slavik, J. (1998). Single and multiple spectral parameter fluorescence microscopy. *In* "Digital image analysis of microbes. Imaging, morphometry, fluorometry and motility techniques and applications" (M.H.F. Wilkinson and F. Schut, Eds.), pp. 93-114. John Wiley and Sons, Ltd, West Sussex, England Barnes and Ellis, New York.

Smiley, K.L., McNeal, M.M., Basu, M., Choi, A.H., Clements, J.D. and Ward, R.L. (2007). Association of gamma interferon and interleukin-17 production in intestinal $CD4^+$ T cells with protection against rotavirus shedding in mice intranasally immunized with VP6 and the adjuvant LT(R192G). *J. Virol.* **81**(8), 3740-3748.

Smith, E.M., Estes, M.K., Graham, D.Y. and Gerba, C.P. (1979). A plaque assay for the Simian rotavirus SA11. *J. Gen. Virol.* **43**, 513-519.

Snodgrass, D.R., Fitzgerald, T.A., Campbell, I., Browning, G.F., Scott, F.M., Hoshino, Y., and Davies, R.C. (1991). Homotypic and heterotypic serological responses to rotavirus neutralization epitopes in immunologically naïve and experienced animals. *J. Clin. Microbiol*. **29**(11), 2668-2672.

Sonna, L.A., Fujita, J., Gaffin, S.L. and Lilly, C.M. (2002). Invited review: Effects of heat and cold stress on mammalian gene expression. *J. Appl. Physiol.* **92**(4), 1725-1742.

Sonna, L.A., Kuhlmeier, M.M., Khatri, P., Cheng, D. and Lilly, C.M. (2010). A microarray analysis of the effects of moderate hypothermia and rewarming on gene expression by human hepatocytes (HepG2). *Cell Stress Chaperones* **15**(5), 687-702.

Spencer, E. and Arias, M.L. (1981). In vitro transcription catalyzed by heat-treated human rotavirus. *J. Virol.* **40**(1), 1-10.

Spaniol, V., Troller, R. and Aebi, C. (2009). Physiologic cold shock increases adherence of *Moraxella catarrhalis* to and secretion of interleukin 8 in human upper respiratory tract epithelial cells. *J. Infect. Dis.* **200**(10), 1593-1601.

Stephen, J. and Osborne, M.P. (1988). Pathophysiological mechanisms in diarrhoeal disease. *In* "Bacterial infections of respiratory and gastrointestinal mucosae" Vol. 24 (W. Donachie, W. Griffiths, and E. Stephen, J. Eds.), pp 149-172. Special Publications of the Society for General Microbiology, IRL Press, Oxford.

Storey, S.M., Gibbons, T.F., Williams, C.V., Parr, R.D., Schroeder, F. and Ball, J.M. (2007). Full-length, glycosylated NSP4 is localized to plasma membrane caveolae by a novel raft isolation technique. *J. Virol.* **81**(11), 5472-5483.

Summers, M.D. and Smith, G.E. (1987). A manual of methods for baculovirus vectors and insect cell culture procedures. *Texas Agricultural Experiment Station Bulletin No. 1555.* pp. 1-54.

Suzuki, H., Konno, T., Kitaoka, S., Sato, T., Ebina, T. and Ishida, N. (1984). Further observations on the morphogenesis of human rotavirus in MA104 cells. *Arch. Virol*. **79**(3-4), 147-159.

Suzuki, H., Kitaoka, S., Konno, T., Sato, T. and Ishida, N. (1985). Two modes of human rotavirus entry into MA104 Cells. *Arch. Virol*. **85**(1-2), 25-34.

Svensson, L., Sheshberadaran, H., Vesikari, T., Norrby, E. and Wadell, G. (1987). Immune response to rotavirus polypeptides after vaccination with heterologous rotavirus vaccines (RIT 4237, RRV-1). *J. Gen. Virol*. **68**(Pt 7), 1993-1999.

Tafazoli, F., Zeng, C.Q., Estes, M.K., Magnusson, K.-E. and Svensson, L. (2001). NSP4 enterotoxin of rotavirus induces paracellular leakage in polarized epithelial cells. *J. Virol.* **75**(3), 1540-1546.

Takahashi, A., Camacho, P., Lechleiter, J.D. and Herman, B. (1999). Measurement of intracellular calcium. *Physiol. Rev*. **79**(4), 1089-1125.

Tao, H., Changan, W., Zhaoying, F., Zinyi, C., Xuejian, C., Xiaoquang, L., Guangmu, C., Henli, Y., Tungxin, C., Weiwe, Y., Shuasen, D. and Weicheng, C. (1984). Waterborne outbreak of rotavirus diarrhoea in adults in China caused by a novel rotavirus. *Lancet* **323**(8387), 1139-1142.

Taraporewala, Z.F., Schuck, P., Ramig, R.F., Silvestri, L. and Patton, J.T. (2002). Analysis of a temperature-sensitive mutant rotavirus indicates that NSP2 octamers are the functional form of the protein. *J. Virol.* **76**(14), 7082-7093.

Tatte, V.S., Rawal, K.N. and Chitambar, S.D. (2010). Sequence and phylogenetic analysis of the VP6 and NSP4 genes of human rotavirus strains: evidence of discordance in their genetic linkage. *Infect. Genet. Evol.* Electronic publication ahead of print.

Tatti, K.M., Gentsch, J., Shieh, W.J., Ferebee-Harris, T., Lynch, M., Bresee, J., Jiang, B., Zaki, S.R. and Glass, R. (2002). Molecular and immunological methods to detect rotavirus in formalin-fixed tissue. *J. Virol. Methods* **105**(2), 305-319.

Tavaria, M., Gabriele, T., Kola, I. and Anderson, R.L. (1996). A hitchhiker's guide to the human Hsp70 family. *Cell Stress Chaperones* **1**(1), 23-28.

Taylor, J.A., Meyer, J.C., Legge, M.A., O'Brien, J.A., Street, J.E., Lord, V.J., Bergmann, C.C. and Bellamy, A.R. (1992). Transient expression and mutational analysis of the rotavirus intracellular receptor: the C-terminal methionine residue is essential for ligand binding. *J. Virol.* **66**(6), 3566-3572.

Taylor, J.A., O'Brien, J.A., Lord, V.J., Meyer, J.C. and Bellamy, A.R. (1993). The RER-localized rotavirus intracellular receptor: a truncated purified soluble form is multivalent and binds virus particles. *Virology* **194**(2), 807-814.

Taylor, J.A., O'Brien, J.A. and Yeager, M. (1996). The cytoplasmic tail of NSP4, the endoplasmic reticulum-localized non-structural glycoprotein of rotavirus, contains distinct virus binding and coiled coil domains. *EMBO J*. **15**(17), 4469-4476.

Thomas, D., Tovey, S.C., Collins, T.J., Bootman, M.D., Berridge, M.J. and Lipp, P. (2000). A comparison of fluorescent $Ca^{2+}$ indicator properties and their use in measuring elementary and global $Ca^{2+}$ signals. *Cell Calcium* **28**(4), 213-223.

Tian, P., Hu, Y., Schilling, W.P., Lindsay, D.A., Eiden, J. and Estes, M.K. (1994). The nonstructural glycoprotein of rotavirus affects intracellular calcium levels. *J. Virol.* **68**(1), 251-257.

Tian, P., Estes, M.K., Hu, Y., Ball, J.M., Zeng, C.Q. and Schilling, W.P. (1995). The rotavirus nonstructural glycoprotein NSP4 mobilizes $Ca^{2+}$ from the endoplasmic reticulum. *J. Virol.* **69**(9), 5763-5772.

Tian, P., Ball, J.M., Zeng, C.Q. and Estes, M.K. (1996a). The rotavirus nonstructural glycoprotein NSP4 possesses membrane destabilization activity. *J. Virol.* **70**(10), 6973-6981.

Tian, P., Ball, J.M., Zeng, C. Q. and Estes, M.K. (1996b). Rotavirus protein expression is important for virus assembly and pathogenesis. *Arch. Virol. Suppl.* **12**, 69-77.

Tian, P., Ottaiano, A., Reilly, P.A., Udem, S. and Zamb, T. (2000). The authentic sequence of rotavirus SA11 nonstructural protein NSP4. *Virus Res.* **66**(2), 117-122.

Tihova, M., Dryden, K.A., Bellamy, A.R., Greenberg, H.B. and Yeager, M. (2001). Localization of membrane permeabilization and receptor binding sites on the VP4 hemagglutinin of rotavirus: implications for cell entry. *J. Mol. Biol.* **314**(5), 985-992.

Tô, T.L., Ward, L.A., Yuan, L. and Saif, L.J. (1998). Serum and intestinal isotype antibody responses and correlates of protective immunity to human rotavirus in a gnotobiotic pig model of disease. *J. Gen. Virol.* **79**(Pt 11), 2661-2672.

Torres-Vega, M.A., González, R.A., Duarte, M., Poncet, D., López, S. and Arias, C.F. (2000). The C-terminal domain of rotavirus NSP5 is essential for its multimerization, hyperphosphorylation and interaction with NSP6. *J. Gen. Virol*. **81**(Pt 3), 821-830.

Trask, S.D. and Dormitzer, P.R. (2006). Assembly of highly infectious rotavirus particles recoated with recombinant outer capsid proteins. *J. Virol.* **80**(22), 11293-11304.

Tsien, R.Y., Pozzan, T. and Rink, T.J. (1982). Calcium homeostasis in intact lymphocytes: cytoplasmic free calcium monitored with a new, intracellularly trapped fluorescent indicator. *J. Cell Biol*. **94**(2), 325-334.

Uhnoo, I., Riepenhoff-Talty, M., Dharakul, T., Chegas, P., Fisher, J.E., Greenberg, H.B. and Ogra, P.L. (1990). Extramucosal spread and development of hepatitis in immunodeficient and normal mice infected with rhesus rotavirus. *J. Virol.* **64**(1), 361-368.

Valenzuela, S., Pizarro, J., Sandino, A.M., Vásquez, M., Fernández, J., Hernández, O., Patton, J. and Spencer, E. (1991) Photoaffinity labeling of rotavirus VP1 with 8-azido-ATP: identification of the viral RNA polymerase. *J. Virol.* **65**(7), 3964-3967.

Varghese, V., Das, S., Singh, N.B., Kojima, K., Bhattacharya, S.K., Krishnan, T., Kobayashi, N. and Naik, T.N. (2004). Molecular characterization of a human rotavirus reveals porcine characteristics in most of the genes including VP6 and NSP4. *Arch. Virol.* **149**(1), 155-172.

Vasconcelos, D., Norrby, E. and Oglesbee, M. (1998). The cellular stress response increases measeles virus-induced cytopathic effect. *J. Gen. Virol.* **79**(Pt-7), 1769-1773.

Vaughn, J.L., Goodwin, R.H., Tompkins, G.J. and McCawley, P. (1977). The establishment of two cell lines from the insect *Spodoptera frugiperda* (Lepidoptera; Noctuidae). *In Vitro* **13**, 213-217.

Velázquez, F.R., Matson, D.O., Calva J.J., Guerrero, M.L., Morrow, A.L., Carter-Campbell, S., Glass, R.I., Estes, M.K., Pickering, L.K. and Ruiz-Palacios, G.M. (1996). Rotavirus infections in infants as protection against subsequent infections. *N. Engl. J. Med.* **355**(14), 1022-1028.

Velazquez, F.R., Matson, D.O., Guerrero, M.L., Shults, J., Calva, J.J., Morrow, A.L., Glass, R.I., Pickering, L.K. and Ruiz-Palacios, G.M. (2000). Serum antibody as a marker of protection against natural rotavirus infection and disease. *J. Infect Dis.* **182**(6), 1602-1609.

Vende, P., Piron, M., Castagné, N. and Poncet, D. (2000). Efficient translation of rotavirus mRNA requires simultaneous interaction of NSP3 with the eukaryotic translation initiation factor eIF4G and the mRNA 3' end. *J. Virol.* **74**(15), 7064-7071.

Vesikari, T., Karvonen, A., Puustinen, L., Zeng, S.Q., Szakal, E.D., Delem, A. and De Vos, B. (2004). Efficacy of RIX4414 live attenuated human rotavirus vaccine in Finnish infants. *Pediatr. Infect. Dis. J.* **23**(10), 937-943.

Vesikari, T., Clark, H.F., Offit, P.A., Dallas, M.J., DiStefano, D.J., Goveia, M.G., Ward, R.L., Schödel, F., Karvonen, A., Drummond, J.E., DiNubile, M.J. and Heaton, P.M. (2006a). Effects of the potency and composition of the multivalent human-bovine (WC3) reassortant rotavirus vaccine on efficacy, safety and immunogenicity in healthy infants. *Vaccine* **24**(22), 4821-4829.

Vesikari, T., Matson, D.O., Dennehy, P., Van Damme, P., Santosham, M., Rodriguez, Z., Dallas, M.J., Heyse, J.F., Goveia, M.G., Black, S.B., Shinefield, H.R., Christie, C.D.C., Yitalo, S., Itzler, R.F., Coia, M.L., Onorato, M.T., Adeyi, B.A., Marshall, G.S., Gothefors, L., Campens, D., Karvonen, A., Watt, J.P., O'Brien, K.L., DiNubile, M.J., Clark, H.F., Boslego, J.W., Offit, P.A. and Heaton, P.M. (2006b). Safety and efficacy of a pentavalent human-bovine (WCS) reassortant rotavirus vaccine. *N. Engl. J. Med*. **354**(1), 23-33.

Vesikari, T., Karvonen, A., Prymula, R., Schuster, V., Tejedor, J.C., Cohen, R., Meurice, F., Han, H.H., Damaso, S. and Bouckenooghe, A. (2007). Efficacy of human rotavirus vaccine against rotavirus gastroenteritis during the first 2 years of life in European infants: randomised, double-blind controlled study. *Lancet* **370**(9601), 1757-1763.

Vesikari, T., Itzler, R., Karvonen, A., Korhonen, T., Van Damme, P., Behre, U., Bona, G., Gothefors, L., Heaton, P.M., Dallas, M., Goveia, M.G. (2009). RotaTeq, a pentavalent rotavirus vaccine: efficacy and safety among infants in Europe. *Vaccine* **28**(2), 345-351.

Vizzi, E., Calviño, González, R., Pérez-Schael, I., Ciarlet, M., Kang, G., Estes, M.K., Liprandi, F. and Ludert, J.E. (2005). Evaluation of serum antibody responses against the rotavirus nonstructural protein NSP4 in children after Rhesus rotavirus tetravalent vaccination or natural infection. *Clin. Diagn. Lab. Immun.* **12**(10), 1157-1163.

Vogt, Jr., R.F., Phillips, D.L., Henderson, L.O., Whitfield, W. and Spierto, F.W. (1987). Quantitative differences among various proteins as blocking agents for ELISA microtiter plates. *J. Immunol. Methods* **101**(1), 43-50.

Ward, R.L., Bernstein, D.I., Young, E.C, Sherwood, J.R., Knowlton, D.R. and Schiff, G.M. (1986). Human rotavirus studies in volunteers: determination of infectious dose and serologic response to infection. *J. Infect. Dis.* **154**(5), 871-880.

Ward, R.L, Bernstein, D.I., Shukla, R., Young, E.C., Sherwood, J.R., McNeal, M.M., Walker, M.C., Schiff, G.M. (1989). Effects of antibody to rotavirus on protection of adults challenged with a human rotavirus. *J. Infect. Dis.* **159**(1), 79-88.

Ward, R.L., Clemens, J.D., Knowlton, D.R., Rao, M.R., van Loon, F.P., Huda, N., Ahmed, F., Schiff, G.M. and Sack, D.A. (1992). Evidence that protection against rotavirus diarrhea after natural infection is not dependent on serotype-specific neutralizing antibody. *J. Infect. Dis*. **166**(6), 1251-1257.

Ward, R.L., McNeal, M.M., Sander, D.S., Greenberg, H.B. and Bernstein, D.I. (1993). Immunodminance of the VP4 neutralization protein of rotavirus in protective natural infections of young children. *J. Virol.* **67**(1), 464-468.

Ward, R.L. and Bernstein, D.I. (1994). Protection against rotavirus disease after natural rotavirus infection. US Rotavirus Vaccine Efficacy Group. *J. Infect. Dis.* **169**(4), 900-904.

Ward, R.L. and Bernstein, D.I. (1995). Lack of correlation between serum rotavirus antibody titers and protection following vaccination with reassortant RRV vaccines. US Rotavirus Vaccine Efficacy Group. *Vaccine* **13**(13), 1226-1232.

Ward, R.L., Knowlton, D.R., Zito E.T., Davidson, B.L., Rappaport, R. and Mack, M.E. (1997a). Serologic correlates of immunity in a tetravalent reassortant rotavirus vaccine trial. US Rotavirus Vaccine Efficacy Group. *J. Infect. Dis.* **176**(3), 570-577.

Ward, R.L., Mason, B.B., Bernstein, D.I., Sander, D.S., Smith, V.E., Zandle, G.A. and Rappaport, R.S. (1997b). Attenuation of a human rotavirus vaccine candidate did not correlate with mutations in the NSP4 protein gene. *J. Virol.* **71**(8), 6267-6270.

Ward, R.L. (2003). Possible mechanisms of protection elicited by candidate rotavirus vaccines as determined with the adult mouse model. *Viral Immunol.* **16**(1), 17-24.

Ward, R.L., Clark, H.F., Offit, P.A. and Glass, R.I. (2004). Live vaccine strategies to prevent rotavirus disease. *In* "New Generation Vaccines" (M. M. Levine, J.B. Kaper, R. Rappuoli, M.A. Liu and M.F. Good, Eds), 3rd ed, pp 607-620. Marcel Dekker, Inc, New York.

Ward, R.L., Kirkwood, C.D., Sander, D.S., Smith, V.E., Shao, M., Bean, J.A., Sack, D.A. and Bernstein, D.I. (2006). Reductions in cross-neutralizing antibody responses in infants after attenuation of the human rotavirus vaccine candidate 89-12. *J. Infect. Dis.* **194**(12), 1729-1736.

Ward, R. (2009). Mechanisms of protection against rotavirus infection and disease. *Pediatr. Infect. Dis. J.* **28**(Suppl 3), S57-S59.

Ward, R.L. and Bernstein, D.I. (2009). Rotarix: a rotavirus vaccine for the world. *Vaccines* **48**(2), 222-228.

Warwicker, J. and O'Connor, J. (1995). A model for vicilin solubility at mild acidic pH, based on homology modeling and electrostatics calculations. *Protein Eng.* **8**, 1243-1251.

Webb, A.C., Bradley, M.K., Phelan, S.A., Wu, J.Q. and Gehrke, L. (1991). Use of the Polymerase Chain Reaction for screening and evaluation of recombinant baculovirus clones. *BioTechniques* **11**(4), 512-519.

Welch, W.J. (1991). The role of heat-shock proteins as molecular chaperones. *Curr. Opin. Cell Biol.* **3**(6), 1033-1038.

Westerman, L.E., McClure, H.M., Jiang, B., Almond, J.W. and Glass, R.I. (2005). Serum IgG mediates mucosal immunity against rotavirus infection. *Proc. Natl. Acad. Sci. USA.* **102**(20), 7268-7273.

Widdowson, M.A., Bresee, J.S., Gentsch, J.R. and Glass, R.I. (2005). Rotavirus disease and its prevention. *Curr. Opin. Gastroenterol.* **21**(1), 26-31.

Winslow, M.M. and Crabtree, G.R. (2005). Immunology. Decoding calcium signaling. *Science* **307**(5706), 56-57.

Woo, S.D. (2001). Rapid detection of Multiple Nucleopolyhedroviruses using Polymerase Chain Reaction. *Mol. Cells* **11**(3), 334-340.

Xu, A., Bellamy, A.R. and Taylor, J.A. (1998). BiP (GRP78) and endoplasmin (GRP94) are induced following rotavirus infection and bind transiently to an endoplasmic reticulum-localized virion component. *J. Virol.* **72**(12), 9865-9872.

Xu, A., Bellamy, A.R. and Taylor, J.A. (1999). Expression of translationally controlled tumour protein is regulated by calcium at both the transcriptional and post-transcriptional level. *Biochem. J.* **342**(Pt 3), 683-689.

Xu, A., Bellamy, A.R. and Taylor, J.A. (2000). Immobilization of the early secretory pathway by a virus glycoprotein that binds to microtubules. *EMBO. J.* **19**(23), 6465-6474.

Xu, M., Fu, Y., Sun, J., Zhang, J., Feng, M., Cheng, X. and Xu, J. (2010). Analysis of rotavirus NSP4 genotypes and age-dependent antibody response against NSP4 in Shanghai, China. *Jpn. J. Infect. Dis.* **63**(4), 280-282.

Yolken, R.H., Peterson, J.A., Vonderfecht, S.L., Fouts, E.T., Midthun, K., and Newburg, D.S. (1992). Human milk inhibits rotavirus replication and prevents experimental gastroenteritis. *J. Clin. Invest*. **90**(5), 1984-1991.

Yu, J. and Langridge, W.H.R. (2001). A plant-based multicomponent vaccine protects mice from enteric diseases. *Nat. Biotechnol.* **19**(6), 548-552.

Yu, J., Dennehy, P., Keyserling, H., Westerman, L.E., Wang, Y., Holman, R.C., Gentsch, J.R., Glass, R.I. and Jiang, B. (2005). Serum antibody responses in children with rotavirus diarrhea can serve as proxy for protection. *Clin. Diagn. Lab. Immunol.* **12**(2), 273-279.

Yuan, L., Ward, L.A., Rosen, B.I., To, T.L. and Saif, L.J. (1996). Systemic and intestinal antibody-secreting cell responses and correlates of protective immunity to human rotavirus in a gnotobiotic pig model of disease. *J. Virol.* **70**(5), 3075-3083.

Yuan, L., Kang, S.Y., Ward, L.A., To, T.L. and Saif, L.J. (1998). Antibody-secreting cell responses and protective immunity assessed in gnotobiotic pigs inoculated orally or intramuscularly with inactivated human rotavirus. *J. Virol.* **72**(1), 330-338.

Yuan, L., Geyer, A., Hodgins, D.C., Fan, Z., Qian, Y., Chang, K.O., Crawford, S.E., Parreňo, V., Ward, L.A., Estes, M.K., Conner, M.E. and Saif, L.J. (2000). Intranasal administration of 2/6-rotavirus-like particles with mutant *Escherichia coli* heat-labile toxin (LT-R192G) induces antibody-secreting cell responses but not protective immunity in gnotobiotic pigs. *J. Virol.* **74**(19), 8843-8853.

Yuan, L., Iosef, C., Azevedo, M.S., Kim, Y., Qian, Y., Geyer, A., Nguyen, T.V., Chang, K.O. and Saif, L.J. (2001). Protective immunity and antibody-secreting cell responses elicited by combined oral attenuated Wa human rotavirus and intranasal Wa 2/6-VLPs with mutant *Escherichia coli* heat-labile toxin in gnotobiotic pigs. *J. Virol.* **75**(19), 9929-9238.

Yuan, L. and Saif, L.J. (2002). Induction of mucosal immune responses and protection against enteric viruses: rotavirus infection of gnotobiotic pigs as a model. *Vet. Immunol. Immunopathol.* **87**(3-4), 147-160.

Yuan, L., Honma, S., Ishida, S.-I., Yan, X.-Y., Kapikian, A.Z. and Hoshino, Y. (2004a). Species-specific but not genotype-specific primary and secondary isotype-specific NSP4 antibody responses in gnotobiotic calves and piglets infected with homologous host bovine (NSP4[A]) or porcine (NSP4[B]) rotavirus. *Virology* **330**(1), 92-104.

Yuan, L., Ishida, S.-I., Honma, S., Patton, J.T., Hodgins, D.C., Kapikian, A.Z. and Hoshino, Y. (2004b). Homotypic and heterotypic serum isotype-specific antibody responses to rotavirus nonstructural protein 4 and viral protein (VP)4, VP6, and VP7 in infants who received selected live oral rotavirus vaccines. *J. Infect. Dis.* **189**(10), 1834-1845.

Yuan, L., Azevedo, M.S., Gonzalez, A.M., Jeong, K.I., Van Nguyen, T., Lewis, P., Iosef, C., Herrmann, J.E. and Saif, L.J. (2005). Mucosal and systemic antibody responses and protection induced by a prime/boost rotavirus-DNA vaccine in a gnotobiotic pig model. *Vaccine* **23**(3), 3925-3936.

Yuan, L., Honma, S., Kim, I., Kapikian, A.Z. and Hoshino, Y. (2009). Resistance to rotavirus infection in adult volunteers challenged with a virulent G1P1A[8] virus correlated with serum immunoglobulin G antibodies to homotypic viral proteins 7 and 4. *J. Infect. Dis.* **200**(9), 1443-1451.

Zambrano, J.L., Díaz, Y., Peña, F., Vizzi, E., Ruiz, M.-C., Michelangeli, F., Liprandi, F. and Ludert, J.E. (2008). Silencing of rotavirus NSP4 or VP7 expression reduce alterations in $Ca^{2+}$ homeostasis induced by infection of cultured cells. *J. Virol.* **82**(12), 5815-5824.

Zanardi, L.R., Haber, P., Mootrey, G.T., Niu, M.T. and Wharton, M. (2001). Intussusception among recipients of rotavirus vaccine: reports to the vaccine adverse event reporting system. *Pediatrics* **107**(6), E97.

Zárate, S., Espinosa, R., Romero, P., Guerrero, C.A, Arias, C.F. and López, S. (2000a). Integrin α2β1 mediates the cell attachment of the rotavirus neuraminidase-resistant variant nar3. *Virology* **278**(1), 50-54.

Zárate, S., Espinosa, R., Romero, P., Méndez, E., Arias, C.F. and López, S. (2000b). The VP5 domain of VP4 can mediate attachment of rotaviruses to cells. *J. Virol.* **74**(2), 593-599.

Zárate S., Cuadras, M.A., Espinosa, R., Romero, P., Juárez, K.O., Camacho-Nuez, M., Arias, C.F. and López, S. (2003). Interaction of rotaviruses with Hsc70 during cell entry is mediated by VP5. *J. Virol.* **77**(13), 7254-7260.

Zerbini, M., Musiani, M. and La Placa, M. (1985). Effect of heat shock on Epstein-Barr virus and cytomegalovirus expression. *J. Gen. Virol.* **66**(Pt 3), 633-636.

Zerbini, M., Musiani, M. and La Placa, M. (1986). Stimulating effect of heat shock on the early stage of human cytomegalovirus replication cycle. *Virus Res.* **6**(3), 211-216.

Zhang, M., Zeng, C. Q.-Y., Dong, Y., Ball, J.M., Saif, L.J., Morris, A.P. and Estes, M.K. (1998). Mutations in rotavirus nonstructural glycoprotein NSP4 are associated with altered virus virulence. *J. Virol.* **72**(5), 3666-3672.

Zhang, M., Zeng, C. Q.-Y., Morris, A.P. and Estes, M.K. (2000). A functional NSP4 enterotoxin peptide secreted from rotavirus-infected cells. *J. Virol.* **74**(24), 11663-11670.

Zhang, W., Azevedo, M.S., Wen, K., Gonzalez, A., Saif, L.J., Li, G., Yousef, A.E. and Yuan, L. (2008). Probiotic *Lactobacillus acidophilus* enhances the immunogenicity of an oral rotavirus vaccine in gnotobiotic pigs. *Vaccine* **26**(29-30), 3655-3661.